Sedimentary processes and stratigraphic record of the shelf to slope transition; an example from the Karoo Basin, South Africa.

Thesis submitted in accordance with the

requirements of the University of Liverpool for the

degree of Doctor in Philosophy

by

George Edward Davys Jones

March 2013

Abstract

Exposures of the lower Waterford Formation, Karoo Basin, South Africa provide rare three-dimensional control to an exhumed low-gradient basin margin, which permits increased understanding of sub-seismic scale process-regime and lateral variability. The study section overlies a 500-m-thick channelized submarine slope succession and is subdivided into eight mappable parasequences clinothems. The central 40 km 2D reference profile parallel to depositional dip (i.e. west-to-east) enables characterization of the shelf-to-slope transition for two successive clinothems and the establishment of robust criteria for identifying the shelf edge at outcrop.

The two clinothems exhibit differing process responses to the gradient increase at the shelf edge rollover. The fluvial-dominated, mouth-bar clinothem of WfC 3 exhibits a 5 km dip-parallel zone of extensional growth faulting at the shelf edge with limited delivery of sediment beyond the shelf edge rollover. In contrast, WfC 4 is a wave and storm dominated shoreface-clinothem that supplied a thick upper slope turbidite succession via closely spaced gullies at the shelf edge and a large upper slope channel. This suggests that the delivery of sediment to deep-water settings is governed by parameters other than the presence and proximity of a fluvial point source, which is heavily advocated in current models for shelf construction.

It would be common practice to attribute variability between successive clinothems on a single 2D dip profile to lateral variability across the basin margin. However, two additional, sub-parallel dip profiles across depositional strike to the north and south of the reference profile indicate significant 3D variability in the nature of the clinothems. A greater supply of sediment to the upper slope in the north of the region, in the absence of a clear fluvial driver, suggests that the deltaic/shoreface system was able to transit quickly to the shelf edge and establish itself in that position for an extended period. Increasing parasequence thickness toward the north indicates greater accommodation in this area throughout the lower Waterford succession. It is therefore likely that differential subsidence across the margin controlled the position of the shelf edge and maintained a narrower shelf in the north, which would have had significant influence on sediment routing paths, diverting them to the north.

Abundant shelf-confined soft sediment deformation in successive clinothems along all three dip margin profiles is attributed to instability on the frontal slopes of inner shelf deltas, due to high rates of sediment supply. The basinward splitting and abrupt thinning of deformed packages beyond the inferred shelf edge rollover shows that the presence of soft-sediment deformation alone is not an adequate criterion with which to define the shelf edge rollover.

The significant thickness of shelf deposits without subaerial exposure indicates that the margin was subject to a relatively high subsidence rate but that the rate of sediment supply was sufficient to drive the system to the shelf edge and deliver sand to the slope without the development of incised valleys. Therefore, the lower Waterford Formation is considered a high accommodation / high supply system. This study provides a high-resolution outcrop-based dataset with three-dimensional constraints. It enables greater understanding of the controls on basin margin construction, and the sub-seismic scale processes that control the spatial and temporal variability of sediment delivery to the slope and basin floor.

Acknowledgements

I would like to thank my supervisors Stephen Flint, David Hodgson and Rufus Brunt for the opportunities they provided me with, and for their continuous support, encouragement and guidance throughout. I would also like to thank them for the numerous other benefits I have experienced, namely, field trips to the Ross, Ireland; Ainsa Basin; Spain; Book Cliffs Utah and for all the excellent days spent in the Karoo.

I am also grateful to the Slope 3 project sponsors Anadarko, BHP Billiton, BP, Chevron, Conoco-Phillips, ExxonMobil, GDF-Suez, Maersk Oil, Murphy, Petrobras, Schlumberger, Shell, Statoil, Total, Tullow, VNG Norge, and Woodside, for their financial support of this Ph.D. studentship.

DeVille Wickens is thanked for the discussions, logistics, and regional knowledge. We also acknowledge landowners in the Laingsburg area for access, and thank John Kavanagh, Emma Morris, Heather Rawcliffe, Ashley Clarke, Kehinde Olafiranye, Alice Gulliford, and Laura Edwards for their assistance.

A special thanks to colleagues Emma Morris, Alice Gulliford, John Kavanagh, Rufus Brunt and Willem Van de Merwe for healthy discussion and making my stay at Liverpool so pleasurable. Finally, thanks to my parents and especially Elise, for the hours of spell checking as well as constant support and encouragement.

Contents

Abstract 1

Acknowledgements 2

Contents 3

List of figures 7

List of tables 11

Chapter 1 12

Introduction 12

1.1. Introduction to the SLOPE project 13

1.2. Background rationale 13

1.3. Aims of the PhD project 18

1.3.1. Key objectives of this thesis 18

1.4. Thesis layout 23

1.5. Contribution by authors to the manuscripts 25

1.6. Shelf edge deltas: a brief review 26

1.6.1. Classification of deltas 26

1.6.2. Clinoform scale and margin accretion. Shelf edge deltas and the accretion / development of basin margins 28

1.6.3. Shelf edge delta architecture 29

1.6.4. Sedimentary characteristics of shelf edge delta systems (lithofacies distribution) 32

1.6.4.1. Facies landward of the shelf edge 32

1.6.4.2. Facies basinward of the shelf edge 33

1.6.5. Generation of shelf margin deltas 35

1.7. Sequence stratigraphy: an overview 37

1.7.1. Shallow marine sequence stratigraphy: concepts and limitations 38

1.7.1.1. Flooding surfaces 38

1.7.1.2. Sequence boundaries 38

1.7.1.3. Parasequences, parasequence sets and systems tracts 38

1.7.1.4. Depositional sequences and systems tracts 40

1.8. Dataset and methods 42

1.9. Geological setting of the study area 44

1.9.1. Geological evolution of southern Africa/western Gondwana 45

1.9.1.1. Ordovician to middle Carboniferous 45

1.9.1.2. Formation and evolution of the Karoo Basin and the Cape Fold Belt 46
1.9.1.3. Late Carboniferous to Permian deposits of the Karoo Supergroup 48
Chapter 2 50
Lithofacies and depositional processes 50
Chapter 3 72
Environments of deposition and stratigraphic interpretation 72
3.1. Sedimentary facies associations 73
3.1.1. Upper slope setting (Fig. 3.3D) 76
3.1.2. Shelf edge rollover setting (Fig. 3.3C) 77
3.1.3. Shelf setting (Fig. 3.3B) 78
3.1.4. Coastal plain setting (Fig. 3.3A) 80
3.2. Margin development 82
3.3. Shelf-slope-basin configuration 86
3.4. Sequence stratigraphy 87
Chapter 4 91
Contrast in the process response of stacked clinothems to the shelf-slope rollover 91
4.1. Abstract 92
4.2. Introduction 93
4.3. Geologic setting 95
4.4. Terminology 96
4.5. Lower Waterford Formation stratigraphy 96
4.5.1. Facies and facies associations 97
4.6. Stratigraphic correlation and interpretation 101
4.7. Dip-parallel depositional architecture of WfC 3 and WfC 4 103
4.7.1. Downdip character of WfC 3 103
4.7.1.1. Ouplaas section 103
4.7.1.2. N1 section 104
4.7.1.3. Blockhouse section 106
4.7.1.4. Hartbeesfontein section 111
4.7.2. Downdip character of WfC 4 111
4.7.2.1. Ouplaas section 111
4.7.2.2. N1 section 111
4.7.2.3. Blockhouse section 112

4.7.2.4. Hartbeesfontein section 113
4.8. Position of the shelf edge rollover 116
4.9. Variability between clinothems WfC 3 and WfC 4 117
4.10. Discussion 117
4.10.1. Controls on clinothem architecture 118
4.10.2. Subaerial exposure of the shelf edge rollover? 119
4.10.3. Limitations of identifying the shelf edge rollover from a 1D profile 123
4.11. Conclusions 124
Chapter 5 125
Lateral variability in shelf edge process regime and shelf edge trajectory during differential subsidence 125
5.1. Abstract 126
5.2. Introduction 127
5.3. Geological setting 128
5.4. Study area, data and methodology 129
5.5. Stratigraphic framework 130
5.6.1. Summary 136
5.7. Trajectory analysis 138
5.8. Temporal and spatial variability of WfC 3, 4 and 5 142
5.9. Discussion 146
5.9.1. Establishing the deltaic system at the shelf edge rollover 146
5.9.2. Timing of sediment bypass 147
5.9.3. Controls on the lateral variability of the lower Waterford margin 148
5.9.4. Prediction of sediment bypass 150
5.10. Conclusions 152
Chapter 6 154
Controls on the Waterford basin margin architecture 154
6.1. Lower Waterford Formation key aspects 155
6.1.1. Thick shelf succession without evidence for sub-aerial exposure 155
6.1.2. Widespread soft-sediment deformation on the shelf 156
6.2. Interplay between sediment supply, subsidence, and eustasy in the Waterford Formation 158
Chapter 7 160

Conclusions **160**

7.1. Response to initial questions posed in this thesis 161

7.2. Future work 167

7.2.1. When and by what means do basin margins prograde? 167

7.2.2. In basin-fill successions, are shallow-marine systems representative of the sediment delivery regime that supplied the underlying basin-floor and slope? 168

7.2.3. Regional variability of the Waterford Formation 168

References **171**

Appendix A: Palaeo-flow measurements **191**

Appendix B: Log Localities **195**

Appendix C: Correlation panels **197**

List of figures

Figure 1.1: Sediment transport profile. Highlighted is the critical shelf to slope transitional zone, the focus of this work. 14

Figure 1.2 A: Shelf edge delta examples: Miocene, northwest shelf of Australia. Outcrop example from Eocene Central Basin, Spitsbergen. Channel-levee system and shelf edge delta. VSA Author: Zoltan Sylvester Organization, 2010, unpublished data. 17

Figure 1.3: Illustratration of the lateral variability across a basin margin.. 18

Figure 1.4: Classification of shelf deltas in terms of relative sea-level change (Porębski & Steel, 2003). 27

Figure 1.5: (A) Profile outlining the terminology used in this study to describe the basin margin architecture and settings.. 28

Figure 1.6: Seismic section from the New Jersey margin exhibiting a clear increase in gradient associated with the transition from shelf to slope (adapted from Mountain & Proust, 2010). 30

Figure 1.7: Geometry and dimensions of Wisconsinan shelf-margin deltas in the northwest Gulf of Mexico (A and B), the ancestral Mississippi (C) and Rio Grande (D) rivers (from Porębski & Steel, 2003) (modified after Suter & Berryhill, 1985). 31

Figure 1.8: Typical progradational wave and storm-dominated parasequence from the Blackhawk Member, Utah showing a coarsening- and thickening-upward succession. 33

Figure 1.9: Photographs, representative vertical section, and interpretations of middle-slope facies association (Plink-Bjorklund *et al.*, 2001). (B) Alternations of deformed and undeformed beds occurring in the distal mouth-bar succession just basinward of a shelf edge. Slumped bed in centre is 25-cm-thick; Storvola, Spitsbergen (Porębski & Steel, 2003). 35

Figure 1.10: Schematic diagram demonstrating the effects of relative sea-level fall;. 36

Figure 1.11: Stratal pattern in a type-1 sequence deposited in a basin with a shelf break (redrawen from Van Wagoner *et al.*, 1990). Diagram highlights key surfaces and sequences. 37

Figure 1.12: Parasequence stacking patterns in parasequence sets; depositional dip cross-section and well-log expression (from Van Wagoner *et al.*, 1990). 40

Figure 1.13: Typical lower Waterford Formation logged section, exhibiting coarsening and thickening upward parasequences bounded by physically correlated fine-grained units interpreted to contain flooding surfaces (white lines). 43
Figure 1.14: Early Permian geodynamics of Gondwana (from Faure & Cole, 1999). 44
Figure 1.15: Lithostratigraphy of the Western Cape area. Modified (modified from Wickens, 1994). 45
Figure 1.16: Evolution of Cape and Karoo Basins. (A-D) Saladian orogeny and Cape Basin. (EF). Regional uplift and pre-Foreland Karoo Basin. (G-H) Cape Fold Belt orogeny and Foreland Karoo Basin (from Tankard et al., 2009). 47
Figure 2.1: This schematic diagram shows the spatial relationship of key facies from a fluvial dominated position (top right) to a storm and wave influenced setting (bottom left) and the facies transitions observed basinward of these two settings. (MFWWB=mean fair weather wave base, SWWB= storm wave base). (modified from Mountain & Proust, 2010).....51
Figure 3.1: Comparison of seismically imaged basin margin profile from the New Jersey Margin (adapted from Mountain & Proust, 2010) and the outcrop based profile of the Waterford margin constructed as part of this study. Both images are at approximately similar horizontal and vertical scales. 73
Figure 3.2: Schematic diagram depicting a basin margin scale clinothem divided into coastal plain, shelf, rollover, slope and basin floor segments. The diagram also shows typical parasequences for the four key depositional settings relevant to this study (coastal plain, shelf, rollover and slope).....74
Figure 3.3: Graphical representations of typical parasequences in four key depositional settings: (A) Coastal plain (B) Shelf (C) Rollover (D) Upper slope. 76
Figure 3.4: Facies associations of upper slope parasequences.....77
Figure 3.5: Facies associations of shelf edge parasequences. 78
Figure 3.6: Facies associations of shelf parasequence.....79
Figure 3.7: Facies associarions of coastal plain parasequences.....81
Figure 3.8: Overview of the Ladismith road section showing the 9 sand-prone units. White lines represent the regionally extensive and correlatable mudstone units.....82
Figure 3.9: Zoutkloof correlation panel showing the eight lower Waterford parasequences.....83

Figure 3.10: Diagram illustrate how minimum clinoform height is calculated. 87

Figure 3.11: Schematic sequence stratigraphy of the Waterford Formation. All major surfaces, sequences and stacking patterns have been mapped regionally. 89

Figure 4.1: (A, B) Locality maps of southern Africa and the Western Cape Province,.....94

Figure 4.2: (A) Lithostratigraphy of the Western Cape area (redrawn after Wickens, 1994).....95

Figure 4.3: (A) Profile outlining the terminology used in this study to describe the basin margin architecture and settings. (B) Schematic to explain the relationship between a shelf delta clinoform and the preexisting shelf edge to produce a basin margin–scale clinoform. 96

Figure 4.4: Generalized summary log of a typical coarsening- and thickening-upward parasequence from the lower Waterford Formation showing the five main facies associations observed. 99

Figure 4.5: Baviaans north correlation panel showing the seven lower Waterford parasequences (WfC). B. 102

Figure 4.6: Multiple low-angle (0.7°) delta-scale clinoforms dipping basinward (eastward) in WfC (Waterford clinothem) 3. 105

Figure 4.7: (A, B) Rotation of bedding within the growth fault fills of Waterford clinothem (WfC) 3 showing preferential rotation to the west. (C) Thin beds onlapping the margin of a shallow gully feature that cuts into the top of WfC 4. (D) The stepped margin of a shallow gully cutting into the top of WfC 4. 108

Figure 4.8: (A) Interpreted aerial photograph of Waterford clinothem (WfC) 3 at the Blockhouse section showing large-scale extensional deformation in the form of sand-fi lled rotated growth faults.....110

Figure 4.9: Interpreted aerial image of Waterford clinothem (WfC) 4 at the Blockhouse section showing broad shallow gullies cutting down into the top surface. Gullies have been later filled by WfC 5 material. 110

Figure 4.10: (A) Waterford clinothem (WfC) 4 thickening basin-ward beyond the shelf edge rollover comprising undeformed turbidite sandstones and silt-stones. (B) Interbedded sandstone and siltstone making up the basinward-thickening turbidite package of WfC 4. 114

Figure 4.11: (A) Schematic correlation showing the upper slope channel from the Hartbeesfontein section. Log sections are hung from the maximum

flooding surface above Waterford clinothem (WfC) 5. (B) Hartbeesfontein channel geometry corrected for vertical exaggeration. 115
Figure 4.12: (A) Oblique view of the upper slope channel cutting down 60 m into the slope mud-stone succession at the Hartbeesfontein section. (B) Erosive base of channel truncating underling heterolithic slope turbidites. Erosive surface is mantled with channel lag conglomerate (F.11). (C) Amalgamated, medium-grained turbidite channel fill sandstone (F.12). 116
Figure 4.13: Schematic diagram summarizing the different responses of Waterford clinothem (WfC) 3 and WfC 4 to increasing gradient at the shelf edge rollover. Individual clinothems are vertically separated for clarity. See text for details. 119
Figure 4.14: Evolution of Waterford clinothem (WfC) 3 and WfC 4 through time on encountering the shelf edge rollover.. 122
Figure 5.1: (A) Lithostratigraphy of the Western Cape area, redrawn after Wickens (1994). (B) Schematic stratigraphic log of the upper Ecca Group in the Laingsburg depocentre. 129
Figure 5.2: (A) (B) & (C) Locality maps 130
Figure 5.3: Baviaans South, Baviaans North and Zoutkloof correlations panels showing eight lower Waterford parasequences. 132
Figure 5.4: Representative photographs of the facies associations typical of the coarsening and thickening upward parasequences of the lower Waterford Formation. 136
Figure 5.5: Isopach thickness maps for individual parasequences 137
Figure 5.6: Basin margin trajectory profiles for the northern (Zoutkloof), central (Baviaans North) and southern (Baviaans South) dip profiles.. 139
Figure 5.7: Palaeogeographic reconstructions of (A) WfC 3, (B) WfC 4 and (C) WfC 5 each at their most progradational extent. Pie charts represent facies breakdowns for key log localities. 144
Figure 5.8: Facies fence diagrams for (A) WfC 3, (B) WfC 4 and (C) WfC 5. 145
Figure 5.9: Lateral variability observed along the lower Waterford margin in the Laingsburg area. 149
Figure 5.10: Trajectory and sequence stratigraphic interpretations of the lower Waterford Formation.. 152

Figure 6.1: Sediment supply vs. Accommodation and the resulting margin geometries. Note the position of the lower Waterford Formation in the Laingsburg area as a high supply, high accommodation system. 159
Figure 7.1: Cartoon to illustrate variability across a basin margin.. 161
Figure 7.2: Keiskie Pass, South of Calvinia. Photo shows a silt dominated lower slope consisting of heterolithic facies with an abrupt change to thick amalgamated sandstone parasequences. The parasequences only include one thin (~1-m-thick) *in-situ* deformed package. 170
Figure 7.3: Mudstone intervals cut by gully feature replace deformed facies in a typical parasequence facies succession observed in the Laingsburg area, therefore it may be speculated that such gullied delta front settings are a forerunner to extensive deformation.....170

List of tables

Table 2.1: Table showing the translation of axial delta and shoreface facies and their facies associations 52
Table 3.1: Linkage of the 19 delta and shoreface associated facies described in chapter 2 to delta and shoreface facies associations.....75
Table 4.1: Sedimentary facies defined in this study, their key characteristics, and interpreted depositional environments.....100

CHAPTER 1.
INTRODUCTION

This chapter reviews the current state of knowledge on shelf edge delta systems and frames the objectives of the thesis. It introduces the methodology used and summarizes the regional and local stratigraphic context of the field areas. It also presents a short literature review on shelf edge delta systems, including nomenclature and scale, as well as a review of shallow marine sequence stratigraphy.

1.1. Introduction to the SLOPE project

This PhD thesis forms part of Phase 3 of the SLOPE project, a Joint Industry Project undertaken by the *Stratigraphy Group* of the Department of Earth, Ocean and Ecological Sciences, University of Liverpool, in collaboration with the Technical University of Delft (Netherlands). The aims of SLOPE Phase 3 were to study the well-exposed Permian shelf to deepwater depositional systems of the Karoo Basin, South Africa, building on the knowledge gained from phases 1 and 2 of the SLOPE project. The project consisted of three main strands of investigation:

1) Documenting and quantifying the positions, architecture and connectivity of distributive deepwater systems down dip of the well understood slope channel deposits studied in Phase 2.

2) Linking the downhole core and electrofacies from a series of research boreholes to the outcrop-derived slope channel hierarchy established in Phase 2.

3) Characterizing for the first time the slope to shelf transition and understanding the mechanisms of delivery of sand to the slope.

The SLOPE project team involved two full-time Post-Doctoral researchers (Dr. Rufus Brunt and Dr. Willem Van der Merwe) working on Strand 1; two PhD students, Emma Morris (Strand 2) and George Jones (Strand 3, this work), and several graduate research assistants who assisted with fieldwork. The project ran from June 2009 to June 2012 and involved six field seasons with a total of 250 field days. A consortium of 17 petroleum companies (ExxonMobil, BP, Statoil, Maersk, Woodside, Petrobras, Total, Shell, Chevron, GDF Suez, VNG Norge, ConocoPhillips, Tullow, BHPBilliton, Anadarko, Murphy and Schlumberger) sponsored the project financially. While all the individual works were integrated into the SLOPE project deliverables, each thesis had its own clearly identified objectives and work programme conducted by the individual researcher.

1.2. Background rationale

The depositional profile (Fig. 1.1) is an integral concept in sedimentology and sequence stratigraphy. It helps us to understand how sediment is transported from the hinterland to its final resting place in sedimentary basins (Allen, 2008). Sedimentary systems begin with mountainous upland areas, which supply sediment by physical, chemical and biological weathering and erosion by rivers and streams, to low-relief subaerial areas that are dominated by a combination of transport (bypass) and deposition (storage) (Romans & Graham, 2013). These subaerial, transport dominated zones transition seaward to the subaqueous shelf, slope and basin floor settings, which are characterized by long term sediment deposition, which leads to lasting accumulation, burial and lithification (Romans *et al.*, 2009; Sømme *et al.*, 2009). The depositional profile is characterized by a number of key transitional zones. This study focuses on the transition from the subaqueous shelf to the submarine slope (Fig. 1.1), which represents a key transitional zone of increased gradient and associated change in sedimentary processes (Sømme *et al.*, 2010). Understanding changes in the process regime through time is critical for predicting the partitioning of coarse-grained sediment between the shelf, the slope, and the basin floor (Southard & Stanley, 1976; Dixon *et al.*, 2012a).

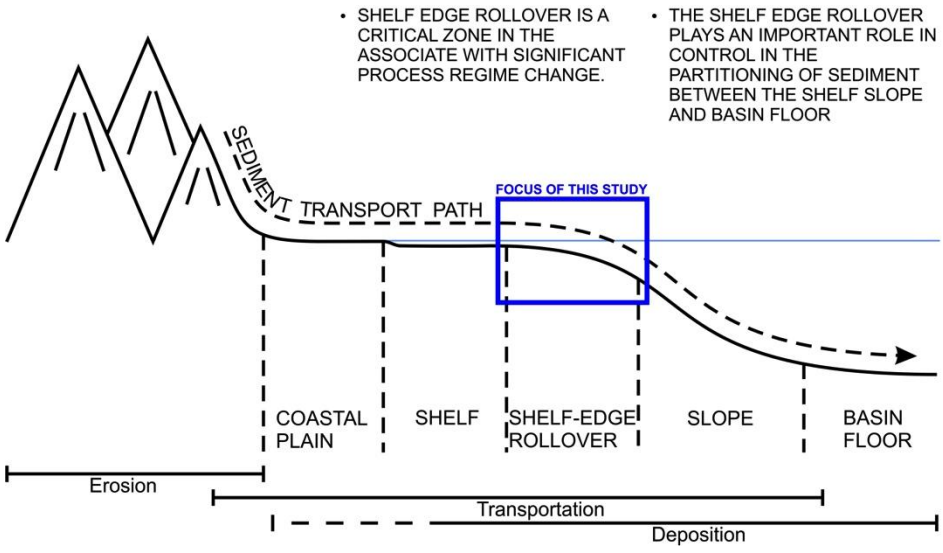

Figure 1.1 Sediment transport profile from drainage basin, which supplies sediment through weathering and erosion, to terrestrial lowlands that are dominated by sediment bypass and finally the subaqueous shelf to basin floor settings where deposition becomes increasingly dominant. Highlighted is the critical shelf to slope transitional zone, the focus of this work.

Many published studies on long-term sedimentary processes and stratigraphic architecture of basin margins have focussed on 2D (two-dimensional) profiles, typically oriented parallel to the main sediment transport route (Pyles & Slatt, 2007; Covault *et al.*, 2009; Helland-

Hansen, 2010; Mountain & Proust, 2010), regardless of the fact that a number of studies recognize basin margins as inherently three-dimensional (Allen & Posamentier, 1994; Martinsen & Helland-Hansen, 1995; Driscoll & Karner, 1999; Johannessen & Steel, 2005; Moscardelli *et al.*, 2012). Over recent years 3D reflection seismic datasets have been employed to constrain the lateral as well as temporal variability in the architecture of basin margins (e.g. Suter & Berryhill, 1985; Matteucci & Hine, 1987; Poag *et al.*, 1990; Tesson *et al.*, 1990; Sydow & Roberts, 1994; Morton & Suter, 1996; Kolla *et al.*, 2000; Hiscott, 2001; Pinous *et al.*, 2001; Krassay & Totterdell, 2003; Houseknecht *et al.*, 2009; Ryan *et al.*, 2009; Moscardelli *et al.*, 2012; Sanchez *et al.*, 2012b, a). A number of these studies have highlighted the weakness of considering basin margin development only in 2D, which has been implicitly understood if not widely tested or documented. Furthermore, seismic-reflection studies suffer from a lack of sub-seismic detail, such as core, with which to calibrate seismic facies. This lack of subseismic detail is improving with seismic datasets being tied to core e.g. Pleistocene Lagniappe Delta (Kindinger, 1988), Mississippi Delta (Sydow & Roberts, 1994; Winn *et al.*, 1995; Kolla *et al.*, 2000), New Jersey margin (Mountain & Proust, 2010).

Bathymetric datasets that image modern day and Holocene basin margins (Fig. 1.2C) confirm the lateral variability in subsidence patterns (hence relative sea-level change), margin physiography, distribution of sediment supply points, discharge rates and process regime (e.g. Olariu & Steel, 2009). However, these datasets are limited by their short time window and can only be partially employed to support understanding of long-term stratigraphic development of basin margins.

Many outcrop-based studies of exhumed basin margin successions also suffer the limitations of 3D control. Examples include the Battfjellet Formation, Spitsbergen (Helland-Hansen, 2010) (Fig. 1.2B), Magallanes Basin, Chile (Covault *et al.*, 2009) and the Lewis Shale, Wyoming (Pyles & Slatt, 2007). Only a few studies document any lateral variability (usually <10 km across strike) whilst still recording extensive dip profiles, such that the shelf edge rollover position can be constrained (Wild *et al.*, 2009; Charvin *et al.*, 2010; Dixon *et al.*, 2012a). Yet, outcrop based studies do provide greater vertical resolution than seismic data (Covault *et al.*, 2009), thus increased understanding of sub-seismic architecture and process regime, as well as resolving temporal changes in processes operating in margin settings that cannot be obtained from modern or seismic datasets.

Bridging the gap between the broad architectural elements observed so well in 3D seismic datasets, and the outcrop based process observations that improve understanding of transitional zones such as the shelf edge rollover, remains a significant challenge. In order to advance our knowledge of controls on sediment dispersal patterns and long-term variability in basin margin development, datasets with 3D constraints and sub-seismic resolution are crucial.

A) SEISMIC EXAMPLE FROM MIOCENE SHELF EDGE DELTAS, NORTHWEST SHELF OF AUSTRALIA

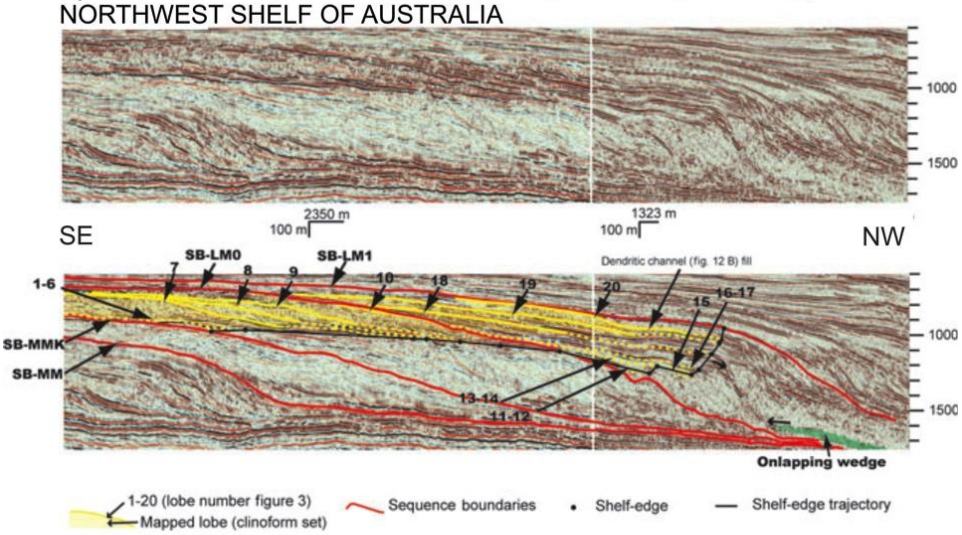

B) OUTCROP EXAMPLE FROM EOCENE CENTRAL BASIN, SPITSBERGEN

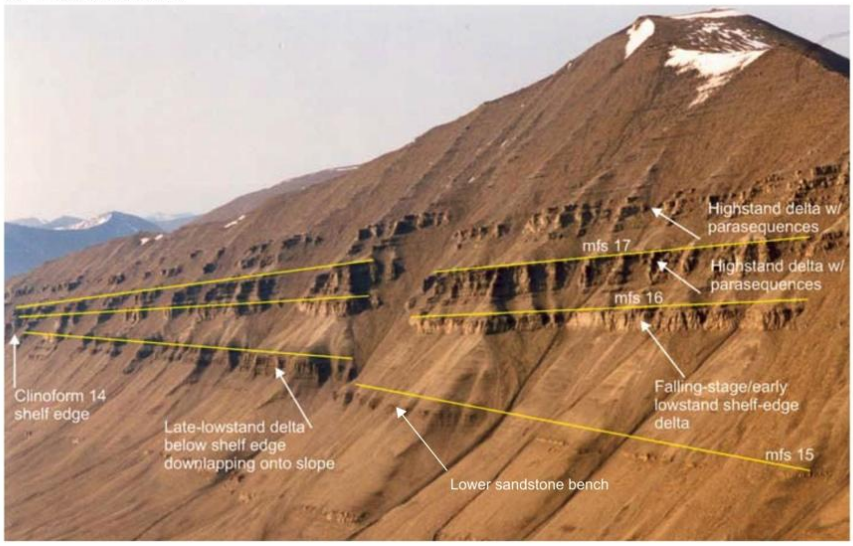

C) MODERN BATHYMETRIC EXAMPLE

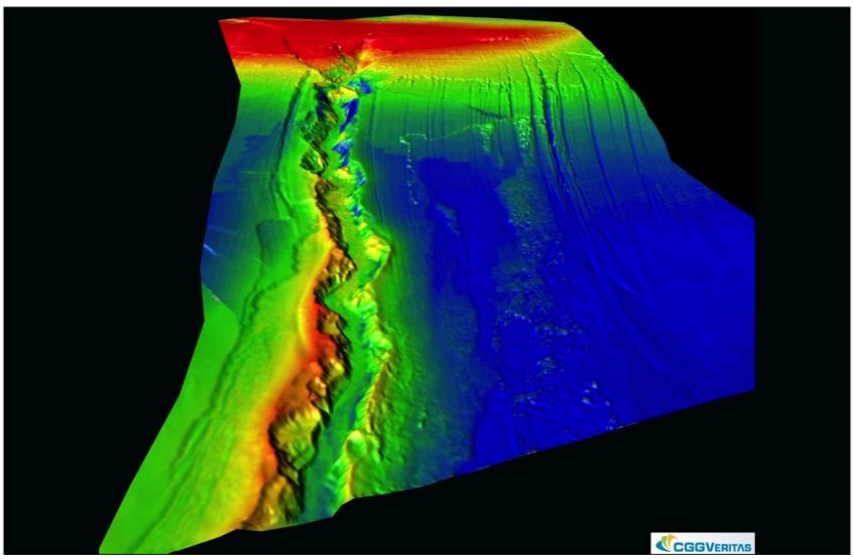

Figure 1.2 A: Miocene shelf edge deltas, northwest shelf of Australia. Northern dip-oriented (southeast-northwest) seismic profile showing delta lobes (yellow shading) and time lines corresponding to lobes located outside the plane of the profile (dashed yellow lines), shelf edge positions relative to times of lobe deposition (black dots) and shelf edge trajectory (black line) (from Sanchez *et al.*, 2012b). (B) Outcrop example from Eocene Central Basin, Spitsbergen. Example of a shelf edge delta (labelled Clinoform 14) draping halfway down a shelf-margin slope on Storvola. The lower sandstone bench represents basin-floor fans of an older clinoform that peeled off the shelf at the left hand end of the mountain. The sandstone bench above has its shelf edge a few kilometres to the SE. Note the limited dip extent and the 2D nature of the outcrop face (Porębski & Steel, 2006). (C) Channel-levee system and shelf edge delta. This perspective view shows the top surface a channel-levee system, draped with thickness information (red = thick, blue = thin). Note the slope gullies sourced by the youngest delta lobe (upper left corner of the image). VSA Author: Zoltan Sylvester Organization, 2010, unpublished data.

Understanding the mechanisms involved in sediment transfer from the shelf to the slope and basin floor is a complicated multi-faceted issue (Porębski & Steel, 2003; Johannessen & Steel, 2005; Dixon *et al.*, 2012a). Shelf edge trajectory analysis (Helland-Hansen & Gjelberg, 1994; Helland-Hansen & Hampson, 2009) and traditional sequence stratigraphic models (Vail *et al.*, 1977b; Posamentier & Vail, 1988b; Van Wagoner *et al.*, 1988; Galloway, 1989; Martinsen & Helland-Hansen, 1995; Posamentier & Allen, 1999; Steel & Olsen, 2002; Johannessen & Steel, 2005; Catuneanu *et al.*, 2009) remain the most cited methods for the prediction of down dip sandstone deposits. However, both these models focus heavily on relative sea-level fluctuations as the mechanism controlling delivery beyond the shelf edge rollover. The basic premise states that reduced accommodation on the shelf due to relative sea-level fall drives the fluvio-deltaic system towards the shelf edge (Posamentier & Vail, 1988b). Sea-level fall below the shelf edge results in incision and bypass of sediment to deeper parts of the basin (e.g. Posamentier & Vail, 1988b; Van Wagoner *et al.*, 1990; Mutti & Davoli, 1992; Milton & Dyce, 1995; Marjanac, 1996; Normark *et al.*, 1998; Johannessen & Steel, 2005). However, when these models are applied to 2D datasets, variability in across strike physiography, sediment supply and process regime are not always fully considered (Driscoll & Karner, 1999), and profiles are rarely back-stripped to account for differential subsidence that might have modified the original trajectory.

In order to better understand these depositional systems as a whole, but particularly to constrain when and how sediment is delivered across the shelf edge, the routing pathways and the presence and distribution of down dip sandstone deposits, it is necessary to integrate high-resolution observations from outcrop with the 3D understanding traditionally afforded by reflection seismic datasets. This study integrates detailed outcrop observations and interpretations of three 40-km-long sub-parallel dip profiles, which provide a 3D outcrop dataset that is comparable in scale to seismic surveys. This dataset offers a unique opportunity to document the spatial and temporal variability of the shelf to

slope transition across successive parasequences, and to consider the partitioning of sediment between the shelf, slope and basin floor. The ability to place detailed process based observations within the 3D-constrained depositional architecture of an exposed basin margin provides a unique opportunity to address the key controls on sediment bypass to deep water settings (Fig. 1.3), and leads to better prediction of slope and basin floor sand deposits, a critical factor affecting hydrocarbon exploration.

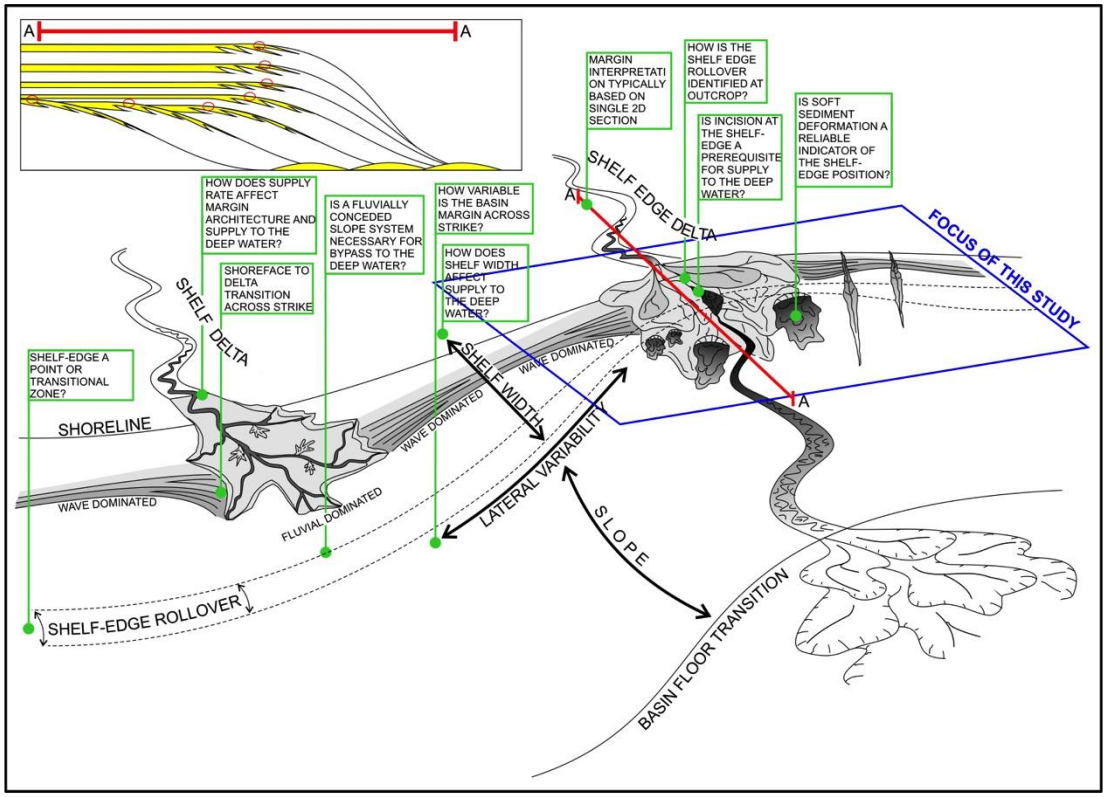

Figure 1.3: Illustration showing lateral variability across a basin margin. The area of focus in this study, the shelf-to-slope transition zone, is highlighted by the blue box. Flags represent key research questions and critical points to be addressed in this thesis. The red line represents a typical 2D line of section upon which interpretations of controls on basin margin architecture and the prediction of deep water sand deposits are commonly based.

1.3. Aims of the PhD project

1.3.1. Key objectives of this thesis

The main objectives of this thesis are: (1) to document the architectural and stratigraphic evolution of the Permian lower Waterford Formation; (2) to understand the temporal (stratigraphic) and spatial (palaeogeographic) variability in the transition from the continental shelf to upper slope; (3) to constrain the sedimentary process record during basin margin progradation and (4) to determine the balance of external and internal

controls on basin margin development. These objectives are framed in four key research questions that will be returned to in the conclusions.

A. What factors control the spatial and temporal variability of sand delivery to the slope and basin floor, and is fluvial incision of the shelf rollover necessary for the delivery of sand to deep marine settings?

Rationale: The progradation of a shelf-delta or shoreface system to a position at the shelf edge rollover is a favourable scenario for the delivery of significant quantities of coarse-grained sediment to the submarine slope and basin floor (Edwards, 1981; Suter & Berryhill, 1985; Porębski & Steel, 2003; Carvajal & Steel, 2009). Conventionally, relative sea-level fall has been regarded as a primary control on driving the fluvio-deltaic system to the shelf edge (Posamentier & Vail, 1988a; Van Wagoner *et al.*, 1990; Mutti & Davoli, 1992; Milton & Dyce, 1995; Marjanac, 1996; Normark *et al.*, 1998; Steel & Olsen, 2002; Johannessen & Steel, 2005; Porębski & Steel, 2006; Ainsworth *et al.*, 2008; Steel *et al.*, 2008).

Sea-level fall below the shelf edge promotes incision of the shelf by fluvial feeder systems (e.g. Posamentier & Vail, 1988b; Van Wagoner *et al.*, 1990; Mutti & Davoli, 1992; Milton & Dyce, 1995; Marjanac, 1996; Normark *et al.*, 1998; Johannessen & Steel, 2005). Identification of such incisional features and their corresponding sub-aerially exposed interfluve surfaces, plays a critical role in sequence stratigraphic analysis and the prediction of down dip deepwater sandstone deposits (Fig. 1.3). Examples of large scale shelf edge fluvial incision at outcrop have been well documented from the Eocene succession of Spitsbergen (Plink-Bjorklund *et al.*, 2001; Mellere *et al.*, 2002), which have been interpreted to be driven by exposure of the shelf edge due to relative sea-level fall. Episodes of relative sea-level fall at a basin margin are characterized by downstepping clinothem geometries, particularly in ramp settings (Fig. 1.3 insert) (Posamentier *et al.*, 1992). In shelf-slope settings relative sea-level fall below the shelf edge is more typically characterized by incision of the shelf and bypass of sediment to the slope and basin floor, and the presence of interfluves adjacent to sites of incision. Understanding the variability in scale of shelf edge incision across a margin, or even the necessity for sub-aerial exposure of the shelf edge (e.g. Talling, 1998), is an important step in predicting the location and scale of potential reservoir sandstones.

These accommodation-driven scenarios (Steel *et al.*, 2008) have been complemented by models that emphasize the role of sediment supply rates in establishing shelf edge deltas.

Burgess & Hovius (1998) used data from 24 modern river systems to demonstrate the importance of fluvial sediment supply, shelf width, shelf volume and shelf transport rates and the effect these parameters have on delta transit times to the shelf edge. In addition, the effect of fluvial processes operating at the shelf edge has been highlighted as a key mechanism for delivery of sediment beyond the shelf edge, due to transit times (<100 thousand years (Burgess & Hovius, 1998)) with which the fluvial system can cross the shelf and focus delivery of sediment to the shelf edge (Kolla & Perlmutter, 1993; Flood & Piper, 1997; Posamentier & Allen, 1999; Plink-Björklund & Steel, 2004; Johannessen & Steel, 2005; Petter & Steel, 2006). More recently Dixon *et al.* (2012b) considered the importance of processes operating at the shelf edge on delivery of sediment to the slope and basin floor and showed that wave and storm dominated systems redistribute sediment along the margin rather than supplying it beyond the shelf edge.

B. How is the shelf edge rollover identified at outcrop?

The shelf edge rollover represents a critical transitional zone that is significant to the partitioning of sediment between the shelf slope and basin floor (Sømme *et al.*, 2010). Seismic volumes can be easily manipulated to identify subtle stratal relationships and geometric changes (e.g. Stewart, 2011), and the physical transition from shelf to slope is easily identifiable in horizontally shortened seismic images (Fig. 1.2A) as a break-in-slope at the clinoform rollover (Suter & Berryhill, 1985; Sydow & Roberts, 1994; Kolla *et al.*, 2000; Hiscott, 2001; Pinous *et al.*, 2001; Krassay & Totterdell, 2003; Houseknecht *et al.*, 2009; Ryan *et al.*, 2009; Mountain & Proust, 2010). Identifying the shelf edge rollover at outcrop, however, is more challenging because without the vertical exaggeration shown in seismic displays, the rollover becomes a subtle zone of transition several kilometres long (in a dip sense), rather than a point on a basin profile (Fig. 1.2A). Examples where the physically linked slope to shelf transition can be documented are rare, due to the usually limiting extent of outcrop (e.g. Tanqua depocentre, South Africa (Wild *et al.*, 2009; Dixon *et al.*, 2012a), Magallanes basin, Chile (Covault *et al.*, 2009; Romans *et al.*, 2009; Hubbard *et al.*, 2010), Central basin, Svalbard (Mellere *et al.*, 2002; Deibert *et al.*, 2003; Johannessen & Steel, 2005; Carvajal & Steel, 2006; Uroza & Steel, 2008) Lewis Shale, Wyoming (Pyles & Slatt, 2007). Criteria for identifying shelf edge deltas and associated rollover at outcrop have been established from short, steep and commonly relatively coarse grained basin margins (Porębski & Steel, 2003), these criteria include:

- the very large scale of the clinoforms, that can be an order of magnitude greater in amplitude than that of mid- and inner-shelf deltas;
- the resultant thick, strike-elongated isopach image of shelf-margin deltas is commonly augmented by growth faulting;
- sigmoidal dip cross-sectional shape, with the thickest part located near the offlap break of a pre-existing shelf margin;
- the landward pinch-out by onlap onto shelf shales and the basinward pinch-out by downlap within hemipelagic shales;
- evidence of foreshortened stratigraphy;
- the characteristic turbidite-prone nature of the delta-front/prodelta segment;
- the abundance and large scale of slope-controlled soft-sediment deformation;
- the absence of a paralic ‘‘tail’’ along the delta’s trailing edge.

Therefore, it is important to establish criteria for the identification of the shelf edge rollover for fine grained (fine sand or finer) and low gradient systems. Such criteria may also aid identification of the rollover in other settings with limited dip or lateral exposure, and from 1D well datasets.

C. What is the relationship between soft-sediment deformation processes and proximity to the shelf edge?

There is a wide range of pre-requisite conditions and processes that lead to the deformation of unlithified sediments. Published datasets have suggested a strong link between soft sediment deformation processes and position with respect to a shelf edge setting (Fig. 1.3), where by deformation increases with proximity to the increased gradient at the shelf edge. Most notably, sediment transport across subaqueous breaks-in-slope such as the shelf edge rollover are interpreted to be dominated by gravity driven processes such as mass transport events (Collinson *et al.*, 1991; Stow, 1994; Sydow & Roberts, 1994; Galloway, 1998; Lee *et al.*, 2009; Pratson *et al.*, 2009; Oliveira *et al.*, 2011). Over steepening and repeated collapse of the shelf edge break in slope, is thought to trigger mass transport complexes and initiation of turbidity currents, thus contributing to an effective gravity-driven sediment delivery system (Wild *et al.*, 2009).

Two of the best documented examples of soft sediment deformation in a shelf edge position are the Mississippi and Niger deltas. The continental margin off the Niger Delta is undergoing margin-scale deformation by gravity tectonics caused by rapid seaward

sediment progradation above a deep basal detachment (Meisling *et al.*, 2000), which suggests that large portions of the thick sediment prism are slowly moving downslope by gravity gliding or sliding, in a manner analogous to giant mass movements or mega-landslides (Damuth, 1994). Deformation styles are categorized by Damuth (1994) as: (1) an upper extensional zone of listric growth faults beneath the outer shelf; (2) a translational zone of diapirs and shale ridges beneath the upper slope; and (3) a lower compressional zone of imbricated thrust structures (toe thrusts) beneath the lower slope and rise. Seismic data tied to core from the Mississippi delta (Mayall *et al.*, 1992) show a very different scale and style of deformation to that of the Niger Delta. The dataset described from the two vertically stacked shelf edge deltas in Canyon block 109 which are dominated by soft sediment deformation shows that the two deltas exhibit similar vertical profiles and facies associations. A typical profile begins with a mud-dominated delta slope, followed by slump-dominated upper delta slope deposits, which are overlain by mouth-bar deposits; deformation is attributed to the increased gradients associated with shelf edge deltas.

The wide range of deformation processes produced in the shelf to slope transitional setting can obscure primary depositional processes and result in complicated stratigraphic successions. Therefore, understanding the stratigraphic distribution of soft sediment deformation processes and products may enable better understanding of depositional setting relative to the shelf edge rollover, which is significant to the interpretation of outcrop examples with limited lateral exposure.

D. What role does differential subsidence play on the stratigraphic development of Karoo Basin margin during deposition of the lower Waterford Formation?

Examples of shelf margin development can be grouped broadly into sediment-supply-driven and accommodation-driven systems (Steel *et al.*, 2008). The debate surrounding the control of relative sea-level fluctuations and the effect on margin architecture encourages investigations that attempt to distinguish between eustatic and tectonic controls on depositional sequences and the delivery of sediment to deepwater settings. The effect of subsidence on depositional systems varies depending on tectonic setting, but is commonly related to *extensional* or flexural loading leading to intraplate stresses, and regional crustal loading (Romans & Graham, 2013). On a smaller scale, tectonic changes can control accommodation across a basin margin by influencing the morphology of the shelf edge and the position of sediment routing and storage, such that sediment supply rates may vary across a basin margin (Moscardelli *et al.*, 2012). Understanding the effect of interaction

between eustatic sea-level change and tectonic processes on stacking patterns is critical to the application of sequence stratigraphic and trajectory models as predictive tools. Forced regressive deltaic sequences from the Holocene, Canada (Hart & Long, 1996) have shown how glacio-eustatic rebound can outpace rates of global eustatic sea-level rise and force the progradation of deltaic sequences. Moscardelli *et al.* (2012) also show how local basin tectonic factors can produce significant lateral and vertical stratigraphic variability along the palaeo-Orinoco shelf edge, offshore Trinidad margin during the Pleistocene to Holocene. The increasing recognition that sediment bypass to deepwater settings under any condition of sea-level stand has increased the emphasis on untangling the relative impact of eustatic and tectonic sea-level change, sediment supply rates, margin physiography, volumes and dynamics of continental shelves in order to incorporate such variability into more accurate predictive models.

1.4. Thesis layout

This thesis contains 7 chapters. Chapters 4 and 5 are scientific papers that have been submitted to international journals for publication. At the time of submission of this thesis, chapter 4 has been accepted by *Geosphere* in December 2012. Chapter 5 has been submitted to Basin Research (March 2013) and is in review.

Chapter 1: This chapter introduces the geological problems addressed by this thesis, outlines the content of each chapter, and poses the key questions that will be dealt with throughout the thesis. It presents a short literature review on shelf edge delta systems, including nomenclature and scale, as well as a review of shallow marine sequence stratigraphy. The final section of the introduction covers the regional and local geological setting of the field area.

Chapter 2: This chapter contains the descriptions and interpretations of the sedimentary facies encountered within the lower Waterford Formation of the Laingsburg depocentre. They represent an integral component in the interpretation of the margin development. This sedimentary facies scheme is based on lithology, grain-size and sedimentary structures, which are related to depositional process.

Chapter 3: Building on the detailed lithofacies descriptions laid out in chapter 2, the purpose of chapter 3 is to establish lithofacies associations and to provide depositional context within the dip profile of a single basin margin scale clinoform. Chapter 3 also deals with the description and interpretation of the lower Waterford Formation stratigraphy,

which constitutes 8 parasequences (Waterford Clinothems (WfC) 1-8). Following the description of individual parasequences, an evaluation of architecture, stacking patterns, facies association variability and the identification of key surfaces is carried out. A sequence stratigraphic analysis is undertaken in order to constrain the stratigraphic evolution of the margin, which provides context for the following three chapters.

Chapter 4 (manuscript in press in *Geosphere*): This chapter leads on from the broad facies association descriptions and sequence stratigraphic interpretation made in chapter 3. It focuses on the detailed facies and architectural variability within two successive basin margin scale clinothems as they encounter the shelf edge rollover and transition onto the slope. It also establishes key criteria for identifying the clinoform rollover in a low gradient, fine-grained, mixed influence system. These criteria represent a fundamental aspect of this thesis and are integral to the interpretations made in chapters 5 and 6.

Chapter 5 (manuscript under review in *Basin Research*): Integrates data from three sub-parallel 2D dip profiles to provide 3D coverage of the changes in architectural and facies distribution across the lower Waterford margin. Discussion focuses on the factors that led to greater sediment supply to the upper slope in the north of the study area without clear evidence for a fluvial driver, during a period of steeply rising margin trajectory, factors which contradict established hypotheses for sand delivery beyond the shelf edge rollover.

Chapter 6: addresses two unusual aspects of the lower Waterford Formation. Firstly, the significant thickness of shelf stratigraphy (>300 m) that does not exhibit any sign of subaerial exposure, and secondly the ubiquitous occurrence of extensive soft sediment deformation recorded landward of the shelf edge rollover. These two key features are discussed in the context of sediment supply and accommodation and how this has affected long term stratigraphic evolution of the basin margin.

Chapter 7: provides a synthesis and answers the questions posed in chapter 1. Areas of possible further future work are also presented.

Appendix A: Palaeocurent rose diagrams for WfC 1 - 8

Appendix B: is a list of the names, GPS coordinates, of all sedimentary logs measured in the Laingsburg depocentre.

Appendix C: Baviaans South, Baviaans North and Zoutkloof correlation panels.

1.5. Contribution by authors to the manuscripts

Chapter 4 ***(Contrast in the process response of stacked clinothems to the shelf-slope rollover)***

G. Jones: principal investigator and main author

D.M. Hodgson: fieldwork assistance, discussion, manuscript review

S.S. Flint: fieldwork assistance, discussion, manuscript review

DOI number: 10.1130/GES00796.1

Chapter 5 ***(Lateral variability in shelf edge process regime and trajectory of a subsiding basin margin)***

G. Jones: principal investigator and main author

D.M. Hodgson: fieldwork assistance, discussion, manuscript review

S.S. Flint: fieldwork assistance, discussion, manuscript review.

1.6. Shelf edge deltas: a brief review

1.6.1. Classification of deltas

Classification schemes for deltas have previously focussed on the morphology produced by the sum of the process regimes acting upon the deltaic system. Galloway (1975) classified deltas based upon the relative influence of fluvial, wave and tidal processes. This was later augmented by Orton (1988) and Orton & Reading (1993) to incorporate sediment calibre or grain size. Other classification schemes have focussed on delta geometries (topset/foreset relationship) (Gilbert, 1990), and delivery system type (Holmes, 1965; Chough *et al.*, 1990). However, more recent studies have moved away from steady-state models biased toward the present day highstand of sea-level. The establishment and widespread application of sequence stratigraphic analysis has shown how deltas vary in their external geometry and internal characteristics in response to falling and rising of sea-level (e.g. McMaster *et al.*, 1970; Suter & Berryhill, 1985; Postma, 1995; Kolla *et al.*, 2000; Tesson *et al.*, 2009). This has led to classification of deltas based upon position on the shelf. Four broad delta-types are recognized: *bayhead*, *inner-shelf*, *mid-shelf* and *shelf edge* (Fig. 1.4) (Edwards, 1981; Suter & Berryhill, 1985; Reading & Collinson, 1996; Porebski and Steel, 2003). These four main delta types are characterized by a number of key features that relate to the hydrodynamic processes and water depth into which the delta is prograding. **Bayhead deltas** develop during regional sea-level rise, that sees the development of estuarine settings during the infilling of flooded valleys. This results in small, dip elongate and commonly tidally dominated deltas (Dalrymple *et al.*, 1992; Nichol *et al.*, 1996). **Inner-shelf deltas** tend to be wide and thick with significant aggradationally stacked paralic facies, which is characteristic of deposition during highstand conditions (Porębski & Steel, 2003). **Mid-shelf deltas** are considered to be thin, patchily developed, exhibiting low angle clinoforms (Suter & Berryhill, 1985). **Shelf edge deltas** are considered to develop during falling or lowstand sea-level conditions, or when sediment supply is high enough to permit complete across shelf transit of the delta, which enables the delta to be positioned at or near a pre-existing shelf edge break. Shelf edge deltas are commonly thick, localized, strike-oriented wedges of strata, that bear signs of slope failure (Suter & Berryhill, 1985). The thickness of shelf edge deltas can extensive due to increase accommodation resulting from extensional growth faulting (Edwards, 1981), but this need not be the case. The clear relationship between delta type and available accommodation (relative sea-level change) enables prediction of delta location and broad facies distribution.

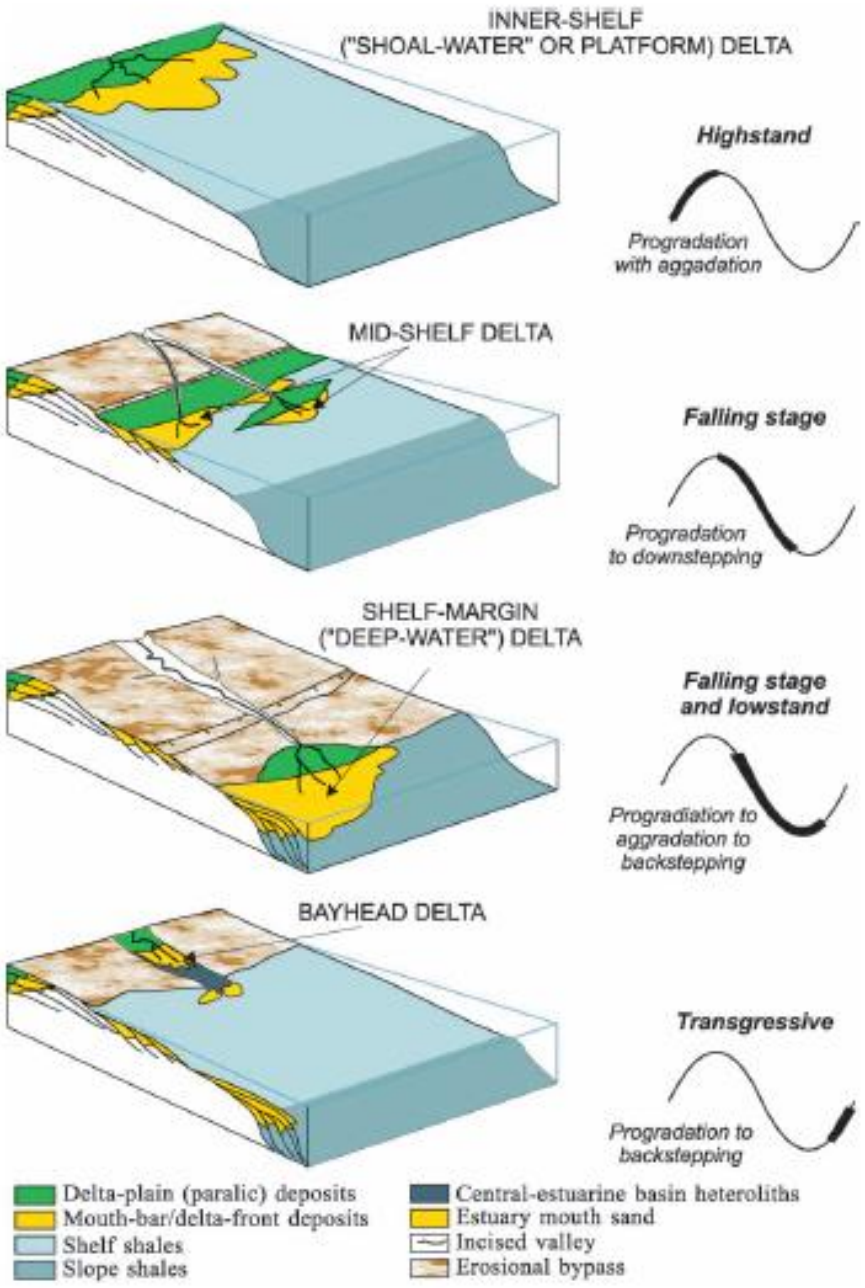

Figure 1.4: Classification of shelf deltas in terms of relative sea-level change (Porębski & Steel, 2003).

1.6.2. Clinoform scale and margin accretion. Shelf edge deltas and the accretion / development of basin margins

The term “clinoform” is commonly applied to the entire sigmoid surface shape, including the topset, foreset and bottomset (Fig. 1.5), but it was originally applied only to the sloping segment of such a surface (Rich, 1951). The term “clinothem” is used herein to describe a 3D body of rock that is bounded by clinoform surfaces (Steel & Olsen, 2002). Clinothems comprise three fundamental depositional components: topsets, foresets, and bottomsets (Fig. 1.5A). The upper clinoform break in slope between the topset and foreset (clinoform slope) surface, which forms a zone of increased gradient rather than a point, is referred to as the shelf edge rollover. The lower clinoform break is referred to as the ‘rollunder’ or base-of-clinoform slope and represents the transition from slope to basin floor**.** Clinoform geometries tend to change basinward as the delta progrades from the outer shelf to the shelf edge, so therefore it is important not to confuse shelf-margin-scale clinoforms with shelf delta-scale clinoforms. The former have heights of hundreds of meters, whereas shelf delta -scale clinoforms are generally tens of meters high (Fig. 1.5) (Helland-Hansen & Hampson, 2009). In this study we document basin-margin scale clinothems with amplitude of 100s of metres and shelf delta clinothems with heights of a few 10s of metres.

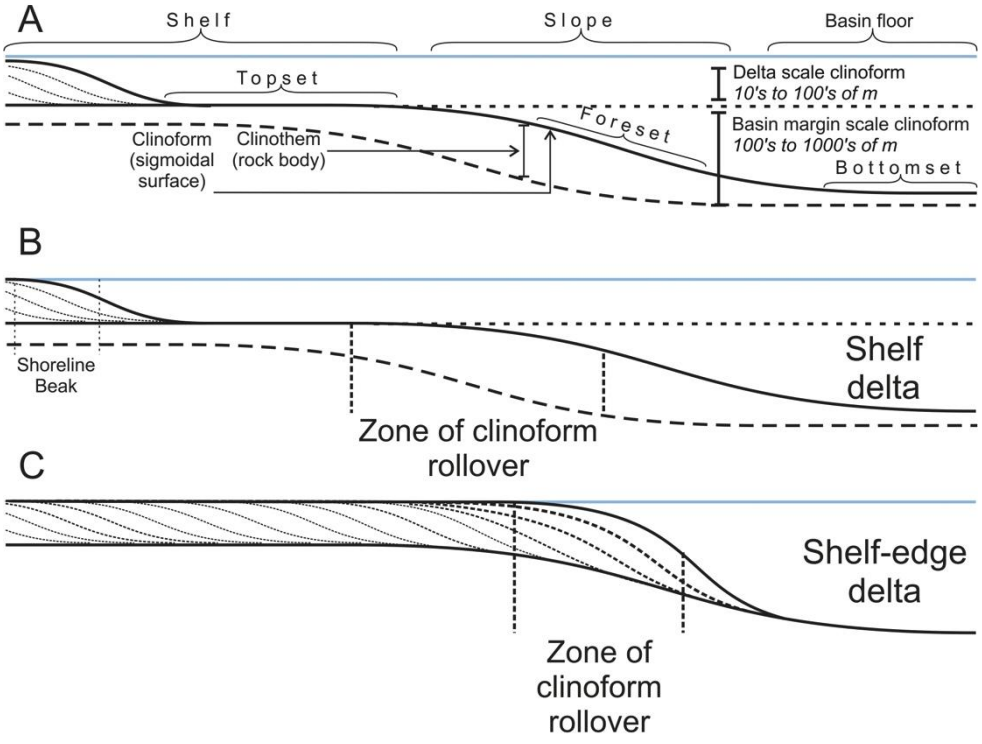

Figure 1.5: (A) Profile outlining the terminology used in this study to describe the basin margin architecture and settings. (B) & (C) Distinguishing between shelf scale clinoforms formed by delta progradation and basin margin scale clinoforms produced by basin margin accretion when the shelf delta clinoform coincides with the basin margin clinoform.

The establishment of a delta system at the shelf edge is one of the main ways sediment is passed over the shelf edge to the slope and basin floor, and is therefore the primary way in which basin margins prograde (Helland-Hansen *et al.*, 2012). On encountering the shelf edge, the front of the delta then progrades and merges onto a pre-existing slope and, as a result, steepens as the commonly muddy foresets / toesets extend and downlap on to the slope or basin floor segment (Posamentier & Allen, 1999; Kolla *et al.*, 2000).

By constraining thickness variability and facies distribution in combination with stratigraphic context it is possible to recognize clinoform geometries in the parasequences of the lower Waterford Formation. Although the complete clinoform profile of topset, foreset and bottomset cannot be recognized along the complete profile of each parasequence, it is possible to observe dip-elongate stratal packages in the lower stratigraphy that thin basinward and are overlain by packages that thicken basinward beyond their interpreted shelf edge rollover position (see chapter 4). This transition from basinward thinning to basinward thickening stratal packages is interpreted to represent the transition from clinoform toe-sets on the middle to lower slope, to shelf and upper slope top-sets within a flooding surface-bounded parasequence. The stratigraphic thickness between the shelf edge rollover and the furthest correlatable position confirms that these are basin margin scale clinoforms.

1.6.3. Shelf edge delta architecture

Shelf edge deltas share many characteristics with inner and mid shelf deltas, however their position at or near to a significant break in slope has a considerable effect on their external geometries and the processes operating. Identifying shelf edge delta systems from high-resolution seismic images is relatively straightforward due to the vertical exaggeration of such seismic sections (Fig. 1.6), which produces a notable angular relationship between the topset and foreset.

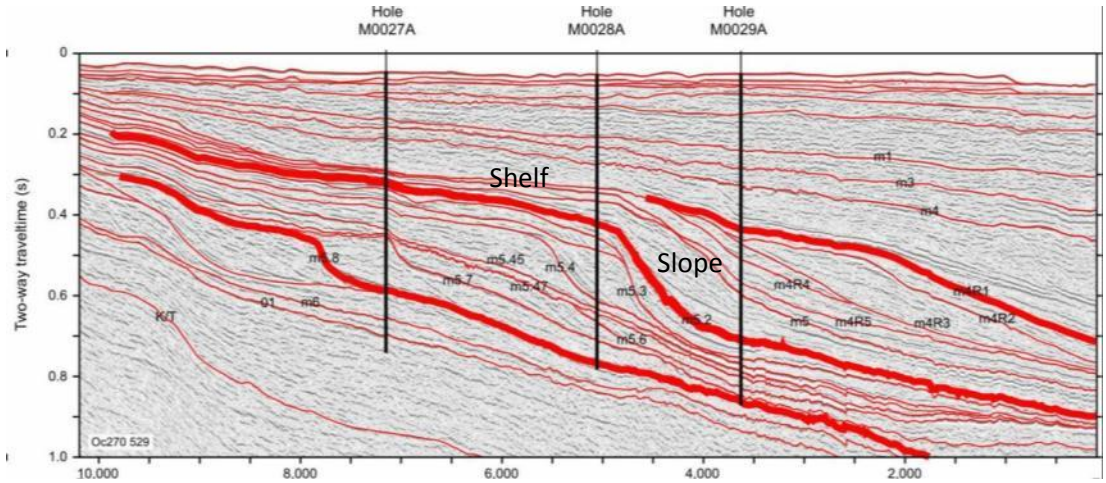

Figure 1.6: Seismic section from the New Jersey margin exhibiting a clear increase in gradient associated with the transition from shelf to slope (adapted from Mountain & Proust, 2010).

Recognition of shelf edge deltas from outcrop or well datasets is more difficult due to the limitations of outcrop exposure. Steel *et al.* (2000) suggested that the key to recognizing ancient shelf-margin deltas is in the correct identification of the ancient shelf edge break, for which a detailed understanding of the architecture and process operation is crucial. The Eocene shelf edge delta examples from Spitsbergen are exceptional for their complete shelf-slope-basin floor record. These relatively short and steep basin margin clinothems facilitate identification of the change in gradient from shelf to slope (Fig. 1.2B). However, in low gradient systems at outcrop, such as the Kookfontein Formation, Karoo Basin, South Africa (Wild *et al.*, 2009; Dixon *et al.*, 2012a), where identifying the shelf edge is difficult due to the lack of a marked gradient change between the shelf and slope, there is a gradual process and facies change across the rollover which could be a zone of change up to 10-km-long in a dip sense.

The progradation of a fluvio-deltaic system to a position at the shelf edge where it encounters a significant increase in water depth (associated with the shelf edge break), results over time in a change from a progradational to more aggradational stacking pattern, due to the inability of the delta to fill all the available accommodation beyond the shelf edge (Muto & Steel, 1992). This results in sequestering of sediment along the margin due to the redistributing effects of wave and storm energy and slow relative sea-level rise. Therefore shelf edge deltas are commonly characterized by substantial strike-elongate sand bodies. Suter & Berryhill (1985) recognized shelf edge deltas from the late Quaternary, northwest Gulf of Mexico and demonstrated through isopach thickness maps that they often exhibit multi-lobate, arcuate and lunate bodies at the shelf edge (Fig. 1.7). In dip profile, shelf edge deltas show significant basinward thickening (Plink-Bjorklund *et al.*,

2001; Porębski & Steel, 2003), attaining a maximum thickness just basinward of the shelf edge rollover (a key criterion for identifying the shelf edge; Porębski & Steel (2003)) and then thin and downlap onto the slope. Growth faulting of the shelf edge deltaic deposits is a common feature of high supply, over-steepened shelf edge settings observed in seismic datasets; similar features have also been documented at outcrop (Rider, 1978; Coleman *et al.*, 1998; Wignall & Best, 2004; Maloney *et al.*, 2012). Listric extensional faulting at the shelf edge results in the creation of local accommodation, resulting in trapping of sediment.

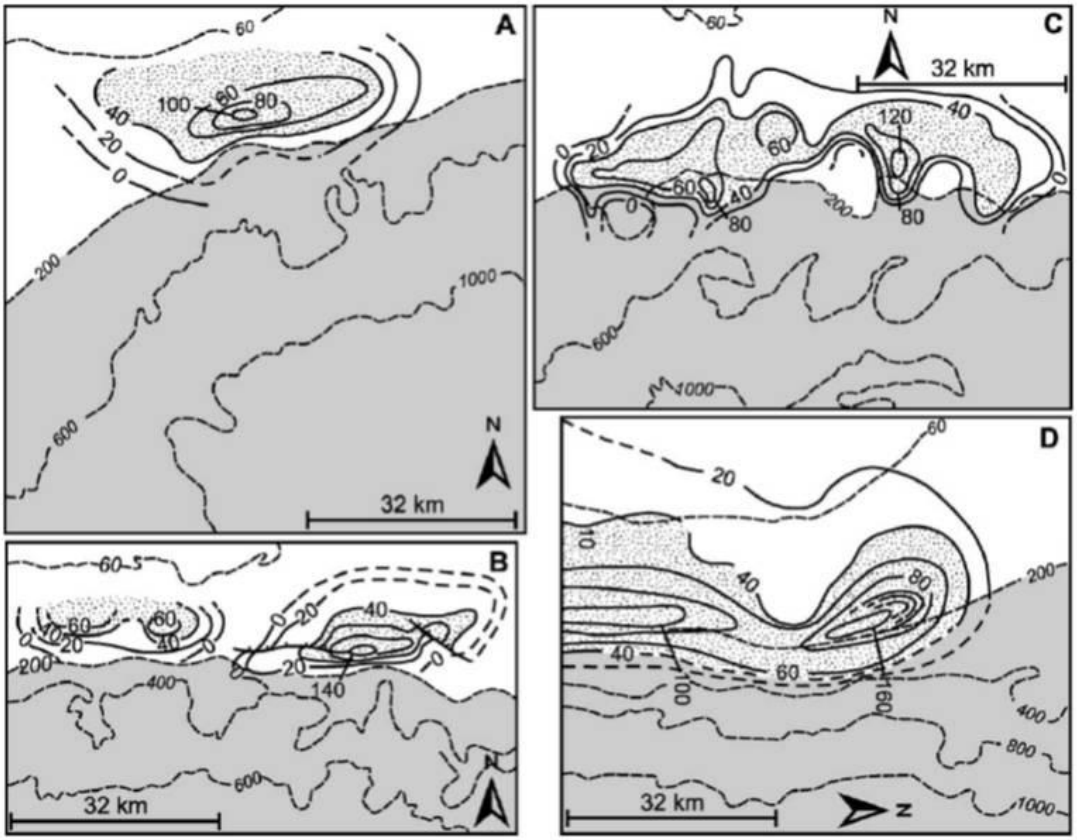

Figure 1.7: Geometry and dimensions of Wisconsinan shelf-margin deltas in the northwest Gulf of Mexico (A and B), the ancestral Mississippi (C) and Rio Grande (D) rivers. Deltaic depocentres are dotted; shaded areas correspond to continental slope (from Porębski & Steel, 2003) (modified after Suter & Berryhill, 1985).

1.6.4. Sedimentary characteristics of shelf edge delta systems (lithofacies distribution)

1.6.4.1. Facies landward of the shelf edge

The shelf edge break represents a significant geomorphological feature, and exerts a considerable influence on the processes operating on and around the shelf and slope transition, which in turn controls the distribution of facies belts (Johannessen & Steel, 2005). Studies of large scale outcrops where the shelf to slope transition is identifiable can be supplemented by detailed facies data (Collinson *et al.*, 1991; Steel *et al.*, 2000; Plink-Bjorklund *et al.*, 2001; Mellere *et al.*, 2002; Johannessen & Steel, 2005; Carvajal & Steel, 2006; Løseth *et al.*, 2006; Uroza & Steel, 2008; Covault *et al.*, 2009; Hubbard *et al.*, 2010). Such studies reveal significant changes in sedimentary processes and transfer mechanisms from the shelf to the slope.

Landward of the shelf edge rollover, shelf facies typically follow a vertical succession that coarsens and thickens upward similar to the 'parasequence' described by Van Wagoner *et al.* (1990) and is interpreted to record a single episode of delta progradation (Fig. 1.8). A typical individual parasequence starts with an offshore mudstone or fine-grained siltstone package. These fine-grained packages are extensive, overlie the sandy top of the underlying parasequence, and are considered to represent an increase in water depth. Above the offshore mudstone and siltstone facies are heterolithic coarse siltstone and sandstone beds that are commonly planar or unidirectional ripple laminated. These interbedded facies are often referred to as shoreface-to-offshore transition or prodelta deposits, depending on the nature of the up-dip or overlying system. Heterolithic sandstone and siltstone units coarsen- and thicken-upward, becoming increasingly amalgamated into sandy proximal delta front and mouth bar deposits (Bhattacharya & Walker, 1992; Mayall *et al.*, 1992; Reading & Collinson, 1996; Hart *et al.*, 1997; Plink-Bjorklund *et al.*, 2001; Bhattachary, 2006), or shoreface facies if away from the main fluvial entry point (Hampson & Howell, 2005). Mouth bar deposits can form thick units consisting of bedded (up to metre scale) or amalgamated, clean, well sorted sandstone. The very top of a parasequence commonly exhibits a transition into subaerial deposits or a transition back into heterolithic facies. Most parasequences are capped by offshore deposits associated with the next flooding surface. Basinward correlation of shelf parasequence facies shows a transition into increasingly heterolithic prodelta facies with the loss of mouthbar and shoreface deposits, and increasing mudstone and siltstone offshore facies. Continual thinning and fining of the sandy component results in a transition into offshore mudstone succession (Winn *et al.*,

1995; Morton & Suter, 1996; Macquaker *et al.*, 2007), if the shelf edge rollover is not encountered.

Figure 1.8: Typical progradational wave and storm-dominated parasequence from the Blackhawk Member, Utah showing a coarsening- and thickening-upward succession.

1.6.4.2. Facies basinward of the shelf edge

On encountering a pre-existing shelf margin break in slope, deltaic systems commonly exhibit significant facies change due to the increase in gradient associated with the transition to the steeper slope setting (Johannessen & Steel, 2005). In published examples, this transition is characterized by a change from the well-established coarsening- and thickening-upward deltaic parasequences (outlined above) to a setting dominated by

currents driven by gravity and density excess, and the deposition of turbidites, extensive soft sediment deformation, and erosion (gullies and channels) (Fig. 1.9A & B).

Parasequences that extend beyond the shelf edge commonly comprise thick intervals of sheet turbidite deposits that consist of clean, sharp based sandstone beds that range in thickness from 3 -15 cm and are normally graded. Internally they are plane-parallel to current-ripple laminated. (Mellere *et al.*, 2002) also noted numerous dip elongate channels and chutes cutting slope turbidite packages. The external geometries of upper slope turbidite packages show that these facies associations can be laterally extensive with relatively short dip extents. Examples from the Eocene of Spitsbergen (Mellere *et al.*, 2002) show limited runout distances of 1-2 km where they are seen to fine and thin, downlapping basinward into offshore facies. Up dip, slope turbidite deposits can be traced back to oversteepened mouth bar and distributary channel systems. Determining the processes leading to deposition of these sandy slope turbidite deposits is difficult, but it is likely that they were supplied directly from distributary channels, which have been shown to play a key role in the delivery of sand beyond the shelf edge rollover (Morton & Suter, 1996; Johannessen & Steel, 2005; Carvajal & Steel, 2009).

The increased gradient encountered by prograding fluvio-deltaic systems at a shelf margin promotes far more mass transport and soft sediment deformation (Mayall *et al.*, 1992; Winn *et al.*, 1995) than is commonly observed in inner or mid shelf deltaic systems (Fig. 1.9B), where sediment calibre and supply rates control deformation (Coleman *et al.*, 1998). Heterolithic sheet turbidite packages beyond the shelf edge commonly alternate with highly deformed mouthbar and shoreface sandstones with examples from the Karoo Basin (Wild *et al.*, 2009; Oliveira *et al.*, 2011), Mississippi Canyon (Mayall *et al.*, 1992), Namurian of County Clare, Ireland (Pulham, 1989) and the Eocene of Spitsbergen (Steel *et al.*, 2000; Plink-Bjorklund *et al.*, 2001). All exhibit prolific soft sediment deformation at the shelf edge. As a result, the occurrence of abundant soft-sediment deformation has widely been attributed to proximity to the shelf edge rollover (e.g. Stow, 1994; Galloway, 1998; Lee *et al.*, 2009; Pratson *et al.*, 2009; Oliveira *et al.*, 2011).

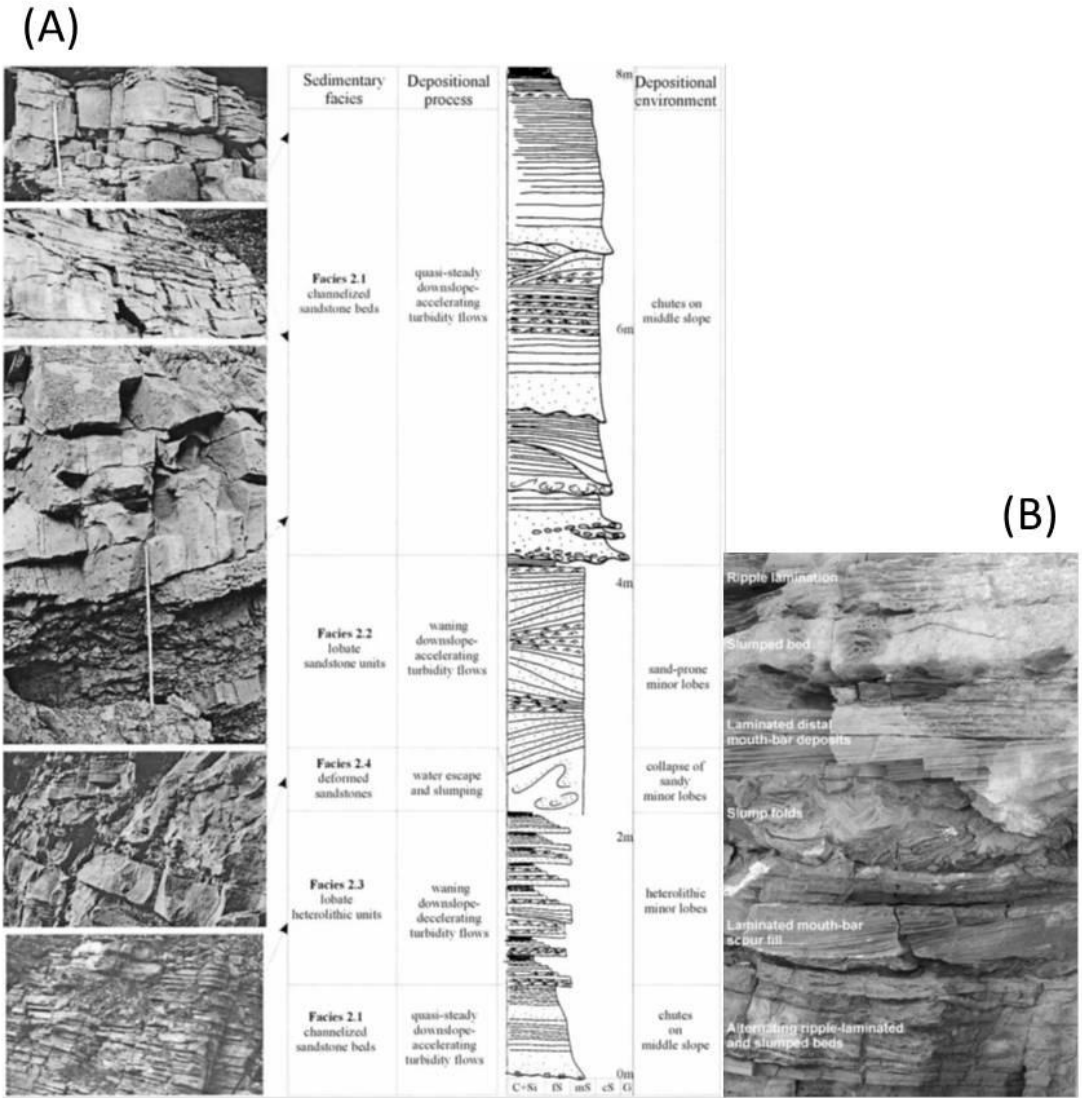

Figure 1.9: (A) Photographs, representative vertical section, and interpretations of middle-slope facies association (Plink-Bjorklund *et al.*, 2001). (B) Alternations of deformed and undeformed beds occurring in the distal mouth-bar succession just basinward of a shelf edge. Slumped bed in centre is 25-cm-thick; Storvola, Spitsbergen (Porębski & Steel, 2003).

1.6.5. Generation of shelf margin deltas

Lowering of relative sea-level results in reduced accommodation on the shelf (Posamentier *et al.*, 1988) driving progradation of the deltaic systems to the shelf edge. Further relative sea-level fall promotes incision of the fluvial feeder system into the shelf (e.g. Posamentier & Vail, 1988a; Van Wagoner *et al.*, 1990; Mutti & Davoli, 1992; Milton & Dyce, 1995; Marjanac, 1996; Normark *et al.*, 1998; Johannessen & Steel, 2005) resulting in entrenchment and focussing of fluvial supply to the shelf edge (Fig. 1.10B). In addition, the role of sediment supply as a major controlling factor for the development of basin margins

and the delivery of sediment to the slope and basin floor is widely recognized (Carvajal & Steel, 2006). High sediment supply rate systems have the ability to out-pace accommodation generation, thus enabling progradation of deltaic systems to the shelf edge under a range of conditions (Burgess & Hovius, 1998; Muto & Steel, 2002). Porębski & Steel (2006) used data from modern deltas to highlight that given sufficient sediment supply, deltas are capable of prograding to the shelf edge even during rising sea-level within a characteristic short transit time (100 Ky). Further studies of modern rivers have considered the importance of drainage basin area, relief, climate, bedrock type and tectonic evolution of the supply region on sediment flux (Milliman & Syvitski, 1992; Hovius, 1998; Syvitski & Milliman, 2007). The importance of sediment supply rate is emphasized by the modern day Mississippi river delta which, despite present day highstand conditions, has been able to prograde to within 30 km of the shelf edge in the last 7000 years (Frazier, 1976).

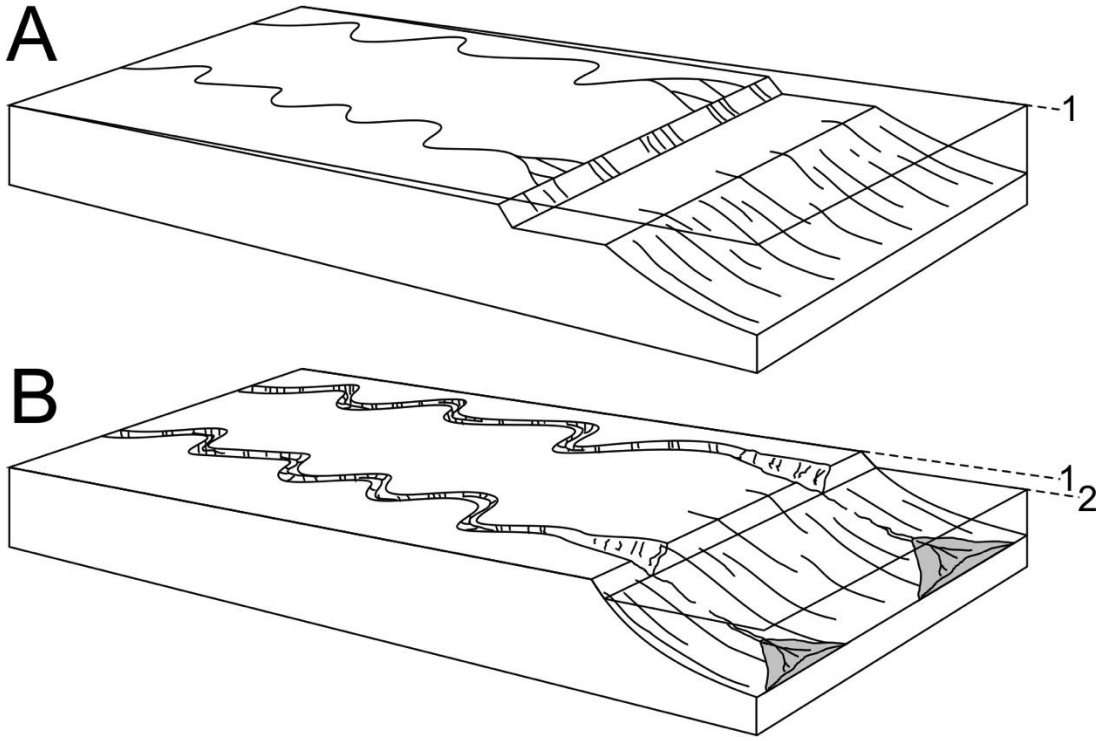

Figure 1.10: Schematic diagram demonstrating the effects of relative sea-level fall; (A) High stand condition, deltaic system shelf confined with no bypass to the basin floor. (B) Relative sea-level fall below the shelf edge resulting in incision of the shelf and bypass of sediment to the slope and basin floor.

1.7. Sequence stratigraphy: an overview

The widespread acceptance of relative sea-level change as one of the main factors that controls the development of shelf edge delta systems and the delivery of sediment to deep water settings means that sequence stratigraphic analysis can be applied in order to understand and predict the timing and occurrence of sedimentary facies.

Van Wagoner *et al.* (1988) defined sequence stratigraphy as "the study of rock relationships within a chronostratigraphic framework of repetitive, genetically related strata bounded by surfaces of erosion or non-deposition, or their correlative conformities". Although originally developed from the recognition of repeating patterns of reflector styles and termination patterns in early regional 2D seismic reflection surveys, sequence stratigraphic principles have since been readily applied to outcrop, core, and well log datasets (see Van Wagoner *et al.*, 1990 amongst others; Johnson *et al.*, 2001; Droz *et al.*, 2003).

Sequence stratigraphic models are concerned with understanding changes in available accommodation through time and the effect this has on the partitioning and distribution of sediment within a basin as a function of changes in relative sea-level (Emery & Myers, 1996; Coe *et al.*, 2003), accommodation is therefore the 3D expression of relative sea-level change. Sequence stratigraphic interpretations are based on the recognition of key bounding surfaces of regional extent, such as sequence boundaries, flooding and maximum flooding surfaces and the stacking pattern of strata that are bounded by these surfaces (Fig. 1.11).

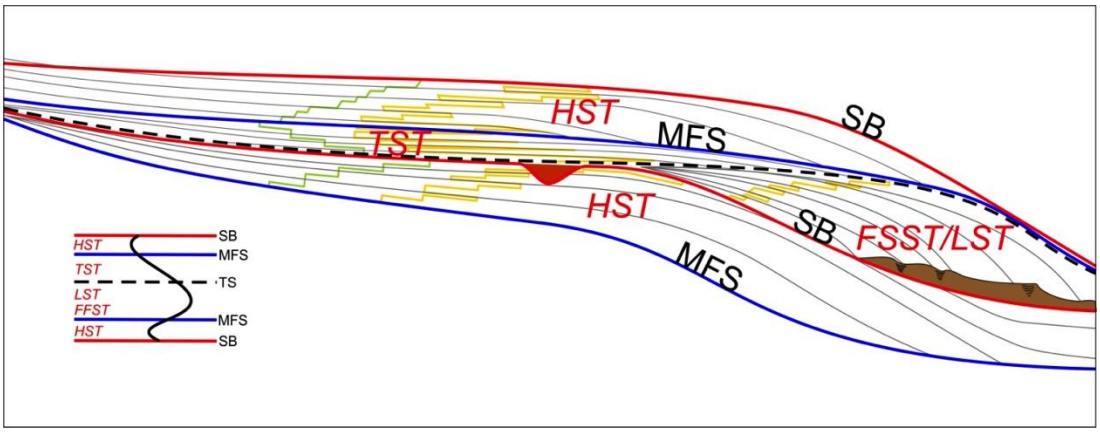

Figure 1.11: Stratal pattern in a type-1 sequence deposited in a basin with a shelf break (redrawen from Van Wagoner *et al.*, 1990). Diagram highlights key surfaces and sequences.

Advancements in acquisition and interpretation of 3D seismic data have led to continued testing and refinement of sequence stratigraphic models. The definition, terminology and interpretation of sequence stratigraphy has been contentious at times (Mitchum (1977), Vail *et al.* (1977d), Miall (1991), Ashton E. (2002), Catuneanu (2002), Coe *et al.* (2003) and

Bertram *et al.* (2006) amongst others). This thesis will follow the scheme of Van Wagoner *et al.* (1990) but with the inclusion of a four part systems tract division.

1.7.1. Shallow marine sequence stratigraphy: concepts and limitations

1.7.1.1. Flooding surfaces

Relative sea-level rise possibly in combination with reduced sediment supply forces the depositional system to step landward, resulting in the deposition of fine grained offshore facies over shallow water or emergent facies, producing a flooding surface in shallow-water settings or the expression of a flooding surface in deep-water settings (Fig. 1.11). A parasequence flooding surface separates younger from older strata across which there is evidence of an abrupt increase in water depth (Van Wagoner *et al.*, 1990), and usually separates two coarsening and thickening and/or fining and thinning upward units. It is commonly characterized by a condensed horizon reflecting very slow deposition (Van Wagoner *et al.*, 1990).

Parasequence flooding surfaces are typified by finer grained sediments, typically pelagic or hemipelagic deposits. When a flooding surface separates a transgressive systems tract (TST) from a highstand systems tract (HST) it is termed a maximum flooding surface (MFS).

1.7.1.2. Sequence boundaries

The sequence boundary is a key stratal surface produced as a result of reduced accommodation due to a fall in relative sea-level (Fig. 1.11) (Posamentier *et al.*, 1988; Posamentier & Vail, 1988a). This fall in relative sea-level forces the basinward regression of the system resulting in basinward facies dislocation where relatively distal facies are abruptly overlain by proximal facies without preservation of the intervening succession of coarsening and thickening upward strata. Typically in shallow marine settings a sequence boundary may be recorded as a laterally extensive abrupt juxtaposition of subaerial fluvial deposits and palaeosols on offshore mudstone facies. The sequence boundary can be traced down dip to a correlative conformity (Mitchum, 1977) where it is may be marked by an abrupt increase in sand supply if the up dip supply regime has the capable of delivering sufficient sediment out into the basin.

1.7.1.3. Parasequences, parasequence sets and systems tracts

Van Wagoner *et al.* (1990) defined a parasequence as “A relatively conformable succession of genetically related beds or bedsets, bounded by marine flooding surfaces and their

correlative surfaces". In the clastic shallow marine environment, parasequences are typically coarsening and thickening upward packages that exhibit facies trends consistent with a shallowing depositional environment, and are interpreted to represent single episodes of shoreline progradation.

Repeated episodes of shoreline progradation produces a succession of genetically related parasequences with a distinctive stacking pattern, known as a parasequence set (Fig. 1.12). In many cases, parasequence sets are bounded by major marine-flooding surfaces and their correlative surfaces (Van Wagoner *et al.*, 1988). The observed stacking pattern is produced by the long term vertical and horizontal migration path of the shoreline, as viewed along a depositional dip cross section, and is classified as either progradational, aggradational or retrogradational.

Progradational parasequence sets (Fig. 1.12A) result from successive parasequences advancing further basinward than the preceding parasequence, due to the long term rate of sediment supply exceeding the rate of accommodation generation. This can be recognized in vertical section by successive parasequences showing an increasing proportion of shallower facies. In cross section, successive parasequences will exhibit basinward migration of facies belts.

Retrogradational parasequence sets (Fig. 1.12C) develop when successive parasequences reach a less basinward position than the preceding one due to the rate of accommodation generation exceeding the rate of sediment supply. The result is a net landward migration of facies belts and an overall deepening upwards trend. In a single vertical section, a progressive decrease in the proportion of shallower water facies would be expected.

Aggradational parasequence sets (Fig. 1.12B) are characterized by successive parasequences reaching a similar position as the underlying parasequence, and therefore each parasequence exhibits similar facies distributions as the ones above and below. This aggradational stacking pattern occurs when supply and accommodation generation are equally balanced. In a vertical section the same repeated pattern of facies would be expected.

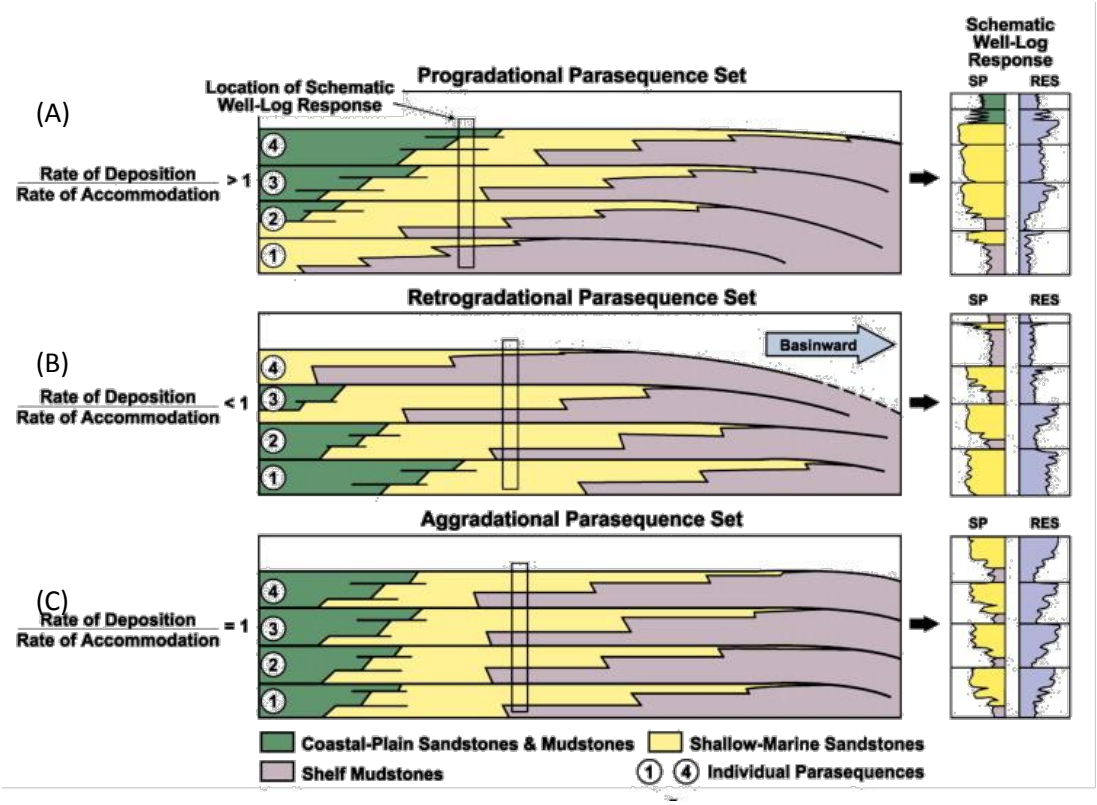

Figure 1.12: Parasequence stacking patterns in parasequence sets; depositional dip cross-section and well-log expression (from Van Wagoner *et al.*, 1990).

1.7.1.4. Depositional sequences and systems tracts

Patterns produced by the stacking of parasequence sets are used in conjunction with key surface boundaries and the position within a sequence to define systems tracts (Van Wagoner *et al.*, 1988). A sequence is defined as a relatively conformable succession of genetically related strata bounded by unconformities or their correlative conformities. They differ from a parasequence set because they contain more than one parasequence stacking geometry and are always bounded by sequence boundaries (Fig. 1.11).

Each sequence represents a complete cycle of relative sea-level change, and therefore can be broken down into a predictable succession of systems tracts divided by key surfaces. A number of sequence stratigraphic approaches have been proposed, starting with the three system tract scheme developed by Exxon researchers in the 1960s. This method divides a complete relative sea-level cycle into an isochronous sequence boundary (SB) overlain by a Low Stand Systems Tract (LST). There then follows a Transgressive Systems Tract (TST) and a subsequent Maximum Flooding Surface (MFS) before the High Stand Systems Tract (HST) (Vail *et al.*, 1977b; Jervey, 1988; Posamentier *et al.*, 1988; Van Wagoner *et al.*, 1990; Vail *et al.*, 1991). However a four system tract scheme has since been widely advocated, which suggests that the HST begins with the end of transgression and ends with the onset of

relative sea level fall. Therefore a Falling Stage Systems Trace (FSST) has been proposed, beginning at the onset of relative sea-level fall and concluding with the end of relative sea level fall which is associated with a subareal unconformity or a regressive surface of marine erosion (sequence boundary). However, the exact positioning of the sequence boundary is still a point of discussion; Plint & Nummedal (2000) worked on ramp margin settings, and placed the sequence boundary separating the FSST from the LST at the lowest point of relative sea-level. In ramp settings, the prograding shoreface is able to keep pace with falling relative sea-level until the initiation of sea-level rise. However in more typical basin margins where there is a pronounced break in slope (such as the margin documented in this study), the falling stage systems tract is often inhibited by the significant increase in water depth beyond the shelf edge rollover, and is therefore physically separated from the LST by significant subaerial exposure or a regressive surface of marine erosion (SB) expressed as a basinward shift in facies. The four system tract scheme begins with the sequence boundary that is placed at the position subject to the highest rate of relative sea-level fall (the F inflection point on the relative sea-level curve).

Lowstand Systems Tract (LST) – The LST represents a period of relative sea-level fall, which is generally consistent with widespread erosion and development of incised valleys as the shelf becomes fully exposed. LST concludes with the end of regression and the start of transgression, leading to the development of a retrogradational stacking pattern. Within the LST a specific pattern of deposition is expected; initial rapid fall of relative sea-level is often associated with slope and basin floor fan deposits, but as relative sea-level begins to slowly rise, basin floor deposits give way to increased deposition on the upper slope and the start of deposition at the shelf edge.

Transgressive Systems Tract (TST) – The TST overlies the LST and represents the retrogradational stepping of the depositional systems across the shelf. Backstepping of the system continues due to the increasing rate of relative sea-level rise until the time of maximum transgression, when the maximum flooding surface (MFS) is formed. Incised valleys cut during the preceding LST are filled during the early TST and an open marine shelf is produced.

Highstand Systems Tract (HST) – Following the MFS the rate of relative sea-level rise slows, meaning that increasing sediment supply can progressively increase the ability of the system to prograde. As a result, the HST begins with a broadly aggradational parasequence

stacking pattern that becomes increasingly progradational due to increasing then decreasing rate of relative sea-level rise until the time of maximum transgression.

Falling Stage Systems Tract (FSST) - As relative seal level starts to fall, this is marked by an increasingly progradational to downstepping parasequence stacking pattern due to an increasing rate of reduction of shelf accommodation, increasing up dip subaerial exposure and fluvial incision which in turn supplies more sediment to the rapidly prograding shoreline. Such rapid rates of supply and limited accommodation enable deltaic systems to rapidly move across the shelf.

1.8. Dataset and methods

This study represents the first detailed study of the lower Waterford (the initial 250 m of Waterford stratigraphy) from the Laingsburg Deposcentre South Africa (Fig. 1.13).

The field data collected for this study were acquired via a combination of logging sections, measurement of palaeocurrents and walking out of parasequences and key surfaces over 10s of km. The data collected included:

- In excess of 16,000 m of logged section recorded at a cm-scale. Logged sections can be divided into *extended* and *detail* logs. Extended logs aimed to capture the regional stratigraphic framework and large scale architecture. They usually recorded >400 m of stratigraphy and are spaced at intervals of several kilometres. Detail logs were collected to capture specific smaller scale architectural detail; they capture on average 20 – 50 m of section with a spacing of 10s of metres.
- 1,220 palaeocurrent measurements.

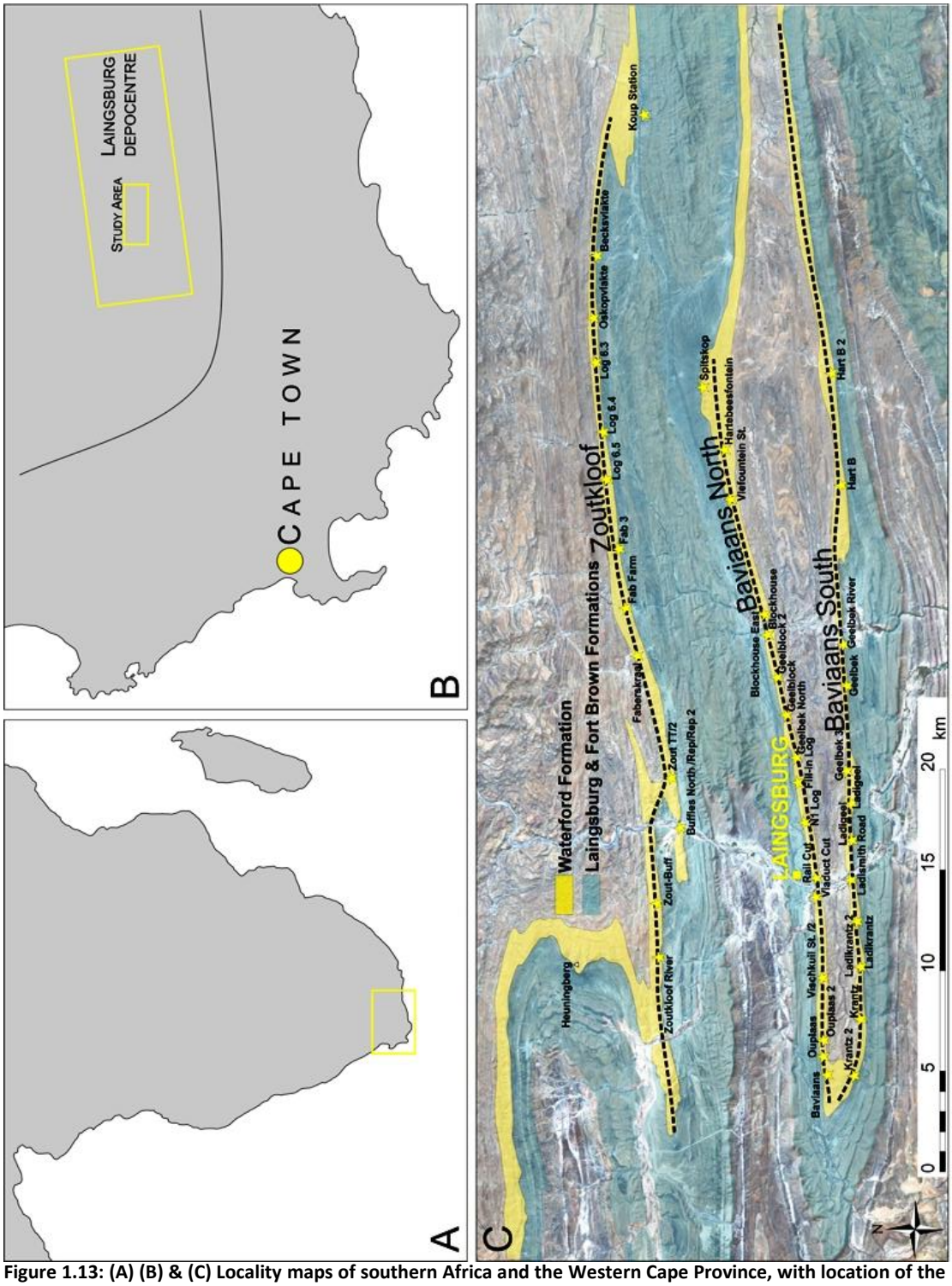

Figure 1.13: (A) (B) & (C) Locality maps of southern Africa and the Western Cape Province, with location of the Laingsburg depocentre and study area indicated. (C) Aerial image of the study area showing the three dip profiles and the locations of logged sections (yellow stars) referred to in the text.

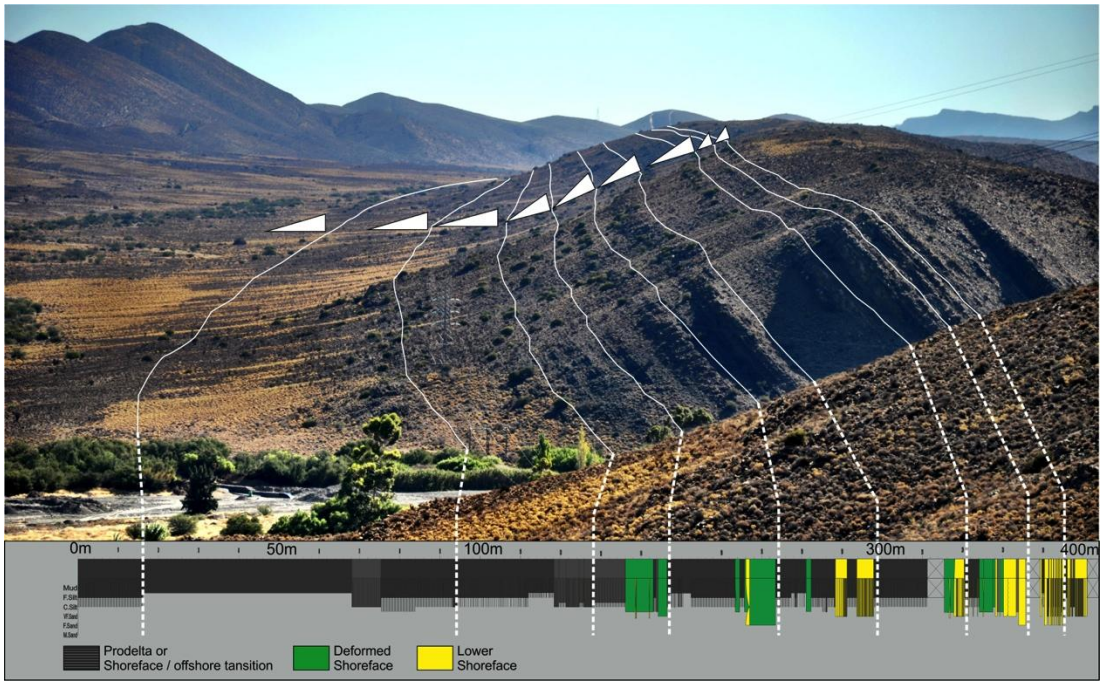

Figure 1.14: Typical lower Waterford Formation logged section, exhibiting coarsening and thickening upward parasequences bounded by physically correlated fine-grained units interpreted to contain flooding surfaces (white lines). Photo taken looking west (up dip) of the Ladismith road log locality.

Robust regional correlations were established by physically walking out parasequence flooding surfaces in order to constrain large scale architecture and facies variability. Across strike correlation was achieved by physically walking beds around the noses of the post depositional fold structures. The products of this extensive data collection program were three regional stratigraphic correlation panels that record facies distributions. Dip panel datasets were integrated to produce regional fence diagrams which provide a 3D understanding of architectural and facies variability over the 900 km^2 study area.

Further analysis of facies distribution was undertaken by integrating the facies breakdown data to produce isopach thickness maps for individual facies association. Interpretation of facies association maps combined with palaeocurrent indicator data enabled reconstruction of depositional palaeogeographical maps. By constructing palaeogeographical maps for successive clinothems it was possible to constrain the stratigraphic evolution of the basin margin.

1.9. Geological setting of the study area

The Palaeozoic to early Mesozoic tectono-stratigraphic development of southern Africa and the Karoo Basin can be related to the large-scale evolution of western Gondwana (Fig. 1.14). De Wit & Ransome. (1992) summarized four main episodes of compression and extension that affected the southern margin of Gondwana: (1) The Pan-Gondwanan convergence that occurred around 650 ± 100 Ma, which has been interpreted to be the result of fusion of greater Gondwana; (2) early Palaeozoic extension that took place at 500 Ma ±100 Ma and is considered to be related to the break-up of the greater proto-Gondwana and the subsequent formation of an extensive Atlantic-type passive margin along the southern edge of Gondwana; (3) late Palaeozoic convergence that occurred at 300 ± 100 Ma and is understood to relate to the assembly of Pangaea and the development of a Variscan-aged fold-thrust belt; and (4) mid to late Mesozoic extension ~150 ± 50 Ma, which resulted in the break-up of Gondwana and the subsequent opening of the southern oceans.

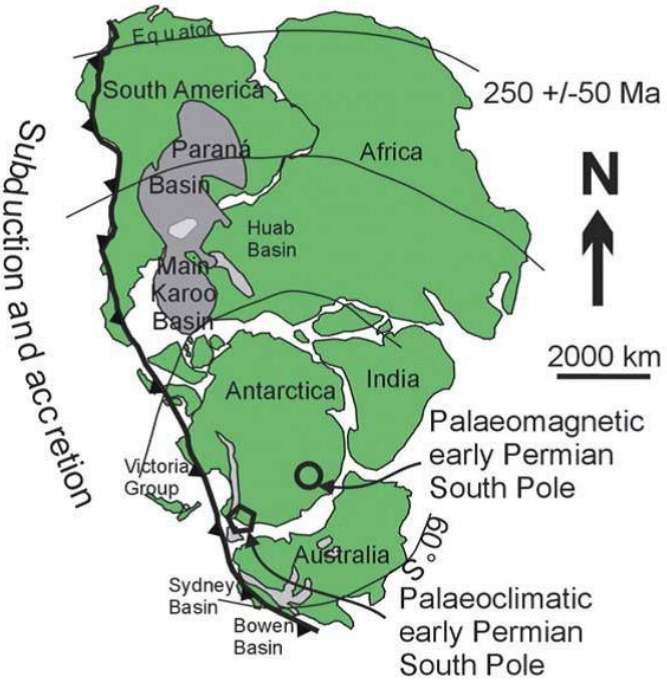

Figure 1.15: Early Permian geodynamics of Gondwana (from Faure & Cole, 1999).

Two mega-successions were deposited in southern Africa between the early Ordovician and early Jurassic. These are the Cape Supergroup (Ordovician-Carboniferous) and the Karoo Supergroup (late Carboniferous - Jurassic) and they are separated by a major unconformity (Fig. 1.15A) (Visser, 1987; Visser, 1997; Tankard *et al.*, 2009). The unconformity, which represents a ~30 Ma year hiatus, is interpreted to reflect uplift resulting from the mid-

Carboniferous assembly of Pangaea (Veevers *et al.*, 1994). Deposition of the Cape Supergroup spans from the Early Ordovician to Early Carboniferous and comprises shallow marine, deltaic and fluvial deposits (Veevers *et al.*, 1994). The overlying Karoo Supergroup represents ~5,500 m of tillites, deep marine to fluvial deposits deposited between the late Carboniferous and the early Jurassic (Fig. 1.15A).

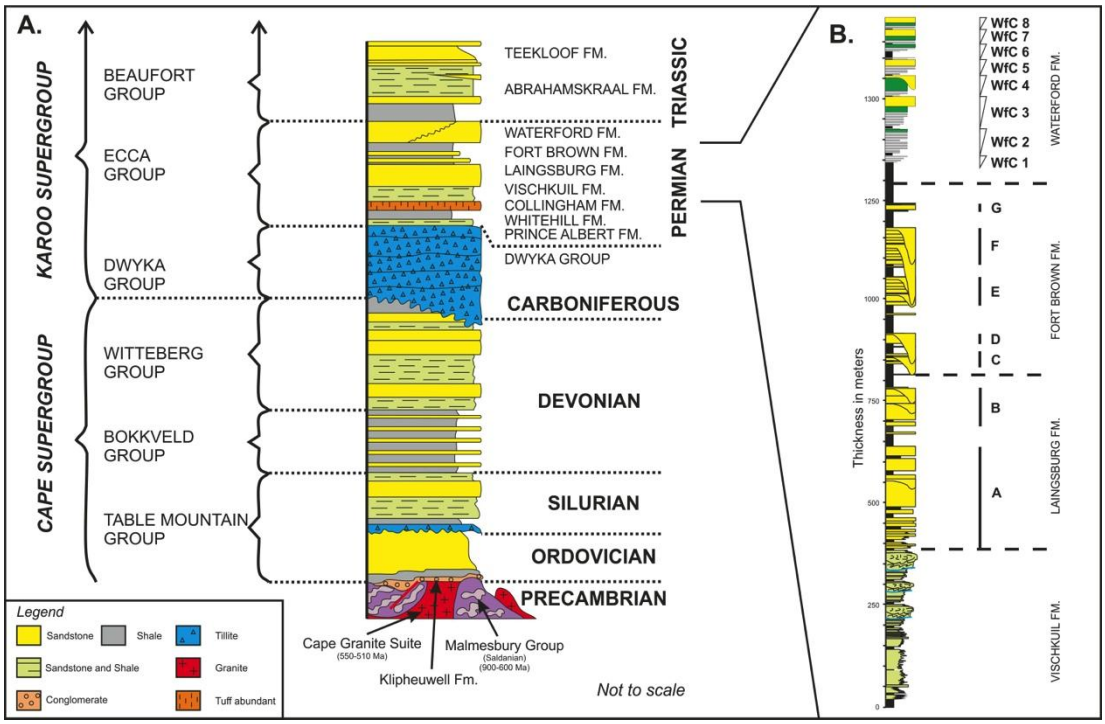

Figure 1.16: Lithostratigraphy of the Western Cape area. Modified (modified from Wickens, 1994).

1.9.1. Geological evolution of southern Africa/western Gondwana

1.9.1.1. Ordovician to middle Carboniferous

Basement material in the Western Cape region consists of Proterozoic meta-sedimentary rocks of the Malmesbury Group, into which intruded the Cambrian Cape Granite Suite (Scheepers & Armstrong, 2002; Tankard *et al.*, 2009). These units are unconformably overlain by the ~8,000-m-thick Palaeozoic sedimentary succession of the Cape Supergroup. These shallow marine, deltaic and fluvial deposits thicken towards the south into an east-west trending depo-axis (Broquet, 1992; Turner, 1999). Tankard *et al.* (1982) suggested that sediments were derived from a cratonic source to the north and are interpreted to have undergone significant reworking by shallow marine processes on a stable shelf setting in order to produce quartz-rich sands. The Cape Supergroup is divisible into three main groups: (1) Table Mountain Group, fluvial and shallow marine orthoquartzites; (2) Bokkeveld Group, shallow marine deposits; (3) Witteberg Group, shallow marine and fluvial deposits. Deposition is understood to have ceased due to the gradual collision of the

Panthalassan micro-continent during the late Devonian and early Carboniferous (Visser & Praekelt, 1998). This 'Hercynian' contractional deformation resulted in large areas of uplift and the progressive restriction of the Bokkeveld and Witteberg basin, culminating in an unconformity that marks the top of the Witteberg Group.

1.9.1.2. Formation and evolution of the Karoo Basin and the Cape Fold Belt

The Karoo Basin, along with other major southern Gondwanan basins (Paraná, Beacon and Bowen Basins), has long been interpreted to have developed in response to accretionary tectonics along the southern Gondwanan margin during the Late Palaeozoic (Johnson, 1991; Cole, 1992; De Wit & Ransome., 1992; Gresse *et al.*, 1992; Hälbich, 1993; Veevers *et al.*, 1994; Catuneanu *et al.*, 1998; López-Gamundí & Rossello, 1998; Visser & Praekelt, 1998; Faure & Cole, 1999; Catuneanu, 2004). The northward subduction of the Panthalassan plate beneath the Gondwana continent resulted in the formation of a magmatic arc (Johnson, 1991; Visser, 1993). Continued subduction along the margin resulted in continued northward compression and the development of a fold thrust belt inboard of the magmatic arc (Visser, 1987; Veevers *et al.*, 1994; Visser & Praekelt, 1998). For this reason the Karoo Basin has long been considered a retroarc foreland basin with an associated fold thrust belt (the Cape Fold Belt) lying along the southern margin of the basin (Visser, 1987; Johnson, 1991; Cole, 1992; De Wit & Ransome., 1992; Veevers *et al.*, 1994; Catuneanu *et al.*, 1998; Visser & Praekelt, 1998; Catuneanu, 2004).

More recent studies that have focussed on sediment provenance (Andersson *et al.*, 2004; Van Lente, 2004) and radiometric dating of the Ecca Group (Fildani *et al.*, 2007) have revealed inconsistencies in these earlier interpretations, which have led to a reassessment of the tectono-sedimentary evolution of the Karoo Basin and the timing of the Cape Fold Belt uplift and its ability to source the Karoo Basin fill. Based on provenance data and seismic stratigraphy (Tankard *et al.*, 2009), the Cape Fold Belt has been reinterpreted as Triassic in age, postdating much of the Karoo Basin fill and not being responsible for early Karoo Basin subsidence (Tankard *et al.*, 2009) (Fig. 1.16). Only the upper section of the basin-fill (the upper Beaufort Group) shows a compositional match with the Cape Fold Belt. As a result an alternative interpretation for the evolution of the Karoo Basin has been offered by Tankard *et al.* (2009), who suggested that the basin formed within the continental interior of Gondwana as a sag-like basin, with subsidence driven by long wavelength dynamic topography related to the mass imbalance of the subducting slab.

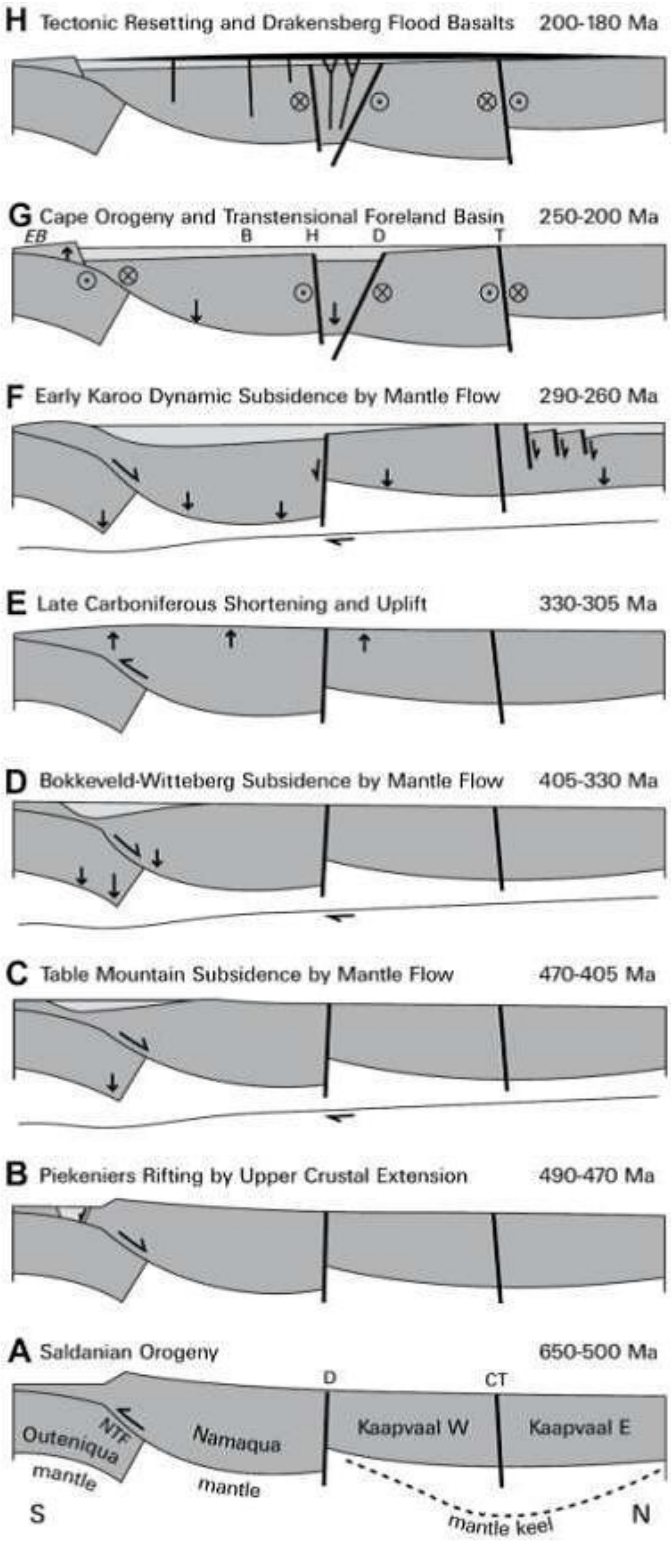

Figure 1.17: Evolution of Cape and Karoo Basins. (A-D) Saladian orogeny and Cape Basin. (E-F). Regional uplift and pre-Foreland Karoo Basin. (G-H) Cape Fold Belt orogeny and Foreland Karoo Basin (from Tankard et al., 2009).

1.9.1.3. Late Carboniferous to Permian deposits of the Karoo Supergroup

The Karoo Supergroup overlies the regional unconformity at the top of the Witteberg Group. The onset of Karoo sedimentation began with a ~800-m-thick succession of diamictites, varves and glacio-fluvial deposits of the Dwyka Group. Deposition of this glacial succession resulted from the migration of Gondwana over the South Pole and the coinciding Carboniferous glacial period at approximately 300-310 Ma. Zircon age dates derived from ash beds situated immediately above the Dwyka Group suggest an end to the glacial succession in the south-western Karoo at 289 Ma (Bangert *et al.*, 1999). However, glacial conditions are considered to have continued elsewhere in Gondwana and cycles of glaciation/deglaciation have been interpreted as a primary driver for controlling the stratigraphy of the overlying Ecca Group (Flint *et al.*, 2011b).

The final fragmentation of the Dwyka ice sheet as Gondwana moved away from the South Pole led to extensive areas of south-western Gondwana becoming flooded. Postglacial sedimentation is represented by the 2000-m-thick Ecca Group. The basal Prince Albert Formation (Fig. 1.15A) has a maximum thickness of 180 m and consists predominantly of shale and cherty shale beds with inter- to supra-tidal carbonates (Visser, 1993). It is overlain by 30 m of carbonaceous black shales of the Whitehill Formation (Fig. 1.15A) (Visser, 1993). These initial postglacial formations are thin sequences characterized by highly-condensed, sediment-starved shallow water facies that indicate low subsidence rate and minimal rates of sediment supply.

The Collingham Formation (Fig. 1.15A) marks a significant lithological change from dark condensed shales to siliciclastic turbidites with ash beds (Visser, 1993). The Collingham Formation is between 30 and 70-m-thick and is divided into the Zoutekloof and Buffels River Members that are separated by the regional Matjiesfontein chert (Fig. 1.15A) (Viljoen, 1994), which is used a distinctive regional basal marker bed from which overlying stratigraphic correlations are hung.

In the Laingsburg depocentre the Collingham Formation (Fig. 1.15A) is conformably overlain by the 380-m-thick Vischkuil Formation which consists of mud-capped silty turbidites with three extensive soft-sediment deformed units in the upper section (van der Merwe *et al.*, 2009) (Fig. 1.15B), which are interpreted as large mass transport events derived from an unstable shelf/slope. The overlying 500-m-thick Laingsburg Formation represents basin floor fan deposits (Sixsmith *et al.*, 2004; Prélat & Hodgson, 2013) (Fig. 1.15B). Unit A is a

300-m-thick sandy basin floor fan system and is overlain by Unit B, which represents a ~150-m-thick transitional base of slope channelized lobe system (Flint *et al.*, 2011b). The overlying Fort Brown Formation represents a transition to a channelized slope succession consisting of 5 sand prone units C – G that are separated by thick mudstone intervals (Figueiredo *et al.*, 2010; Hodgson *et al.*, 2011c). The Laingsburg and Fort Brown Formations have been interpreted to represent the progradation of the basin margin to the northeast (Flint *et al.*, 2011b). Continued progradation is marked by the ~400-m-thick Waterford Formation (the focus of this study) (Fig. 1.15B), which is characterized by a series of coarsening and thickening up parasequences (Fig. 1.13). The upper Waterford Formation comprise and addition 100 -150 m of thin (<10 m) shelf style parasequences that transitional gradually into subaqueous coastal plain deposits (F.17, 18, 19) (Fig.1.16). This study represents the first detailed work undertaken on the lower Waterford Formation in the Laingsburg area. The Ecca Group is conformably overlain by the ~ 5,000 m fluvial Beaufort Group (Veevers *et al.*, 1994; Johnson *et al.*, 1997; Cole & Whipplinger, 2001) (Fig. 1.1).

CHAPTER 2.
LITHOFACIES AND DEPOSITIONAL PROCESSES

Presented here are the descriptions and interpretations of the facies encountered within the lower Waterford Formation of the Laingsburg depocentre; they represent an integral element in understanding of the margin development and as a result will be referred to in various levels of detail through the subsequent chapters. This facies scheme is based on lithology, grain-size and sedimentary structures, which are related to depositional process.

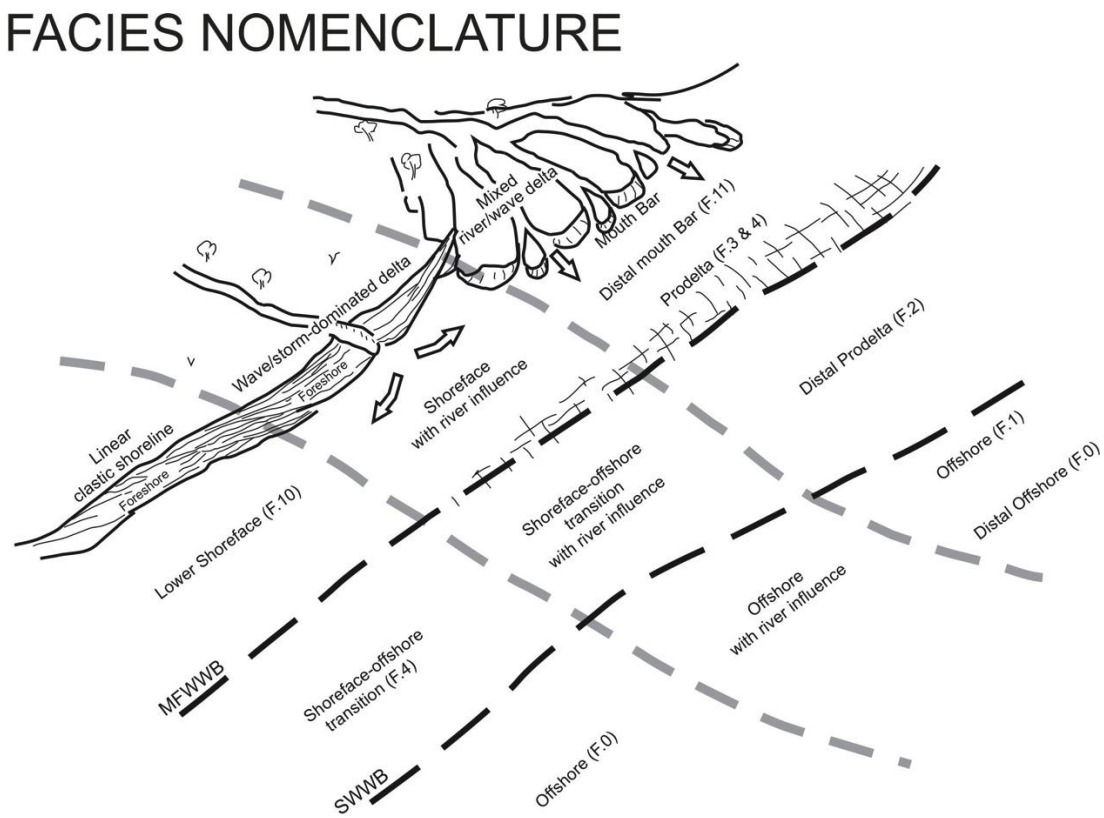

Figure 2.1 This schematic diagram shows the spatial relationship of key facies from a fluvial dominated position (top right) to a storm and wave influenced setting (bottom left) and the facies transitions observed basinward of these two settings. (MFWWB = mean fair weather wave base, SWWB = storm wave base). (modified from Mountain & Proust, 2010)

Facies and facies associations				
	Facies		Facies associations	
Facies No.	Delta (Based on chapter 4)	Shoreface	Delta	Shoreface
F.0	Distal offshore		Offshore	
F.1	Offshore			
F.2	Distal prodelta		Prodelta	
F.3	Prodelta			
F.4		Shoreface-offshore transition		Shoreface-offshore transition
F.5	Margin of mass flow deposit		Deformed lower delta front	Deformed shoreface
F.6	Axis of mass flow deposit			
F.7	*In-situ* deformed			
F.8	Lower delta front		Wave-dominated upper delta front with fluvial influence	
F.9	Delta front			
F.10		Lower shoreface		Lower shoreface
F.11	Distal mouthbar		Distal mouthbar	
F.12	Bioturbated prodelta		Bioturbated prodelta	
F.13		Bioturbated Shoreface-offshore transition		Bioturbated Shoreface-offshore transition
F.14	Channel lag conglomerate		Slope channel fill	
F.15	Slope channel fill			
F.16	Upper slope turbidites		Upper slope turbidites	
F.17	Distributary channel sandstone		Coastal plain	
F.18	Overbank or floodplain deposits			
F.19	Interdistributary bay deposits			

Table 2.1: Table showing the translation of axial delta and shoreface facies and their facies associations

F.0 – Distal offshore

Shelf mudstone unit above WfC 5 (person on boundary, mudstone to right).

Parasequence-bounding mudstone used as regional marker. Notebook 20-cm-long.

Characteristics

Feature	Values and interpretation
Depositional environment	Distal offshore shelf or slope
Description	Structureless mudstone, black in colour (no bioturbation observed). Concretionary nodules occur in most fine grained interval. Rare mm-scale lamination of fine siltstone and very fine sandstone. Bioturbation not observed.
Sedimentary structures	Typically structureless. Little to no internal stratification seen at outcrop. Thin laminations of very fine silt may be seen in fresh samples
Process interpretation	Hemipelagic fall-out and supply by very low-density turbidity currents in conditions of low clastic input. Mode of deposition ensures regional coverage of the mudstone deposits. Hence they are invaluable as correlation markers; this is particularly true of the mudstone markers above Unit G and WfC 5 (Fig. 1.16)
Bed thickness range	0.01 m
Net : Gross range	0 - 5%
Basal bounding surface	Sharp or gradational from underlying sandstone dominated parasequence (F.10)
Upper bounding surface	Gradational, occasionally sharp / erosional (F.1, 2)
Outcrop thickness	Very variable. From 10s of cm to 10s of m, typically thickening down-dip
Outcrop width / geometry	Very extensive, mapped laterally and down-dip through the entire Laingsburg area (Fig.1.13). Mudstones are thickest to the north (Fig.1.13)
Example localities	Mudstones are ubiquitous and are well developed between Unit G and WfC 1 and between WfC 5 and WfC 6 (Fig. 1.16).

F.1 - Offshore

Thinly laminated siltstone deposited by low-density turbidity currents. WfC 1, Heuningberg (Fig. 1.13).

Thinly laminated siltstone, occasional occurrence of starved ripple laminae. Lens cap for scale.

Characteristics

Feature	Values and interpretation
Depositional environment	Offshore
Description	Exposure typically looks thinly laminated, comprised of fine, medium and coarse siltstone. Siltstone laminations tend to be mm thick although 2-10 cm beds do occur. Bioturbation index = 1/5.
Sedimentary structures	Generally starved ripple lamination
Process interpretation	Deposition by low density turbidity currents and minor suspension fallout
Bed thickness range	Laminations are 1-5 mm, occasionally reaching 100 mm.
Net : Gross range	10 - 20%
Basal bounding surface	Normally gradational from distal offshore mudstone (F.0)
Upper bounding surface	Gradational into overlying interbedded siltstone and sandstone (F.2,3,4)
Outcrop thickness	Packages up to 20-m-thick
Outcrop width / geometry	Regionally extensive, thickens basinward attaining a maximum thickness where shelf (shoreface) facies F.8,9,10 pinch out, which is geographicaly and temporaly variable across the study area.
Example localities	Marks the initiation of each Waterford parasequence but is most prevalent in WfC 1 & 2 (Fig. 1.16)

F.2 - Distal Prodelta

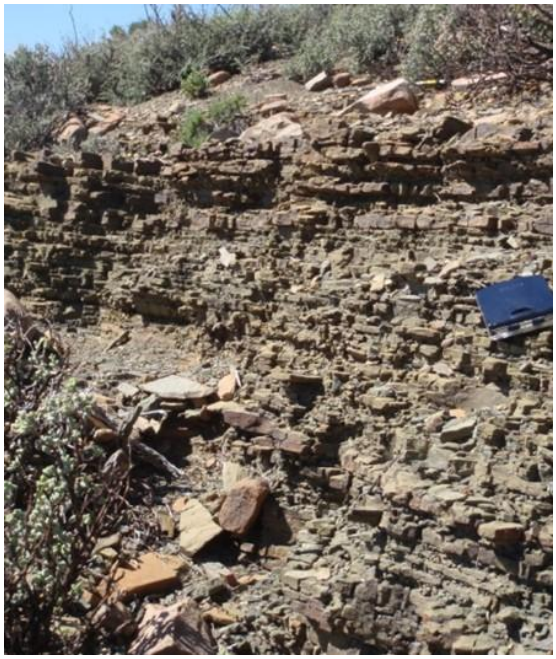

Thinly bedded, ripple laminated heteroliths. Upper WfC 1, N1 locality. Compass for scale

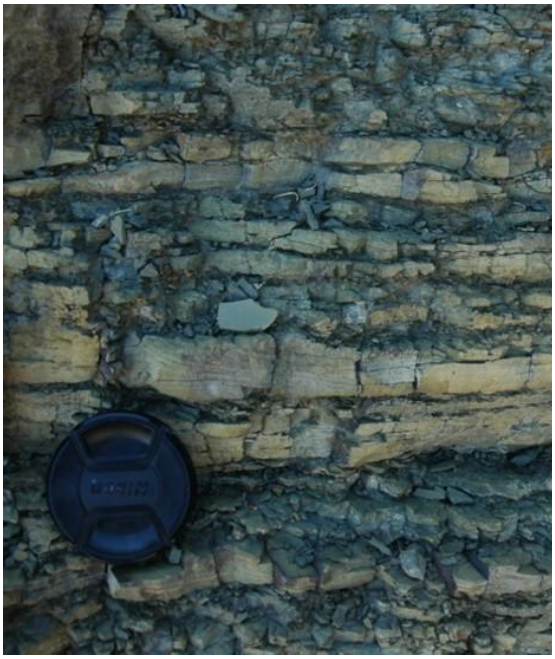

Close up of facies from Rail Cut log. Ripple laminated beds have poorly defined bed bases and tops.

Characteristics

Feature	Values and interpretation
Depositional environment	Distal prodelta
Description	Rhythmically interbedded fine and coarse siltstone. Normal grading of beds often observed. Bioturbation index = 1/5.
Sedimentary structures	Predominantly starved ripple laminae, lenticular and flaser bedded, occasional parallel laminated. Bed bases are sharp with gradational to sharp tops.
Process interpretation	Deposition by low density turbidity currents
Bed thickness range	Siltstone bed thickness 0.01 – 0.03 m
Net : Gross range	15 – 35%
Basal bounding surface	Packages have gradational bases from F.1 & 2
Upper bounding surface	Packages generally grade into overlying interbedded siltstone and sandstone (F.3,4)
Outcrop thickness	Packages up to 15-m-thick
Outcrop width / geometry	Occurs locally down dip of supply point
Example localities	N1 log locality (Fig. 1.13)

F.3 - Prodelta

Heterolithic sandstone beds from WfC 1 Waterkloof log locality (Fig. 1.13). 1.5m logging pole for scale

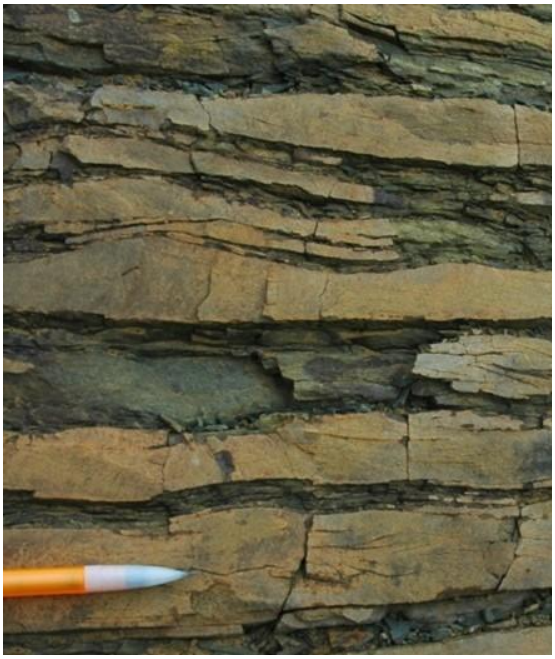

Sandstone beds 2 – 5-cm-thick, typically unidirectional current ripple laminated with symmetrical ripple reworked tops, Rail Cut log locality (Fig. 1.13)

Characteristics

Feature	Values and interpretation
Depositional environment	Prodelta
Description	Very regular interbedding of fine siltstone and very fine-grained sandstone. Bed bases are sharp and occasionally slightly erosive. Bed tops are sharp to gradational. Bioturbation index = 0-1/5.
Sedimentary structures	Predominantly unidirectional ripple laminated but occasionally parallel laminae and climbing ripple laminated. Bed tops often reworked by orbital currents
Process interpretation	Deposited by low density turbidity currents
Bed thickness range	Sandstone beds 0.01 – 0.05 m
Net : Gross range	30 – 50%
Basal bounding surface	Gradational from F.1,2,
Upper bounding surface	Gradational, coarsening up into bedded sandstone (F.8,9,10) but commonly erosive where overlain by deformed material (F.5,6,7)
Outcrop thickness	Packages up to 10-m-thick
Outcrop width / geometry	Occurs locally down dip of supply point
Example localities	N1 log locality (Fig. 1.13)

F.4 – Shoreface-offshore transition

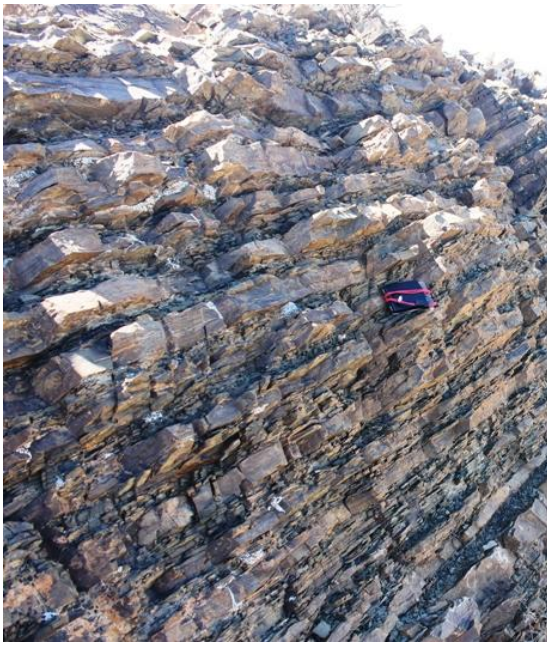

Heterolithic sandstone beds from WfC 2 Waterkloof log locality (Fig. 1.13). Compass for scale

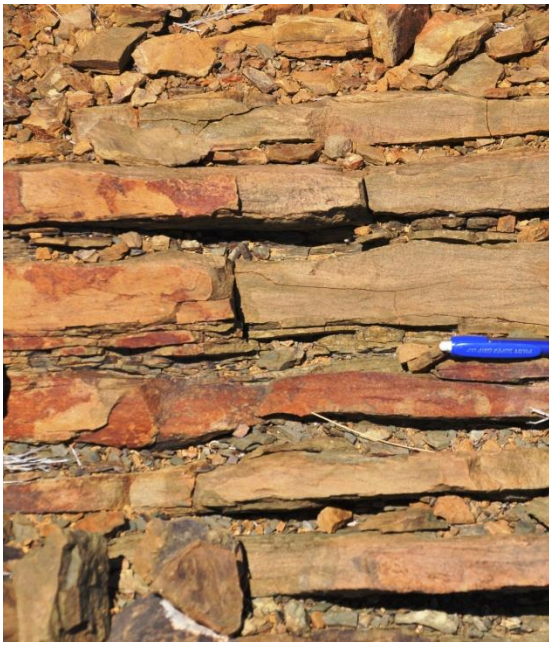

Sandstone beds 2 – 5-cm-thick, typically unidirectional current ripple laminated with wave reworked tops

Characteristics

Feature	Values and interpretation
Depositional environment	Shoreface-offshore transition
Description	Heterolithic fine siltstone and very fine sandstone beds. Bed bases are sharp and occasionally slightly erosive. Bed tops are sharp to gradational. Greater wave influence than prodelta deposits. Bioturbation index = 0-1/5.
Sedimentary structures	Unidirectional ripple laminated beds, strongly reworked by orbital currents
Process interpretation	Deposited by low density turbidity currents
Bed thickness range	Sandstone beds 0.01 – 0.10 m
Net : Gross range	30 – 50%
Basal bounding surface	Gradational from offshore deposits (F.1,2,3)
Upper bounding surface	Gradational top coarsening up into bedded sandstone (F.8,9,10) but commonly where overlain by deformed material (F.5,6,7)
Outcrop thickness	Packages up to 10-m-thick
Outcrop width / geometry	Regionally extensive, thickens basinward attaining a maximum thickness where shelf (shoreface) facies F.8,9,10 pinch out, which is geographicaly and temporaly variable across the study area
Example localities	Present in all lower Waterford parasequences. Thickens in the north of the study area

F.5 – Margin of mass flow deposit

Structureless poorly sorted silty sandstone. Beds 20-30-cm-thick separated by thin, foundered ripple laminated sandstone beds, Buffels North Repeat locality (Fig. 1.13).

Structureless poorly sorted silty sandstone. Rail Cut locality (Fig. 1.13). Pencil for scale.

Characteristics

Feature	Values and interpretation
Depositional environment	Shelf delta fron and distal shelf delta front. Depositional margin of mass flow
Description	Dark-green-grey, poorly sorted, coarse siltstone to very fine sandstone (sandy siltstone) often overlying prodelta deposits.
Sedimentary structures	Structureless, lacks clasts that are characteristic of more proximal debrites. Bed bases are sharp, bed tops are sharp with occasional symmetrically rippled tops
Process interpretation	Off axis or distal deposit associated with a debrite, comprising only the finer grained matrix of more proximal debris-flows. Lacks sandstone clasts
Bed thickness range	0.1 - 0.75 m
Net : Gross range	40%
Basal bounding surface	Sharp and usually occur above interbedded siltstone and sandstone (F.1,2,3,4,)
Upper bounding surface	Sharp or erosive, often overlain by debrite facies (F.6,7)
Outcrop thickness	Individual beds of deformed material are 0.1 – 0.6-m-thick. Packages of marginal mass transport material up to 5-m-thick
Outcrop width / geometry	Extensive individual beds can be traced for hundreds of metres
Example localities	WfC 4 (Fig.1.16), Buffels North section (Fig. 1.13)

F.6 – Axis of mass flow deposit

Heavily deformed and disaggregated debrite deposit. WfC 4 (Fig. 1.16), Buffels North locality (Fig. 1.13).

Heavily deformed and disaggregated sandstone blocks. Note rounding of sandstone blocks indicating down slope transportation. Logging pole (1.5 m) for scale.

Characteristics

Feature	Values and interpretation
Depositional environment	Shelf delta front
Description	Dark green-grey, coarse siltstone to very fine sandstone matrix with deformed and disaggregated rafts and fine grained sandstone blocks.
Sedimentary structures	Heavily deformed with disaggregated, rafts and rounded sandstone blocks
Process interpretation	Debris-flow
Bed thickness range	0.3-1.2 m
Net : Gross range	Variable
Basal bounding surface	Sharp or erosive, usually overlying interbedded sandstone and siltstone (F.1,2,3,4) or marginal mass flow deposits (F.5)
Upper bounding surface	Sharp or irregular, overlain by *in-situ* deformed deposits (F.7)
Outcrop thickness	Individual events 0.3-1 m but produce amalgamated packages 3 – 4-m-thick
Outcrop width / geometry	Widespread, individual deformed intervals can be correlated for kms
Example localities	Prevalent across the study area. Excellent examples in Buffels North area (Fig. 1.13)

F.7 - *In-situ* deformed

In-situ deformed structureless sandstone blocks. Formed as dense sandstones are deposited onto unconsolidated, water-laden substrate. WfC 4, Heuningberg (Fig. 1.13 & 1.16). 20-cm-long notebook for scale.

Contrast the small scale water escape deformation in this photo with the large scale deformation structures in the photograph to the left. Coin for scale (right hand side).

Characteristics

Feature	Values and interpretation
Depositional environment	*In-situ* deformation in shoreface clinothem on shelf
Description	Deformed fine sandstone.Deformation ranges in size from small scale (centimetres) ball and pillow structures and detached pseudonodules, up to large scale (metres) loaded bed bases and larger flame structures. Bioturbation absent.
Sedimentary structures	Ball and pillow structures, flame structures.
Process interpretation	Sediment deformed *in-situ* by abrupt loading, resulting in the vertical movement of fluids and sediment.
Bed thickness range	0.2 - 2.0 m
Net : Gross range	Variable
Basal bounding surface	Irregular, generally overlie debrite facies (F.6)
Upper bounding surface	Gradational, becoming less deformed into bedded or amalgamated sandstone (F.8,9,10)
Outcrop thickness	Variable from 0.1 m – 5 m, generally occurring in the upper part of coarsening and thickening up packages
Outcrop width / geometry	Widespread, individual deformed intervals can be correlated for kms
Example localities	WFC 4 (Fig. 1.16), Heuningberg (Fig. 1.13)

F.8 - Lower delta front

Generally tabular sandstone beds locally lenticular. WfC 5, Heuningberg (Fig. 1.13 & 1.16).

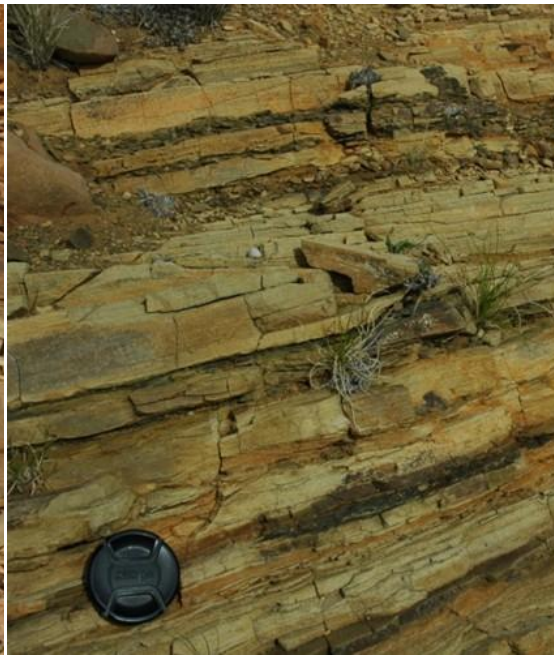

Tabular sandstones with planar and unidirectional flow. Convex up laminations (HCS) and occasional scours also present.

Characteristics

Feature	Values and interpretation
Depositional environment	Lower delta front, fluvial dominated, storm and wave influenced
Description	Generally tabular bedded fine sandstone. Often have symmetrical rippled top surfaces with sharp occasional erosive bases. Bioturbation absent.
Sedimentary structures	Predominantly includes: climbing ripple and parallel lamination. Locally structureless or HCS.
Process interpretation	Rapid deposition of sand from suspension in fluvial distributary area. Reworking by wave and storm processes
Bed thickness range	0.1-0.2 m
Net : Gross range	85 %
Basal bounding surface	Overlying or laterally gradational from distal mouth bar deposits (F.11)
Upper bounding surface	Gradational into amalgamated lower shoreface sands. Can be sharp and erosive (F.10)
Outcrop thickness	Packages are in the range of 2 – 4-m-thick
Outcrop width / geometry	Tabular sheet like geometries, locally lenticular with occasional scours
Example localities	WfC 3 (Fig. 1.16) N1 locality (Fig.1.13).

F.9 – Delta front

Generally tabular sandstone beds locally lenticular. Upward increased amalgamation of beds. WfC 5, Baviaans North limb.

Tabular sandstones with convex up laminations (HCS) and occasional scours

Characteristics

Feature	Values and interpretation
Depositional environment	Delta front, fluvial dominated, storm and wave influenced
Description	Commonly amalgamated, occasionally tabular fine sandstone beds. Often sharp symmetrical rippled tops surfaces with occasional erosive bases. Bioturbation absent.
Sedimentary structures	Variable, includes parallel lamination, unidirectional climbing laminating, structureless. Locally wave and storm influenced with HCS.
Process interpretation	Rapid deposition of sand from suspension fluvial distributary setting. Reworking by wave and storm processes
Bed thickness range	0.1-0.3 m
Net : Gross range	90 %
Basal bounding surface	Overlying or laterally gradational from distal mouth bar deposits (F.11)
Upper bounding surface	Gradational into prodelta or offshore deposits top surface can be sharp and erosive (F.3,4)
Outcrop thickness	Packages are in the range of 2 – 4-m-thick
Outcrop width / geometry	Tabular sheet like geometries, locally lenticular with occasional scours
Example localities	WfC 3 (Fig.1.16) N1 locality (Fig. 1.13).

F.10 - Lower Shoreface

Amalgamated sandstone beds exhibiting HCS and swales. Waterkloof River locality.

Tabular sandstones with convex up laminations (HCS) and occasional scours

Characteristics

Feature	Values and interpretation
Depositional environment	Lower shoreface, dominated by storm and wave processes
Description	Generally tabular fine sandstone beds. Often have symmetrical rippled top surfaces with sharp occasional erosive bases and sharp symmetrical rippled tops. Bioturbation absent.
Sedimentary structures	Variable, includes parallel lamination, structureless, symmetrical ripple laminae, HCS. Locally occurring sigmoidal geometries; pinching and swelling of beds
Process interpretation	Rapid deposition of sand from suspension in distal or lateral to fluvial distributary mouths. Reworking by wave and storm processes
Bed thickness range	0.1-0.4 m
Net : Gross range	95 %
Basal bounding surface	Gradational, from either bedded sandstone (F.8) or *in-situ* deformed sandstone (F.7)
Upper bounding surface	Variable. Sharp transition into mudstone (F.0) or laminated siltstones (F.1,2), often associated with small shallow scouring and mantled by mudstone rip-up clasts. Gradational tops fine and thin into bioturbated interbedded sandstone and siltstone facies (F.12,13)
Outcrop thickness	Packages are in the range of 2 – 4-m-thick
Outcrop width / geometry	Tabular sheet like geometries, locally lenticular with occasional scours. Present in more proximal settings, predominantly above WfC 3 (Fig. 1.16)
Example localities	WfC 5 (Fig. 1.16) N1 locality (Fig. 1.13).

F.11 – Distal mouth bar

Amalgamated sandstone dominated by low angle climbing ripple lamination. WfC 3, N1 Log locality. 1.5m logging pole for scale.

Unidirectional climbing ripple laminations occasionally stoss side preserved. Compass for scale.

Characteristics

Feature	Values and interpretation
Depositional environment	Mouth bar, deposited in close vicinity to a sediment input point
Description	Thick amalgamated fine sandstone packages. Facies lack wave influence. High terrigenous content. Bioturbation absent.
Sedimentary structures	Dominated by low angle climbing ripple lamination. Beds 0.2 - 0.5-cm-thick (amalgamated)
Process interpretation	Deposited by rapid deposition on exit of confinement
Bed thickness range	0.2 - 0.5 m
Net : Gross range	80%
Basal bounding surface	Sharp erosive, usually overlying marginal mass flow deposits and debrites (F.5,6)
Upper bounding surface	Sharp erosive, usually by overlying marginal mass flow deposits and debrites (F.5,6)
Outcrop thickness	Package up to 3-m-thick
Outcrop width / geometry	Produces basinward dipping delta scale clinothems that thin and separate down dip over 2 km. Lateral extent is narrow, no more than 6 km
Example localities	Well developed in WfC 3 (Fig. 1.16) along the N1 Section of the Baviaans Northern profile (Fig. 1.13).

F.12 - Bioturbated prodelta /F.13 - Bioturbated shoreface-offshore transition

Ripple laminated, heterolithic siltstone and sandstone beds, representing distal toesets of delta clinothems. WfC 3 (Fig.1.16), Heuningberg (Fig. 1.13). Pencil for scale.

Primary sedimentary structures and bedding almost destroyed by intense bioturbation. Occurs immediately below flooding surfaces, suggesting rising relative sea-level, enabling colonisation.

Characteristics

Feature	Values and interpretation
Depositional environment	Prodelta to distal prodelta, or shoreface-offshore transition setting
Description	Heavily bioturbated, occasional unidirectional and oscillatory ripple lamination. Bed boundaries poorly defined, interbedded coarse siltstone and fine sandstone, observed as fining and thinning up packages at the tops of parasequences
Sedimentary structures	Primary structures destroyed by bioturbation
Process interpretation	Deposition by low-density turbidity currents, deposited into a quiescent offshore setting, enabling an increased level of bioturbation
Bed thickness range	0.01-0.03 m
Net : Gross range	40%
Basal bounding surface	Gradational from F.8,9,10
Upper bounding surface	Gradational from F.0,1,2
Outcrop thickness	Packages generally < 1-m-thick
Outcrop width / geometry	Occurs at the very top of individual lower Waterford parasequences but distribution is irregular, likely to be removed by wave ravinement
Example localities	Top of WfC 1, 2 ,3 across the study area (Fig. 1.16).

F.14 - Channel lag conglomerate

Conglomerate lag at the base of the Hartbeesfontein channel (WfC 4) (Fig. 1.13). Outcrop shown in photo - 1.5 m across.

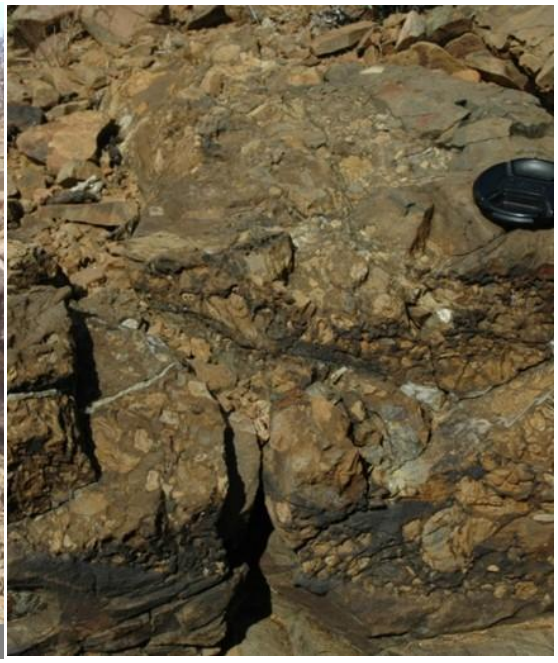

Intra-formational, sub-rounded, matrix supported conglomerate (camera lens cap for scale).

Characteristics

Feature	Values and interpretation
Depositional environment	Slope channel-fill. Conglomerate lag lining erosional channel bases or local scour features
Description	Clast and matrix supported intraformational conglomerate in a medium grained sandstone. Clasts are angular to sub-angular and consist of siltstone and very fine sandstone. Clasts range in size from 1-5 cm
Sedimentary structures	Imbrication of clasts
Process interpretation	Deposited from erosive sediment laden flows
Bed thickness range	0.4 m
Net : Gross range	80%
Basal bounding surface	Sharp erosive into F.0
Upper bounding surface	Gradational to F.15
Outcrop thickness	Confined to small scours or the base of larger incisional features such as slope channels.
Outcrop width / geometry	Highly localized, often associated with significant erosion
Example localities	Base of upper slope channel in WfC 4 (Fig. 1.13) and at the base of WfC 7 (Fig.1.16).

F.15 - Slope channel fill

Oblique view looking down dip of upper slope channel cutting down into underlying slope mud succession. Red line marks erosive base of channel. WfC 4 Hartbeesfontein locality (Fig. 1.13).

Channel fill comprises predominantly structureless occasionally planar laminated, 20-40-cm-thick sandstone beds.

Characteristics

Feature	Values and interpretation
Depositional environment	Upper slope channel
Description	Thinly bedded at base of channel, becoming increasingly thicker bedded and amalgamated upward, fine to medium sandstone. Note the asymmetry to channel fill
Sedimentary structures	Predominantly structureless with occasional cross bedding and planar lamination towards the base of the channel
Process interpretation	Deposited by high density turbidity currents
Bed thickness range	0.1-0.7 m
Net : Gross range	95%
Basal bounding surface	Sharp, erosive, often mantled by significant thicknesses (0.5 m) of intraformational conglomerate lag (F.14).
Upper bounding surface	Sharp, overlain by F.0,3,4,
Outcrop thickness	Confined within erosive channel, 50 m at deepest point of the channel and thins toward the channel margins
Outcrop width / geometry	Confined within a 2-km-wide channel at the Hartbeesfontein locality along the northern limb of the Baviaans syncline
Example localities	WfC 4 Hartbeesfontein locality (Fig.1.13).

F.16 - Upper slope turbidites

Basinward thickening package of sheet turbidites. WfC 4 Vleifontein Log locality (Fig. 1.13). Outcrop height in photo ~40 m

Tabular turbidite beds 4 – 10-cm-thick. Unidirectional ripple laminated occasionally stoss side preserved. 20-cm-long notebook for scale.

Characteristics

Feature	Values and interpretation
Depositional environment	Upper slope
Description	Extensive tabular, fine sandstone beds which produce an aggradational stacking pattern. Beds often have a sigmoidal shape
Sedimentary structures	Predominantly unidirectional ripple lamination, stoss-side preservation occurs locally
Process interpretation	Unconfined turbidity currents deposited beyond the shelf edge
Bed thickness range	0.05 - 0.1 m
Net : Gross range	65%. Interbedded sandstone and mudstone. Sandstone beds are 0.05 – 0.1-m-thick.
Basal bounding surface	Sharp but not erosive from F.0
Upper bounding surface	Sharp, overlain by F.0
Outcrop thickness	Variable, increasing from 30 m to a maximum thickness of 50 m at the Hartbeesfontein locality (Fig.1.13), upper slope turbidite package then thins basinward
Outcrop width / geometry	Occurs only within the most distal 16-km-long Hartbeesfontein section of the Baviaans northern profile (Fig. 1.13)
Example localities	Vleifontein Log locality, Baviaans northern profile (Fig. 1.13).

F.17 – Distributary channel sandstone

Laterally extensive, massive, fine-grained sandstone packages. Sharp based and topped. Buffels North locality.

Erosive base to massive tabular sandstone, overlying interdistributary bay deposits.

Characteristics

Feature	Values and interpretation
Depositional environment	Coastal plain
Description	Extensive tabular fine sandstone packages, fine grained, with internal erosive surfaces.
Sedimentary structures	Predominantly unidirectional ripple lamination, stoss-side preservation occurs locally
Process interpretation	Tractional processes
Bed thickness range	0.5 - 5 m
Net : Gross range	100%.
Basal bounding surface	Erosive into F.18,19
Upper bounding surface	Sharp, overlain by F.19
Outcrop thickness	Individual sandstone packages are between 0.5 & 5-m-thick.
Outcrop width / geometry	Occurs extensively across the study area overlying the typical highly deformed shelf parasequences of the lower Waterford Formation
Example localities	Buffels River North (Fig. 1.13)

F.18 – Inter-distributary crevasse splay

2-m-thick package of pale-grey coarse siltstone beds that exhibit numerous minor scour surfaces. Rail Cut locality.

0.05-0.15 thick siltstone beds that exhibit unidirectional ripple lamination. Bed tops are sharp based and erosive.

Characteristics

Feature	Values and interpretation
Depositional environment	Coastal plain
Description	Pale-grey coarse silt to very fine sand, 5-15-cm-thick beds that exhibit numerous minor scour surfaces,
Sedimentary structures	Predominantly unidirectional ripple lamination but also structureless
Process interpretation	Multiple tractional flows depositing rapidly in an inter-distributary coastal plain setting
Bed thickness range	0.05 - 0.15 m
Net : Gross range	20%.
Basal bounding surface	Erosive into F.19
Upper bounding surface	Sharp amalgamated into F.19
Outcrop thickness	Individual siltstone packages are between 0.5 & 3-m-thick.
Outcrop width / geometry	Occurs extensively across the study area overlying the typical highly deformed shelf parasequences of the lower Waterford Formation
Example localities	Railway cut, Baviaans North profile (Fig. 1.13)

F.19 – Interdistributary bay deposits

Dark grey siltstone package overlain by erosively based channel sandstones. Rail Cut locality.

Dark grey ripple laminated siltstone.

Characteristics

Feature	Values and interpretation
Depositional environment	Coastal plain
Description	Structureless dark grey fine to medium siltstone
Sedimentary structures	Faint ripple lamination
Process interpretation	Suspension fall-out and weak tractional currents
Bed thickness range	Siltstone laminations
Net : Gross range	5%.
Basal bounding surface	Sharp to slightly gradational from F.18
Upper bounding surface	Sharp contact with erosive base of distributary channel sandstone (F.17)
Outcrop thickness	Individual siltstone packages are between 0.5 & 3-m-thick.
Outcrop width / geometry	Occurs extensively across the study area overlying the typical highly deformed shelf parasequences of the lower Waterford Formation
Example localities	Railway cut, Baviaans North profile (Fig. 1.13)

CHAPTER 3.

ENVIRONMENTS OF DEPOSITION AND STRATIGRAPHIC INTERPRETATION

Chapter 3 aims to build on the detailed facies descriptions provided in chapter 2 by establishing key facies associations and providing context for their distribution within the shelf to slope segment of a basin margin scale clinothem (Fig. 3.1). Understanding facies association distribution on a margin profile is not only important for the correct identification of the shelf edge rollover zone (a key feature used in the interpretation of margin trajectory), but also for the establishment of parasequence stacking patterns, which is important in understanding the sequence stratigraphic development of a margin. The latter part of this chapter describes the stratigraphic framework as well as the broad architecture of the margin. It concludes with a sequence stratigraphic interpretation of the lower Waterford margin.

3.1. Sedimentary facies associations

High resolution 3D seismic datasets have provided extensive data on the geometries and architecture of shelf edge delta systems. However there is a notable lack of detailed sub-seismic sedimentary facies information. The data that is available comes from only a limited number of borehole and outcrop studies e.g. Gulf of Mexico, (Sydow & Roberts, 1994; Winn *et al.*, 1995; Kolla *et al.*, 2000), the Eocene Central Basin Spitsbergen (Steel *et al.*, 2000; Plink-Bjorklund *et al.*, 2001; Mellere *et al.*, 2003), the Namurian of County Clare, Ireland (Pulham, 1989; Collinson *et al.*, 1991), the New Jersey Margin (Mountain & Proust, 2010), and Chile (Covault *et al.*, 2009; Hubbard *et al.*, 2010), and Wyoming (Pyles & Slatt, 2007). Bridging the gap between the large scale architectural context afforded by seismic data and the detailed process-based information provided by outcrop studies is a challenge. The extensive outcrop exposure of the lower Waterford Formation provides an opportunity to place detailed process- based observation in an architectural context comparable in scale and geometry to that imaged in seismic datasets (Fig. 3.1).

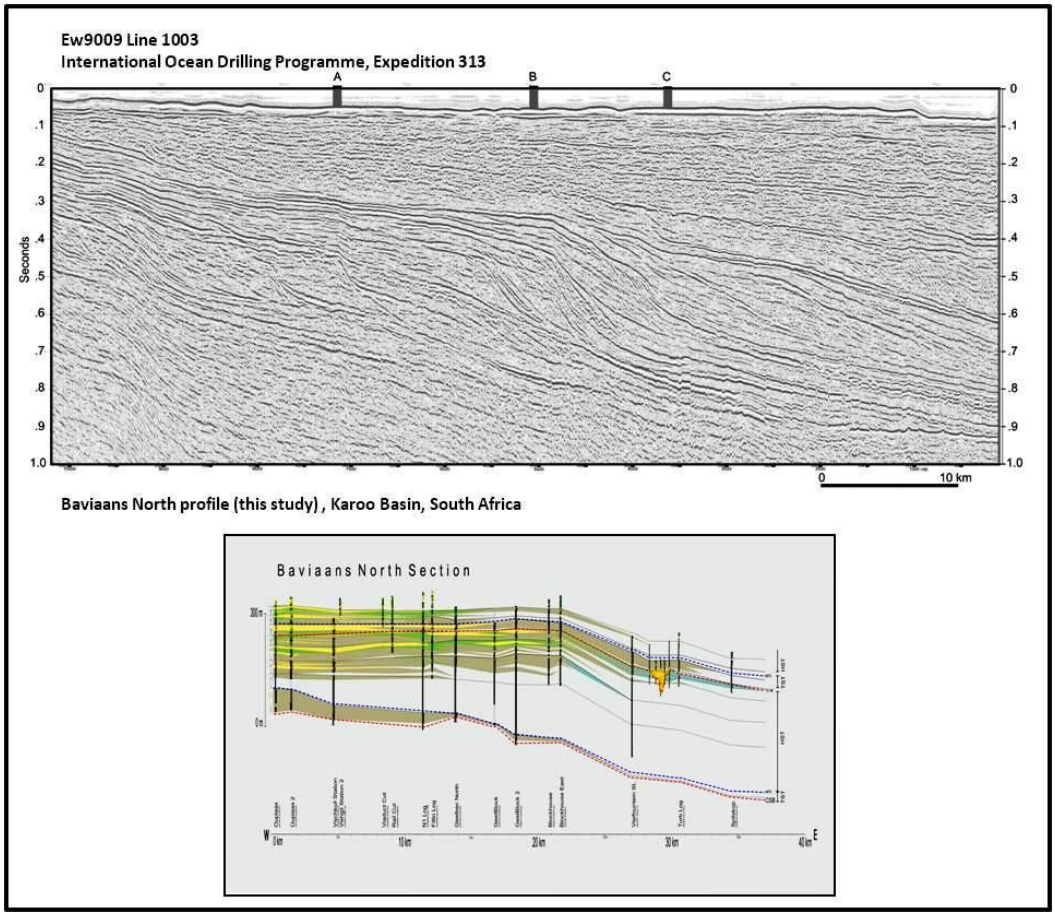

Figure 3.1: Comparison of seismically imaged basin margin profile from the New Jersey Margin (adapted from Mountain & Proust, 2010) and the outcrop based profile of the Waterford margin (For high resolution PDF image see incerted CD) constructed as part of this study. Both images are at approximately similar horizontal and vertical scales.

The lithofacies analysis carried out in this work followed the approach of Mutti & Ricci Lucchi (1975) in considering a sedimentary *facies* as a "layer or group of layers showing lithological, geometrical and sedimentological characteristics which are different from those of adjacent layers. A facies is considered to be the product of a specific depositional mechanism or several related mechanisms acting at the same time". A *facies association* is a "combination of two or more facies forming sedimentary bodies of various scales and degrees of organization". A facies association is considered to be the preserved spatial expression of a depositional environment or process". In this work the prefix *litho-* is added to *facies* used by Mutti & Ricci Lucchi (1975) in order to strictly relate them to the lithological characteristics and to avoid confusion with other categories of facies (e.g. seismic facies). Based on these premises, nine lithofacies were recognized, described and interpreted in this work.

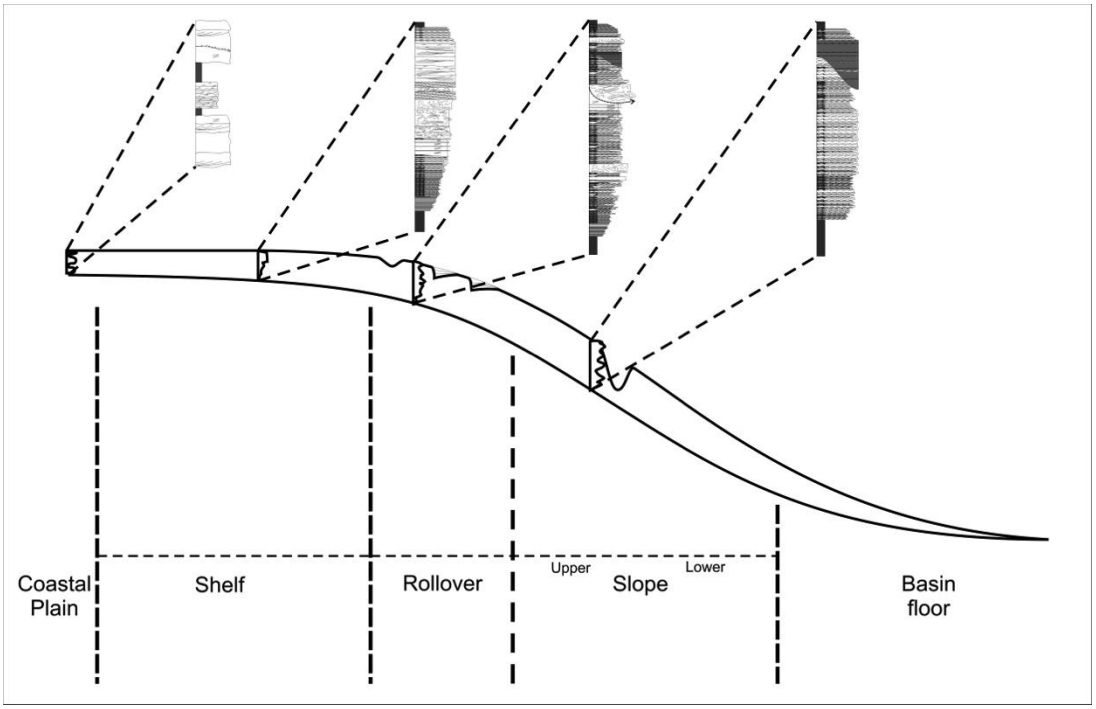

Figure 3.2: Schematic diagram depicting a basin margin scale clinothem divided into coastal plain (CP), shelf (S), shelf edge rollover (SR), upper slope (US), lower slope (LS) and basin floor (BF) segments. The diagram also shows typical parasequences for the four key depositional settings relevant to this study (coastal plain, shelf, rollover and slope). Parasequences are typicaly 10's of meters thick.

The sedimentary facies scheme established in chapter 2 is based on lithology, grain size and sedimentary structures, and is considered to be the product of a specific depositional mechanism or several related mechanisms acting at the same time. Facies can be grouped based on the broadly similar process that acted during their deposition (Table. 3.2). Therefore, sedimentary facies associations identified in the lower Waterford Formation can

be attributed to four broad depositional environments: 1) coastal plain (CP), 2) shelf (S), 3) shelf edge rollover (SR) and 4) upper slope (US) (Fig. 3.2). The different environments of deposition will be described at the scale of parasequences from distal to proximal settings, which is also the typical stratigraphic arrangement observed in this progradational succession.

<table>
<tr><th colspan="6">Facies and facies associations</th></tr>
<tr><td></td><td colspan="2">Facies</td><td colspan="2">Facies associations</td><td>Depositional settings</td></tr>
<tr><td>Facies No.</td><td>Delta (Based on rollover paper)</td><td>Shoreface</td><td>Delta</td><td>Shoreface</td><td>(CP)= coastal plain, (S) = shelf, (SR)= Shelfc edge rollover, (US)= Upper slope</td></tr>
<tr><td>F.0</td><td colspan="2">Distal offshore</td><td colspan="2">Offshore</td><td>S, SR, US,</td></tr>
<tr><td>F.1</td><td>Offshore</td><td></td><td colspan="2" rowspan="2"></td><td rowspan="2"></td></tr>
<tr><td>F.2</td><td>Distal prodelta</td><td rowspan="2"></td></tr>
<tr><td>F.3</td><td>Prodelta</td><td rowspan="2">Prodelta</td><td rowspan="2"></td><td rowspan="2">S, SR, US</td></tr>
<tr><td>F.4</td><td></td><td>Shoreface-offshore transition</td><td>Shoreface-offshore transition</td></tr>
<tr><td>F.5</td><td colspan="2">Margin of mass flow deposit</td><td rowspan="3">Deformed lower delta front</td><td rowspan="3">Deformed shoreface</td><td rowspan="3">S, SR</td></tr>
<tr><td>F.6</td><td colspan="2">Axis of mass flow deposit</td></tr>
<tr><td>F.7</td><td colspan="2">In-situ deformed</td></tr>
<tr><td>F.8</td><td>Lower delta front</td><td rowspan="2"></td><td rowspan="3">Wave-dominated upper delta front with fluvial influence</td><td rowspan="3"></td><td rowspan="3">S, SR</td></tr>
<tr><td>F.9</td><td>Delta front</td></tr>
<tr><td>F.10</td><td></td><td>Lower shoreface</td><td>Lower shoreface</td></tr>
<tr><td>F.11</td><td>Distal mouthbar</td><td></td><td colspan="2">Distal mouthbar</td><td>S</td></tr>
<tr><td>F.12</td><td>Bioturbated prodelta</td><td></td><td rowspan="2">Bioturbated prodelta</td><td rowspan="2"></td><td rowspan="2">S, SR</td></tr>
<tr><td>F.13</td><td></td><td>Bioturbated Shoreface-offshore transition</td><td>Bioturbated Shoreface-offshore transition</td></tr>
<tr><td>F.14</td><td colspan="2">Channel lag conglomerate</td><td colspan="2" rowspan="2">Slope channel fill</td><td>S, US</td></tr>
<tr><td>F.15</td><td colspan="2">Slope channel fill</td><td>US</td></tr>
<tr><td>F.16</td><td colspan="2">Upper slope turbidites</td><td colspan="2">Upper slope turbidites</td><td>US</td></tr>
<tr><td>F.17</td><td colspan="2">Distributary channel sandstone</td><td colspan="2" rowspan="3">Coastal plain</td><td rowspan="3">CP</td></tr>
<tr><td>F.18</td><td colspan="2">Overbank or floodplain deposits</td></tr>
<tr><td>F.19</td><td colspan="2">Interdistributary bay deposits</td></tr>
</table>

Table 3.1: Linkage of the 19 delta and shoreface associated facies described in chapter 2 to delta and shoreface facies associations. Key depositional settings: US = Upper slope, R = Shelf edge rollover, S = Shelf, CP = Coastal plain.

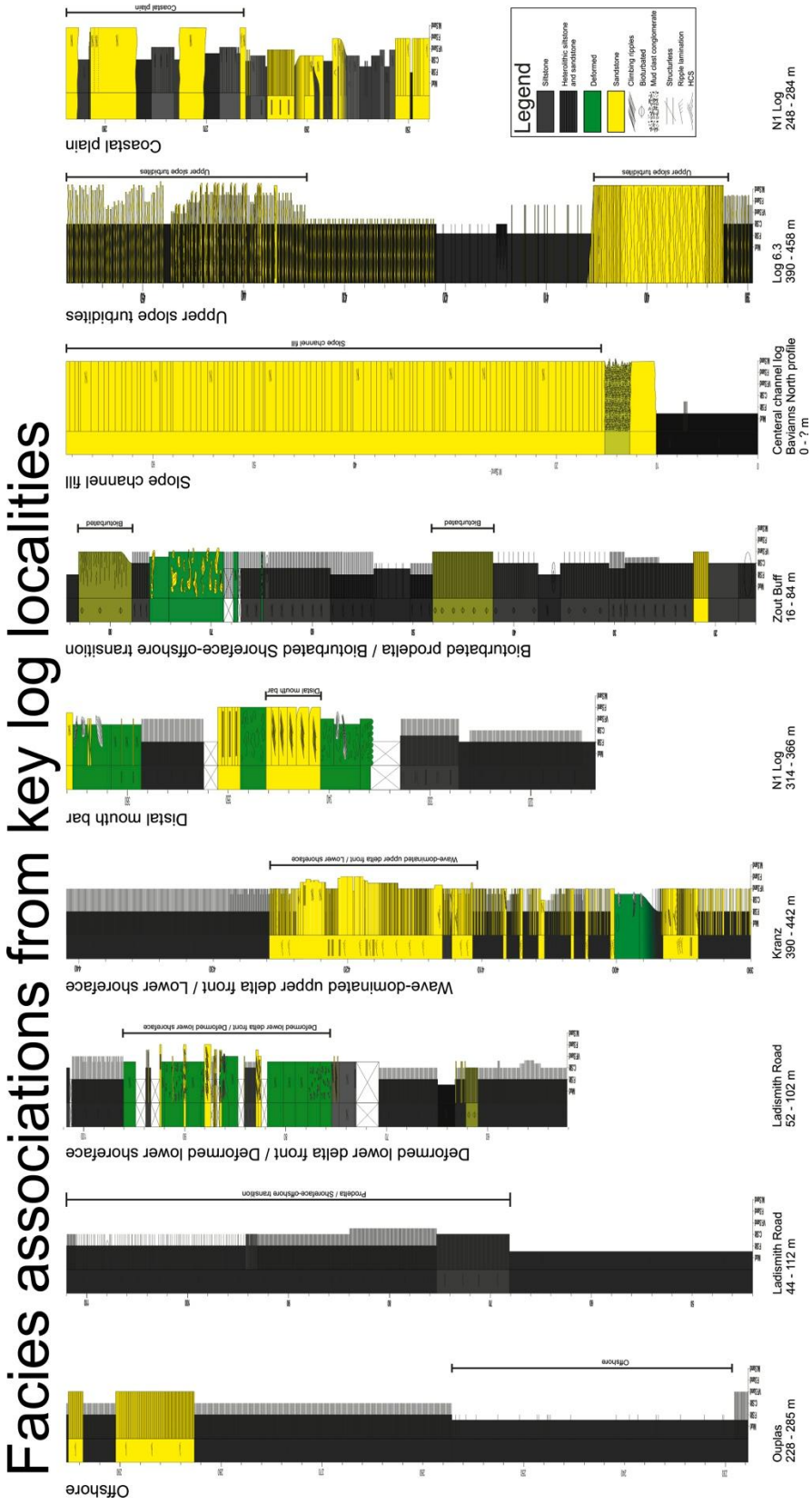

Figure 3.3 Logged intervals of key facies from type sections. For stratigraphic context of loged intervals refer to Apendix C for full corelation pannels.

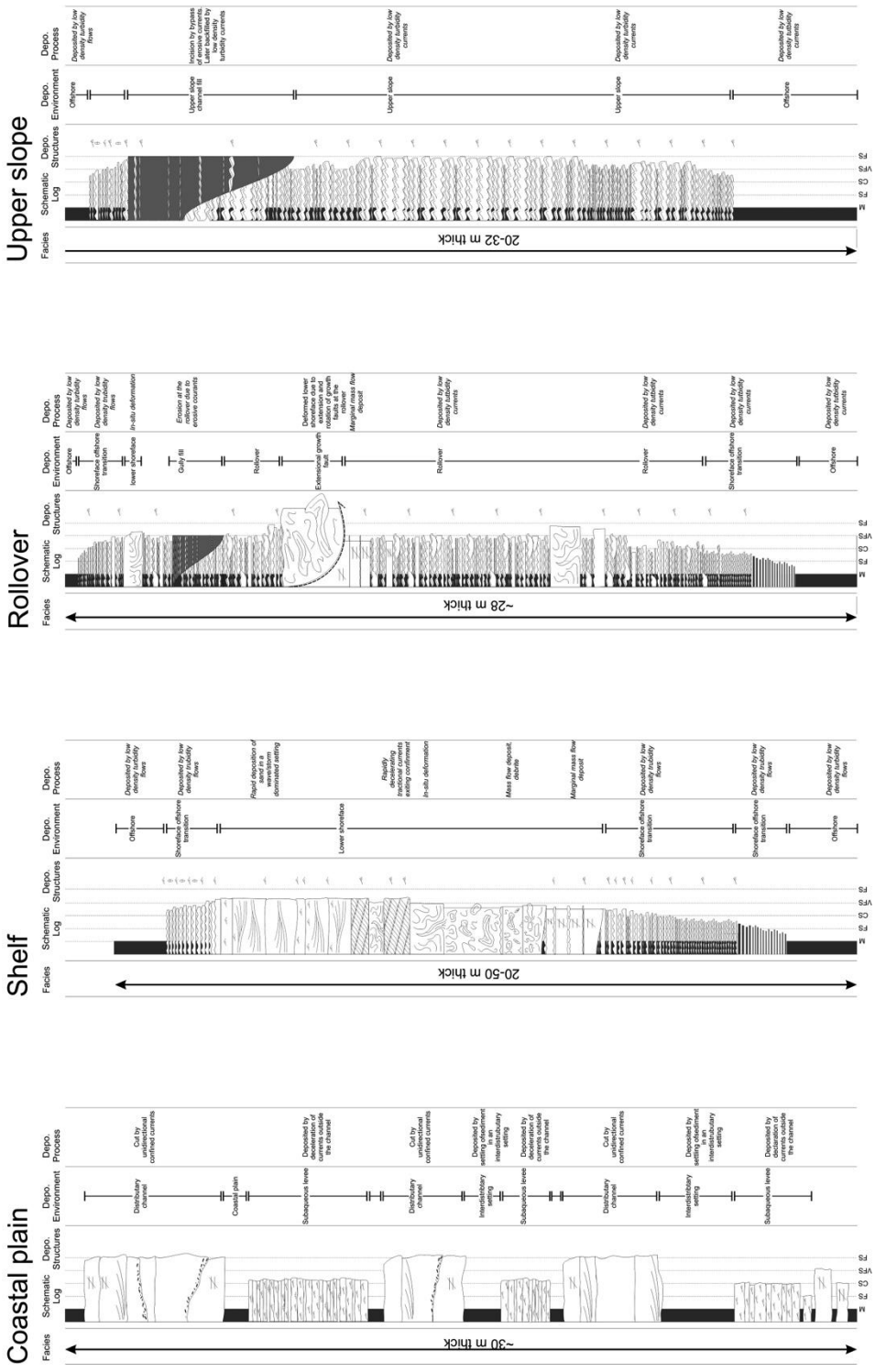

Figure 3.4: Graphical representations of typical parasequences in four key depositional settings: (A) Coastal plain (B) Shelf (C) Rollover (D) Upper slope. Logs exhibit chariceristicsof typical depositional settings but are not representative of specific localities.

3.1.1. Upper slope setting (Fig. 3.4D)

Typically, parasequences on the upper slope are thicker than those on the shelf, and exhibit an aggradational profile (Fig. 3.5A) with a sharp base above offshore mudstones (Fig. 3.5B) and a fining- and thinning-upward trend at the top of the parasequence (Fig. 3.4D). The dominant facies of upper slope parasequences are thin (<5 cm), tabular, planar- and ripple-laminated, very fine-grained sandstone and siltstone beds, deposited from dilute and unconfined turbidity currents (F.16) (Fig. 3.5D). Locally, medium-bedded successions exhibit climbing-ripple laminated and stoss-side preserved, sigmoidal climbing ripple lamination that suggests rapid deposition from turbidity currents (Fig. 3.3H) (Fig. 3.5C). Large scale isolated channel-fill features have been observed with up to 60 m of incision, cutting down from the top of upper slope parasequences into the underlying slope mudstone succession (chapter 4). The fills of the channels are dominated either by amalgamated sandstones (F. 15) (Fig. 3.3G) and mudstone clast conglomerates (F.14) or by heterolithic deposits (F.4). The presence of channel-fills cutting into thick turbidite packages is consistent with an increased gradient and delivery of sediment to the upper slope with incision and transport of coarse-grained sediment farther into the basin.

3.1.2. Shelf edge rollover setting (Fig. 3.4C)

The main distinguishing features between parasequences at the shelf edge rollover area with their up dip shelf counterparts are a basinward thickening trend, an increase in erosional features (chapter 4) (Fig. 3.6B & E), gravity-driven soft-sediment deformation (Fig. 3.6A), and a decrease in *in-situ* soft sediment deformation. These parasequences exhibit an asymmetrical profile that coarsens and thickens upward from mudstone (F.0) into heterolithic weakly normally graded and current ripple laminated siltstones and sandstones (F.4) (Fig. 3.3B). The heterolithic packages interfinger with thicker bedded, tabular, sigmoidal ripple laminated slope turbidite deposits (F.16)) (Fig. 3.6C & D). Styles of deformation vary across the shelf edge rollover and include mass flow deposits (F.5, F.6) (Fig. 3.6C) that thin abruptly basinward across the rollover zone. The lower shoreface deposits (F.10) that characterize the upper part of shelf parasequences are less well developed or heavily *in-situ* deformed at the shelf edge rollover. Jones *et al.* (2013) (chapter 4) describe landward thickening wedges of rotated sandstones interpreted as the fills of small growth faults (Fig. 3.6A). There is also a significant increase in abundance and scale of scours (Fig. 3.6B & E), these features are interpreted as small channel- and gulley-fills.

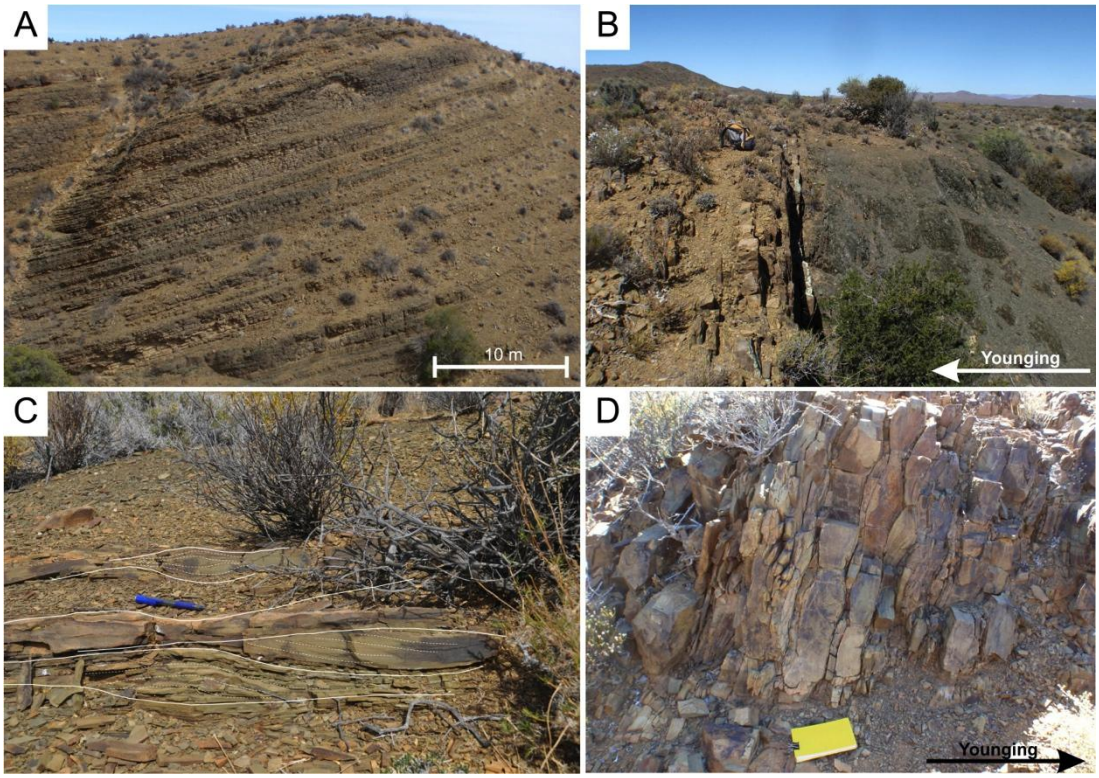

Figure 3.5: Facies associations of upper slope parasequences. (A) Undeformed turbidite sandstone and siltstone package thickening basinward beyond the shelf edge rollover (B) Typical sharp base to basinward thickening slope turbidite deposits. (C) & (D) Interbedded to amalgamated sandstone beds making up the basinward thickening turbidite package. Beds exhibit sigmoidal bedforms with stoss-side preserved climbing ripple lamination, indicating rapid deposition from turbidity currents. For high resolution image see incerted CD.

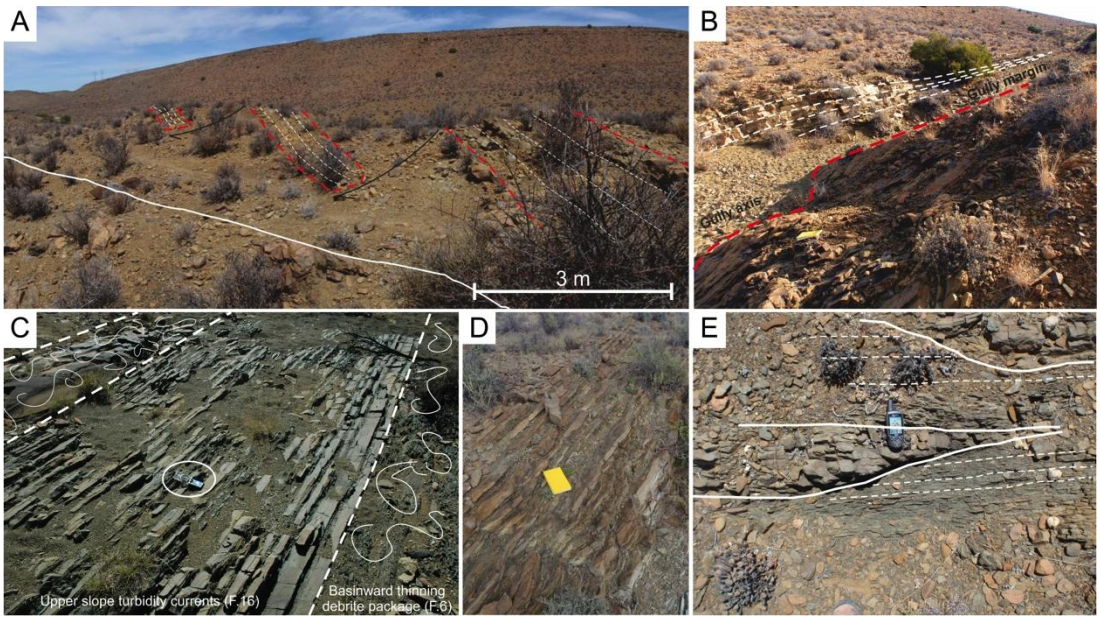

Figure 3.6: Shelf edge facies associations. (A) Rotation of bedding above growth fault of WfC 3 on the Baviaans North section, showing preferential rotation to the west. Solid white line indicates the lower datum used to constrain the geometries of the growth faults. (B) The stepped margin of a shallow gully cutting into the top surface of WfC 4 along the Baviaans North section. (C) Interfingering of heterolithic upper slope turbidite deposits and deformed facies that thin rapidly basinward at the shelf edge. (D) Interbedded sandstone and siltstones; sandstone beds have sheet geometries, internally sigmoidal current ripple

laminated, and sharp, occasionally erosional bases. Tops are sharp and unidirectional ripple laminated. (E) Small erosive sandstone filled scours cutting into offshore and shoreface-offshore transition facies. Erosive scours are numerous at the rollover position and are commonly 2-m-wide with 0.5-m of incision with mud chip lags mantling the erosion surface. For high resolution PDF image see inserted CD-ROM.

3.1.3. Shelf setting (Fig. 3.4B)

Typically, the arrangement of sedimentary facies in shelf parasequences results in an overall coarsening and thickening upward profile (Fig. 3.4B & 3.7A). Bases of parasequence consist of fine-grained, dark-grey predominantly thinly bedded mudstone and siltstone offshore deposits (F.0 & 1) (Fig. 3.7D) (Fig. 3.3A), interpreted to be deposited by dilute turbidity currents. Offshore deposits coarsen and thicken upward into prodelta or shoreface-offshore transition deposits consisting of interbedded, normally-graded thin sandstone and siltstone beds that exhibit unidirectional ripple lamination (F.2, 3 & 4) (Fig. 3.3B) and are therefore interpreted as the deposits of low density turbidity currents. Commonly, multiple packages of soft sediment deformation dominate the middle portions of shelf parasequences (F.5, 6 & 7). The lower part of the deformed package usually consists of structureless, poorly-sorted sandy siltstone (F.5) overlain by contorted and rounded fine-grained sandstone blocks supported by a poorly sorted sandy siltstone matrix (F.6) (Fig. 3.7C). These disaggregated units are interpreted as debrites in a deformed shoreface-offshore transition zone environment. In the upper part of the deformed sandstones package, upward directed features are consistent with *in-situ* deformation (Oliveira *et al.*, 2011) (F.7) (Fig. 3.3C) (Fig. 3.7E). These facies are interpreted to represent deposition in an unstable lower shoreface environment. Typically, the upper part of the shelf parasequence consists of undeformed, amalgamated sandstones exhibiting hummocky cross-stratification and wave and current ripple lamination (F.10) (Fig. 3.3D) (Fig. 3.7B), which suggests deposition in a wave-dominated lower shoreface setting. Locally, climbing-ripple sandstone dominated packages overlie the soft-sediment deformed units (F.11). The abundance of climbing ripple lamination suggests rapid deposition from unidirectional tractional currents. The local lack of wave influence, scouring and the abundant silt and mud content of the sandstone indicates a high terrigenous content, which supports a fluvial dominated distal mouth bar setting with flows depositing rapidly on exit from up-dip confinement (Al-Aasm *et al.*, 1996; Johannessen & Steel, 2005; Olariu & Bhattacharya, 2006; Enge *et al.*, 2010) (chapter 4) (Fig. 3.3E). Commonly a fining- and thinning-upward package of bioturbated shoreface-offshore transition deposits consisting of heterolithic sandstones is preserved at the top of the parasequence (F.12 &13) (Fig. 3.3F). This is interpreted to be due to a reduction in sediment supply associated with a rise in relative sea-level.

3.1.4. Coastal plain setting (Fig. 3.4A)

Overlying the shelf parasequences in the Laingsburg area is a ~300-m-thick succession of coastal plain parasequences (Fig. 3.3I). In many sections the transition from coarsening- and thickening-upward parasequences dominated by *in-situ* deformation to an undeformed coastal plain succession is relatively abrupt and commonly marked by shallow erosive scours filled by intra-formational clast supported conglomerate (F.14) (Fig. 3.8B). The westward (up dip) (Fig. 1.13) limit of outcrop means that shelf parasequences cannot be traced landward into coastal plain parasequences.

Massive, fine-grained sandstone packages (0.5-6-m-thick) are sharp based and topped (F.17) (Fig. 3.8A) and contain minor cross bedding at bed bases. Locally, erosional surfaces cross-cut the larger sandstone units. The lateral extent of sandstone bodies varies from a few metres to hundreds of metres. The siltstone dominated packages range in thickness from 0.4 to 5-m and can be divided into two distinct facies (Fig. 3.8C). The first consists of structureless, dark grey siltstone with occasional coarse siltstone laminations (F.18). The second consists of green-grey, coarse siltstone beds (5-15-cm-thick) (F.19). The siltstone beds are generally poorly sorted and exhibit minor normal grading at the very top of the bed. Internally, beds are unidirectional ripple laminated but also exhibit a high degree of internal scouring. Bed bases are commonly highly erosive; bed tops are generally sharp but often amalgamated.

The sharp based, erosive nature of the sandstones combined with their geometry and stratigraphic context, leads to their interpretation as distributary channel sandstone bodies. The thin bedded, unidirectional ripple laminated, coarse siltstones indicate multiple decelerating tractional flows depositing rapidly. This facies is bounded by finer grained structureless siltstones and is interpreted to represent overbank or floodplain deposits. Palaeosols are not well developed. The fine-grained structureless siltstones represent deposition by suspension settling in an inter-distributary bay setting.

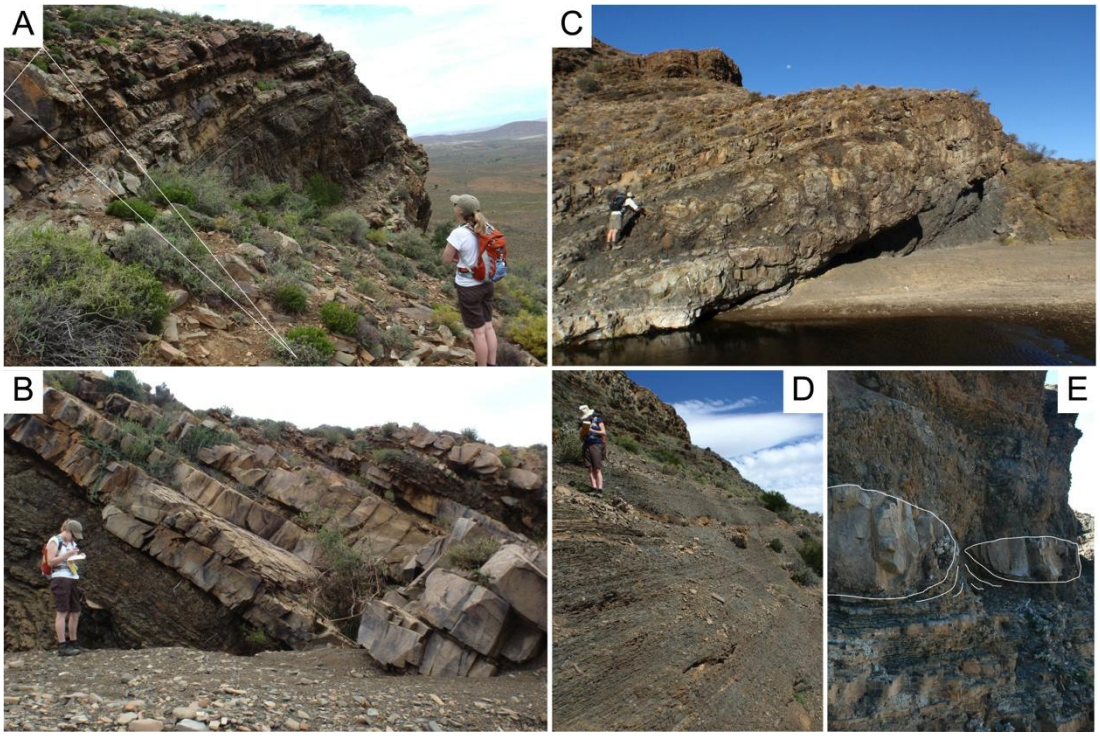

Figure 3.7: Shelf parasequence facies associations. (A) Typical coarsening and thickening up shelf parasequence, approximately 25-m-thick. (B) Thick-bedded, amalgamated, fine-grained, lower shoreface sandstone. (C) Heavily deformed and disaggregated deposits. (D) Thinly laminated siltstone deposited by low density turbidity currents as distal delta toesets. (E) *In-situ* deformed structureless sandstone blocks related to foundering into unconsolidated, water-laden substrate. For high resolution PDF image see incerted CD.

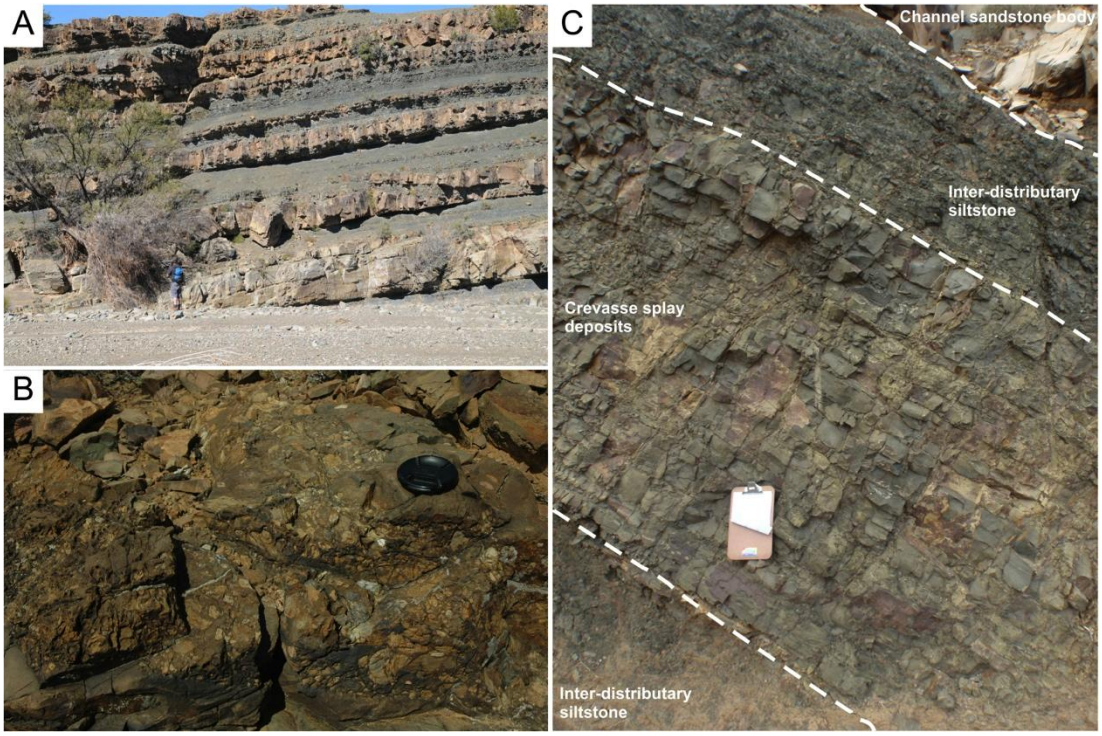

Figure 3.8: Coastal plain facies associations. (A) Tabular sandstone and siltstone deposits. Sandstone packages are tabular and extensive for many hundreds of metres; internally packages exhibit erosive channel cuts and accretionary surfaces but generally lack internal lamination. (B) Locally large erosive surfaces cross-cut the sandstone units and are commonly mantled by intra-formational conglomerate lags with clasts that are sub-

rounded and matrix supported (camera lens cap for scale). (C) Separating the tabular sandstone packages are fine grained units consisting of (1) structureless dark grey siltstone, interpreted as inter-distributary deposits and (2) Pale-grey coarse silt, 5-15-cm-thick siltstone beds that exhibit unidirectional ripple lamination but also numerous minor scour surfaces, interpreted as crevasse splay deposits. For high resolution PDF image see incerted CD.

3.2. Margin development

The Waterford Formation is part of a 1.8-km-thick shallowing-upward basin margin succession (Flint *et al.*, 2011b) (chapter 1). The upper Fort Brown to lower Waterford succession can be divided into 9 sand-prone units separated by regionally extensive and correlatable mudstone units. Stratigraphically from the base, these sand-prone units are referred to as Unit G, and Waterford Clinothems (WfC) 1-8 (Fig. 1.15 & 3.9). The east–west orientation of the post depositional fold axes and east-north-east palaeoflow direction make the Laingsburg depocentre an ideal locality to constrain depositional process variability and architectural development of the upper slope to shelf. This chapter focuses on the Zoutkloof syncline from the up-dip Zoutkloof River locality to the Koup Station locality, 41 km down dip (Fig. 3.10). The ~400-m-thick succession from base Unit G to WfC 8 represents the transition from mudstone dominated middle to upper slope, through the shelf edge rollover to a wave dominated, fluvial influenced shelf setting.

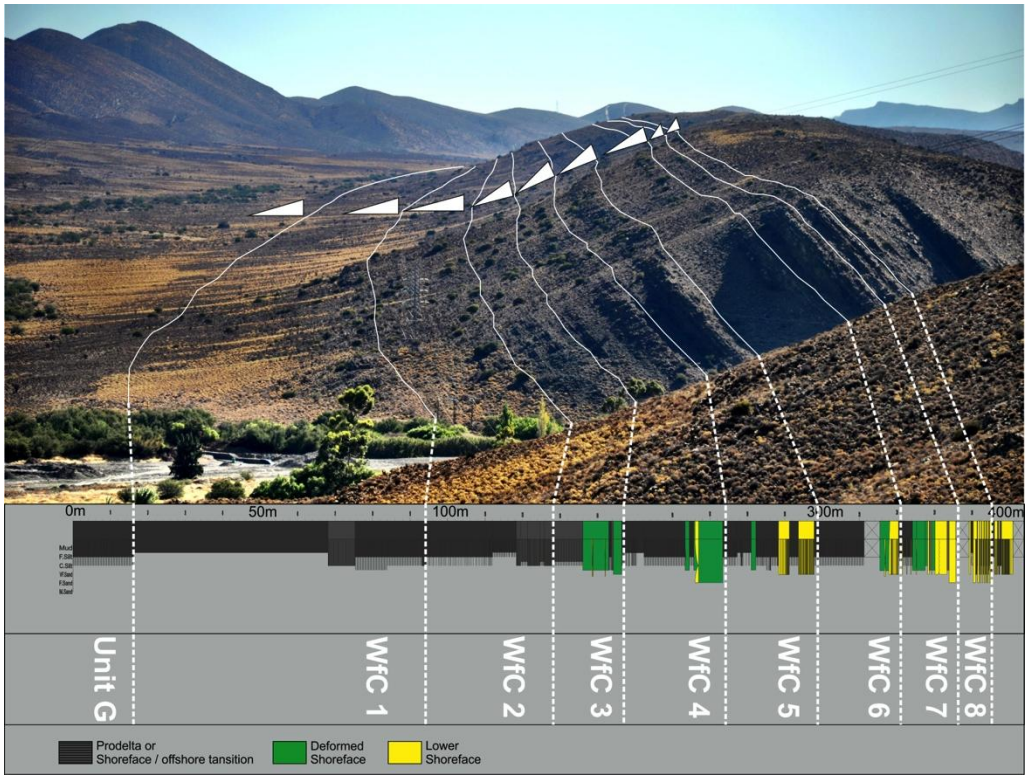

Figure 3.9: Overview of the Ladismith road section showing the 9 sand-prone units. White lines represent the regionally extensive and correlatable mudstone units. Locality: Ladismith road log section.

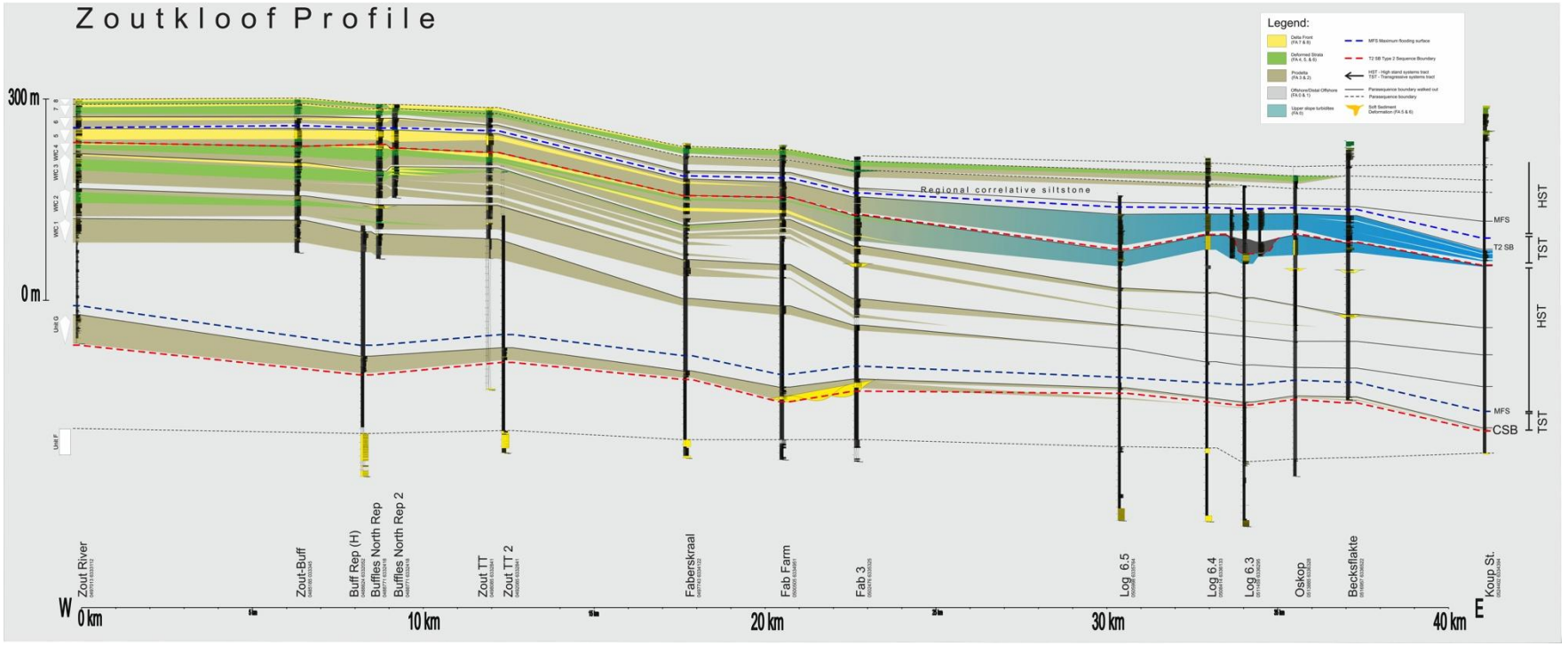

Figure 3.10: Zoutkloof correlation panel (Fig. 1.13) showing the eight lower Waterford parasequences. Bounding flooding surfaces are shown as well as interpreted maximum flooding surfaces and sequence boundaries. The panel uses Unit F as a correlation unit. Prodelta strata are khaki, deformed strata are green and amalgamated sandstone bodies are yellow and show the maximum progradational extent of the lower Waterford Formation. Upper slope turbidite deposits are blue. For high resolution PDF image see incerted CD.

Unit G is 42-m-thick in the proximal Zoutkloof River (Fig. 3.10) area and the sandy component thins basinward (eastward) to 19-m at Faberskraal Farm (Fig. 3.10). Generally, Unit G exhibits an irregular, but overall symmetrical vertical-profile that comprises predominantly heterolithic thin-bedded siltstones and sandstones (F.1, 2 & 3), with areas of thicker (7-28 cm) siltstone to very fine sandstones beds that are characterized by sigmoidal, stoss side-preserved climbing ripple lamination (F.16), which indicate rapid deposition from sediment gravity flows. The deposits share characteristics of submarine levee deposits identified in the underlying stratigraphy (e.g. Kane & Hodgson, 2011). At Faberskraal Farm (Fig. 3.10) a broad ~300-m-wide, shallow (<15 m) incision surface lined with a thin mudstone clast conglomerate cuts down from midway in Unit G and is filled by structureless amalgamated fine-grained sandstone (F.15). East of Faberskraal Farm, Unit G thins, becoming dominated by tabular turbidite sandstones interpreted as off-axis lobe deposits (Personal communication with Brunt, 2012). The stratigraphic context, the dominance of fine grained low density turbidites in the proximal exposures of Unit G, and the occurrence of local channelization, suggest an upper slope setting with local intraslope lobes. The reason for the development of intraslope lobes is not clear, although this may relate to differential compaction above the underlying stratigraphy.

Unit G is overlain by a regionally extensive 80-m-thick mudstone marker package (Fig. 3.10), above which WfC 1 – 3 are considered to be upper slope to shelf parasequences. In the most proximal exposures, these parasequences are 45 – 25-m-thick and are characterized by their symmetrical profiles that initially coarsen and thicken then fine and thin upward (Fig. 310). WfC 1 consists of a coarsening up succession (F.0 & 4) interpreted as a siltstone dominated upper slope parasequence with limited coarse sediment supply beyond the shelf edge rollover. By contrast, WfC 2 and 3 are typical shelf parasequences, dominated by extensive soft sediment deformation (F.5, 6 & 7) and lower shoreface deposits (F.10), which mark a basinward stepping over WfC 1. These two parasequences change basinward into siltstone dominated slope parasequences beyond their respective shelf edges (Fig. 3.10).

Proximal exposures reveal that WfC 4 and 5 are notably thinner than the underlying parasequences (Fig. 3.10) at 20 and 15-m-thick respectively, and they typically exhibit a more asymmetrical coarsening- and thickening-upward profile with sharp top surfaces. In its proximal position, WfC 4 is a shelf parasequence, but it exhibits the greatest degree of soft sediment deformation (F.5, 6 & 7) of all the lower Waterford Formation parasequences. The WfC 4 shelf edge rollover is situated slightly further basinward than

that of WfC 3 (Fig. 3.10). Dip correlations of WfC 4 reveal that it transitions basinward through a typical rollover parasequence (Fig. 3.4C), characterized by erosion and increasing dominance of turbidites, to a characteristically sand dominated slope parasequence, dominated by extensive sheet turbidites and an absence of soft sediment deformation (Fig. 3.4 A-D & 3.10). A late stage, mud-filled channel cuts down from the slope turbidite deposits indicating sediment bypass and delivery further out into the basin. This channel occurs at the same stratigraphic interval and in a similar interpreted upper slope setting as the turbidite-filled channel documented in chapter 4.

In its proximal exposures WfC 5 (Fig. 3.10) is a typical coarsening and thickening upward parasequence with a sharp reworked top surface that exhibits typical shelf parasequence characteristics, but is distinctive due to a lack of significant soft sediment deformation and the abundance of amalgamated lower shoreface deposits (F.10). Basinward correlations show a similar transition to that seen in WfC 4, from rollover parasequence to sandstone dominated slope parasequence.

Abruptly overlying the reworked top surface of WfC 5 is a regionally extensive fine grained marker unit that is thin (<5 m) and siltstone dominated in the most proximal (westerly) exposures and thicker (>30 m) and mudstone dominated in the most distal (easterly) localities.

WfC 6, 7 and 8 (Fig. 3.10) are typically thinner (8 – 15 m) than the underlying parasequences and are characterized by a uniform thickness along their dip profiles. They are interpreted as shelf parasequences (Fig. 3.4B) dominated by deformed and lower shoreface deposits (F.6 & 7). Regional correlation of WfC 6, 7 and 8 of reveals basinward stepping of the system, and WfC 6 and 7 pass into the regional fine grained marker unit (Fig. 3.10). The sandy component of WfC 6 has a relatively limited dip extent with deformed and lower shoreface deposits confined to positions landward of the shelf edge rollover established by WfC 5. WfC 7 shows further basinward progradation, but again the sandy component is confined to the shelf (Fig. 3.10). Regional correlation of WfC 8 shows that deformed and lower shoreface deposits typical of a shelf parasequence are present along almost the entire Zoutkloof profile and therefore represents a significant basinward stepping of the system with little aggradation. WfC 6, 7 and 8 are interpreted to represent the progradation and reestablishment of the deltaic system after the underlying regional transgression. Overlying WfC 8 several similar, thin (<10 m) shelf style parasequences have

been recorded, however, due to their highly variable nature they have not been correlated with the same degree of confidence.

3.3. Shelf-slope-basin configuration

Despite the extensive dip exposure of the lower Waterford Formation along the Zoutkloof panel (>41 km) (Fig. 3.10) it is still not possible to constrain a complete dip profile from coastal plain to basin floor. Therefore, a combination of quantitative and qualitative methods has been employed in order to better understand the character and architecture of the lower Waterford clinoforms and their development through time.

The migration path of the shelf edge rollover is commonly described from seismic datasets and has increased our understanding of the depositional architecture and stratigraphic evolution of basin margins (e.g. Suter & Berryhill, 1985; Morton & Suter, 1996; Monteverde *et al.*, 2008; Ryan *et al.*, 2009; Vanessa Kertznus & Ben Kneller, 2009; Sanchez *et al.*, 2012b, a). Constraining the position of successive shelf edge rollover positions has been key to understanding the basin margin architecture and the stratigraphic evolution of the lower Waterford Formation. The dip profile exposure along the Zoutkloof profile not only allows the identification of the shelf edge rollover but also enables sedimentary processes, stacking patterns and depositional architecture at the shelf edge rollover, to be constrained for successive basin margin scale clinothems; their lateral variability is discussed in chapter 5.

Water depth is understood to be one of the primary controls on the geometry of basin margin clinothems, in particular the height of the stratal units as they prograde into the basin (Steel & Olsen, 2002). Porębski & Steel (2003) suggested that basin margin scale clinoform geometries are generally not produced if the maximum relief (water depth) from shelf to basin floor is less than 150-200 m. In settings where water depth is greater than 200 m a well-established link between increasing water depth and greater clinoform amplitude has been established (Driscoll & Karner, 1999; Steel & Olsen, 2002; Uličný *et al.*, 2002).

Basin floor deposits (toesets) associated with the lower Waterford Formation clinothems have not been identified, making it difficult to establish the height of the clinothems observed. However, it is possible to make minimum estimates of clinoform heights. The pinching and thinning out of deformed strata combined with an increase in thickness of the parasequence is interpreted to represent a position at or close to the clinoform rollover

(Jones *et al.*, 2013) (chapter 4). Physical correlation of parasequences from the shelf edge rollover to the most distal intra-slope position (Koup Station locality (Fig. 3.10) enables the vertical stratigraphic thickness between the toeset and shelf edge rollover of the clinoform to be measured. This therefore provides a minimum, compacted clinoform height.

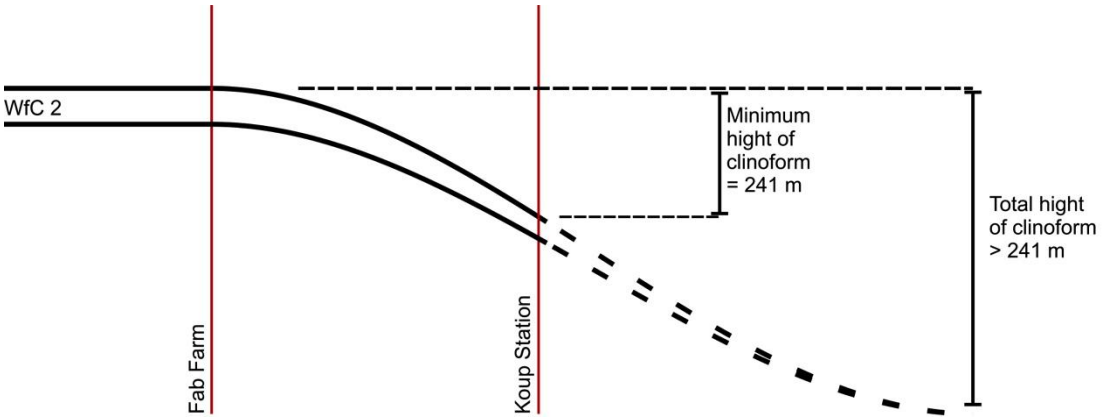

Figure 3.11: Minimum clinoform height is calculated using the most proximal and distal logged sections hung from a base datum, and measuring the stratigraphic thickness difference between the two clinoform intersection points. The base datum is probably dipping basinward. WfC 2 is the first clinoform with a clearly identifiable rollover and therefore has the longest observable foreset length; this provides a minimum compacted clinoform height of 241-m. However, without a mapped time equivalent basin floor control point it is not possible to give a maximum clinoform height value.

WfC 2 is the oldest clinoform to exhibit an identifiable shelf edge rollover. As a result, its exposed coeval slope segment is the longest of the lower Waterford Formation clinothems, which means that it exhibits the greatest stratigraphic thickness between shelf edge rollover and its correlated toeset. A minimum, compacted, clinoform relief of 241 m is calculated for WfC 2.

Increasing basinward compaction of stratal packages due to the fining and thinning of the clinothems results in steepening of buried shelf gradients, which can change the clinoform trajectory. Despite this, the fact that no evidence for any subaerial exposure along any of the 8 clinothem topsets (a distance of >40 km) and the constant thickness of shelf parasequences suggests that shelf gradients must have been low, in the region of 0.01° (see chapter 4). The amplitude of any relative sea-level fall was also low, which is indicated by the absence of incised valleys. Quantifying clinoform gradient for the lower Waterford Formation is difficult but a number of key indicators such as slope length, subtle geometric change between shelf and slope and the fine grain size suggest that this was a low gradient basin margin-scale system.

3.4. Sequence stratigraphy

Above Unit G there is a marked change in the style of sedimentary processes and stacking patterns from the underlying 500-m-thick submarine slope succession. In the absence of a chronostratigraphic framework and the inability to map units all the way down dip into basin floor mudstones means we are not able to apply the criteria of Flint *et al.* (2011b) to define sequence sets, composite sequences and composite sequence sets.

Above Unit G (Fig. 3.12) is a thick regional mudstone, which is interpreted to contain the deepwater equivalent of a maximum flooding surface. WfC 1 – WfC 4 show a clear progradational stacking pattern with well-developed topsets (Fig. 3.10), consistent with a highstand systems tract where sediment supply was able to outpace accommodation generation (Fig. 3.12). The change from progradational to aggradational stacking pattern and absence of subaerial exposure and fluvial incision associated with WfC 4 is consistent with a regressive surface of marine erosion (sequence boundary) (Fig. 3.12) (Vail *et al.*, 1977b; Van Wagoner *et al.*, 1990). The sequence boundary is placed along the erosive surface near the top of WfC 4 due to the fine grained mudstone flooding surface at the base of the channel fill that separates WfC 4 from 5. The sequence boundary is associated with significant slope turbidites (chapter 4). WfC 5, which does not prograde as far basinward as WfC 4, represents the transgressive systems tract (Fig. 3.12). The regional mudstone interval overlying WfC 5 is interpreted to include the next offshore equivalent of a maximum flooding surface (MFS) and WfC 6, 7 and 8 exhibit a strongly progradational stacking pattern which is interpreted as a return to a HST (Fig. 3.12).

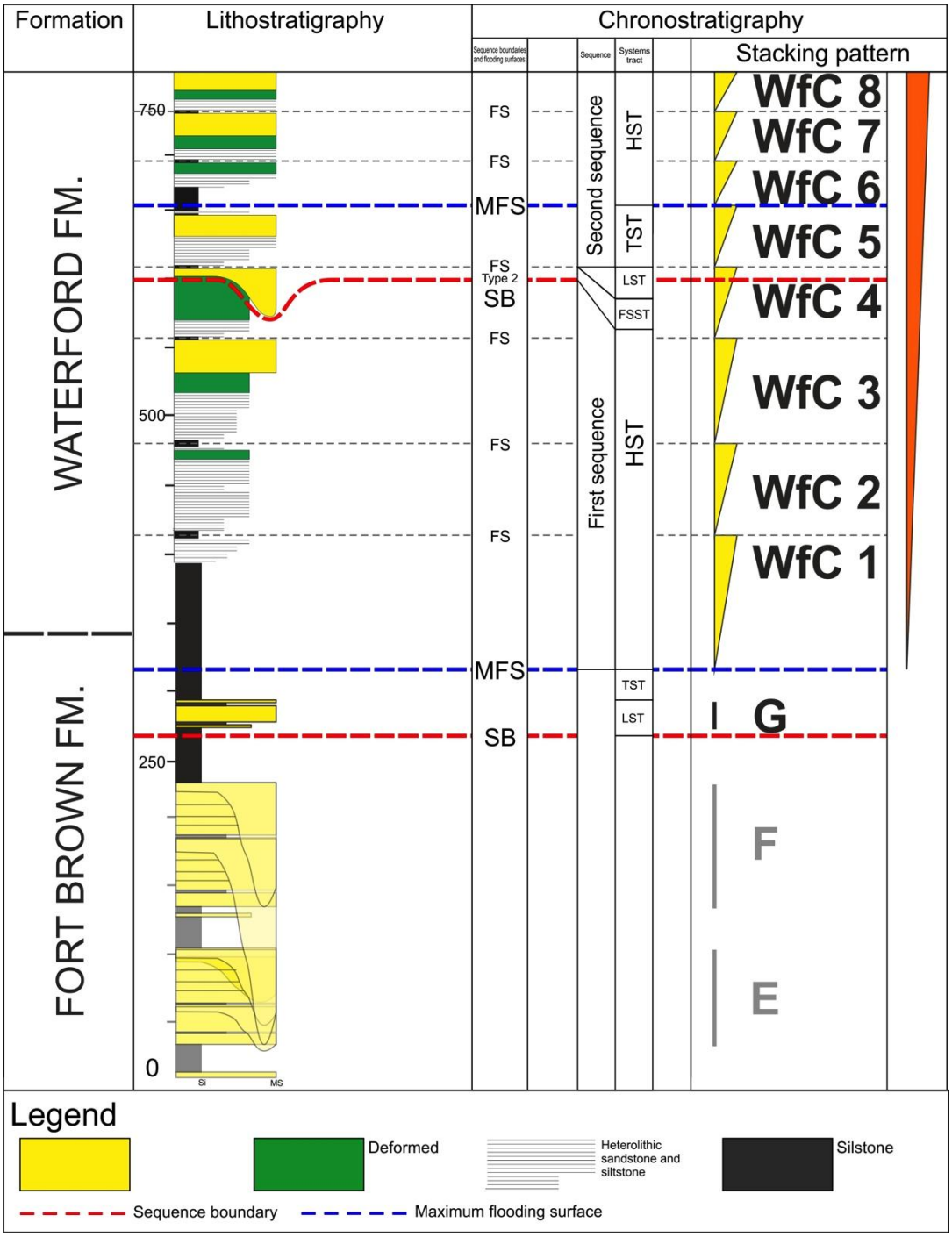

Figure 3.12: Schematic sequence stratigraphy of the Waterford Formation. All major surfaces, sequences and stacking patterns have been mapped regionally.

Overlying WfC 8 is a succession of thin (<10 m) shelf style parasequences. However, due to outcrop constraints neither corresponding shelf edge rollover positions nor a landward transition into coastal plain deposits can be identified; therefore it is difficult to establish a stacking pattern for this interval. A candidate sequence boundary is indentified in the upper Waterford Formation (informal name) and is placed at the base of WfC 15 at 327 m at the Buffels North locality. The surface is marked by a major jump in grain-size in the form of

intra-formational conglomerate lags (Fig. 3.8B) that separate deformed and lower-shoreface shelf deposits from undeformed coastal plain deposits (Fig. 3.4A). The conglomerate lag that marks the transition from shelf to coastal plain deposits occurs in isolated shallow scours, but is recorded at a similar stratigraphic interval across the study area. Further work on the upper Waterford Formation is required to test the regional significance of this surface.

CHAPTER 4.

CONTRAST IN THE PROCESS RESPONSE OF STACKED CLINOTHEMS TO THE SHELF-SLOPE ROLLOVER

This chapter leads on from the broad facies association descriptions and sequence stratigraphic interpretation made in chapter 3. It focuses on the detailed facies and architectural variability within two successive basin margin scale clinothems as they encounter the shelf edge rollover and transition onto the slope. It also establishes key criteria for identifying the clinoform rollover in a low gradient, fine-grained, mixed influence system. These criteria represent a fundamental aspect of this thesis and are integral to the interpretations made in chapters 5 and 6.

4.1. Abstract

Two stacked parasequences exposed continuously along a 35 km dip profile in the Permian lower Waterford Formation, Karoo Basin, South Africa, form basin margin–scale clinothems, and their internal facies distributions have been mapped out from shelf to upper submarine-slope settings. Sedimentary facies changes have been determined by walking out key surfaces between measured sections. The two parasequences (Waterford clinothems WfC 3 and WfC 4) share progradational profiles, but WfC 3 is characterized by a strong fluvial influence, whereas overlying WfC 4 is a wave-storm–dominated delta front system. When correlated basinward the two clinothems exhibit stratigraphic thickening as well as differing process responses to the increased gradient at the shelf edge rollover. WfC 3 exhibits synsedimentary, wedge-shaped rotational growth faults. These growth faults trapped sand at the shelf edge rollover, so minimal sand was delivered to the upper slope; therefore, the coarse grained component of the clinothem downlaps into the slope mudstones within 7 km of the shelf edge rollover. In contrast, the top of WfC 4 is marked by closely spaced gullies cut into deformed delta front deposits. The delta front deposits pass into sand-prone slope turbidites 3 km downdip. Locally these turbidites are truncated by a 60-m-thick turbidite-sandstone– filled slope channel fill. In this case most of the slope delivery is associated with a wave-dominated process regime. It is important to consider the sequence stratigraphic setting of clinothems in such analyses; WfC 4 represents a minimum accommodation point in a depositional sequence and is overlain by a regressive surface of marine erosion (sequence boundary). Despite wave and storm dominance, the low accommodation and high sediment supply at that time is interpreted to have driven sand beyond the gullied shelf edge rollover. Therefore, the delivery of sediment to deep-water settings is governed by parameters other than the presence and proximity of a fluvial point source, which is heavily advocated in current models for shelf construction.

4.2. Introduction

The shelf edge rollover zone is critical for understanding the mechanisms and timing of sediment and organic carbon transfer from continents to oceans. The stratigraphic record of the rollover area is complicated due to the interaction of current- and gravity-driven sedimentary processes (Johannessen & Steel, 2005), but provides a vital archive for the reconstruction of changes in relative sea-level and rates of sediment supply (Helland-Hansen & Hampson, 2009).

Datasets utilized to study the delivery of sediment across the shelf edge rollover include bathymetric data from present-day shelf margins, seismic reflection datasets from Quaternary to ancient successions that can be tied to well information, and outcrop studies of exhumed ancient basin margin successions. Present-day systems are invaluable in studying both downdip and across-strike variability in shelf to slope morphology (e.g. O'Grady *et al.*, 2000; Olariu & Steel, 2009; Goff *et al.*, 2010). Typically, these case studies are limited to a single time slice during a period of high sea-level when few systems are active at the shelf edge. Understanding how changes in parameters such as eustatic sea-level, subsidence rate, sediment supply, and climate affect the depositional architecture and morphology of the shelf to slope transition requires a stratigraphic perspective.

High-resolution reflection seismic datasets that illustrate the depositional architecture of the shelf-to-slope profile have significantly increased our understanding of the long-term morphological evolution of basin margins (Saller *et al.*, 2004; Johannessen & Steel, 2005; Ryan *et al.*, 2009). The physical transition from shelf to slope is easily identifiable in horizontally shortened seismic images as a break in slope (Suter & Berryhill, 1985; Sydow & Roberts, 1994; Kolla *et al.*, 2000; Hiscott, 2001; Pinous *et al.*, 2001; Krassay & Totterdell, 2003; Houseknecht *et al.*, 2009; Ryan *et al.*, 2009). When combined with information from cored wells, integrated studies have allowed the geometries of clinoforms to be defined and mapped, and rates of margin progradation established (e.g. Mountain & Proust, 2010).

Subsurface and modern datasets suffer from a lack of high-resolution stratigraphic and sedimentological details that permit process-based interpretations to augment the analysis of morphological and architectural change. This gap in data coverage can be filled by the use of large-scale (seismic scale) stratigraphic successions at outcrop where the transition from shelf to slope can be physically defined and characterized (Mellere *et al.*, 2002; Johannessen & Steel, 2005; Carvajal & Steel, 2006; Løseth *et al.*, 2006; Uroza & Steel, 2008; Covault *et al.*, 2009; Hubbard *et al.*, 2010). Few outcrop studies present analysis of multiple

stacked shelf edge systems, where long-term trends and changes in sedimentary processes and transfer mechanisms across the shelf-to-slope transition are considered. Common observations of single shelf edge successions is that a fluvial process regime at the shelf edge transfers more sediment basinward than a wave-dominated process regime (e.g. Carvajal & Steel, 2009; Dixon *et al.*, 2012b), and successive shelf edge rollover strata are normally similar in their process response to increased gradient (e.g. Mellere *et al.*, 2002; Pyles & Slatt, 2007; Dixon *et al.*, 2012a).

Here we report on changes in process regime and sediment transfer mechanisms across stacked shelf edge rollovers from the seismic-scale outcrops of upper Permian deposits in the Laingsburg depocenter, Karoo Basin, South Africa (Fig. 4.1). Our objectives are to (1) document the stratigraphic variability in sedimentary facies, stacking patterns, and downdip sediment transfer mechanisms in the transition from shelf to upper slope; (2) examine the influence of erosional and depositional processes, and the distribution of soft-sediment deformation processes, in the resolution gap between core and seismic information in subsurface datasets; (3) assess the criteria used to identify the position of the shelf edge rollover at outcrop; and (4) evaluate the interplay between controls on the basinward delivery of sediment by comparing stacked parasequences.

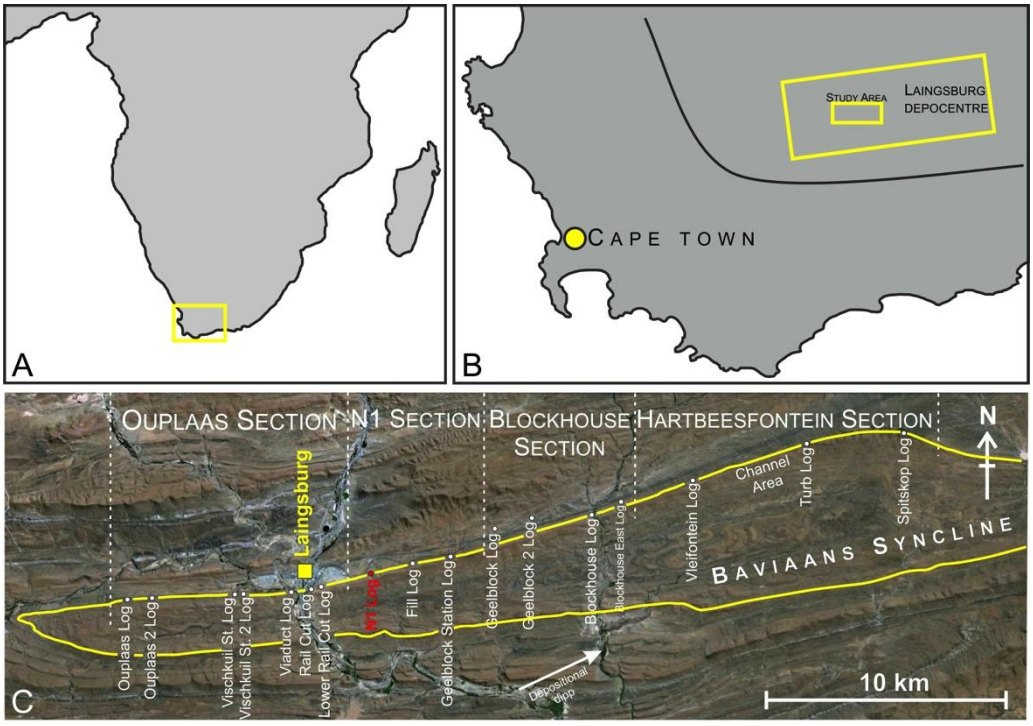

Figure 4.1: (A, B) Locality maps of southern Africa and the Western Cape Province, with location of the Laingsburg depocenter and study area indicated. (C) Aerial image of the study area showing locations of logged sections and localities referred to in the text. Note the N1 log locality (in red), which is used as the type section. White dots indicate logged sections.

4.3. Geologic setting

The Karoo Supergroup in the Laingsburg area is 5500-m-thick and is divided into the Dwyka Group (late Carboniferous to Early Permian glacial deposits), Ecca Group (Permian clastic marine sediments), and the Beaufort Group (Permian–Triassic fluvial sediments) (Fig. 4.2A). Accommodation during the time of deposition of the Ecca Group was generated by regional subsidence driven by dynamic topography related to subduction of the oceanic plate (Mitrovica *et al.*, 1989; Tankard *et al.*, 2009).

Within the Ecca Group the Vischkuil Formation represents distal basin-plain deposits (2009; van der Merwe *et al.*, 2010), overlain by basin-floor fan deposits of the Laingsburg Formation (Sixsmith *et al.*, 2004). An overlying submarine slope succession of the Fort Brown Formation is dominated by channel-levee complexes and entrenched slope valleys (Figueiredo *et al.*, 2010; Hodgson *et al.*, 2011a). Continued progradation is marked by the ~400-m-thick Waterford Formation, the focus of this study, which comprises a mixed river- and wave-influenced deltaic succession (Oliveira *et al.*, 2011). The ability to document a complete vertical stratigraphic transition from erosional slope channel-levee systems (Fort Brown Formation) to shelf deltas (Waterford Formation) implies that the shelf edge rollover will be encountered within the vertical stratigraphic section. Extensive downdip exposures allow the physical identification of the shelf edge rollover along a clinoform profile.

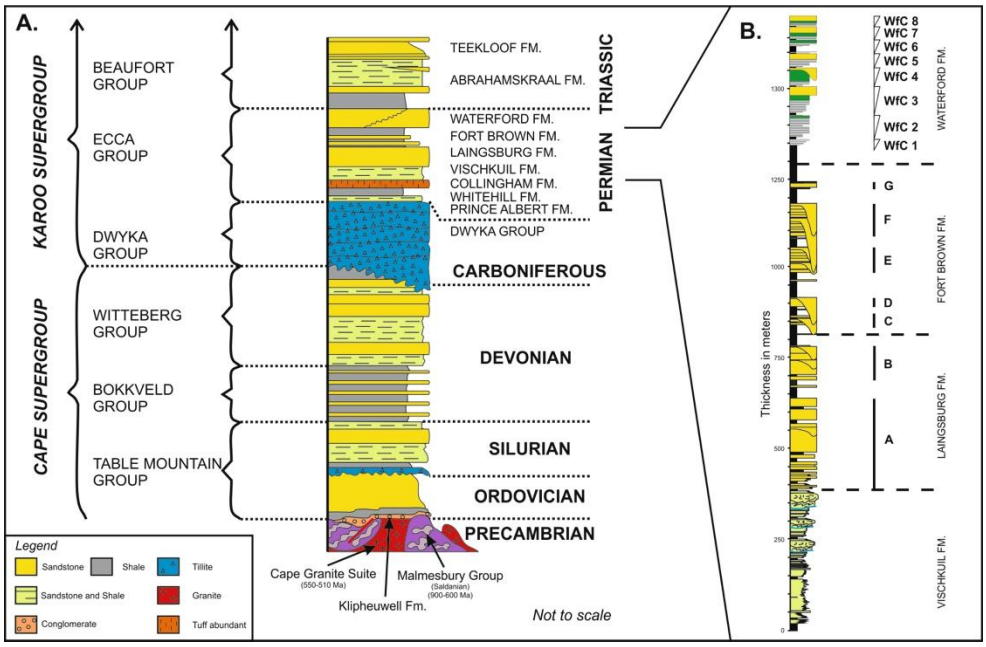

Figure 4.2: (A) Lithostratigraphy of the Western Cape area (redrawn after Wickens, 1994). (B) Schematic stratigraphy of the upper Ecca Group in the Laingsburg depocenter. The lower Waterford Formation detail is based upon the N1 log locality type section and shows the seven studied parasequences. The focus of this study is on Waterford clinothem (WfC) 3 and WfC 4.

4.4. Terminology

Clinoform geometries are common to a number of depositional settings and the focus here is on two scales: (1) shelf-slope basin (basin margin) scale (hundreds to thousands of metres high), and (2) shelf-delta scale (tens to hundreds of metres high) (Helland-Hansen & Hampson, 2009). The term clinoform is commonly applied to the entire sigmoid surface shape (Fig. 4.3), but it was originally applied only to the sloping segment of such a surface (Rich, 1951). The term clinothem is used herein to describe a three-dimensional (3D) body of rock that is bounded by clinoform surfaces (Steel & Olsen, 2002). Clinothems are a key component of sedimentary successions and have been used to interpret the interplay between changes in sediment supply and relative sea-level (Vail *et al.*, 1977b). This interplay drives the stacking pattern of clinoforms at all scales, such that a shoreline or shelf-delta clinoform can merge with a basin margin–scale clinoform to produce a compound clinoform. The upper clinoform break in slope is referred to as the shelf edge rollover. The lower clinoform break in slope (the toe of clinoform) has not been identified in this study.

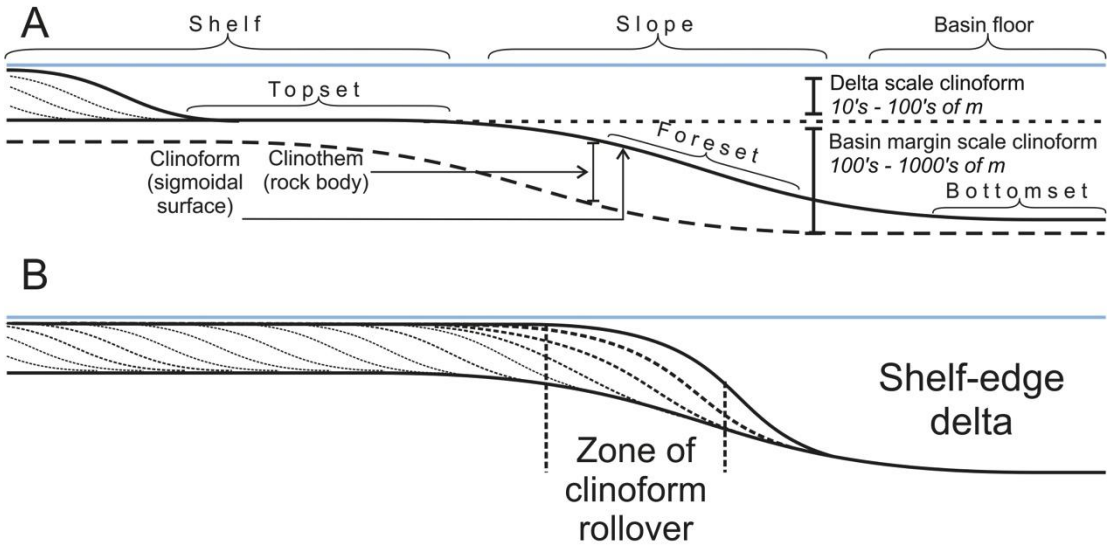

Figure 4.3: (A) Profile outlining the terminology used in this study to describe the basin margin architecture and settings. (B) Schematic to explain the relationship between a shelf delta clinoform and the preexisting shelf edge to produce a basin margin–scale clinoform.

4.5. Lower Waterford Formation stratigraphy

Analysis of the 360-m-thick lower Waterford Formation was facilitated through the collection of 17 detailed sedimentary logs (>4.5 km cumulative thickness). Regionally persistent mudstones have been physically walked out between logged sections in order to establish a robust stratigraphic framework along a single well-exposed 35 km dip profile

(Fig. 4.1C). The informaly named upper Waterford Formation comprise and addition 100 - 150 m of thin (<10 m) shelf style parasequences that transitional gradually into subaqueous coastal plain deposits (F.17, 18, 19) and eventually fluvial deposits of the Beaufort Formation (Fig. 4.2).

4.5.1. Facies and facies associations

The lower Waterford Formation comprises 7, 45–15-m-thick packages (Fig. 4.2B) that are bounded by regionally correlated mudstones. Within these packages 13 individual facies are recognized that can be grouped into 7 broad facies associations (Table 4, 1; Fig. 4.4). Individual packages differ subtly in their stratigraphic profiles and internal facies arrangement. All packages broadly coarsen and thicken upward (asymmetrical), yet the basal 2 fine and thin upward in their upper 1–3 m, producing a more symmetrical profile. The upward-fining tops consist of the highly bioturbated heterolithic facies, F.10 (Table 1). Packages are increasingly asymmetrical higher in the stratigraphy, and their tops are characterized by either a thin (<1 m) heterolithic and bioturbated package, or a sharp top surface.

Generally, the lower coarsening-upward part of each package comprises 0.4–45 m of laminated siltstone and thin, very fine grained ripple-laminated sandstone beds (F.2 and F.3; Table 1), overlain by a 0.5–5-m-thick unit of heavily deformed sandy siltstone and silty sandstone. The upper part of a typical package comprises 0.5–8 m of amalgamated sandstones that are dominated by low-angle to concave-upward lamination; locally, however, some units contain persistent unidirectional climbing ripple-laminated sandstone beds. Basal heterolithic successions are interpreted as dilute turbidity current deposits in a prodelta facies association. The deformation structures indicate evidence for downslope mass transport and vertical foundering, and these deposits are interpreted as a deformed lower delta front succession (F.4–F.6; Table 1). The low-angle to hummocky cross-stratified deposits are interpreted as wave-dominated upper delta front (F.7 and F.8; Table 1), but the climbing ripple-laminated sandstones indicate rapid deposition from flows with a high suspended load (F.9; Table 1).

The vertical facies succession recorded in each package is typical of parasequences described by (Van Wagoner *et al.*, 1990), and each parasequence is interpreted as the record of an episode of delta progradation. Each para-sequence is bounded by a mudstone or fine grained-siltstone package interpreted as distal offshore facies (F.0 and 1; Table 1). These fine-grained packages are considered to represent an increase in water depth,

consistent with containing the offshore expression of a flooding surface, and form the basis for stratigraphic correlation (Fig. 4.5). The seven correlatable para-sequences are herein referred to as Waterford clinothems 1–7 (WfC 1–WfC 7). The use of the term clinothem is supported by (1) stratigraphic context, (2) the basinward thickening of physically correlated parasequences, and (3) the departure from the typical vertical clinothem facies succession, examples of which are mapped basinward across the shelf to slope transition.

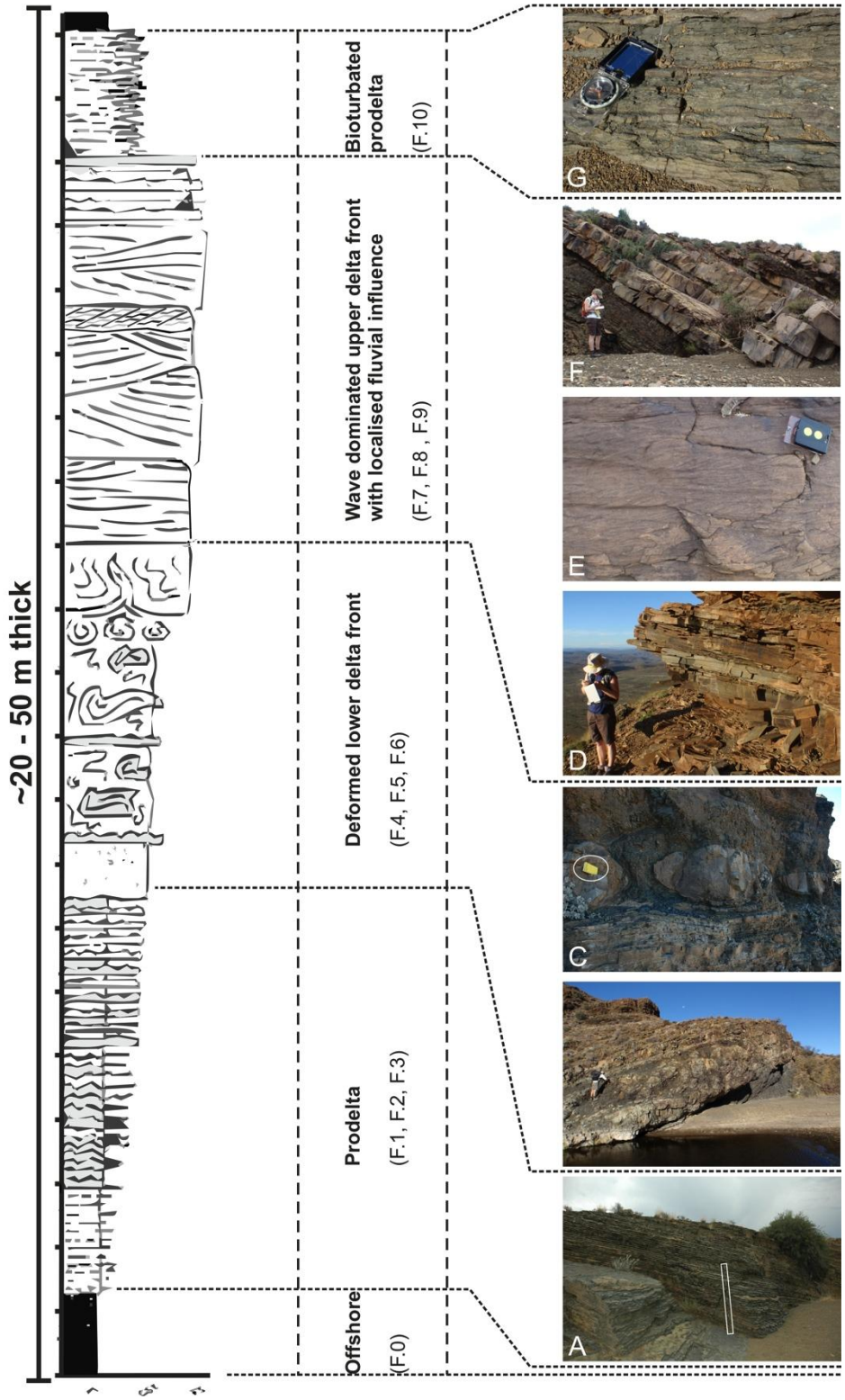

Figure 4.4: Generalized summary log of a typical coarsening- and thickening-upward parasequence from the lower Waterford Formation showing the five main facies associations observed. (A) F.3—(prodelta), 1.5 m Jacob staff for scale. (B) F.5—debris flow (downslope transport of mass flow). (C) F.6—*in-situ* deformed sandstone (deformed sandstone and/or siltstone with vertical structures), notebook for scale. (D) F.7—bedded sandstone (lower delta front). (E) F.9—amalgamated, climbing ripple-dominated sandstone (distal mouth bar), compass clinometer for scale. (F) F.8—thick-bedded, amalgamated, fine-grained sandstone (delta front). (G) F.10—heavily bioturbated heterolithic siltstone and sandstone (bioturbated offshore), compass clinometer for scale.

Facies	Description	Interpreted process	Depositional setting	Facies associations
F.0	Structureless, dark gray fine-grained claystone and siltstone	Deposited by hemipelagic fallout	Distal offshore	Offshore
F.1	Finely laminated fine and coarse siltstone	Deposited by hemipelagic fallout in an off shore environment	Offshore	
F.2	Interbedded, ripple and parallel laminated, fine and coarse siltstone	Deposition by low-density concentration turbidity currents	Distal prodelta	Prodelta
F.3	Interbedded, thin, unidirectional ripple-laminated fine sandstones and coarse siltstone	Deposited by low-density turbidity currents in a setting below fairweather wave base	Prodelta	
F.4	Structureless, dark green-gray, poorly sorted, coarse siltstone to very fine sandstone (sandy siltstone)	Debris flow	Margin of mass flow deposit	Deformed lower delta front
F.5	Dark green-gray, coarse silt to very fine sand matrix, containing heavily deformed and disaggregated rafts and rounded fine sandstone blocks	Debris flow	Axis of mass flow Deposit	
F.6	Deformed siltstone and sandstone. Deformation ranges in size from small -scale (centimetres) ball and pillow structures and detached pseudonodules, to large-scale (metres) loaded bed bases and larger flame structures	Sediment deformed *in-situ* by abrupt loading, resulting in the vertical movement of fluids and sediment	Deformed sandstone and/or siltstone with vertical structures	
F.7	Bedded fine sandstone, typically 10–30-cm-thick beds that show a range of sedimentary structures, including parallel, climbing and current ripple lamination, as well as hummocky and swaley crossstratification. Beds are tabular with sharp bases (occasionally erosive) and symmetrical reworked ripple tops	Deposited by high-density turbidity currents with minor storm reworking	Lower delta front	Wave dominated upper delta front with localized fluvial influence
F.8	Amalgamated fine-grained sandstone, typically structureless but often with convex-up lamination toward the top. Beds can be defined by discrete changes in grain size or a mud-chip lag. Bases are generally sharp but can be loaded and top surfaces have symmetrical ripples with rounded crestlines	Rapid deposition of turbidity currents on exit from confinement	Delta front	
F.9	Amalgamated very fine to fine sandstone, dominated by low angle climbing ripple laminations	Deposited by flows depositing rapidly on exit from channel confinement	Distal mouth bar	
F.10	Heavily bioturbated, thinly bedded fine sandstones. Observed as fining and thinning upward packages at the top of parasequences.	Deposition by low density turbidity currents	Prodelta	Bioturbated prodelta
F.11	Clast-supported medium-grained sandstone. Clasts are angular to subangular and consist of siltstone and very fine sandstone. They range in size from 1 to 5 cm and line the erosional channel base.	Deposited by waning erosive flows at the base of a channel	Channel lag conglomerate	Slope channel fill
F.12	Amalgamated, fine- and medium-grained sandstone deposited within a large erosive surface	Deposited by high-density turbidity currents	Channel fill	
F.13	Interbedded fine sandstones, sigmoidal ripple lamination. Sharp based and occasional erosional. Tops are sharp and unidirectional ripple laminated. Sheet geometry to sandstone beds.	Unconfined turbidity currents deposited beyond the shelf edge	Upper slope turbidites	Upper slope turbidites

Table 4.1: Sedimentary facies defined in this study, their key characteristics, and interpreted depositional environments.

4.6. Stratigraphic correlation and interpretation

The seven Waterford clinothems are separated from the underlying channelized slope succession (Figueiredo *et al.*, 2010; Hodgson *et al.*, 2011a; Brunt *et al.*, 2013) by a regionally extensive 80-m-thick mudstone marker unit. The uppermost channelized slope unit (unit G) is used as a basal datum in this study (Figs. 4.2B and 4.5) (Figueiredo *et al.*, 2010). Waterford clinothems 1 and 2 (WfC 1 and WfC 2; Fig 2B) are 45 – 25-m-thick, and are characterized by a coarsening- and thickening-upward stratigraphic succession of heterolithic siltstone and sandstone beds, with a bioturbated fining- and thinning-upward top, interpreted as prodelta deposits.

The N1 type log (Fig. 4.2B & 4.5) shows that WfC 3 (~38-m-thick) and WfC 4 (~20-m-thick) exhibit asymmetric coarsening- and thickening-upward profiles with a thin (<1 m) upper fining- and thinning-upward section. Unlike WfC 1 and WfC 2, the middle sections of these parasequences are dominated by highly deformed strata showing a range of soft-sediment deformation styles. The deformed sections are overlain sharply by undeformed tabular 5–30 cm sandstone beds with erosional bases and symmetrical rippled tops, passing upward into 40–70-cm-thick beds of amalgamated sandstone that are generally massive or exhibit faint convex-upward laminae sets that represent hummocky cross-stratification generated by storm action. WfC 5 (~19-m-thick) lacks any significant soft-sediment deformation, in contrast to WfC 3 and WfC 4. The lower half is dominated by a coarsening- and thickening-upward package of thin, normally graded, inter-bedded siltstone and very fine sandstone beds (1–4 cm). This is overlain sharply by 1.5 m of tabular bedded sandstone, followed by ~9 m of amalgamated sandstone dominated by parallel, low-angle, and hummocky cross-stratifi cation. The top surface is marked by symmetrical ripples with shallow scours filled with small mudstone chips, consistent with reworking by wave and storm action. Abruptly overlying this reworked surface is a regionally extensive ~30-m-thick mudstone unit that provides a stratigraphic key marker across the entire study area. It is thinner and more siltstone dominated in the most proximal (western) outcrops, and thicker and more mudstone dominated in the most distal (eastern) outcrops (Fig. 4.5).

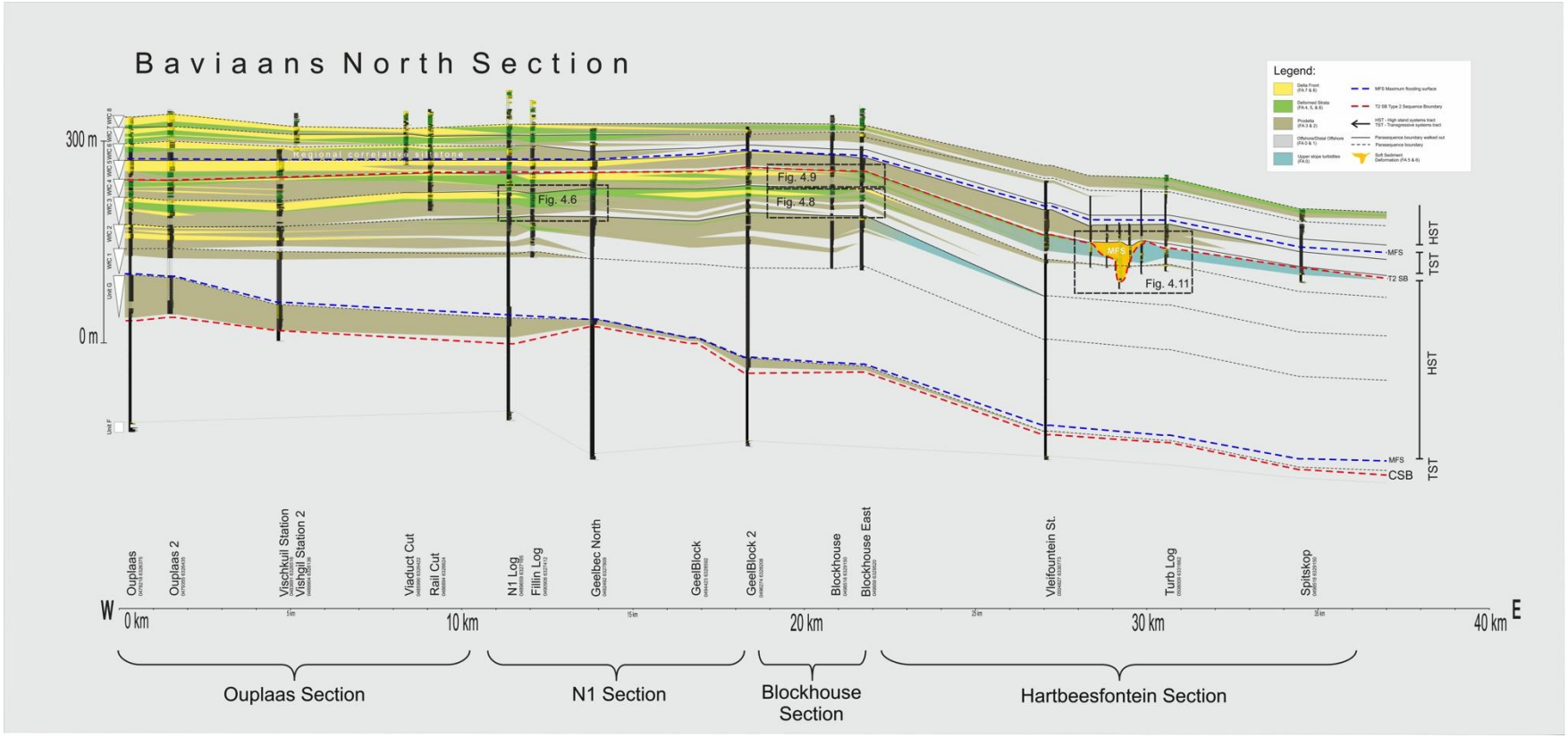

Figure 4.5: Baviaans north correlation panel (Fig. 1.13) showing the seven lower Waterford parasequences (WfC). Bounding flooding surfaces are shown as well as interpreted maximum flooding surfaces and sequence boundaries. CSB composite sequence boundary. The panel uses unit G as a datum. Prodelta strata are khaki, deformed strata are green and amalgamated sandstone bodies are yellow and show the maximum progradational extent of the lower Waterford Formation. Upper slope turbidite deposits are blue. For high resolution PDF image see incerted CD.

4.7. Dip-parallel depositional architecture of WfC 3 and WfC 4

The architectural variability of WfC 3 and WfC 4 as observed along the 37 km oblique dip profile of the northern limb of the post depositional Baviaans syncline (Fig. 4.1C) is described in detail here; 17 measured sections were logged and all key surfaces were walked out between logs. The following describes the sedimentology and stratigraphy of the Ouplaas (most proximal), N1, Blockhouse, and Hartbeesfontein (most distal) key sections for WfC 3 and WfC 4 (Figs. 4.1C).

4.7.1. Downdip character of WfC 3

4.7.1.1. Ouplaas section

WfC 3 is 24-m-thick with a coarsening- and thickening-upward profile. The lower part of the parasequence is dominated by thin (1–3 cm) beds of siltstone and sandstone (F.3). Sandstone beds exhibit unidirectional current ripple lamination; commonly these thin beds display symmetrical curved-crest ripples on top surfaces. This lower part of WfC 3 is interpreted as low-density turbidity current deposits in a prodelta setting. Symmetrical ripples are interpreted to have resulted from storm waves that reworked bed tops. The middle 3–8-m-thick part of the parasequence is dominated by multiple beds containing soft-sediment deformation. Individual deformed beds vary in thickness between 0.2 m and 1.2 m and exhibit a range of deformation styles. In the lower part of the deformed package thin beds of poorly sorted sandy siltstone with sharp bases and tops have a structureless appearance and are characteristically green-gray (F.4). There is an upward transition to chaotic beds, characterized by deformed sandstone clasts supported by a poorly sorted sandy siltstone matrix (F.5). Both facies are interpreted as debrites (debris-flow deposits). A significant increase in sandstone content in the top 2 m, and a change to flame structures and *in-situ* deformation features (F.6), is characteristic of the upper part of WfC 3, and suggests limited downslope movement. The relatively undeformed upper section of WfC 3 is dominated by nonamalgamated and amalgamated sandstone beds containing hummocky cross-stratification and wave and current ripple lamination, which suggests deposition in a wave-dominated delta front setting (F.7 and F.8). Locally, WfC 3 is overlain abruptly by WfC 4 debrites where the intervening distal offshore mudstone (F.0) was removed by erosion; however, a thin fining- and thinning-upward package of moderately bioturbated sandstone is locally preserved at the top of WfC 3 (F.10). This is interpreted to be due to a reduction in sediment supply associated with a rise in relative sea-level.

4.7.1.2. N1 section

At the N1 locality (Fig. 4.1) the lower third of WfC 3 consists of F.2 and F.3, interpreted as prodelta facies, overlain by a 5-m-thick debrite (F.5). In contrast to the Ouplaas section, the middle part of WfC 3 is dominated by a 5-m-thick package of amalgamated, fine-grained sandstone with abundant climbing ripple lamination (F.9) (mean palaeocurrent direction 082°). The climbing ripple lamination suggests rapid deposition from unidirectional tractional currents with a high suspended load. The lack of wave indicators and the high silt and mud content of the sandstones indicate a high terrigenous component; this supports a fluvially dominated distal mouth bar setting with flows depositing rapidly on exit from updip distributive channels (Al-Aasm *et al.*, 1996; Johannessen & Steel, 2005; Olariu & Bhattacharya, 2006; Enge *et al.*, 2010). The abundance of debrites that interfinger with climbing ripple-laminated sandstones is interpreted as the product of rapid deposition and incremental collapse of a steep, river-dominated upper delta front. The top 1.5 m of the unit comprises amalgamated fine-grained sandstone with hummocky cross-stratification and low-angle lamination (F.8), consistent with a wave-dominated upper delta front. This might reflect progradation and/or overstepping of the delta front over the distal mouth bar at the top of WfC 3 and/or local delta lobe abandonment.

Internally, WfC 3 contains multiple low-angle inclined surfaces (~0.7° using the top of WfC 3 as a horizontal datum) that are 14–16 m in height. Bedsets can be traced between logged sections where they thin, split, and pinch out over a downdip distance of ~1 km. The inclined surfaces are eastward dipping, consistent with both the internal and regional palaeocurrent directions (Fig. 4.6). The sedimentology and geometry support an interpretation of river-dominated shelf-delta–scale clinothems. However, low-angle topsets (Steel & Olsen, 2002) are not recognized. Overall, the geometry of the delta-scale clinothems reveals subtle gradient differences between slightly steeper climbing ripple-dominated sandstone clinothems and overlying, lower angle and thinner wave- and storm-influenced clinothems. This change is interpreted to reflect an increase in the degree of wave and/or storm energy reworking to form a lower gradient. Low-angle delta topsets are interpreted to have been removed during transgressive erosion. This interpretation is supported by the sharp-crested symmetrical ripples and the concentration of mud chips within shallow erosional scours on the top surface of WfC 3.

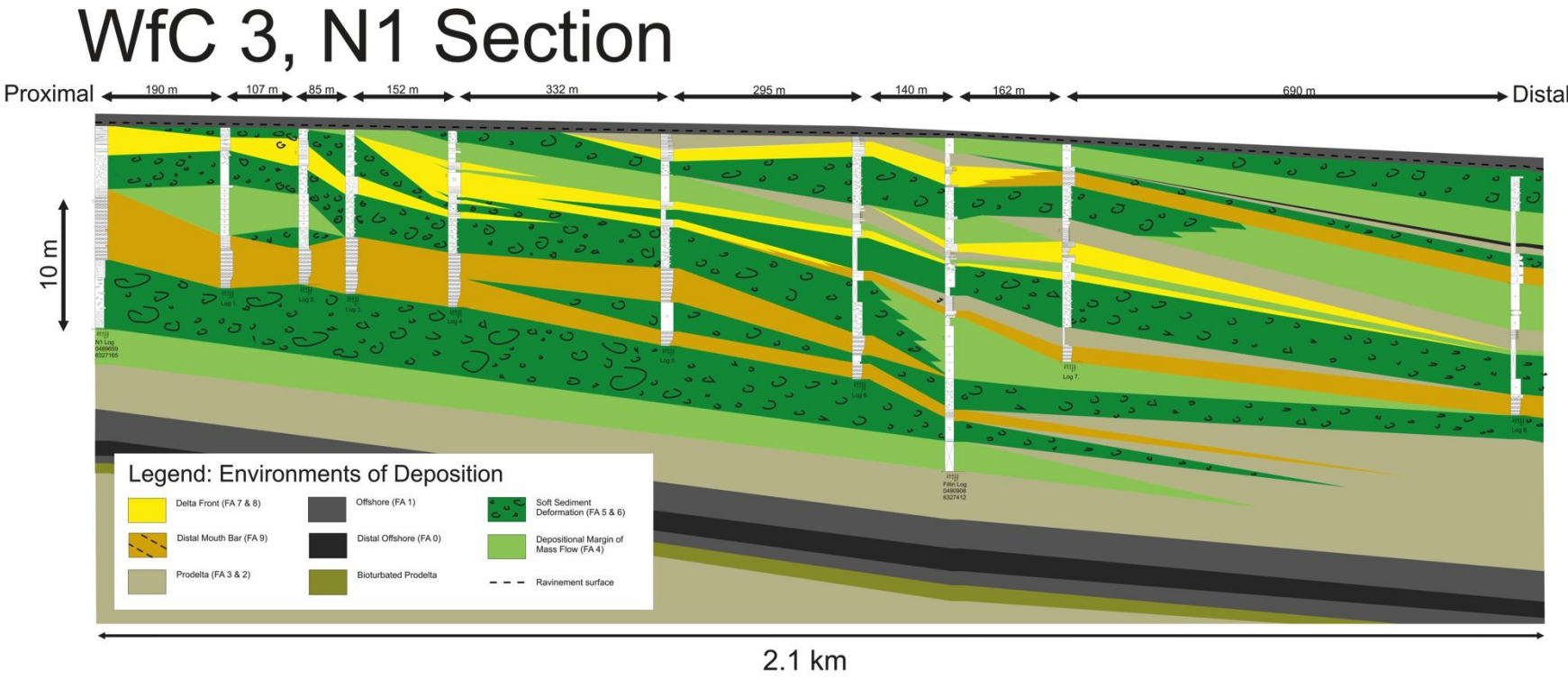

Figure 4.6: Multiple low-angle (0.7°) delta-scale clinoforms dipping basinward (eastward) in WfC (Waterford clinothem) 3.

4.7.1.3. Blockhouse section

This 5.4-km-long dip section comprises pervasively deformed sediments directly downdip of the river-dominated, shelf-delta–scale clinoforms of the N1 section. The zone of deformation starts at the Geelblock log locality in the west (Fig. 4.1C) and increases in intensity downdip toward the Blockhouse East log (Fig. 4.1C). Clinothem thickness increases from 38 m at the N1 to ~48 m at the Blockhouse section.

Mapping the transition of WfC 3 from the N1 to the Blockhouse section has shown that WfC 3 maintains a broadly coarsening- and thickening upward profile, comprising deformed beds and heterolithic sandstones (F.1 and F.2), interpreted as prodelta deposits to the river-dominated shelf-delta clinothems of the N1 section. These prodelta deposits are abruptly truncated at the Geelblock log locality by a 10–12-m-thick wedge-shaped unit of intensely contorted fine to medium-grained sandstone blocks (0.2–3 m diameter) supported by a dark green-gray, poorly sorted sandy siltstone matrix (Fig. 4.7) (F.6). Several other wedges of deformed sediments are identified in this area (Fig. 4.8).

A prominent sharp-based, sharp-topped, 1.0–1.4-m-thick bed forms a datum toward the base of WfC 3 along the Blockhouse section. This marker bed consists of deformed, dark green-gray, poorly sorted, sandy siltstone, with numerous small sandstone pseudonodules. This internal datum enables the stratigraphic position and geometry of the overlying wedge shaped units of intensely contorted sandstone to be constrained. Separating the basal siltstone datum from the intensely deformed material is a package of dark gray ripple-laminated siltstone (F.2). Overlying this package is a dark gray structureless sandy siltstone (F.4) that is locally highly deformed and injected between the overlying intensely deformed sandstones wedges to produce metre-high flame structures.

The fine-grained sandstone-filled wedges that form the upper part of WfC 3 in the Blockhouse section taper and thin to the east. The wedges vary in size from 10-m-long and 2–3-m-thick to ~140-m-long and 19-m-thick. To the west the sandstone wedges terminate against steep, broadly eastward-facing surfaces that shallow downward, and are associated with metre-high fl ame structures in the underlying structureless sandy siltstone. Internally, the wedges are moderately to intensely deformed but contain contorted blocks and bedding that are consistently rotated to be westward facing (Figs. 7A, 7B). Internally, the greatest amount of bed rotation is at the bases of wedges, proximal to the abrupt western margins, but overall, bed dips decrease upward. Not all blocks conform to this westward rotation; a few in the center of the heavily deformed area are orientated randomly. Three

of the larger wedges also contain a 2–3-m-thick interval of the massive dark green-gray silty sandstone that is similar to the underlying material (F.3).

The 2D dip profile of the Blockhouse section means that the wedges are well exposed in cross section, but their 3D geometry is poorly constrained. The distribution and scale of the wedges vary down the section. At the updip end (Geelblock log), wedges are relatively small, widely spaced, and poorly defined; they are usually separated by less deformed amalgamated upper delta front sandstone. At the Blockhouse locality, the size and concentration of the wedges reach a maximum with no separation between individual wedges. Beyond the Blockhouse locality the scale and concentration of the wedges decreases, before passing into undeformed thin-bedded sandstone and siltstone beds at the downdip Blockhouse East log. The top of the wedge fill is commonly less deformed, with a sharp, symmetrical rippled top surface that also marks the top of the parasequence.

The wedge-shaped units are interpreted as growth fault fills due to their steep updip and shallow downdip margins, the rotation of the internal bedding, the minor top truncation of wedge fills, and the flame structures at the steep western margins. Extensional growth faulting is a common feature of oversteepened shelf edge settings that are subject to high sediment supply rates (Rider, 1978; Coleman *et al.*, 1998; Wignall & Best, 2004; Maloney *et al.*, 2012). The rotation of blocks within the void created indicates that the development of the growth fault was synsedimentary. None of the identified faults extends into the overlying stratigraphy of WfC 4; this suggests that extensional faulting was of WfC 3 age. The sense of throw on the faults is normal; the downthrown side to the east. However, it is not possible to measure the displacement because the intensely deformed nature of the sandstone fill does not allow the correlation of beds from the hanging wall to the footwall.

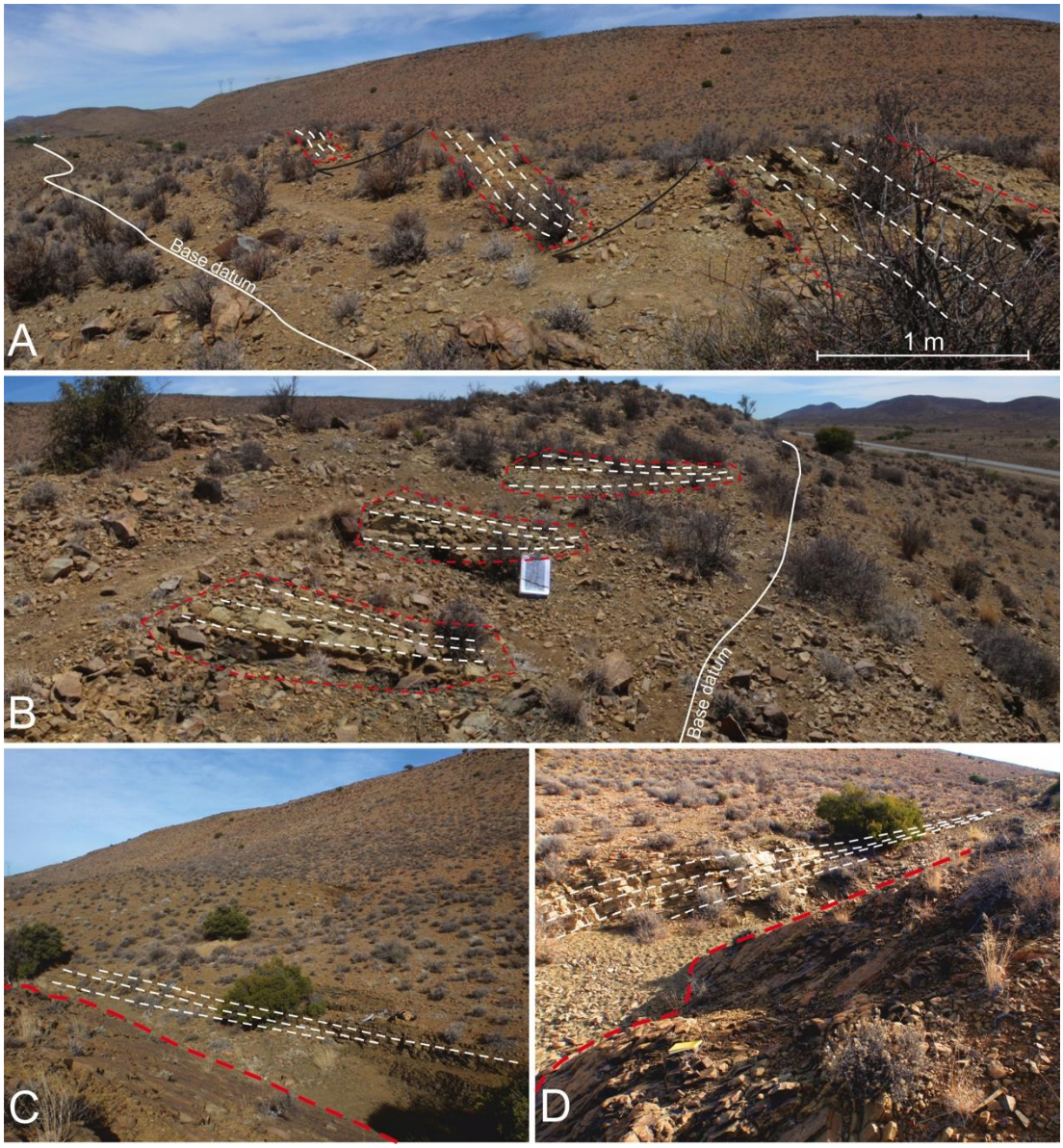

Figure 4.7: (A, B) Rotation of bedding within the growth fault fills of Waterford clinothem (WfC) 3 showing preferential rotation to the west. Solid white line indicates the lower datum used to constrain the geometries of the rotational growth faults. (C) Thin beds onlapping the margin of a shallow gully feature that cuts into the top of WfC 4. (D) The stepped margin of a shallow gully cutting into the top of WfC 4.

There is a general absence of extensional tectonic features in the Karoo basin fill (Tankard *et al.*, 2009; Flint *et al.*, 2011a). The orientation of the growth faults and pattern of sedimentation reported here indicate a close association between sediment deposition at the shelf edge delta front and the formation and development of the growth fault features; this is consistent with a gravitational driver. Rapid deposition of sand by an advancing river-dominated shelf delta above unconsolidated silt-prone prodelta deposits creates a density instability that results in the movement of sediment. The increase in number and scale of the growth faults toward the Blockhouse log locality, and their subsequent reduction in scale and number beyond, suggests that substrate movement was initiated and enhanced

by a gradual increase in gradient eastward through the Blockhouse locality. This is supported by the basinward thickening of WfC 3 in this area.

The trapping of sediment in the growth fault depression, accommodated by movement along the displacement plane, created additional accommodation through loading and rotation. This model is supported by the presence of relatively undeformed but disaggregated blocks of laminated sandstone that fill the depression created by the growth fault.

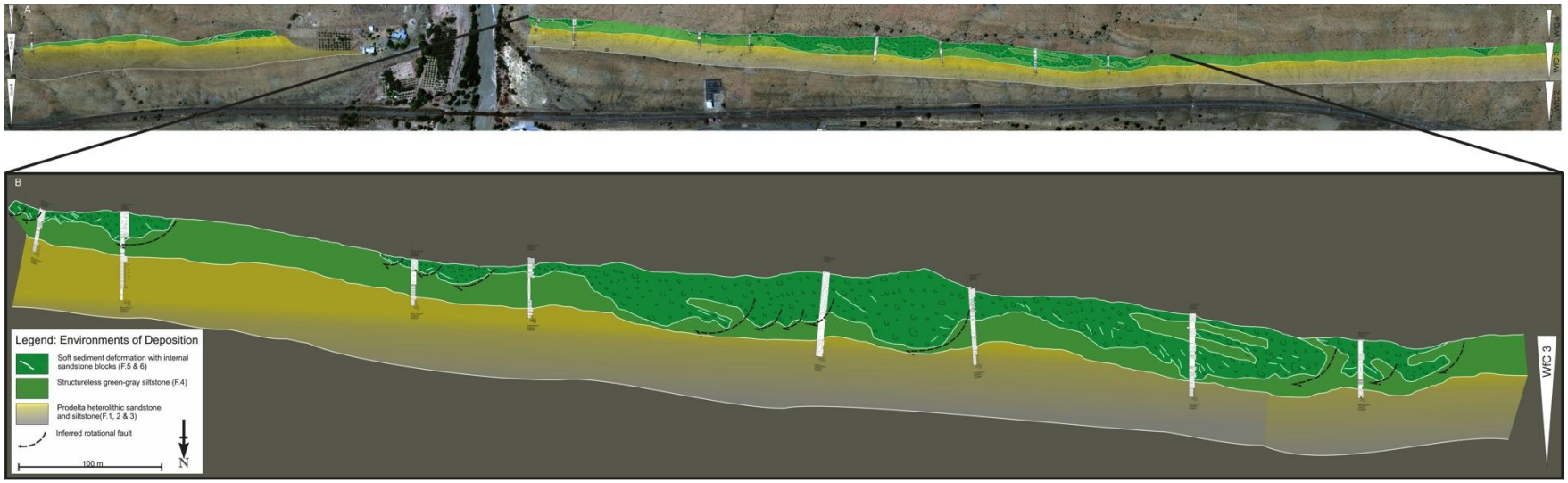

Figure 4.8: (A) Interpreted aerial photograph of Waterford clinothem (WfC) 3 at the Blockhouse section (Fig. 4.1) showing large-scale extensional deformation in the form of sand-fi lled rotated growth faults. Extension direction is to the east. Image is from Google Earth. (B) Close-up of area of most intense rotational deformation within WfC 3 (2× vertical exaggeration). Note consistent rotation of internal sandstone blocks.

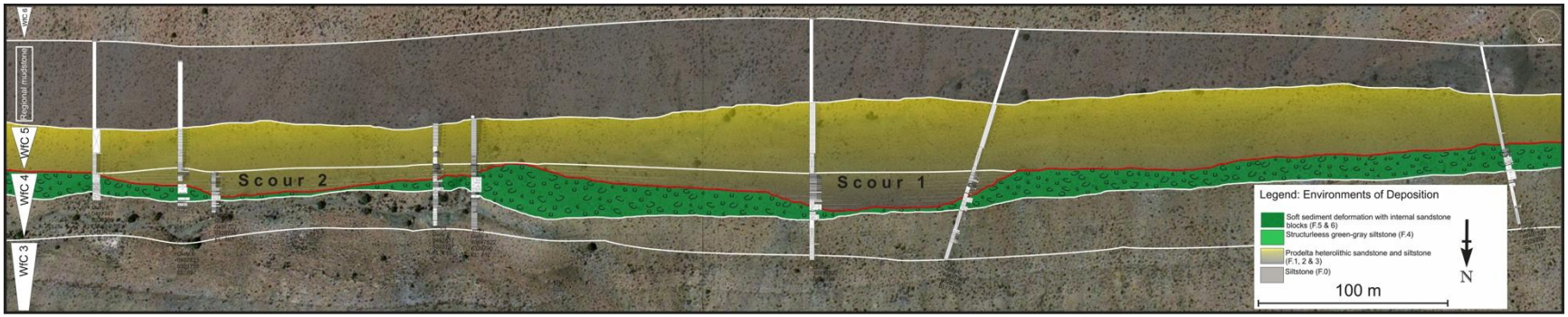

Figure 4.9: Interpreted aerial image of Waterford clinothem (WfC) 4 at the Blockhouse section (Fig. 4.1) showing broad shallow gullies cutting down into the top surface. Gullies have been later filled by WfC 5 material.

4.7.1.4. Hartbeesfontein section

Beyond the Blockhouse East logged section, WfC 3 thins and is dominated by siltstone beds with rare thin sandstone beds. This facies change coincides with no further signs of growth fault features, a marked decrease in soft-sediment deformation, and a lack of sandstone beds. The coarse grained component of WfC 3 gradually thins downdip over the next 7 km, becoming difficult to distinguish from the slope mudstone succession.

4.7.1. Downdip character of WfC 4

4.7.1.1. Ouplaas section

WfC 4 is 23-m-thick and dominated by heavily deformed beds consisting of sandstone clasts supported by a poorly sorted sandy siltstone matrix, interpreted as deformed lower delta front (F.5). The debrite-dominated package is split by a 5-m-thick undeformed hetero lithic siltstone-sandstone package, capped by a single undeformed sandstone bed. Basinward (eastward) of the Ouplaas section, WfC 4 becomes less deformed, with an increase in thin interbedded siltstone and sandstone prodelta deposits in the lower half of the unit. The upper deformed package is retained but is overlain by *in-situ* deformed (F.6) and undeformed wavedominated upper delta front sandstone (F.7 and F.8). The top of WfC 4 is generally sharp with an abrupt change to thinly bedded siltstone above the amalgamated sandstones.

4.7.1.2. N1 section

At the N1 locality WfC 4 is 26-m-thick with a coarsening- and thickening-upward asymmetrical profile (Fig. 4.2B) that is similar in character to the Ouplaas section but with a slight basinward increase in the thickness of the lower heterolithic deposits (F.2 and F.3). The lowermost 1.5 m consists of thinly laminated fine and coarse siltstone overlain by a 7.5-m-thick coarsening- and thickening-upward package of interbedded fine siltstone and very fine grained sandstone. Beds are normally graded, 2 – 4-cm-thick, and have unidirectional ripple lamination and symmetrical rippled top surfaces (F.2 and F.3). These characteristics are consistent with a prodelta setting with sediment delivery by low-density turbidity currents and minor reworking by storm waves. An overlying 3-m-thick package comprises structureless, dark green-gray, coarse siltstone to fine sandstone beds 0.7 – 1.1-m-thick (F.4), interbedded with 0.01–0.3-m-thick undeformed ripple-laminated sandstone beds. The middle portion of WfC 4 comprises two packages (4.8 and 5.6-m-thick) of detached and deformed sandstone pseudonodules supported in a matrix of dark green-gray sandy siltstone (F.5), interpreted as debrites. The upper debrite package grades upward into *in-*

situ deformed sandstone and finally undeformed amalgamated sandstone with internal hummocky cross-stratification. This suggests deposition in a wave-dominated upper delta front environment (F.6), consistent with progradation of a wave- and storm-dominated shoreline. The top 2.8 m of WfC 4 is marked by a fining and thinning-upward package of thinly bedded sandstones that are moderately bioturbated, giving this package a mottled appearance (F.10), and is capped by offshore mudstone. WfC 4 does not exhibit similar shelf-delta–scale clinoforms as seen at this locality in WfC 3, or any evidence for proximity to a fluvial input point.

4.7.1.3. Blockhouse section

WfC 4 at the Blockhouse locality is 24-m-thick, compared to ~25-m-thick updip. Closely spaced scour surfaces cut down from the sharp top surface into deformed lower delta front facies (F.5) that dominate the upper portion of the parasequence in this area (i.e., no undeformed delta front deposits; Figs. 7C, 7D). The erosion surface and fill of two complete scours situated stratigraphically above the most intensely deformed zone (the largest growth fault) in WfC 3 have been characterized in detail along a 2.5 km dip section (Fig. 4.9). Closely spaced short measured sections hung from lower (base WfC 4) and upper datums (top WfC 5) were used to constrain scour dimensions. The distance between the deepest points of the scours is 430 m; scour 1 is 186-m-wide and 9.8 m deep and scour 2 is 275-m-wide and 13.6 m deep (Fig.4.10). The scour margins are marked by steps, interpreted to indicate multiple erosive events cutting into the underlying deformed sandstones (Fig. 4.7D). The western margins are slightly steeper than the eastern sides. Scour orientation is 038° (scour 1) and 028° (scour 2), consistent with the north-northeast–east-northeast palaeocurrent trend recorded throughout the lower Waterford Formation. The stepped morphology, the orientation with regional palaeoflow, and the palaeogeographic context support an interpretation that the scours represent straight shelf edge to upper slope gullies.

The basal fills of scours 1 and 2 are dominated by fine-grained stratified dark gray siltstone (F.1 & 2) that forms a drape marking the parasequence boundary flooding surface between WfC 4 and WfC 5. The fill thickens and coarsens upward and comprises heterolithic fine-grained sandstone beds (F.3) that onlap the margins of the gullies (Fig. 4.7C). Beds are commonly sharp based and occasionally erosive, and bed tops commonly exhibit symmetrical ripples. Internally, beds exhibit climbing ripple lamination, suggesting rapid deposition from density currents that preferentially concentrated in the topographic lows

of the gullies. The accumulation of fine-grained sediment at the bases of the scours indicates that the gully features were cut but remained unfilled before being later filled by deposits of the advancing delta front of WfC 5.

4.7.1.4. Hartbeesfontein section

East of the Blockhouse section (basinward of the shallow gully fills) WfC 4 exhibits distinctly different facies and architecture, and increases in thickness from ~24 m to a maximum of ~35 m (Figs. 5, 10A, and 10B) at the Vleifontein Station log (Fig. 4.1C). The main deformed lower delta front package splits into discrete <1-m-thick deformed beds that thin toward and pinch out within a 1.4-km-wide area of no exposure occupied by the present-day Geelbek River. The increase in clinothem thickness coincides with a marked change in facies from soft-sediment deformed lower delta front deposits to undeformed heterolithic sandstones and siltstones (F.13; Figs. 10A, 10B). The sandstone beds are extensive and tabular, typically 7 – 15-cm-thick, with sharp or erosive bases and asymmetric rippled top surfaces. Sandstone beds are well sorted, weakly normally graded, with climbing (sigmoidal) ripple laminations that locally are stoss-side preserved; these characteristics are consistent with an interpretation of rapid deposition from turbidity currents. This basinward-thickening wedge of turbidites is sharp based with a broadly aggradational profile. Just beyond the point at which the basinward thickening wedge of turbidites reaches its maximum thickness, these deposits are incised 1-km-wide and 55-m-deep sandstone-filled incision surface (Fig. 4.11A) that cuts down from the top of WfC 4, and is the same stratigraphic surface as the gully features observed updip along the Blockhouse section. The erosive basal surface cuts down into the muddy slope succession beneath the turbidite wedge (Fig. 4.12B) and is marked by a distinct increase in grain size and a discontinuous clast-supported intraformational pebble conglomerate (Fig. 4.12B) (F.11) at the deepest point of erosion. The incision surface is asymmetric in cross section, with a shallow western margin and a steep eastern margin that is mantled by a large amount of carbonate nodule clasts. However, there is little asymmetry to the fill, which consists of thick, amalgamated medium- to fine-grained sandstones (F.12) that are generally structureless and/or dewatered, but that occasionally display localized current ripple- and cross-laminated units (Fig. 4.12C). The scale of the incision surface, the basal mudstone clast conglomerates, and the turbiditic fill supports an interpretation of a slope channel fill. It is possible from the small number of palaeocurrent measurements available and the orientation of the channel margins to infer a north-eastward palaeoflow. The doubling in thickness of WfC 4 associated with the basinward-thickening wedge of turbidites suggests

that this was an area of increased accommodation basinward. Coupled with the evidence for localized erosion and bypass, the Hartbeesfontein section is interpreted to be beyond the shelf edge rollover for WfC 4, on the upper slope. WfC 4 progressively thins and pinches out into the slope mudstone succession over the next 6 km downdip, beyond the Spitskop log section (Fig 1C).

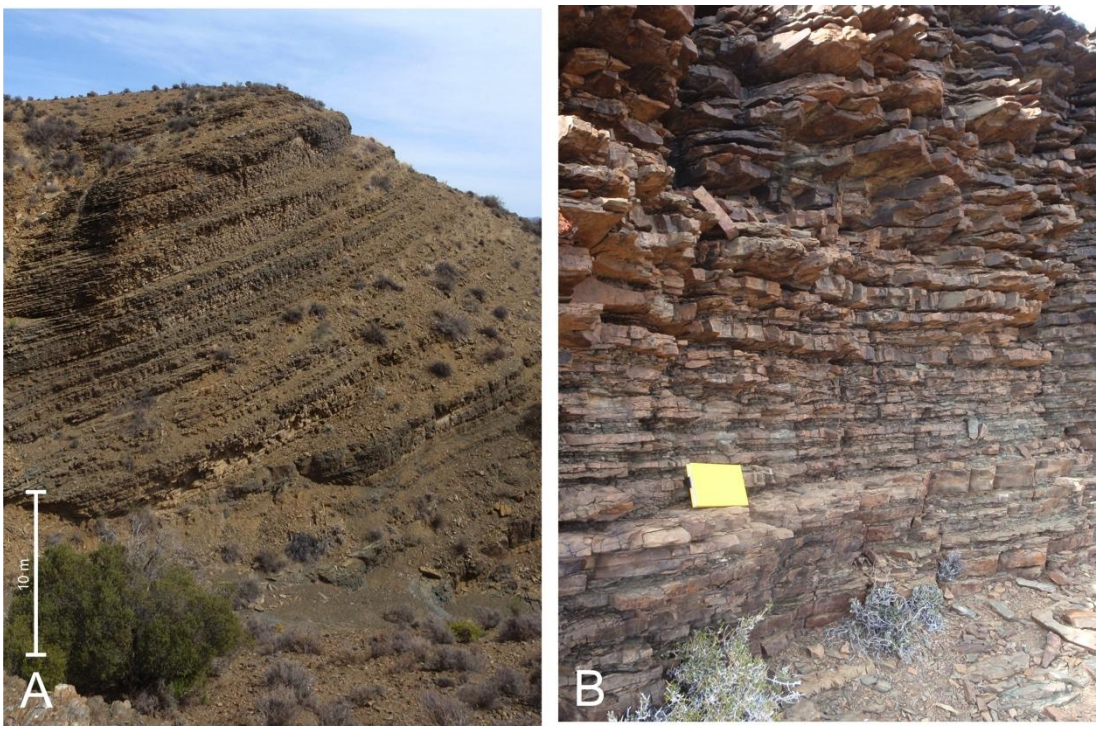

Figure 4.10: (A) Waterford clinothem (WfC) 4 thickening basin-ward beyond the shelf edge rollover comprising undeformed turbidite sandstones and silt-stones. (B) Interbedded sandstone and siltstone making up the basinward-thickening turbidite package of WfC 4. Sandstone beds have sheet geometries, internally sigmoidal current ripple lamination, and sharp, occasionally erosional bases. Tops are sharp and unidirectional ripple laminated.

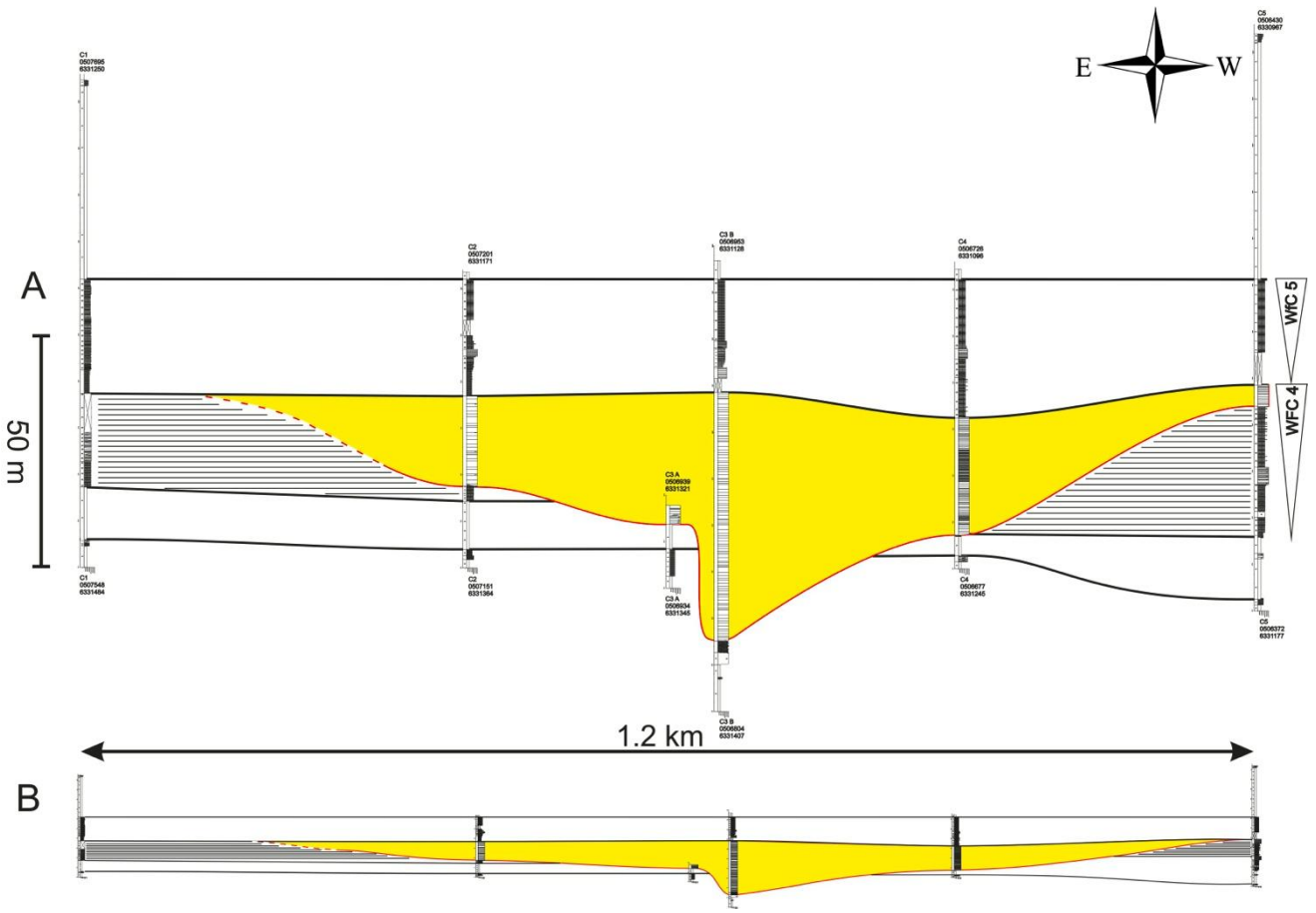

Figure 4.11: (A) Schematic correlation showing the upper slope channel from the Hartbeesfontein section. Log sections are hung from the maximum flooding surface above Waterford clinothem (WfC) 5. (B) Hartbeesfontein channel geometry corrected for vertical exaggeration.

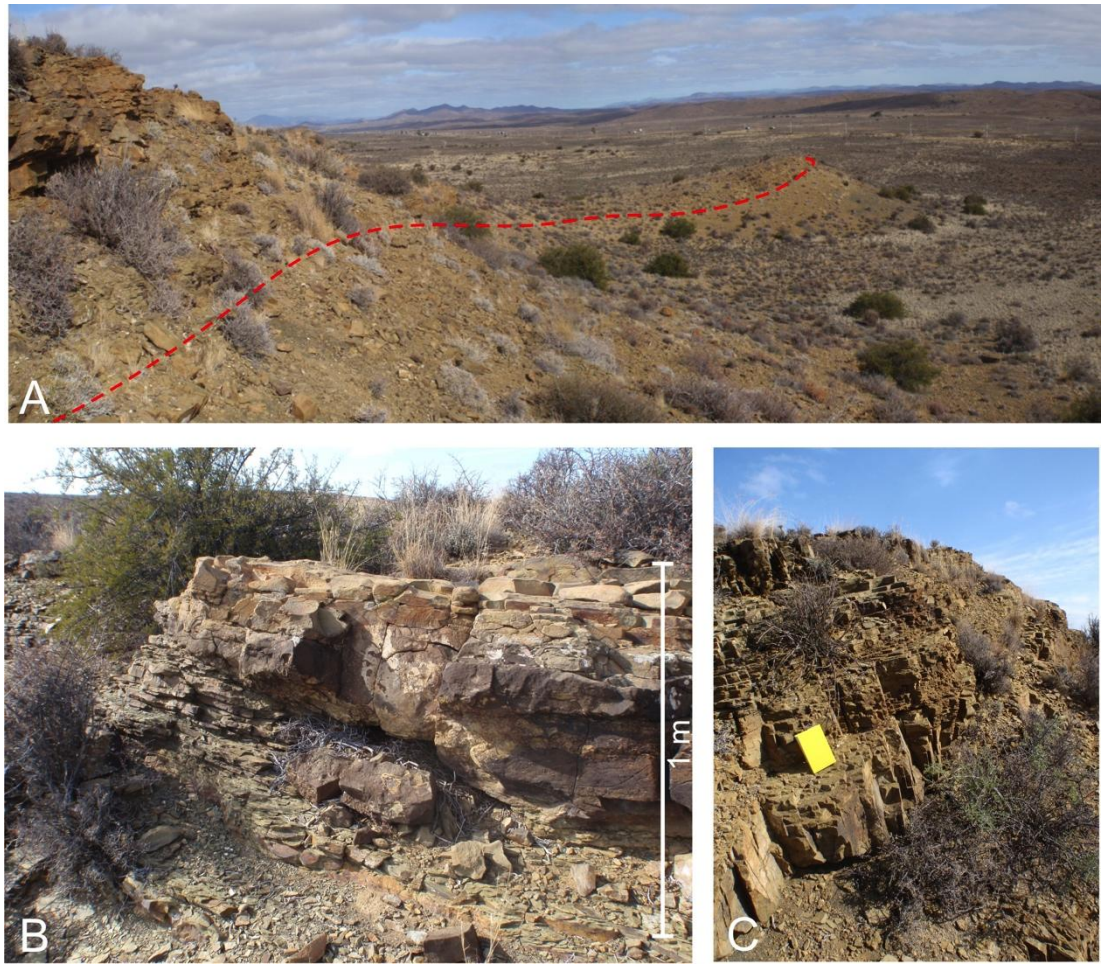

Figure 4.12: (A) Oblique view of the upper slope channel cutting down 60 m into the slope mud-stone succession at the Hartbeesfontein section. (B) Erosive base of channel truncating underling heterolithic slope turbidites. Erosive surface is mantled with channel lag conglomerate (F.11). (C) Amalgamated, medium-grained turbidite channel fill sandstone (F.12).

4.8. Position of the shelf edge rollover

The zone of extensional deformation coincident with basinward thickening along the Blockhouse section of WfC 3 is compelling evidence for a downdip increase in gradient. The context provided by the extensive outcrop shows river-dominated shelf-delta–scale clinoforms updip of the deformation zone. Basinward thickening through the zone of deformation is observed, followed by thinning and pinching out of WfC 3 into muddy slope deposits beyond the deformation zone. The Blockhouse section is interpreted as the shelf edge rollover zone for WfC 3.

For WfC 4, the contextual setting of shore-face deposits updip of a discrete zone of gully incision and a basinward-thickening package of turbidites incised by an upper slope channel places the shelf edge rollover position in the same Blockhouse area. This interpretation is

supported by the thickening of clinothems at (WfC 3) and beyond (WfC 4) the Blockhouse locality (Fig. 4.5); this is a key geometric criterion (Dixon et al., 2012a) and is consistent with an increase in accommodation beyond the shelf edge rollover.

4.9. Variability between clinothems WfC 3 and WfC 4

Differences in processes and architecture between clinothems WfC 3 and WfC 4 at the shelf edge rollover highlight the stratigraphic variability possible between successive clinothems (Fig 13). Both show broadly progradational profiles with similar thickness and shelf edge rollover positions. However, WfC 3 is characterized by a strong fluvial influence and shelf-delta–scale internal clinoforms. In contrast, the character of WfC 4 indicates a wavestorm-influenced delta front setting. Along the Blockhouse section, WfC 3 and WfC 4 exhibit quite different process responses to the preexisting shelf break. Amalgamated sandstones at the top of WfC 3 are heavily deformed and segregated into a series of rotational growth fault structures consistent with the increase in gradient encountered at the shelf edge rollover.

In contrast, rotational growth fault features did not develop along the Blockhouse section in WfC 4, although soft-sediment deformation is widespread. WfC 3 has a gradational top, whereas the top of WfC 4 is sharp and highly erosive locally, with broad shallow gully fills. Beyond the interpreted shelf edge rollover, WfC 3 thins and downlaps into the slope mudstone succession. WfC 4 thickens beyond the shelf edge rollover; this is associated with a change in process to extensive turbidity current deposits that are incised by an upper slope channel, and is consistent with increased sediment supply beyond an incised shelf edge rollover. WfC 4 thins and pinches out into the slope mud-stone succession 10 km beyond the pinch-out of WfC 3.

4.10. Discussion

Architectural and sedimentary facies change along a dip profile is commonly described based on a single basin margin clinothem (e.g. Uroza & Steel, 2008; Charvin *et al.*, 2010) or a succession of clinothems that appear similar at seismic resolution (Pyles & Slatt, 2007). Successive clinothems are commonly reported to have similar facies associations and architecture (Mellere *et al.*, 2002; Dixon *et al.*, 2012a). The two stacked clinothems described and interpreted here record significantly different process responses to sedimentation at a similar geographic shelf edge rollover position.

4.10.1. Controls on clinothem architecture

The interpreted rollover zone of WfC 3 is marked by a 5 km dip length zone of extensional deformation and basinward clinothem thickening (Figs. 7A, 7B, and 8). Sand was trapped in the depressions created by extensional growth faults at the shelf edge, contributing to limited sand supply directly basinward of the rollover. WfC 4 is wave and storm dominated and is characterized by a narrower (~2 km dip length) shelf edge rollover zone with widespread erosion and gullying coincident with basinward thickening and significant amounts of sand transferred beyond the shelf edge rollover (Figs. 7C, 7D, and 9).

The presence of fluvial feeder systems close to the shelf edge rollover has been shown to play a key role in the delivery of sand beyond the rollover (Morton & Suter, 1996; Johannessen & Steel, 2005; Carvajal *et al.*, 2009). Fluvial systems are able to supply a significant amount of sediment to a focussed area at the shelf edge. They also have the potential to incise and degrade the shelf edge rollover zone and promote the initiation of turbidity currents on the upper slope through hyperpycnal flows or mouth bar collapse. Fluvial systems are therefore effective at delivering sediment beyond the shelf edge through gravity-driven processes. It has also been suggested that a dominance of storm and wave processes at the shoreline reduces the potential for delivery of sediment beyond the shelf edge due to (1) the along-margin distributive effect of these processes on sand dispersal patterns and (2) the limited potential to incise the shelf edge rollover and create conduits due to the lack of focus (Carvajal & Steel, 2006). Therefore, wave- and storm-dominated settings have been proposed to be important in the development of thick packages of sediment along the shelf edge with limited downslope sediment supply (Carvajal & Steel, 2009).

Given that deltas in both the studied clinothems reached the rollover area, a simple prediction following the established conceptual model above would be that the fluvial-dominated WfC 3 would supply more sediment beyond the shelf edge rollover with the development of turbidites downdip. Although only a 2D oblique-dip panel constrains the interpretation presented here, the data show that in this case the wave-dominated clinothem was more efficient at supplying coarse-grained sediment across the shelf edge rollover.

Basinward sand supply across the shelf edge rollover can occur in wave- and storm-dominated settings during highstands of sea-level under a number of circumstances: (1) if a narrow shelf significantly reduces delta transit times to the shelf edge (Piper & Normark,

2001), (2) where there is strong longshore sand transport into canyons that incise into the shelf (Boyd *et al.*, 2008; Covault & Graham, 2010), (3) under high sediment supply conditions where shelf redistribution processes are weak (Weber *et al.*, 1997), (4) where a sub marine canyon has incised across much of the shelf (Lobo *et al.*, 2006; Fernández-Salas *et al.*, 2007; Covault & Graham, 2010), and (5) where extreme storms can produce strong storm-surge ebb currents that incise shoreface sandstones and canyon walls and resuspend and redistribute sediment offshore (e.g. Dail *et al.*, 2007; Goff *et al.*, 2010; Rogers & Goodbred, 2010). An increase in sedimentation rate through time has the potential to influence the architecture of successive clinothems. There is no evidence for incision of the shelf edge rollover in the fluvial-dominated WfC 3, but it appears that the rate of sediment input was high enough to drive synsedimentary growth faults, resulting in sand being sequestered around the rollover area. In contrast, WfC 4 was able to step farther into the basin possibly due to a prolonged period of higher sediment supply; this period of maximum regression is consistent with a significant amount of sediment transfer across the shelf edge. This point is expanded upon in the following.

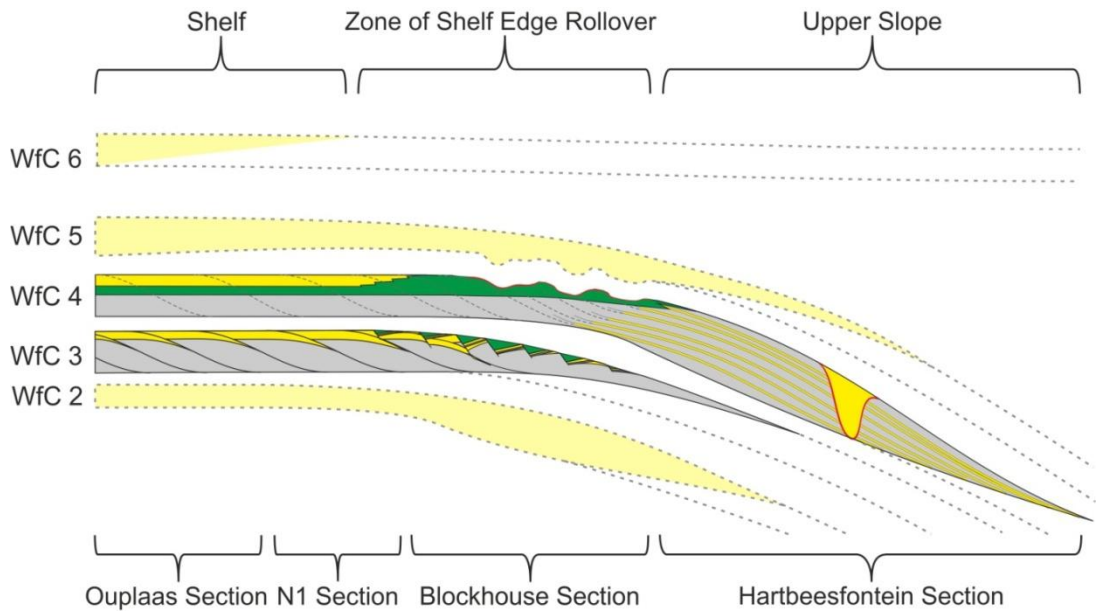

Figure 4.13: Schematic diagram summarizing the different responses of Waterford clinothem (WfC) 3 and WfC 4 to increasing gradient at the shelf edge rollover. Individual clinothems are vertically separated for clarity. See text for details.

4.10.2. Subaerial exposure of the shelf edge rollover

Changes in relative sea-level have been widely invoked as one of the main factors controlling clinoform architecture and facies distribution (Steel & Olsen, 2002; Porębski & Steel, 2006; Ainsworth *et al.*, 2008; Steel *et al.*, 2008). Lowering of relative sea-level results in reduced accommodation on the shelf (Posamentier *et al.*, 1988) and promotes incision of

the fluvial feeder system into the shelf (e.g. Posamentier & Vail, 1988b; Van Wagoner *et al.*, 1990; Mutti & Davoli, 1992; Milton & Dyce, 1995; Marjanac, 1996; Normark *et al.*, 1998; Johannessen & Steel, 2005). Examples of large-scale shelf edge fluvial incision at outcrop have been well documented from the Eocene succession from Spitsbergen (Plink-Bjorklund *et al.*, 2001; Mellere *et al.*, 2002; Carvajal & Steel, 2009). However, is the exposure of the shelf edge rollover due to relative sea-level fall necessary for incision and sediment bypass?

The basinward-thickening package of unconfined, upper slope turbidites situated beyond the WfC 4 rollover is strong evidence that reduced accommodation on the shelf enabled progradation beyond the shelf edge rollover zone. Widespread erosion at the shelf edge rollover and incision on the upper slope along the top surface of WfC 4 indicates that there was a late-stage change from accretion to incision. This may have been due to relative sea-level falling below the shelf edge rollover, but this would have resulted in widespread subaerial exposure of the more proximal shelf areas. Assuming the shelf edge was at sea-level, a typical shelf gradient of 0.01° (Miall, 1991; Cattaneo & Steel, 2003; Sømme *et al.*, 2009), and a minimum shelf width of 21 km (the distance from the most proximal Ouplaas locality to the shelf edge rollover zone at the Blockhouse locality), the Ouplaas locality would have been 3.6 m above sea-level. Despite this, no evidence for subaerial exposure (rootlets, desiccation cracks, or soil horizons) or widespread truncation of the underlying deposits has been found within WfC 4. This suggests that the amplitude of any relative fall in sea-level was not great enough to expose the shelf edge rollover (Fig. 4.14). The stacking pattern of parasequences in the lower Waterford Formation is an important additional line of evidence on the accommodation history. A composite sequence boundary is interpreted at the base of unit G (Figueiredo *et al.*, 2010), as this unit marked a significant change in depositional style from the underlying slope channel-levee systems (Flint *et al.*, 2011a). The regional fine-grained unit above unit G (Figs. 2B and 5), which is interpreted to represent a long-term rise in relative sea-level, is consistent with a transgressive systems tract (TST) and early highstand systems tract and includes the offshore equivalent of the maximum flooding surface. The overlying succession shows a clear progradational stacking pattern from WfC 1 to WfC 4 (Fig. 4.5), consistent with a (HST). The regional correlation demonstrates that WfC 5 marks a slight landward step relative to WfC 4 (retrogradational stacking), and the overlying regional 30-m-thick mudstone is interpreted to include the offshore expression of the next maximum flooding surface. WfC 4 therefore represents the maximum regression in the lower Waterford sequence, and the change in stacking pattern from progradational to retrogradational. Due to the absence of subaerial exposure and

fluvial incision, this change in stacking pattern is interpreted as a regressive surface of marine erosion (sequence boundary) (Vail *et al.*, 1977b; Van Wagoner *et al.*, 1990). The regressive surface of marine erosion is placed along the erosive surface at the top of WfC 4 due to the fine-grained mudstone observed in the base of the gullies that separated WfC 4 from WfC 5. Therefore, the gully fills are included as part of the TST of a second sequence. The maximum supply of sand over the shelf edge is associated with the most regressive parasequence in sequence 1 and supports the notion that in high supply settings sediment can be delivered over the shelf edge rollover without subaerial exposure (Burgess & Hovius, 1998; Carvajal & Steel, 2009), under a wave- and storm-dominated process regime.

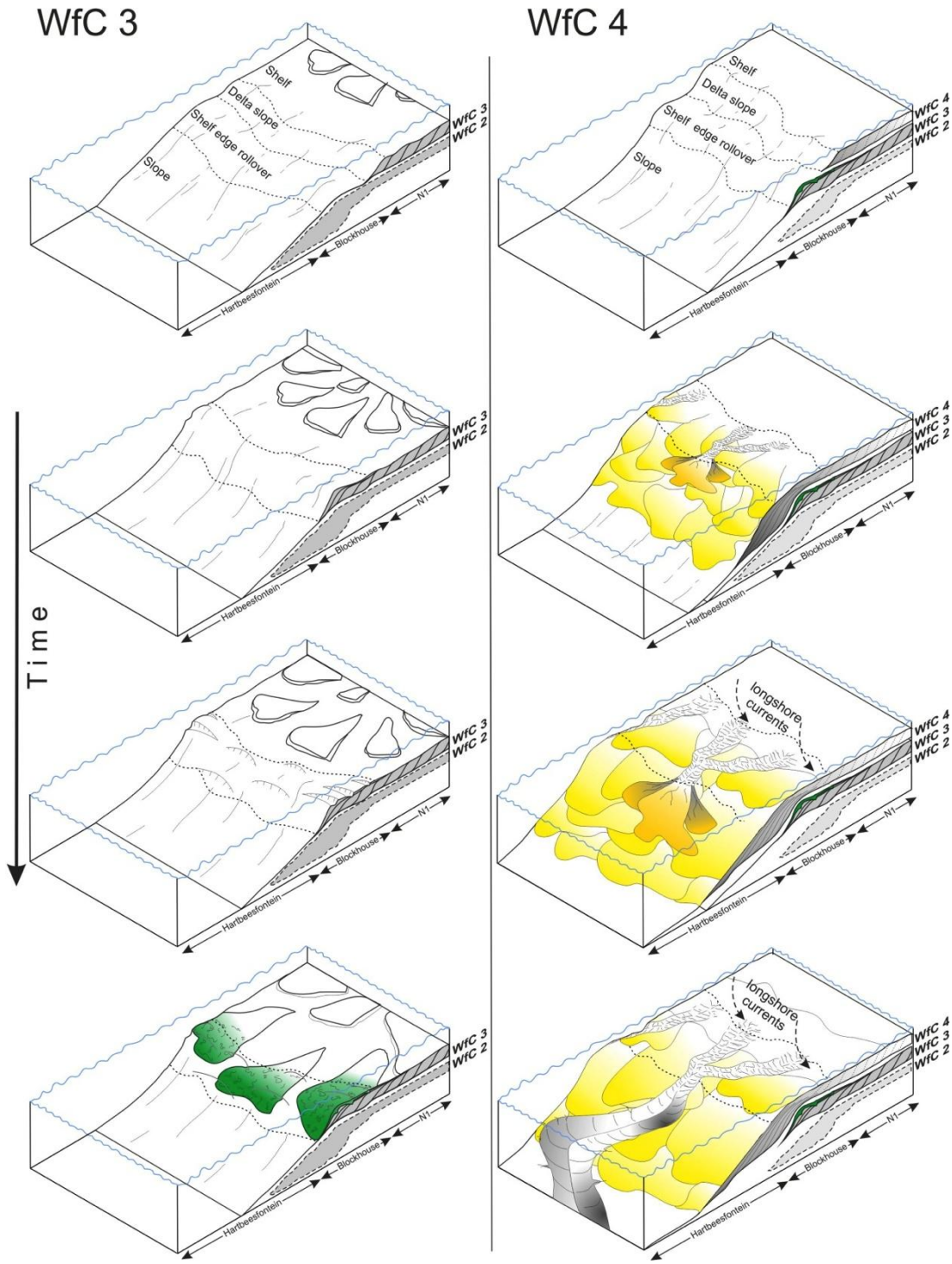

Figure 4.14: Evolution of Waterford clinothem (WfC) 3 and WfC 4 through time on encountering the shelf edge rollover. WfC 3 encountered the shelf edge rollover, but sediment was trapped in rotational growth faults, preventing progradation onto the upper slope. WfC 4 was able to supply sediment beyond the shelf edge rollover and cut shelf edge gullies as well as a turbidite-filled slope channel, despite the shelf never becoming subaerially exposed within the study area.

4.10.3. Limitations of identifying the shelf edge rollover from a 1D profile

Many clastic basin-fill successions pass upward from slope to shelf settings, and therefore any 1D section should pass through the shelf edge rollover at some stratigraphic position, unless the basin margin has a ramp geometry. Given the regional context provided by the large outcrop extent of WfC 3 and WfC 4, a number of criteria have been derived to define the shelf edge rollover zone in a mixed influence system along a 2D dip profile. Attention has also been drawn to the potential variability of successive clinothems. Therefore, attempting to identify the shelf edge rollover from a 1D section or from outcrop with limited lateral exposure will be subject to significant limitations.

1. Without regional depositional dip context, recognizing gradient change across the shelf to slope transition will not be possible because the change is subtle.

2. Distinguishing turbidites deposited beyond the shelf edge rollover from delta front turbidites associated with inner shelf deltas is challenging without being able to record their run-out distances, and could lead to misinterpretation of the position on the shelf-slope profile.

3. Basinward thickening of clinothems coincident with a change to sediment gravity flow deposits is a key criterion for identifying the rollover (Dixon *et al.*, 2012a), and this is difficult to determine in one dimension.

4. The occurrence of abundant soft-sediment deformation has been attributed to proximity to the shelf edge rollover (e.g., (Stow, 1994; Galloway, 1998; Lee *et al.*, 2009; Pratson *et al.*, 2009; Oliveira *et al.*, 2011). However, as shown in the regional correlation of WfC 3 and WfC 4, soft-sediment deformation is abundant from the most proximal exposures at Ouplaas to the Blockhouse section, a distance of ~25 km, without significant thickness changes in the packages. These features are attributed to instability on the slopes of inner shelf deltas.

5. Landward-rotated growth fault features are common in shelf edge deltas (Rider, 1978; Coleman *et al.*, 1998). The abrupt thinning of deformed packages beyond the inferred shelf edge rollover further indicates that simply the presence of soft-sediment deformation is not sificiant criteria for identifying the shelf edge rollover, but rather that the scale and process of deformation are more accurate indicators of proximity to the shelf edge rollover zone (Oliveira *et al.*, 2011).

4.11. Conclusions

The large-scale outcrops of the Waterford Formation have enabled a set of criteria to be developed for the identification of exhumed shelf edge rollovers on a large, low-gradient basin margin. These criteria vary as a function of the river- or wave-dominated process regime of the parasequence at the shelf edge. The criteria include widespread erosion or gullying, extensional growth faults, an increase in large-scale soft-sediment deformation, and basinward thickening of parasequences (associated with increased amounts of thin turbidite beds) over a zone of several kilometres in a basinward direction. Although the criteria were developed for a low-gradient setting, they may also offer a reference point for other, more complex basin margins or other outcrop settings with limited dip or lateral exposure. Although the literature is replete with examples in which soft-sediment deformation is used to suggest proximity to the shelf edge rollover (Oliveira *et al.*, 2011), this study shows that the presence of soft-sediment deformation alone is not an adequate criterion with which to define the shelf edge rollover; in the case of the lower Waterford Formation it is simply a common feature of delta-scale clinothems on the shelf.

Process regime and architecture may vary significantly between successive shelf edge rollover successions. High sediment supply to the shelf edge in a river-dominated parasequence drove extensional deformation of the shelf edge rollover that provided an effective trapping mechanism for sand, and limited transfer of sediment beyond the shelf edge rollover. The overlying parasequence is wave and/or storm dominated, but the lower accommodation setting of this parasequence was an important factor in delivery of sediment over the shelf edge, probably in combination with longshore re distribution. The mechanism of sand supply to the upper slope was via a network of gullies (below seismic resolution) and incised upper slope channels cut by subaqueous turbidity currents in the absence of subaerial exposure. This case study shows that it is possible to source deep-water slope turbidite systems from subaqueous wave-dominated regimes at the shelf edge rollover. The significant stratigraphic variability between WfC 3 and WfC 4 at the clinoform rollover highlights the difficulty in identifying the shelf edge rollover position in 1D sections. Interpretations based on individual shelf edge rollover criteria without regional context will lead to the misinterpretation of the shelf edge rollover position, and limit downdip predictive capabilities.

CHAPTER 5.

LATERAL VARIABILITY IN SHELF EDGE PROCESS REGIME AND SHELF EDGE TRAJECTORY DURING DIFFERENTIAL SUBSIDENCE

This chapter builds on the interpretations made in chapter 4 and integrates data from two additional sub-parallel 2D dip profiles to provide 3D coverage of the changes in architectural and facies distribution across the lower Waterford margin. Discussion focuses on the factors that led to greater sediment supply to the upper slope in the north of the study area without clear evidence for a fluvial driver, during a period of steeply rising margin trajectory, factors which contradict established hypotheses for sand delivery beyond the shelf edge rollover.

5.1. Abstract

Sediment supply rate and accommodation regime represent primary factors controlling the depositional architecture of basin margins. Their interaction is commonly presented as a two-dimensional (2-D) problem, although across-strike variability in basin margin physiography and process regime strongly affects sediment partitioning and stratigraphic predictability between the shelf, slope and basin floor. Three >40 km 2D depositional dip profiles from the lower Waterford Formation, Karoo Basin, South Africa, have been correlated to enable characterization of the shelf-to-slope transition for three successive clinothems (WfC 3, 4 & 5) over a 900 km^2 area. This dataset provides a rare opportunity to assess stratigraphic and palaeogeographic changes in sub-seismic scale processes around an ancient shelf edge, and the lateral variability in the trajectory of successive shelf edge rollovers that formed on a low-gradient basin margin over geological time.

The three parallel dip profiles show similar shelf edge rollover trajectories, but this belies significant along-margin variability in process and physiography. To the south, a wider shelf resulted in limited coarse-grained sediment being supplied to the slope for any of the studied clinothems. To the north, consistently higher sediment supply combined with a narrower shelf produced long term sand supply to the slope in all three clinothems, even with a strong wave and storm dominated process regime. However, supply of coarse-grained sediment beyond the shelf edge rollover was not the only method for progradation of the lower Waterford margin. Regional correlations show that significant progradation of the margin took place during highstand times through accretion of fine-grained deposits, resulting in the development of a wide shelf over which successive sand-dominated shelf delta parasequences prograded.

5.2. Introduction

Traditional sequence stratigraphic models provide a tool for prediction of lithologies and key surfaces in space and time and enable a better understanding of how basin margins respond to the principal controlling factors of sediment supply and accommodation change (Vail *et al.*, 1977b; Posamentier & Vail, 1988b; Van Wagoner *et al.*, 1988; Galloway, 1989; Martinsen & Helland-Hansen, 1995; Steel & Olsen, 2002; Johannessen & Steel, 2005). However, many models and approaches, including trajectory analysis, have treated the generation of accommodation and the input of sediment supply as a two-dimensional problem (Driscoll & Karner, 1999). Interpretation of passive margin development and prediction of sedimentary facies distribution is therefore still commonly limited to two-dimensional dip orientated profiles. Examples include the New Jersey margin (Mountain & Proust, 2010), Battfjellet Formation Spitsbergen (Helland-Hansen, 2010), Magallanes Basin Chile (Covault *et al.*, 2009), Lewis Shale Wyoming (Pyles & Slatt, 2007). Yet, observations of modern systems indicate significant along margin variability in terms of subsidence patterns, margin physiography, distribution of sediment supply points, discharge rates and process regime (e.g. Olariu & Steel, 2009). The same parameters will also vary in time, which will result in complexity in spatial and temporal trends.

Commonly, sequence stratigraphic models discriminate different systems tracts based upon clinoform geometry and stacking patterns (Van Wagoner *et al.*, 1990). Oblique clinoforms (those with no topset but a well developed foreset and bottomset) are consistent with periods where accommodation is low; oblique clinoforms are therefore associated with falling relative sea-level during a falling stage to lowstand systems tract. Sigmoidal clinoforms (those with complete topsets) are consistent with periods of positive shelf accommodation, therefore sigmoidal clinoforms are considered to be typical of periods of rising relative sea-level during transgressive and highstand systems tracts (Sangree & Widmier, 1978). Similarly, trajectory models state that flat to falling trajectories during periods of limited or reducing accommodation are typically associated with thin or absent topsets and with significant sediment supply to the foreset and bottomset (Helland-Hansen & Hampson, 2009). In contrast, a rising trajectory during periods of excess accommodation results in sequestering of sediment in the topset with minimal supply to the foreset and bottomset. However, the out of plane variability of such clinoform geometries and trajectory paths has largely been overlooked due to either limitations in the primary dataset or the additional complexity that it introduces. In addition, these models have been

developed from reflection seismic datasets where calibration to sedimentary facies is sparse.

Improved understanding of the three-dimensional variability of basin margins has been afforded by increasingly detailed 3D seismic datasets (Suter & Berryhill, 1985; Matteucci & Hine, 1987; Poag *et al.*, 1990; Tesson *et al.*, 1990; Morton & Suter, 1996; Kolla *et al.*, 2000; Fulthorpe & Austin, 2008; Monteverde *et al.*, 2008; Henriksen *et al.*, 2011; Sanchez *et al.*, 2012a, b) but such datasets still lack the subseismic architectural detail and process information that can be obtained from outcrop. Building on the dataset presented by Jones *et al.* (2013) (chapter 4) from the lower Waterford Formation, Karoo Basin, South Africa; here data from two further parallel dip profiles are introduced to provide a rare three-dimensional (3D), outcrop-based case study on the lateral variability across successive clinothems. Specifically the variability of the large scale sequence stratigraphic architecture and trajectory paths are discussed in conjunction with stratigraphic and palaeogeographic changes in process regime at the shelf edge rollover and what effects this has on the temporal and spatial variability of sedimentary facies including the delivery of sand to the slope and basin floor.

5.3. Geological setting

The Karoo Supergroup in the Laingsburg area of South Africa is 5500-m-thick and is divided into the Dwyka Group (Late Carboniferous to Early Permian aged glacial deposits), Ecca Group (Permian aged clastic marine/marginal marine sediments) and the Beaufort Group (Permo – Triassic fluvial sediments; (Veevers *et al.*, 1994; Johnson *et al.*, 1997; Rubidge *et al.*, 2000; Cole & Whipplinger, 2001) (Fig. 5.1A). Subsidence during Ecca Group time was generated by dynamic topography related to subduction of the oceanic plate (Mitrovica *et al.*, 1989; Tankard *et al.*, 2009).

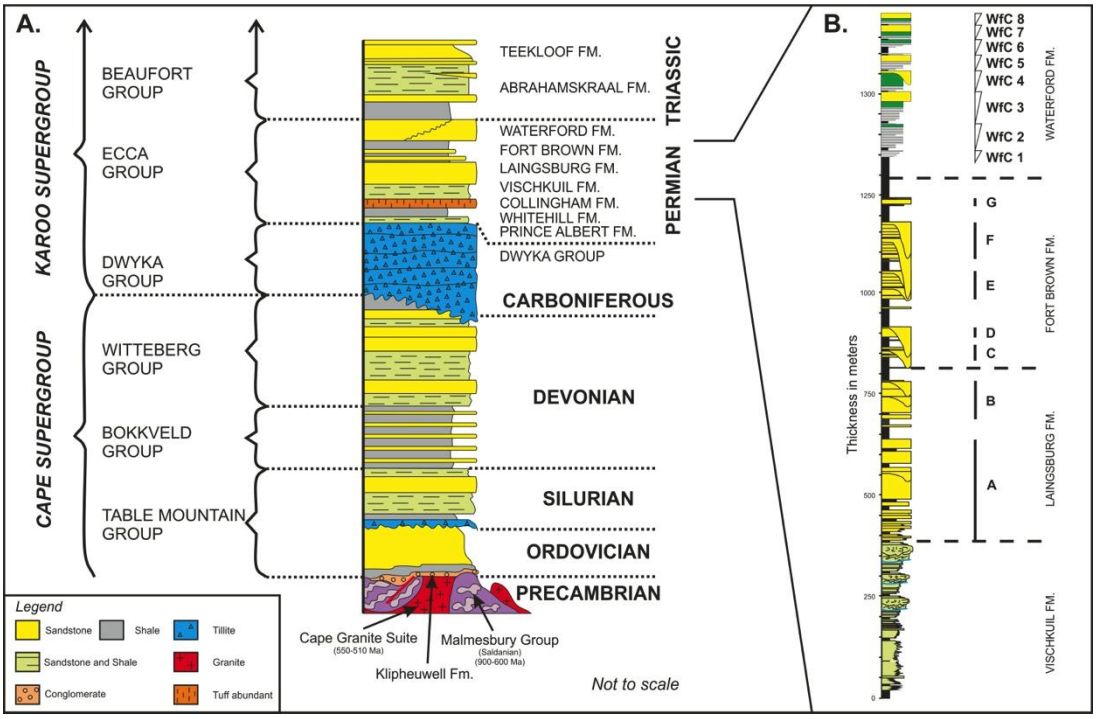

Figure 5.1: (A) Lithostratigraphy of the Western Cape area, redrawn after Wickens (1994). (B) Schematic stratigraphic log of the upper Ecca Group in the Laingsburg depocentre. The lower Waterford Formation detail is based upon a single type section from the Baviaans North dip panel (Fig. 5.2) and shows 8 studied parasequences. The focus of this study is on WfC 3, 4 and 5.

The Ecca Group is a shallowing-upward succession where the basal Vischkuil Formation represents distal basin plain deposits (van der Merwe *et al.*, 2009; 2010) overlain by basin-floor fan deposits of the Laingsburg Formation (Sixsmith *et al.*, 2004). The overlying submarine slope succession of the Fort Brown Formation is dominated by channel-levee complexes and entrenched slope valleys (Figueiredo *et al.*, 2010; Hodgson *et al.*, 2011b). Continued progradation is marked by the ~400-m-thick Waterford Formation, the focus of this study, which comprises a mixed river- and wave-influenced deltaic succession (Wickens, 1994; Oliveira *et al.*, 2011). The complete vertical stratigraphic transition from erosional slope channel-levee systems (Fort Brown Formation) to shelf deltas (Waterford Formation), in combination with extensive down-dip exposures, have allowed the physical identification of the shelf edge rollover along a series of clinoform profiles.

5.4. Study area, data and methodology

The lower Waterford Formation crops out along the limbs of post depositional east-west trending synclines and anticlines, and provides a series of exceptional depositional dip-parallel exposures (>40 km) and significant strike control (~20 km) across the 900 km^2 study area (Fig. 5.2). Analysis included the collection of 51 detailed logged sections (Fig. 5.2C) totalling 15,950 m cumulative thickness. Individual logged sections were physically

correlated by walking regionally persistent fine-grained mudrock units between logs (Fig. 5.3A, B & C panels).

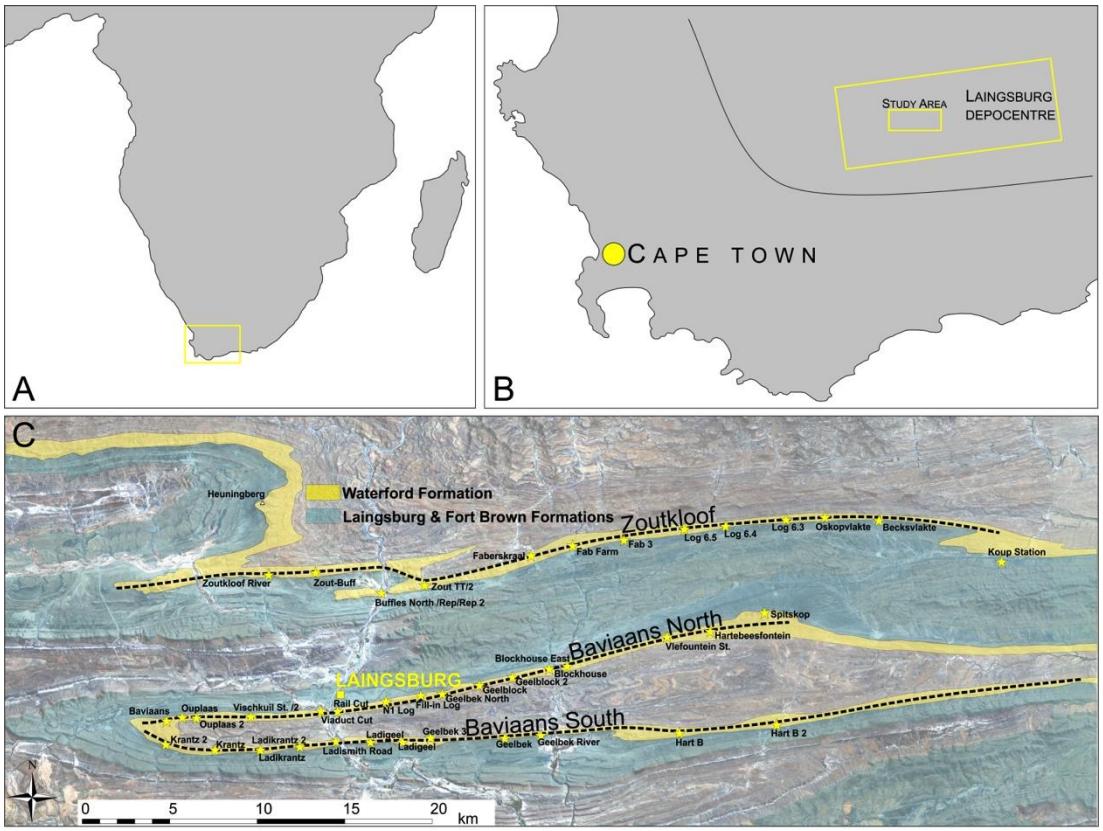

Figure 5.2: (A) (B) & (C) Locality maps of southern Africa and the Western Cape Province, with location of the Laingsburg depocentre and study area indicated. (C) Aerial image of the study area showing the three dip profiles and the locations of logged sections (yellow stars) referred to in the text.

5.5. Stratigraphic framework

Earlier work by Jones *et al.* (2013) recognized multiple, low gradient (<1°) basin margin scale clinothems in the Baviaans North dip profile (Fig. 5.2C, 5.3B). Clinothem geometries were recognized by constraining thickness variability and sedimentary facies distributions in combination with stratigraphic context. Although the complete topset, foreset and bottomset of an individual clinothem cannot be fully delineated due to outcrop constraints, it is possible to recognize basinward thickening of stratal packages that are separated by fine-grained regional mudrock packages interpreted to contain the offshore equivalents to flooding surfaces. This geometric criterion used in the identification of clinothems (Dixon *et al.*, 2012a) is supported by significant facies and architectural changes across the interpreted shelf edge rollover (Jones *et al.*, 2013). These include:

- Large scale extensional deformation (growth faults) at the shelf edge rollover
- Widespread erosion at the shelf edge rollover

- Dominance of sandy turbidites beyond the shelf edge rollover, down dip of delta/shoreface facies
- *In-situ* deformation confined to the shelf and terminating abruptly at the shelf edge rollover

Here we introduce new data from two additional regional dip profiles (the Zoutkloof and Baviaans south profiles) (Fig. 5.3A & B) in order to provide across-strike control on sedimentological characteristics and stratigraphic architecture. The overall palaeoflow is to the NE and E such that the three panels are dip-profiles (Fig. 5.5), landward to the west and basinward to the east.

This chapter uses Table 2.1 and 3.1 in chpters 2 and 3 when referring to facies and facies assoceations.

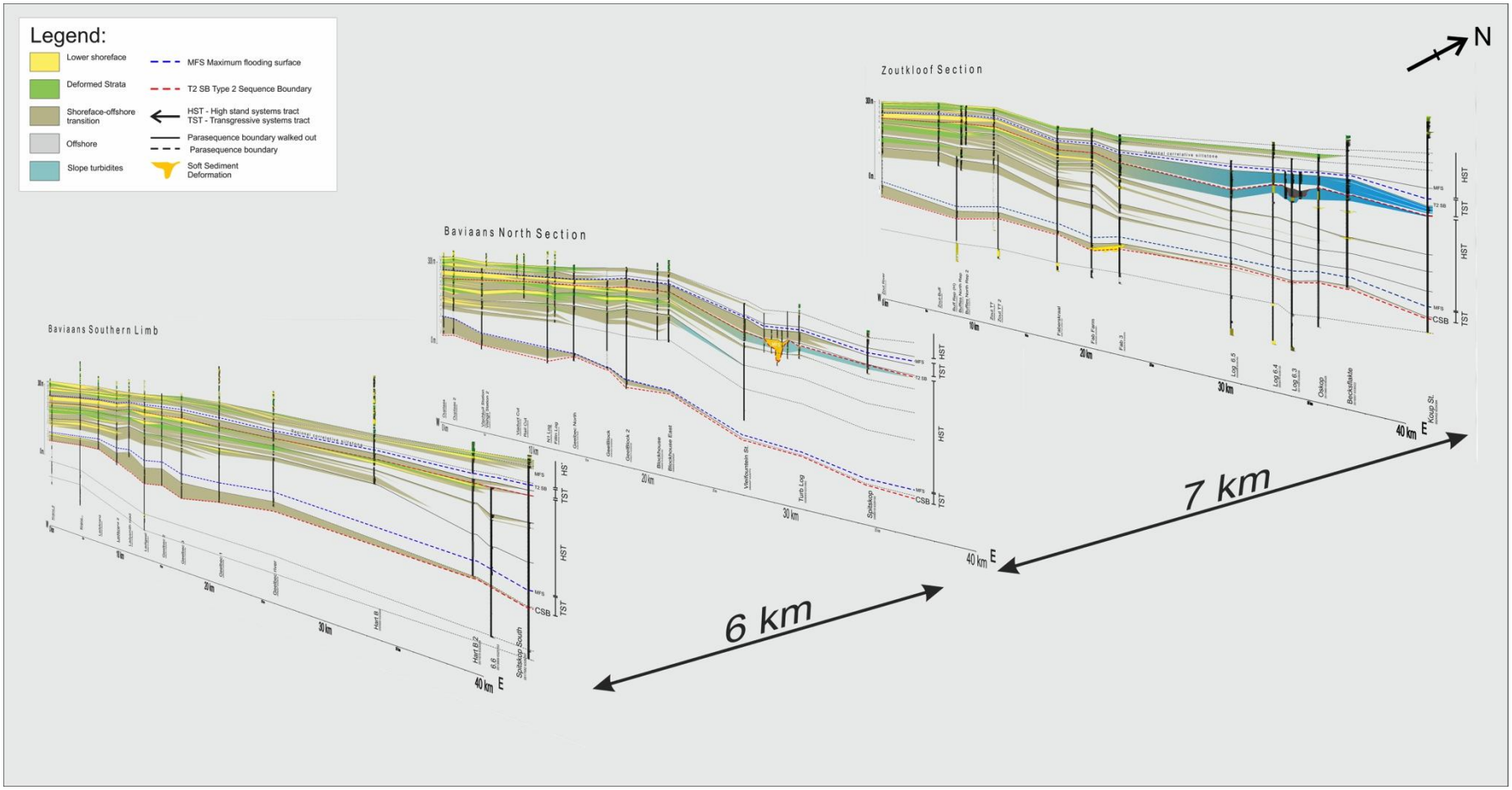

Figure 5.3: Baviaans South, Baviaans North and Zoutkloof correlations panels (Fig. 1.13) showing eight lower Waterford parasequences. Bounding flooding surfaces are shown as well as interpreted maximum flooding surfaces and sequence boundaries. The panels use Unit F as a correlation datum. Prodelta strata are khaki, deformed strata are green and amalgamated sandstone bodies are yellow and show the maximum progradational extent of the lower Waterford Formation. Upper slope turbidite deposits are blue. For high resolution PDF image refer to CD insert.

The lower Waterford Formation comprises 8 regionally correlated stratigraphic units, which are named Waterford clinothems (WfC) 1-8, and are separated from the underlying channelized slope succession by a regionally extensive 80-m-thick mudstone marker unit (Fig. 5.1A) (Jones *et al.*, 2013). Each clinothem exhibits a coarsening- and thickening-upward profile, in some cases with a fining- and thinning-upward upper section. In the up-dip exposures clinothems decrease in thickness stratigraphically from ~140 m to ~20 m. The vertical profile, depositional setting and scale of the stratigraphic packages are consistent with parasequences as described by Van Wagoner *et al.* (1990).

WfC 1 and 2 (138 & 47-m-thick respectively where they are thickest in their most westerly exposures) are dominated by heterolithic siltstone and sandstone beds (F.4) (Fig. 5.4B), but in the most proximal settings WfC 2 contains amalgamated sandstone beds (F.10) (Fig. 5.4E), especially along the Baviaans South and North profiles. Unidirectional and bidirectional paleoflow measurments were taken from ripple foresets, ripple crest, flutes casts and grouves marks. WfC 1 exhibits a dominantly north-east unidirectional paleoflow direction and a more east-north-ease to west-south-west trending bidirectional trend (Fig. 5.5). WfC 2 exhibits a more north-north-west unidirectional paleoflow and stronger east-north-ease to west-south-west trending bidirectional trend. Regional correlation of WfC 1 shows an overall thinning of the sandy component to the south (across strike) and to the east (basinward). The down dip pinch-out of the coarse grained component of WfC 1 shows that it has the least basinward extent of the parasequences and is the only one not present in all three depositional dip profiles (absent for the Baviaans South profile) (Fig. 5.3A). WfC 2 follows the same trend of thinning both southward and eastward, but is present along all three dip profiles and shows a progradational trend relative to WfC 1.

WfC 3 (51-m-thick where it is thickest in its most westerly exposures) has a more asymmetrical profile than the underlying parasequences, especially in more proximal (western) areas. In the proximal exposures of WfC 3 a typical vertical facies transition is recorded from offshore siltstone (F.0) (Fig. 5.4A), to heterolithic shoreface-offshore transition deposits (F.4) (Fig. 5.4B), to deformed debrites (F.4 & 5) and *in-situ* deformed lower shoreface deposits (F.7) (Fig. 5.4C) followed by undeformed, amalgamated lower shoreface sandstones. WfC 3 exhibits a swing toward a more east-north-east unidirectional paleoflow direction when compared to WfC 2 and a similar east-north-east bidirectional trend (Fig. 5.5). Northward and eastward the sandy component of WfC 3 decreases as the overall parasequence thickness increases (from 42 m to a maximum of 78 m). Regional

correlations show that WfC 3 prograded further basinward than the underlying parasequences (Fig. 5.3). Metre-deep sand-filled gullies (Fig. 3.9) in the offshore mudstone facies suggest that WfC3 delivered minor amounts of sediment to the upper slope in the north of the area.

WfC 4 (38-m-thick where it is thickest in its most westerly exposures) exhibits a broadly similar asymmetrical profile and vertical facies succession to WfC 3 across much of its proximal extent, but is notable for the intensity and volume of soft sediment deformed facies (F.5, 6 & 7). WfC 4 exhibits a typical north-east unidirectional and bidirectional paleoflow trend (Fig. 5.5). Eastward and northward, the shoreface-offshore transition and deformed facies associations fine and thin whilst parasequence thickness increases. Central and northern areas exhibit a transition to the east from lower shoreface facies association (F.10) (Fig. 5.4E) and deformed facies (F.5, 6 & 7) (Fig. 5.4C) to a basinward thickening wedge of undeformed heterolithic to amalgamated slope turbidite sandstones (F.16) (Fig. 5.4D & D.1). Two incisional channels cut into the basinward thickening wedge. The channel observed along the Zoutkloof profile is mud filled while the channel on the Baviaans north profile (chapter 4) is filled with thick amalgamated turbidite sandstone (F.14 & 15).

WfC 5 exhibits a strongly asymmetrical profile, and is between 20- and 25-m-thick in its up dip exposures. It differs from the underlying parasequence due to the notable lack of deformed facies and greater thickness of lower shoreface deposits (F.10) (Fig. 5.4E & E.1). WfC 5 is consistent with the underlying parasequences exhibiting a strong north-east unidirectional and north-east to south-west bidirectional paleoflow (Fig. 5.5). Similar down dip facies changes are observed along each of the three parallel dip profiles, where amalgamated lower shoreface (F.10) deposits fine and thin into heterolithic (F.4) (Fig. 5.4B) facies and offshore siltstone (F.0) (Fig. 5.4A). Amalgamated lower shoreface facies (F.10) are extensive in the south of the study area, but they pass into shoreface-offshore transition deposits northwards. Toward the northeast, shoreface-offshore transition deposits pass basinward into upper slope turbidites, similar to WfC 4, indicating a transition from shelf to slope.

Across the study area WfC 5 is overlain by a regional fine-grained marker unit that thickens and fines to the east (basinward). The overlying sand package, WfC 6, 7, and 8 are 32-, 23- and 20-m-thick respectively in their up dip exposures, with coarsening and thickening upward profiles. These upper parasequences are dominated by deformed and amalgamated lower shoreface facies (F.10) in their proximal exposures and a typically thin

offshore (F.0) and heterolithic shoreface-offshore transition (F.4) deposits. The north-east unidirectional and bidirectional paleoflow trend persists throught WfC 6, 7 and 8 (Fig. 5.5). Dip variability for WfC 6 and 7 is consistent with the underlying parasequences as they record a gradual eastward transition from deformed (F.5, 6 & 7) and lower shoreface facies (F.10) (Fig. 5.4E) deposits to heterolithic shoreface-offshore transition (F.4) (Fig. 5.4B) and finally offshore (F.0) (Fig. 5.4A) siltstone. The greatest eastward extent of deformed and shoreface facies is recorded in the south. However, WfC 6 and 7 do not thicken basinward and their sandy components pinch out landward of the sandy part of WfC 3, 4, and 5. The regional correlations of WfC 8 reveal little facies variability across the study area. A small degree of basinward fining is apparent along each of the three dip profiles. However, in the most distal Koup Station locality on the Zoutkloof profile an abrupt transition to offshore (F.0) (Fig. 5.3) facies could be consistent with an increase in gradient at the shelf edge.

Figure 5.4: Representative photographs of the facies associations typical of the coarsening and thickening upward parasequences of the lower Waterford Formation. (A) F.0 - Offshore mudstone, (B) F.4 - Shoreface-offshore transition, (C) F.6 - Deformed, (includes debris-flows transported by mass flow (F.4 & 5) and *in-situ* deformed (F.6) strata with vertical structures). (D) F.10 - Lower shoreface. (E) F.16 - Upper slope turbidites. (F) F.11 - Amalgamated, climbing ripple dominated sandstone (distal mouth bar).

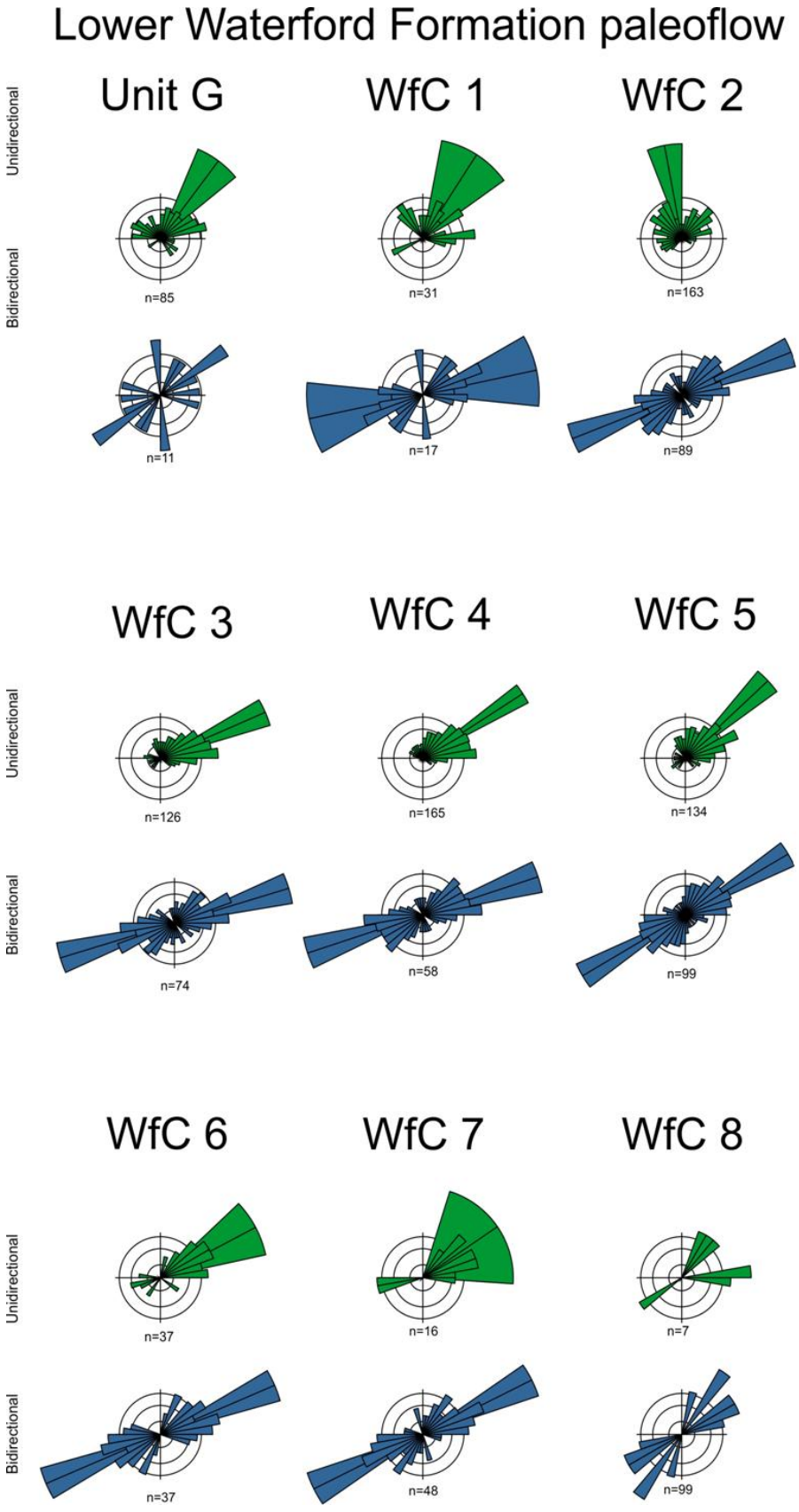

Figure 5.5 Paleoflow directions recorded for each parasequence. Green = unidirectional (internal ripple lamination, flute casts etc). Blue = Bidirectional (rippple crests, grove casts etc)

5.5.1. Summary

Individual parasequences exhibit significant basinward thickening associated with the area of shelf edge rollover. Thickness isopach maps for WfC 3, 4 and 5 (Fig. 5.5) reveal consistent thickening of individual parasequences across-strike toward the north. This trend for thickening to the north is most pronounced in WfC1, the sandy component of which is absent along the southern profile and thickens to ~35 m on the northern profile. Thickening to the north is less pronounced but is present in successive parasequences. Total thickness of the lower Waterford Formation (Units G – WfC 8) increases from 247 m in the south to 360 m in the north on the shelf, and from 305 to 390 m on the slope. The northward thickening of successive parasequences is consistent with a south to north facies trend that shows a decrease in amalgamated lower shoreface facies and deformed facies and an increase in shoreface-offshore transition and offshore facies. The two factors together are indicative of more accommodation to the north. Dominant unidirectional palaeoflow directions are consistently to the north-east, which reflects the progradation of the system in the same direction.

The intense deformation recorded in the shelf deposits of WfC 4 is attributed to an increased rate of progradation across the shelf due to reduced accommodation and high sediment supply (Jones *et al.*, 2013). Rapid progradation of the deltaic system to the shelf edge rollover enabled the supply of sediment to an area of increased gradient beyond the shelf edge, resulting in the deposition of a thick turbidite wedge on the upper slope (Fig. 5.3). The occurrence of two channel-fills provides additional evidence for an interpreted upper slope setting and indicates further bypass of sediment through the upper slope. The preferential distribution of upper slope turbidite deposits to the central and northern areas suggests that WfC 4 prograded further basinward than the underlying parasequences but did not encounter the shelf edge in the south of the region.

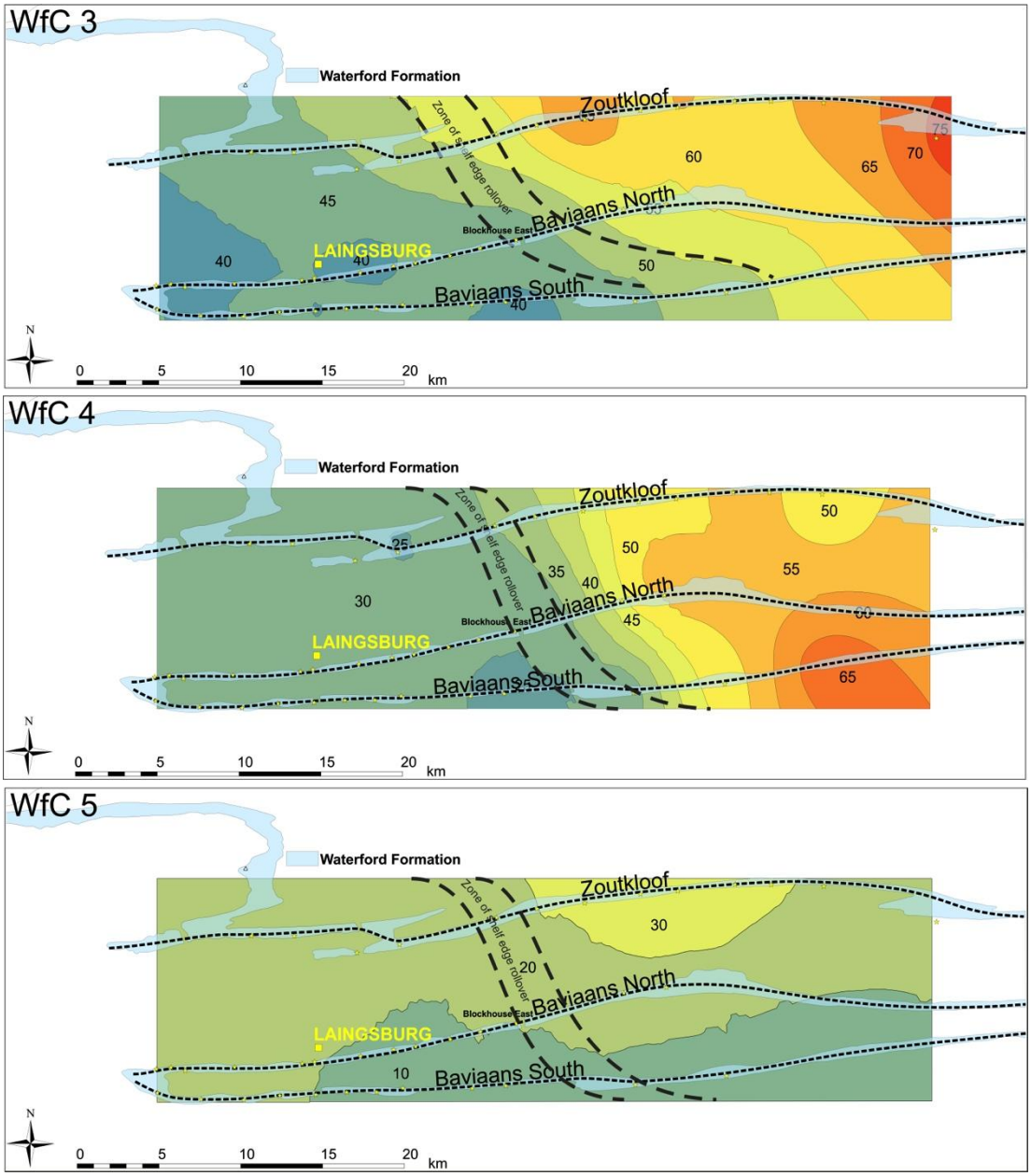

Figure 5.6: Isopach thickness maps for individual parasequences showing thickening beyond the interpreted shelf edge position. Parasequence thickening is consistent with field based observation including: facies, erosion, extensional deformation. In addition to thickening of parasequences beyond the shelf edge rollover position a subtle across strike (northward) thickening trend is also observed. Thicknesses in metres.

The regional correlations (Fig. 5.3) exhibit clear proximal (west) to distal (east) trends in facies and grain-size along each dip profile, with shelf facies (F.5, 6, 7, 8, 9 & 10) transitioning into offshore siltstones (F.0) and/or sandstone dominated upper slope deposits (F.13). The shelf edge rollover is marked by a basinward increase in parasequence thickness (Fig. 5.5) and locally an increase in sediment gravity flow deposits and channelization. An overall north-to-south trend is apparent across the study area; further basinward progradation of shelf facies and an absence of slope deposits is characteristic in the south and successive parasequences thicken to the north. Here, typical shelf facies (deformed and lower shoreface facies deposits) are increasingly confined to up dip positions and upper slope turbidite deposits are better developed.

5.6. Trajectory analysis

The shelf edge rollover is the key feature used in basin margin trajectory analysis where it is used to describe the evolution of a margin through time by tracking the geomorphological breaks in slope for successive clinoforms (Mellere *et al.*, 2002; Steel & Olsen, 2002; Henriksen *et al.*, 2009). Trajectory analysis is commonly applied to seismic datasets where vertical exaggeration of dip profiles produce a pronounced increase in dip of reflectors at the shelf edge, however, seismic datasets lack crucial sub-seismic process sedimentological information (Covault *et al.*, 2009). Trajectory methods have also been applied to outcrop datasets from Spitsbergen (Helland-Hansen, 2010), Tanqua depocentre, Karoo Basin (Wild *et al.*, 2009; Dixon *et al.*, 2012a; Dixon *et al.*, 2012b), Lewis shale Wyoming (Carvajal & Steel, 2006; Pyles & Slatt, 2007) and the Magallanes Basin, Chile (Hubbard *et al.*, 2010) and has been most successful in short, high gradient margin settings where there is a significant beak in slope marking the shelf edge. In the case of low gradient outcrop examples (Wild *et al.*, 2009; Jones *et al.*, 2013) where the change in dip between shelf and slope is less apparent, features consistent with a subtle increase in gradient such as basinward thickening, increase in turbidites, channelization, mass transport deposits, and growth faulting, may be used as a proxy for the rollover position. These criteria were applied to the three parallel dip profiles to establish the pattern and across-strike variability in shelf edge trajectory (Fig. 5.6A, B & C).

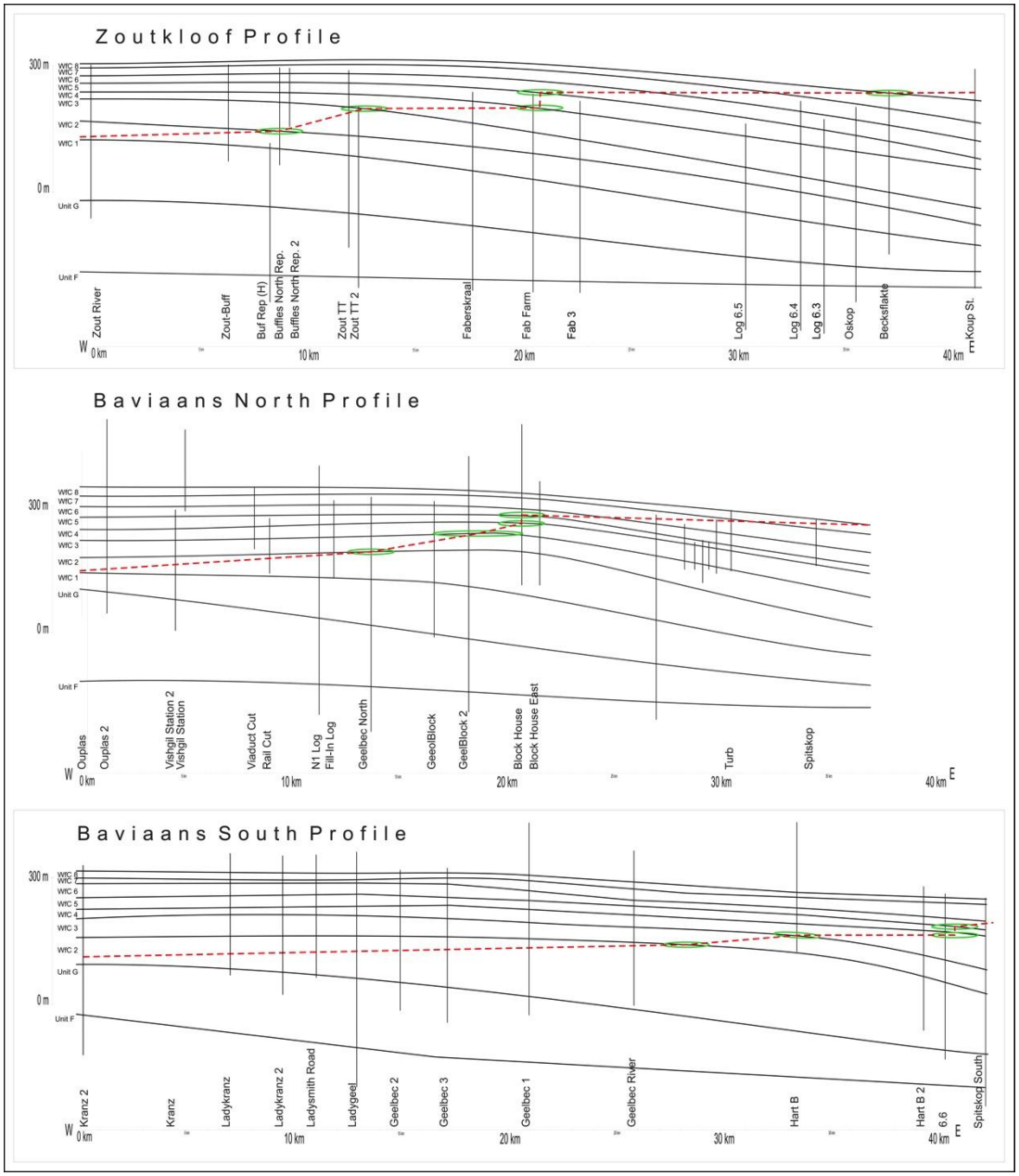

Figure 5.7: Basin margin trajectory profiles for the northern (Zoutkloof), central (Baviaans North) and southern (Baviaans South) dip profiles. Vertical lines represent key logged sections and eastward (basinward) dipping lines lines represent parasequence flooding surfaces. Shelf edge rollover zones (green) are located based upon facies and architectural criteria as well as on isopach thickness maps. Panels are hung from stratigraphic Unit F, and no back-stripping has been attempted.

On the Zoutkloof profile (Fig. 5.6A) WfC 1 consists of toeset deposits with the coeval shelf edge somewhere to the west of the outcrop limit. The shelf edge rollover position of WfC 2 is positioned at the Buffels North locality due to the pinching out of deformed facies in this area and the shallow incision observed along the top surface of the parasequence. WfC 3 exhibits a broad rollover area at the Zout TT locality coincident with an increase in parasequence thickness and a notable decrease in *in-situ* deformed facies (see chapters 3 & 4). The rollover position for WfC 4 and 5 is characterized by a notable increase in thickness

coincident with a facies transition from *in-situ* deformation to heterolithic turbidite sandstones typical of an upper slope setting and an increase in shallow erosive scours. Overlying the regional fine-grained marker unit, the sandy components of WfC 6 and 7 are interpreted to be shelf confined, and show a basinward pinch-out of their sandstone component landward of the WfC shelf edge rollover, whilst their overall parasequence thickness remains constant. WfC 8 shows significant basinward progradation, with facies typical of a shelf setting occurring along almost the entire length of the Zoutkloof profile. An abrupt change from shelf to offshore facies at the Becksvlakte locality indicates an abrupt deepening of the depositional setting, which is consistent with transition over the shelf edge rollover.

On the Baviaans North profile (Fig. 5.6B) WfC 1 consists of toeset deposits with the coeval shelf edge not exposed. The presence of a heterolithic turbidite sandstone package typical of an upper slope setting at the Blockhouse locality and significant basinward thickening of the clinothem provides a down dip limit for the position of the WfC 2 rollover. The rollover positions for WfC 3 and 4 have been comprehensibly documented by Jones *et al.* (2013) and are both situated at the Blockhouse locality. The WfC 3 rollover is characterized by a broad area of growth faults and WfC 4 exhibits extensive erosion in the form of broad shallow gullies. The lower shoreface sandstone component of WfC 5 does not encounter the rollover position. In a similar manner to the Zoutkloof profile, the sandstone components of WfC 6 and 7 are interpreted to be shelf-confined. Overall the parasequences remain a consistent thickness but fine basinward. WfC 8 exhibits characteristics typical of a shelf topset along the entire length of the profile without any basinward thickening of the parasequence; as a result the shelf edge rollover is interpreted to be situated beyond the farthest log section, and may have built basinward through accretion of fine-grained strata during WfC 6, 7, and 8.

The absence of WfC 1 as a sand-prone succession along the Baviaans South profile (Fig. 5.6C) means that the use of dip-related thickness changes to identify the shelf edge rollover for WfC 2 is problematic. The termination of minor amalgamated lower shoreface sandstone and deformed facies occurs at the Geelbek 1 locality. This pinch-out of shelf facies could represent the termination of the sandy component of a shelf-confined parasequence. However, Jones *et al.* (2013) used the termination of extensive deformed shelf facies as a key criterion for identifying the shelf edge rollover; as such the pinch-out of deformed facies provided the best indicator of the transition from shelf to slope. Therefore

the shelf edge rollover for WfC 2 is tentatively placed east of the Geelbek 1 log locality. WfC 3 shows a significant decrease in deformation and a transition to heterolithic shoreface-offshore transition deposits between the Geelbeck River and Hart B log localities. This is considered to be the result of increased gradient at the shelf edge and is consistent with a slight basinward thickening of the parasequence in the same area. WfC 4 exhibits a notable decrease in the amount and intensity of soft sediment deformation and a distinct fining and thickening of the parasequence in the same area, which is consistent with a shelf edge position. WfC 4 exhibits extensive amalgamated lower shoreface deposits and deformation along almost the entire length of the Baviaans South profile. A transition from amalgamated lower shoreface and deformed facies to undeformed heterolithic shoreface-offshore transition sandstone beds is recorded between the Hart B 2 and 6.6 log localities, followed by the complete pinch-out of the sandy component of the parasequence before the Spitskop South locality. Although not conclusive, this abrupt dip-related change in facies may signify an increase in gradient around the shelf edge rollover. The subtle shelf edge rollover of WfC 3 and 4 contrasts to the area of extensional deformation and widespread erosion that characterizes the same rollover 4 km across strike on the Baviaans North profile, and there is no evidence for delivery of sand farther into the basin. WfC 5 exhibits similar architecture and basinward facies change as along the Baviaans North profile. The lower shoreface facies (F.10) and deformed facies of the WfC 5 shelf-delta, fines and thins basinward into shoreface-offshore transition deposits at the Geelbek 3 locality. The entire sandy-prone unit pinches out by the Spitskop South locality. Therefore, the sandy topset of WfC 5 is interpreted to be entirely shelf confined, with minimal apparent progradation of the rollover from WfC 4-to-5. WfC 6 also appears to be entirely shelf confined with the sandy component fining and pinching out down dip, but landward of the established WfC 4 shelf edge rollover. WfC 7 and 8 are dominated by amalgamated lower shoreface (F.10) and deformed facies (F.5, 6 & 7) along the entire length of the Baviaans South profile without exhibiting any significant architectural or facies change, which indicates that the shelf edge rollover lies basinward of the farthest correlated log section.

All three profiles exhibit a broadly similar flat to slightly rising trajectory (Fig. 5.6) with a steeply rising trajectory between WfC 3 and 5. In the absence of topset deposits for the oldest clinothems, this trajectory is interpreted to represent a slowing rate of relative sea-level rise from WfC 1-3, slight relative sea-level fall during WfC 4, followed by a relative sea-level rise from WfC 4-6 and a slowing rate of rise to incipient fall for WfC 8. However, subtle

variations between the three profiles are observed. In the south (Fig. 5.6A), the margin is characterized by a flat to slightly rising trajectory with a significant basinward step recorded between WfC 3 and 4. On the central profile (Fig. 5.6B) the margin exhibits a flat to increasingly steeply rising trajectory with more of an overall rising component than in the south. The absence of an interpreted shelf edge rollover for WfC 8 along the >40 km length of the Baviaans North profile suggests that it must be located farther basinward; therefore a flat trajectory from WfC 5 -8 is suggested. The northern profile (Fig. 5.6C) has an overall flat to rising trajectory, but with a more aggradational component than found to the south. A shelf edge rollover position is recognized for WfC 8, which supports the flat trajectory from WfC 5-8.

5.7. Temporal and spatial variability of WfC 3, 4 and 5

Fig. 5.7A, B and C show palaeogeographic reconstructions for WfC 3, 4 and 5 respectively. Each reconstruction represents the position of greatest basinward advance for each parasequence, based upon palaeoflow direction, sedimentary facies data, clinothem isopach maps and architectural information from 51 localities. The dominant NE to ENE palaeoflow (Fig. 5.5) is sub-parallel to the post depositional folding. The dominance of amalgamated wave and storm dominated lower shoreface sandstones and the lack of obvious sediment input points leads to the interpretation of the lower Waterford Formation in the Laingsburg area as a wave and storm dominated shoreface system.

WfC 3 (Fig. 5.7A) has the least basinward extent of these three clinothems, and consists of wave and storm dominated lower-shoreface facies deposits (F.10) across much of the proximal (western) study area. A fluvial-dominated mouthbar (F.11) at the N1 locality suggests a fluvial input point (Jones *et al.*, 2013). Soft sediment deformed deposits extend further across the shelf than lower shoreface facies sandstones, reaching a position close to the shelf edge rollover. A slight curvature to the margin is interpreted from the distribution of deformed and lower shoreface facies isopach maps as well as facies variability and architectural changes observed at outcrop. Basinward of the interpreted shelf edge rollover position, WfC 3 is characterized by a transition into offshore siltstone and mudstone (F.0, 1, 2, 3, & 4) in the southern and central areas. The north is dominated by significantly thicker offshore and shoreface-offshore transition (F.0 & 4) deposits that contain shallow slope channels indicating minor sediment supply to the upper slope.

In WfC 4 (Fig. 5.7B) soft sediment deformed (F.5, 6 & 7) and lower shoreface facies (F.10) deposits are widespread and extend to the interpreted shelf edge rollover position.

Although mouthbar deposits are not observed, the scale and intensity of deformation on the shelf indicates a high rate of sediment supply (chapter 6). The WfC 4 input points may be either out of outcrop plane and/or have been reworked by wave action. In the south WfC 4 exhibits the greatest basinward advance of shelf facies but still only a subtle and gradational transition to offshore facies. The northern part of the study area is characterized by further evidence of erosion and bypass at the shelf edge and increased delivery of sediment to the upper slope.

WfC 5 (Fig. 5.7C) is aggradational to slightly retrogradational relative to WfC 4, and is notable for its lack of soft sediment deformation. Lower shoreface sandstones (F.10) are thick and extensive in the up-dip (western) areas but did not advance as far as the shelf edge rollover established by WfC 4 in the southern and central areas. However, evidence of sediment bypass, including numerous small bypass scours and a transition from lower shoreface facies deposits (F.10) to amalgamated turbidite sandstones (F.13) are recorded at the Faberskraal Farm locality in the north. Identification of the shelf edge rollover using the isopach thickness maps as well as facies variability and architectural changes observed at outcrop, shows that WfC 5 exhibits a more linear (N-S) trend. Despite the evidence for long term sediment supply to the upper slope in the north, there still remains no direct evidence for sediment input points within WfC 5, which suggests that sediment supply points were either strongly reworked by wave processes or are out of plane.

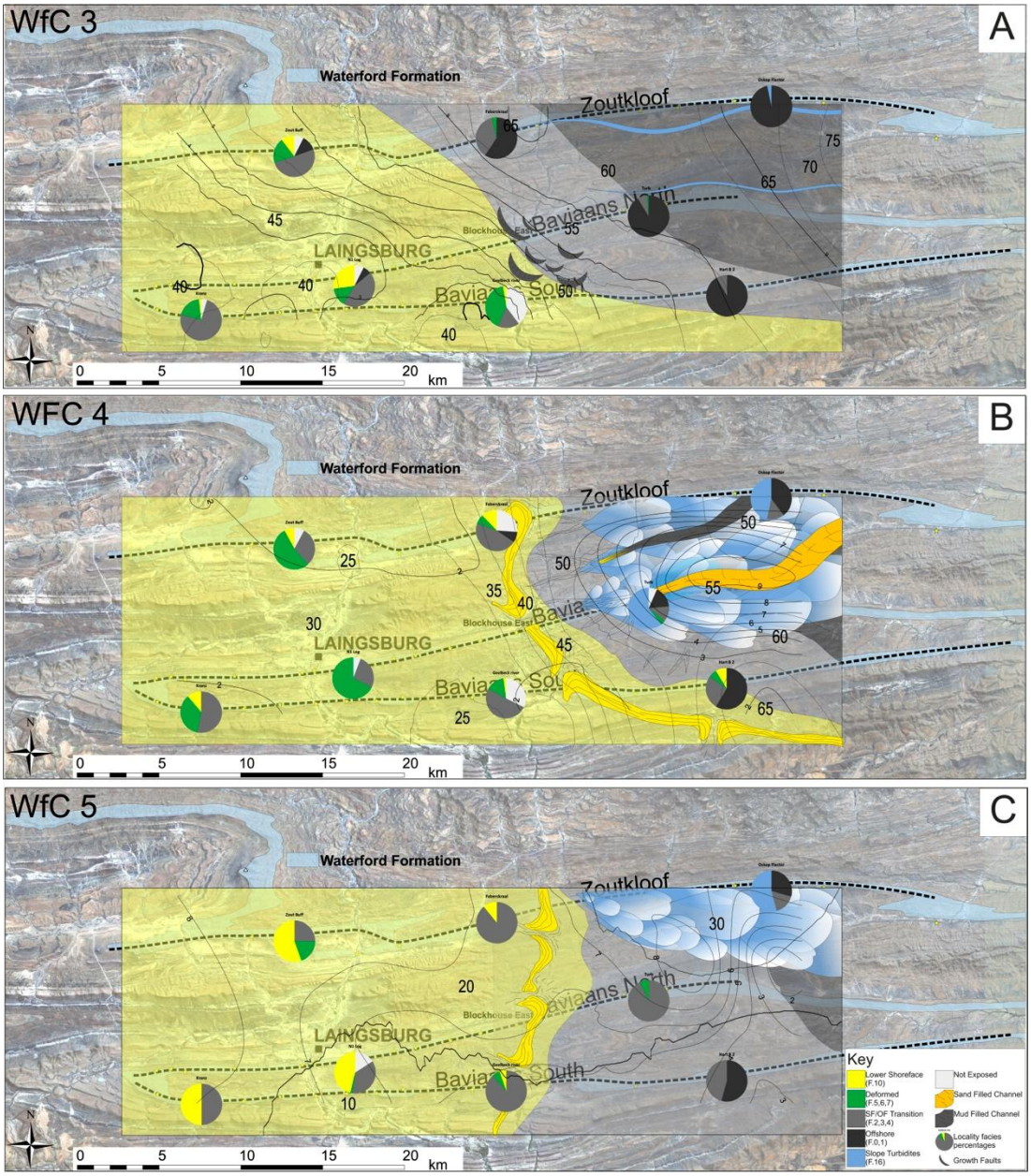

Figure 5.8: Palaeogeographic reconstructions of (A) WfC 3, (B) WfC 4 and (C) WfC 5 each at their most progradational extent. Pie charts represent facies breakdowns for key log localities.

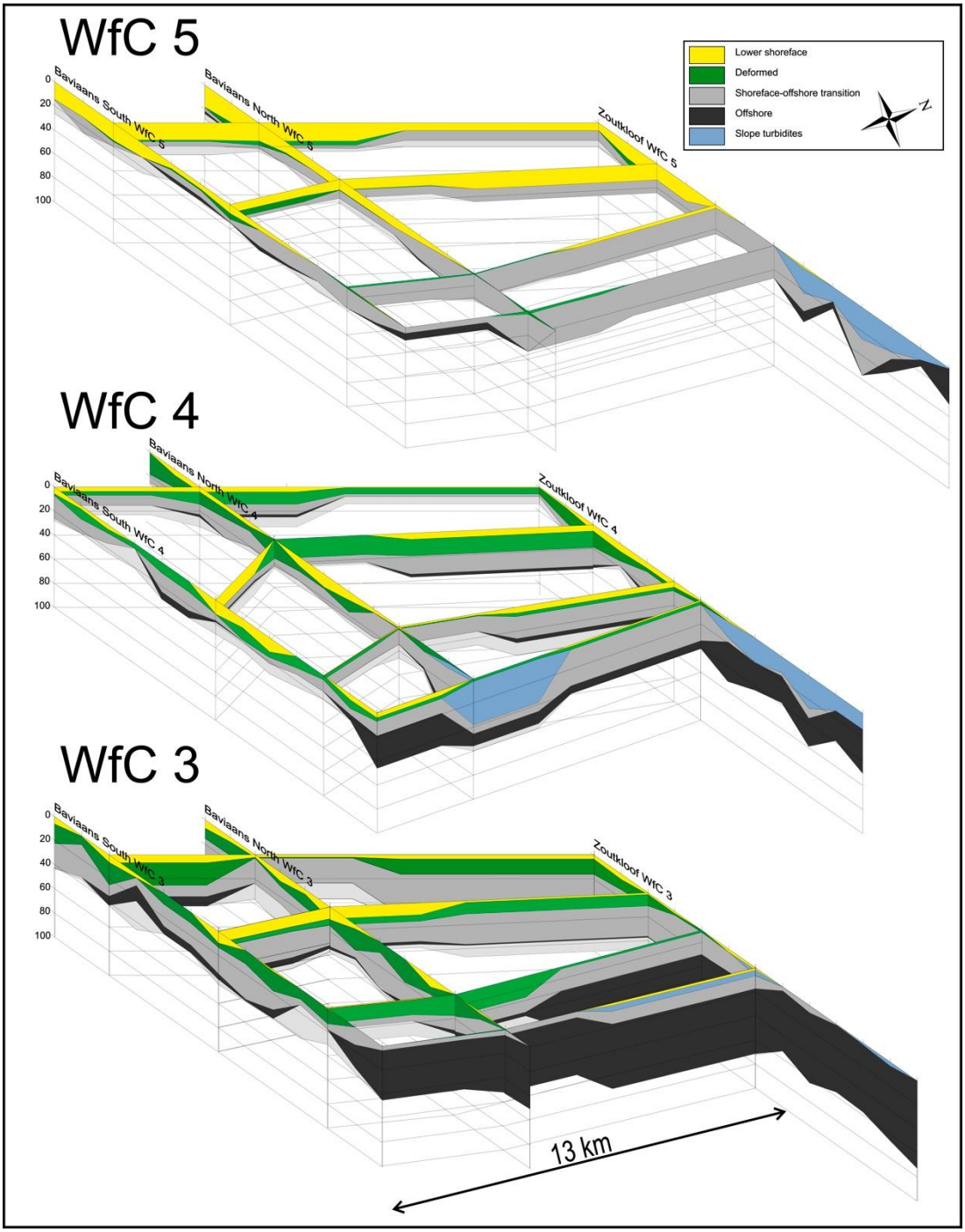

Figure 5.9: Facies fence diagrams for (A) WfC 3, (B) WfC 4 and (C) WfC 5. Note, facies breakdown for individual localities are cumulative. Diagrams show the across-strike thickening of the three clinothems to the north, coupled with an increase in offshore facies and persistent supply of sediment beyond the shelf edge. Basinward thickening of individual clinothems is associated with transition from shelf to slope; and correlates with the down-dip pinching out of deformed facies.

5.8. Discussion

5.8.1. Establishing the deltaic system at the shelf edge rollover

It has been widely documented that shelf edge deltas play a fundamental role in shelf margin accretion (Morton & Suter, 1996; Muto & Steel, 2002; Porębski & Steel, 2003) and that the greatest rate of shelf edge progradation occurs at times when, or in areas where, sediment supply is highest. Dixon *et al.* (2012b) highlighted the importance that process regime (wave, fluvial, tidal) at the shelf edge has on controlling supply of sediment to the slope and basin floor. Fluvial dominated delta systems have the ability to prograde rapidly across a shelf and have greater potential for delivery of sediment to the slope and basin floor, particularly during times of falling or low sea-level (Morton & Suter, 1996; Johannessen & Steel, 2005; Carvajal & Steel, 2009; Sanchez *et al.*, 2012b). The presence of a significant fluvial system at the shelf edge can degrade the shelf edge rollover through incision of the shelf edge, resulting in over steepening and repeated collapse of the delta front, triggering mass transport complexes and initiation of turbidity currents, thus contributing to an effective gravity-driven sediment delivery system (Wild *et al.*, 2009). In contrast, wave and storm dominated shorelines are characterized by low sediment delivery beyond the shelf edge due to redistribution of sediment along the margin by wave and storm processes, and therefore are argued to have limited potential for the development of incisional features that can effectively deliver sediment beyond the shelf edge (Johannessen & Steel, 2005). Jones *et al.* (2013) demonstrated that the wave dominated WfC 4 was more effective at supplying sediment beyond the shelf edge than the fluvial dominated WfC 3 (see chapter 4), which showed no evidence for sediment bypass of the shelf edge rollover. However, the limitations of single 2D dip panel (Baviaans North profile) meant regional robustness of the interpretation could not be tested.

Continued work incorporating data from the Zoutkloof and Baviaans South panels shows that WfC 3, 4 and 5 are typically wave and storm dominated and lack direct evidence of further sediment entry points aside from the one identified within WfC 3 on the Baviaans North profile. Proximity to a fluvial supply was therefore not the main control on the supply of sediment to the slope and basin floor. Fluvial feeders were likely situated outside the study area to supply the wave and storm dominated shorelines with sediment. The shorelines may have the capacity to transfer sediment basinward in settings where shelf redistribution processes are weak (Weber *et al.*, 1997), if the shelf is narrow (Piper & Normark, 2001; Henriksen *et al.*, 2011) or where slope canyons extend across the shelf to the shoreline and receive sand from longshore drift (Covault *et al.*, 2007; Boyd *et al.*, 2008;

Covault & Graham, 2010). It has also been shown that extreme storms can produce strong storm-surge ebb currents that incise shoreface sandstones and canyon walls and re-suspend and redistribute sediment offshore (e.g.Dail *et al.*, 2007; Goff *et al.*, 2010; Rogers & Goodbred, 2010).

The supply of sediment to the upper slope without a clear fluvial driver and during a period of steeply rising margin trajectory contrasts with established models where major sand delivery to the slope and basin floor is expected to occur during a period of flat/falling trajectory (Posamentier *et al.*, 1988; Posamentier & Vail, 1988a; Van Wagoner *et al.*, 1990; Mutti & Davoli, 1992; Milton & Dyce, 1995; Marjanac, 1996; Normark *et al.*, 1998; Johannessen & Steel, 2005) and or at fluvial dominated shelf edge (Morton & Suter, 1996; Johannessen & Steel, 2005; Carvajal & Steel, 2009).

5.8.2. Timing of sediment bypass

An overall flat to slightly rising trajectory from WfC 1 to 8, with a steep rise between WfC 3 and 5 characterizes the lower Waterford margin trajectory along all three dip parallel regional profiles (Fig. 5.6). The southern profile (Fig. 5.6C) exhibits the flattest trajectory profile of the three, and has the smallest rising (aggradational) component between WfC 3 and 5. The central and northern (Fig. 5.6B & C) trajectory paths exhibit successively greater aggradational components to their strongly progradational trajectories. Correlations made by Jones *et al.* (2013) on the Baviaans North profile established that sediment bypass and delivery to the slope occurred only during the interval of steepest rising trajectory (during WfC 4). Although contradictory to the established trajectory model, examples of sediment supply to deepwater settings. The Cenozoic succession offshore eastern Venezuela and Niger Delta (Henriksen *et al.*, 2011) exhibit deepwater fan deposition during stages of ascending shelf edge trajectories, which are attributed to high sediment supply rates. The Zoutkloof profile is also associated with delivery of thicker, more amalgamated slope turbidite packages mainly by WfC 4 and 5. In contrast, the Baviaans South profile reveals that delivery of sediment to the shelf during this period of rising trajectory did not occur uniformly across the entire margin, as the same steeply rising trajectory between WfC 3 and 5 is recorded in the south but is not associated with down dip slope sandstone deposits. The subtle differences in trajectory profiles and the distribution of sediment delivery to the upper slope that is observed across the margin, suggests that there was significant spatial variability in the factors affecting margin development.

5.8.3. Controls on the lateral variability of the lower Waterford margin

The internal facies distribution and stratigraphic architecture of WfC 3, 4 and 5 show significant lateral variability, which provides useful information in the analysis of the critical factors controlling the spatial delivery of sediment to the slope and the stratigraphic development of the margin. The thick turbidite dominated slope succession present in the north of the study area could have developed in several ways:

1) A major fluvial input point lying just to the north of the study area (in the subcrop) close to the shelf edge rollover could have supplied significant volumes of sediment to the slope, and sediment was redistributed to the south beyond the shelf edge.

2) The variability observed in sediment supply to the slope is due to the obliquity of the margin and that slope deposits do occur in the south of the area but lie beyond the final log position and have therefore not been observed.

3) Regional facies isopachs (Fig. 5.5) and the interpreted shelf edge rollover position from the three dip profiles, particularly for WfC 3 and 4, suggests curvature to the basin margin with a narrower shelf in the north (Fig. 5.9). A narrow shelf would result in the prograding delta during a shelf transit would encounter the shelf edge earlier and, as a consequence, the delta would be in a position to deliver sediment to the slope for a longer period. In contrast, a wide shelf would result in the delta taking longer to reach the shelf edge and therefore would have only limited time to deliver sediment to the slope.

The disparity of sand supply to the upper slope along the Waterford margin, combined with the apparent lack of influence from sediment supply points, suggests that shelf width played an important role in the development of the margin. In addition, sediment redistributed across the shelf could be captured in areas where the shelf is narrower.

The lack of sediment supply beyond the shelf edge associated with WfC 3 on the Baviaans North profile and the lack of evidence for strong fluvial supply points further to the north would suggest that it is not proximity to a sediment supply point that resulted in greater supply to the upper slope in the north of the study area. However, it remains possible that such a sediment supply point did sits further to the north that led to more longshore supply to the south, but this remains unexposed or has been eroded away.

The argument for uniform supply of sediment across the margin with slope facies sitting beyond the final log position of the southern Baviaans South profile would appear to be one of the simplest explanations for the observed lateral variability in supply to the slope. However, reconnaissance studies of exposures beyond the final log position of the southern Baviaans South profile show no signs of slope deposits, which is consistent with the lack of evidence for erosion and bypass in shelf edge positions on the southern profile.

Parasequence architecture provides insights into the main external factors controlling shelf width and ultimately the observed lateral facies variability across the margin. A characteristic shown in the fence diagrams (Fig. 5.8) and thickness isopachs maps (Fig. 5.5) is the consistent thickening of parasequences to the north, which also coincides with an increase in delivery of sediment to the upper slope. Overall thickening to the north of successive parasequences below the regional fine-grained interval between WfC 5 and 6, suggests more available accommodation in this area for each parasequence and no suggestion of compensational stacking on the shelf at the scale of the 900 km^2 study area. This interpretation of increased accommodation to the north is reinforced by the more steeply rising basin margin trajectory observed along the northern profile, which is interpreted to reflect sediment supply trying to keep pace with increased subsidence rate. Similar lateral thickness variability in sequences across the New Jersey margin are interpreted to represent depocentre migration due to differential subsidence (Fulthorpe & Austin, 2008)

Assuming that eustatic sea-level changes were consistent across what is a relatively small section of the basin margin, this variability in accommodation can be attributed to differential subsidence. Increased subsidence in the north would result in greater accommodation and a narrower shelf; this would ultimately influence the sediment dispersal pattern of the margin, diverting sediment transport to the north of the area. The driving mechanism for differential subsidence across the margin is not clear. Possible controls include greater tectonic subsidence and/or more compaction of the substrate to the north. A significant increase in thickness of the underlying slope Units E, F and G in the north of the study area, as noted by Figueiredo *et al.* (2010) is consistent with long term creation of accommodation in the north of the region.

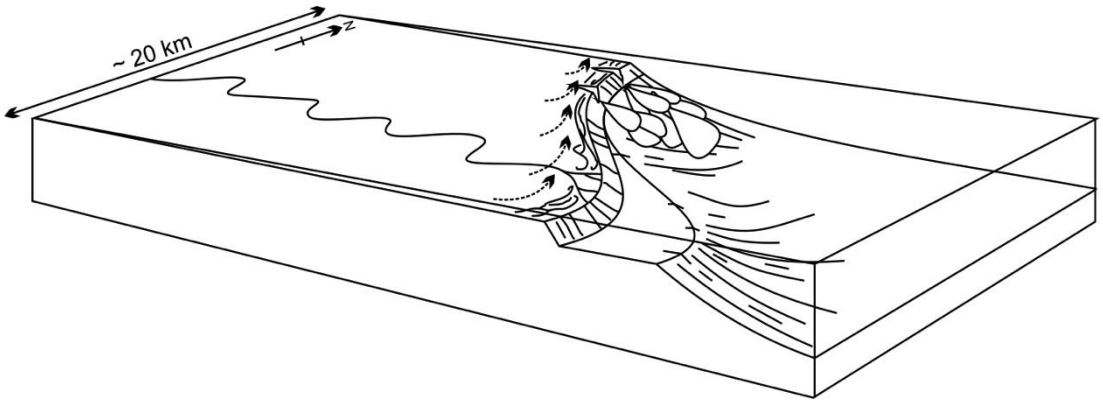

Figure 5.10: Lateral variability observed along the lower Waterford margin in the Laingsburg area. Margin curvature resulted in a narrower shelf to the north, which had a significant bearing on delta transit time to the shelf edge and the time the delta was able to remain at the shelf edge. Longshore process would mean that sediment could be captured by the narrower shelf edge in the north. Thickening of successive clinothems to the north is consistent with greater accommodation in the area and is attributed to long-term differential subsidence.

5.8.4. Prediction of sediment bypass

The delivery of sediment beyond the shelf edge rollover during the interval of steepest rising trajectory is adequately explained by high sediment supply rates outpacing relative sea-level rise and a narrow shelf width in the north, which enabled the deltaic system to prograde to the shelf edge rollover and deliver sediment to the slope and basin floor. However, the ability to bypass sediment to the slope and basin floor during a segment of steeply rising trajectory highlights a weakness in the strict application of the trajectory model when using it as a tool for the prediction of down dip sand deposits (Fig. 5.10A).

Sequence stratigraphic interpretation of the lower Waterford Formation (Fig. 5.10B) can be extended across the margin from that described by Jones *et al.* (2013) for the Baviaans North profile. Jones *et al.* (2013) suggested that the regional fine-grained unit above Unit G represent a long-term rise in relative sea-level consistent with a transgressive systems tract (TST). The overlying succession of WfC 1 – WfC 4 shows a clear progradational stacking pattern, consistent with a highstand systems tract (HST). WfC 5 marks a slight landward step relative to WfC 4 (retrogradational stacking), and is interpreted as a transgressive systems tract (TST). The overlying regional fine-grained interval (Fig. 5.4A) is interpreted to include the offshore expression of the next maximum flooding surface and is followed by progradational stacking of WfC 6 - 8, consistent with a HST. WfC 4, therefore, represents the maximum regression in the lower Waterford sequence, and the 'turnaround' in stacking pattern from progradational to retrogradational. Based on the presence of erosive gullies and channels that cut down from the top surface of WfC 4 across the region, and the fine-grained interval infilling these erosive features (chapter 4), combined with the absence of

subaerial exposure; this turnaround in stacking pattern is interpreted as a regressive surface of marine erosion (sequence boundary) (Vail *et al.*, 1977b; Van Wagoner *et al.*, 1990). The maximum supply of sand over the shelf edge is associated with the regressive surface of marine erosion situated at the top of the most regressive parasequence in sequence 1 (WfC 4). In this instance the sequence stratigraphic model using facies-scale observations more accurately predicts the bypass of sediment beyond the shelf with the presence of a regressive surface of marine erosion at the top of WfC 4 (Fig. 5.10B).

A notable feature of the three depositional dip (Fig. 5.3) panels is the significant basinward step of WfC 8 beyond the previously established, sand dominated, shelf edge rollover position of WfC 4, and the decoupling of the shelf edge trajectory path from the pinch-out of the sandy component of WfC 6 and 7. The basinward step in the deposition of shelf facies associated with WfC 8 requires progradation across a relatively flat shelf setting. The fact that WfC 8 progrades over the top of several hundred metres of fine-grained offshore and slope facies would suggest that progradation of the margin took place through the transport and accretion of fine-grained material by low concentration flows during WfC 6, 7 and 8 time. Correlations reveal that the shelf edge must have prograded a minimum of 15 km (the distance from WfC 5 shelf edge rollover position to the pinch-out of WfC 8 shelf facies) through the accretion of fine-grained sediment under highstand conditions, and therefore represents a significant component of margin progradation comparable to that driven by coarse-grained supply of sediment when deltaic systems are positioned at the shelf edge rollover. Despite the significant volumes of fine-grained sediment transported basinward during rising relative sea-level, neither trajectory nor seismic sequence stratigraphic models recognize or predict accretion of the basin margin without the supply of sand. Comparing relative rates of progradation by coarse-grained and fine-grained material has not been possible due to poor chronostratigraphic constraints, however it is possible to hypothesize that rates of fine-grained progradation are likely to be significantly slower than coarse-grained progradation, yet each may make a comparable contributing to margin development.

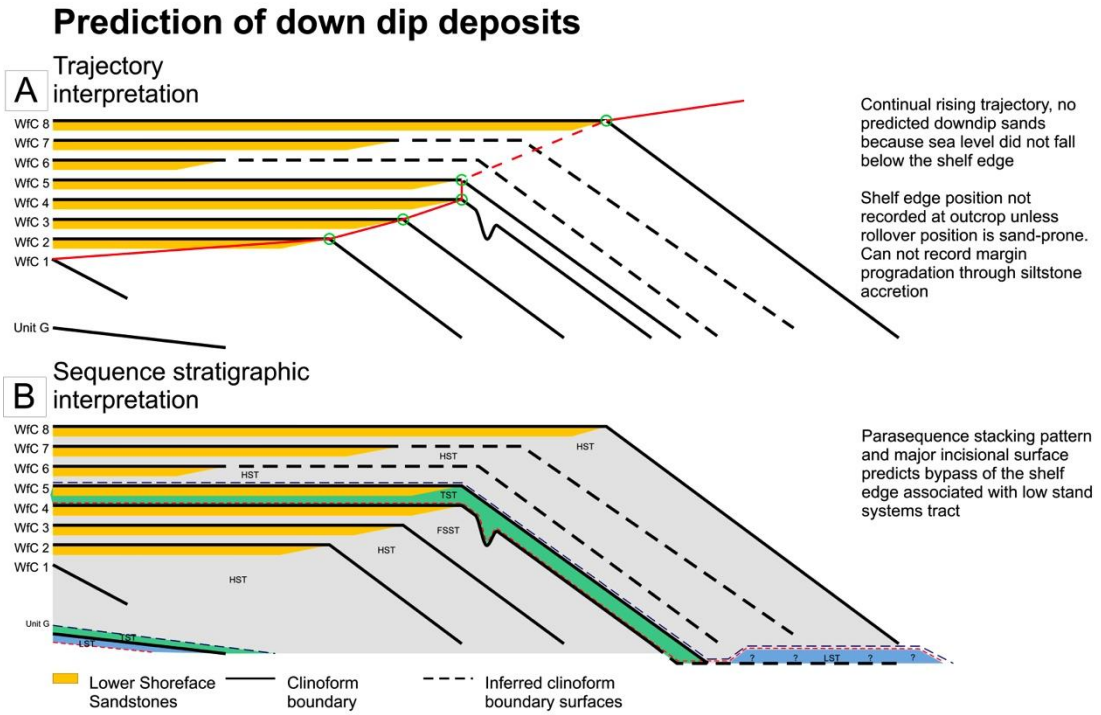

Figure 5.11: Generalized architecture showing Unit G and the 8 overlying clinothems of the lower Waterford Formation. (A) Trajectory interpretation of the lower Waterford Formation showing a flat to slightly rising trajectory with a steepening rise between WfC 3 & 5. Established trajectory model would predict little sediment delivery beyond the shelf edge. However, correlations show the most significant sediment bypass to the slope occurs during the steep rise in trajectory. Bypass of sediment without exposure of the shelf means that a new shelf edge did not develop; therefore the relative sea-level fall is overlooked by the trajectory method, which would fail to predict the presence of lowstand slope turbidites. (B) Sequence stratigraphic interpretation of the lower Waterford Formation places WfC 4 in the falling stage systems tract (FSST) with a sequence boundary overlying it followed by WfC 5, which is part of the transgressive systems tract (TST). The model predicts a lowstand systems tract (LST) further down dip, which is consistent with the strong evidence for sediment bypass of the upper slope in the form of large channels on the Baviaans North and Zoutkloof profiles. It is likely that lowstand deposits lie beyond the final log positions toward the north east of the study area.

5.9. Conclusions

Commonly, published interpretations of the stratigraphic development of basin margins are a single 2D dip profile. The correlation of exhumed clinothems along three deposition dip profiles of the lower Waterford Formation provide a high-resolution dataset with three-dimensional constraints that allows the lateral and temporal variability of the shelf-to-slope transition to be documented.

Plotting successive shelf edge rollover positions for each of the three basin margin profiles is shown to be broadly similar, with a flat to slightly rising trajectory from WfC 1 – 3, followed by steeply rising trajectory between WfC 3 and 5, and a return to a flat to slightly rising trajectory between WfC 5 and 8. Despite the apparent similarities between the three individual trajectory profiles, significant deviation from the established models is observed in terms of the partitioning of sediment between the shelf and slope. Delivery of sand

beyond the shelf edge rollover is during the period of steepest rising trajectory between during WfC 3 and 5 and only in the central and northern part of the study area. The delivery of sediment beyond the shelf edge rollover during rising trajectory and the across-strike variability of sand supply to the slope, suggest that in this case the timing and locus of deposition has little correlation to margin trajectory. Furthermore, the shelf edge system up-dip of where sand is delivered to the slope is wave-dominated (shoreface), suggesting that the process regime need not be restricted to river-dominated systems to induce downslope sediment supply.

Plotting the shelf edge rollover in map view using previously established architectural and facies criteria (Jones *et al.*, 2013) combined with isopach thickness maps, reveals that the lower Waterford Formation margin had an embayed or curved nature. A number of studies have shown the importance of shelf width in the delivery of sediment beyond the shelf edge (Burgess & Hovius, 1998; Muto & Steel, 2002). Extensive shelf facies associations in the south of the region and the absence of upper slope deposits indicate that the prograding shoreface and deltaic system was unable to establish itself at the shelf edge. Yet the long term trend for delivery of sediment to the upper slope in the north of the region suggests that the system was able to transit the shelf more quickly and establish itself in that shelf edge for an extended period. The long-term trend for increasing parasequence thickness toward the north of the area suggests that greater accommodation was present in this area through the lower Waterford succession. It is therefore likely that differential subsidence across the margin controlled the position of the shelf edge and maintained a narrower shelf in the north, which would have had significant influence on sediment routing paths, diverting them to the north.

The delivery of sand to the slope and beyond is therefore recognized to have played a significant role in the development of the lower Waterford margin. However, the extensive shelf deposits of WfC 8 that directly overly thick offshore mudstone deposits, have demonstrated that considerable fine-grained sediment can be deposited beyond the shelf edge during relative sea-level highstand when sand-prone parts of shelf deltas remain shelf-confined, which can contribute to significant margin progradation under such conditions. The results of this study caution against the strict adherence to both the seismic sequence stratigraphic and trajectory method when recording margin development and predicting the timing of significant coarse-grained sediment bypass beyond the shelf edge rollover.

CHAPTER 6.

CONTROLS ON THE WATERFORD BASIN MARGIN ARCHITECTURE

Having focussed on the lateral variability of three key clinothems in chapter 5, and the mechanisms that ultimately controlled the timing and spatial variability of sediment supply beyond the shelf edge rollover, chapter 6 considers two key aspects of the Waterford Formation and their effect on the long term stratigraphic evolution of the basin margin. Firstly, extended logged sections suggest a significant thickness of shelf stratigraphy (>300 m) that does not exhibit any sign of subaerial exposure. Secondly, the Waterford Formation is characterized by the occurrence of extensive soft sediment deformation landward of the shelf edge rollover. These characteristics are discussed in the context of sediment supply and accommodation and how this has affected broader architectural development of the margin.

6.1. Lower Waterford Formation key aspects

Sediment supply rate and relative sea-level change are the primary controls on the development of basin margin stratigraphy; however it is difficult to disentangle their individual effects and to quantify their influences without detailed understanding of supply volumes and rates, subsidence rates and eustasy. Nonetheless, understanding the interplay of these main factors is important in helping to reduce uncertainties relating to the timing and partitioning of sediment between the shelf, the slope and the basin floor. Interpretations presented here enable understanding of the factors that controlled the transgressive and regressive architectural development of the lower Waterford Formation.

The mixed wave- and river-influenced parasequences of the lower Waterford Formation are typically between 50 m and 10-m-thick and are comparable in terms of sedimentary facies and scale with many other documented examples e.g. Book Cliffs (Hampson, 2000; Enge *et al.*, 2010; Schomacker *et al.*, 2010; Hampson *et al.*, 2011), Spitsbergen (Mellere *et al.*, 2002; Deibert *et al.*, 2003; Mellere *et al.*, 2003; Uroza & Steel, 2008; Ponten & Plink-Bjorklund, 2009), Fox Hills Wyoming (Carvajal & Steel, 2006; Carvajal & Steel, 2009), which are widely interpreted to be intimately tied to high frequency eustatic sea-level cycles convolved with background subsidence rate. Yet there are a number of key features of the lower Waterford Formation that differ from other examples. These include:

1. Lack of evidence of subaerial exposure or incised valley-fills in 300 m of shallow marine stratigraphy
2. Widespread and intense soft sediment deformation in shelf delta parasequences

6.1.1. Thick shelf succession without evidence for sub-aerial exposure

Accommodation in a basin is a 3D expression of relative sea-level change, which is defined as being a function of both sea-level change (eustasy) and sea floor movement (sediment compaction, tectonic subsidence, isostasy (Posamentier & Allen, 1993). The significance of relative sea-level change on margin development and architecture becomes apparent when the short-term fluctuations of eustasy and long-term changes in sea floor movement are considered. In a setting where the subsidence rate is low, a fall in eustatic sea-level as part a normal sea-level cycle will outpace subsidence. This results in an overall relative sea-level fall and reduction in accommodation on the shelf, which has the effect of increasing parasequence progradation rates across the shelf. As the rate of relative fall increases, subaerial exposure of part, or all, of the shelf is expected, with the development of incised

valleys to supply shorelines displaced to the outer shelf or shelf edge. Incised valleys are common features of many shelf edge settings, i.e. the Pleistocene Western Gulf of Mexico (Anderson *et al.*, 2004), Clinoform 8 of the Central Basin of Spitsbergen (Mellere *et al.*, 2003) and the Palaeogene Porcupine Basin, offshore western Ireland (Ryan *et al.*, 2009), and are considered the main conduit for sediment supply to the shelf edge. Sequence stratigraphic models predict that during a lowering of relative sea-level, rivers will incise the exposed shelf edge due to a downstream increase in channel gradient (Van Wagoner *et al.*, 1988; Posamentier *et al.*, 1992; Emery & Myers, 1996).

As part of this study a number of extended log sections were completed in order to record the basin fill from upper slope Unit G through to the first coastal plain deposits of the upper Waterford Formation. This succession is 520-m-thick and includes 310 m of stacked shelf strata above WfC 5. This thickness of shallow marine strata contains no evidence for subaerial exposure (e.g. rootlets, desiccation cracks or soil horizons) or widespread truncation (incised valley-fills), which suggests that accommodation on the shelf was always available. However, a high frequency/low magnitude fall in relative sea-level in the case of WfC 4 (as detailed in chapter 4) enabled bypass of sediment to the upper slope without exposing the shelf edge rollover or any of the WfC 4 shelf within the 40 km of depositional dip control. The absence of subaerial exposure and fluvial incision is consistent with a regressive surface of marine erosion (sequence boundary) (Vail *et al.*, 1977b; Van Wagoner *et al.*, 1990) (see chapter 3).Regressive surfaces of marine erosion are typically developed in high subsidence settings such as in the hanging-walls of syn-sedimentary extensional faults (Howell & Flint, 1996). They may track laterally into a subaerial unconformity (sequence boundary), characterized by subaerial exposure in areas of lower subsidence rate.

The presence of a regressive surface of marine erosion (sequence boundary) suggests that the amplitude of any relative fall in sea-level was not great enough to fully expose the shelf, which is contrary to the widely held belief that exposure of the shelf edge rollover is necessary to deliver sediment to the slope and basin floor, and supports the premise that sediment can be delivered to the basin without exposing the shelf edge rollover in high supply settings (Burgess & Hovius, 1998; Carvajal *et al.*, 2009).

6.1.2. Widespread soft-sediment deformation on the shelf

Extensive soft sediment deformation is one of the key characteristics of the lower Waterford Formation. The upward increase in scale and basinward extent of deformation

within parasequences WfC 1-4 marks a change in deformation process from gravity driven mass transport deposits to *in-situ* deformed deposits. WfC 4 is the most intensely and extensively deformed parasequence in the basal HST and is the most regressive. In contrast, the TST parasequence of WfC 5 exhibits only very minor *in-situ* deformation in its most up dip settings. The HST parasequences WfC 6, 7 and 8 in the second Waterford sequence are extensively *in-situ* deformed.

The occurrence of abundant soft sediment deformation has commonly been attributed to proximity to the shelf edge rollover (e.g. Stow, 1994; Galloway, 1998; Lee *et al.*, 2009; Pratson *et al.*, 2009; Oliveira *et al.*, 2011). However it is clear from regional correlations of the lower Waterford Formation and using criteria established by Jones *et al.* (2013) (chapter 4) that soft sediment deformation is more abundant within the topset of each clinothem (landward of the shelf edge rollover) than in the foreset. Deformed zones show relatively little thickness variability in their up-dip exposures, only thinning and splitting where they approach the area of increased gradient / accommodation at the shelf edge rollover (Fig.5.3). The restriction of deformation to the low gradient setting of the shelf suggests that deformation does not indicate proximity to the shelf edge rollover.

Soft sediment deformation is generally associated with a triggering mechanism such as steepening of depositional slope, cyclic loading or rapid sedimentation, however discriminating between these mechanisms is difficult. Soft sediment deformation has been widely attributed to earthquake shaking (Nemec *et al.*, 1988; Barnes & Lewis, 1991; Moore & Shannon, 1991; Hesthammer & Fossen, 1999; Laberg & Vorren, 2000), however in this instance the limited extent of individual deformed intervals is not consistent with shaking of the entire region by earthquakes. Other cyclic loading mechanisms such as storm wave loading could have produced the deformation observed. It is common to see evidence of wave and storm influence in the undeformed lower shoreface sandstones toward the tops of parasequences in the form of HCS (chapter 2 (F.10)), so storm loading of the unconsolidated sea floor may have triggered the deformation. It might be expected that deformation would be at a maximum at the shelf edge rollover and diminish landward due to the attenuation of waves crossing the shallow shelf, but in fact the opposite trend is observed, with deformation diminishing at the shelf edge rollover.

High rates of sediment supply as a trigger for deformation in delta front environments are well documented (Prior & Coleman, 1980; Stow, 1994; Galloway, 1998; Lee *et al.*, 2009; Pratson *et al.*, 2009; Oliveira *et al.*, 2011). Rapid progradation of a delta due to high

sediment flux across a muddy shelf with limited accommodation can result in extensive instability and failure. WfC 4 is the most heavily deformed and thinnest of parasequences 1 to 5 and is capped by a regressive surface of marine erosion (sequence boundary). It therefore represents the parasequence with the lowest accommodation regime, which resulted in most rapid progradation and abundant deformation of the prograding shelf delta. The overlying WfC 5 only shows minor deformation in its up dip area, which is interpreted to be the result of increased shelf accommodation and low progradation rates during relative sea-level rise. The abundance of deformation throughout the lower Waterford Formation suggests that sedimentation input rates were generally high, creating steep, unstable delta-fronts, which was the main driver for the extensive soft-sediment deformation on the shelf.

The case for high sediment input rates driving soft sediment deformation in the shelf parasequences of the lower Waterford Formation, is also supported by the absence of true claystone and ash beds. The fine grained deposits associated with parasequence boundaries can be traced basinward for ~40 km, but they remain siltstone-dominated. This suggests continued high background sedimentation rates, which would prevent deposition of true hemiplegic mudstone. The absence of ash deposits in the Waterford Formation is in direct contrast with the underlying deep water and overlying fluvial deposits (Fildani *et al.*, 2009), which contain numerous ash beds. While a 'volcanic gap' spanning Waterford time is possible, it may be more likely that the high sedimentation rates at the margin and reworking by oscillatory currents limited the preservation of ash beds.

The predominance of shelf confined soft sediment deformation is recorded along all three dip margin profiles and for successive clinothems (chapter 5), and is attributed to instability on the slopes of shelf deltas due to high sediment supply rates. Abrupt basinward splitting and thinning of deformed packages beyond the inferred shelf edge rollover further indicates that the presence of soft-sediment deformation does not indicate proximity to the shelf edge rollover. The detailed study of extensional growth faulting at the shelf edge position of WfC 3 in chapter 4, suggests that the scale and process of deformation are more accurate indicators of proximity to the shelf edge rollover zone.

6.2. Interplay between sediment supply, subsidence, and eustasy in the Waterford Formation

The common feature of parasequences recorded in this study and in many other documented examples e.g. Book Cliffs (Hampson, 2000; Enge et al., 2010; Schomacker et

al., 2010; Hampson et al., 2011), Spitsbergen (Mellere et al., 2002; Deibert et al., 2003; Mellere et al., 2003; Uroza & Steel, 2008; Ponten & Plink-Bjorklund, 2009), Fox Hills Wyoming (Carvajal & Steel, 2006; Carvajal & Steel, 2009) is the occurrence of transgressive episodes that intervene between strongly retrogressive episodes. Transgressive episodes can be explained in by several mechanisms (Helland-Hansen, 2010), of which eustatic rise or tectonic subsidence outpacing sediment supply and delta-lobe switching are the most often cited. By considering a number of the key characteristics of the lower Waterford Formation it has been possible to better understand the factors directly controlling margin trajectory and to disentangle the relative importance of controlling factors.

Deltas are highly dynamic settings where continual delta-lobe switching can conveniently explain the transgressive portion of a prograding parasequence, such as is observed in the lower Waterford and many other documented shallow marine deltaic systems. Helland-Hansen (2010) suggests that the effect of delta lobe switching can be recognised by the disparity in the number of parasequences from one locality to the next due to the limited lateral extent of sandbodies and their intervening transgressive horizons. The avlusion of a distributary delta lobe will result in a reduction in sediment supply resulting in the deposition of increasingly distal facies without an increase in tectonic subsidence or change in eustatic sea level. The 3D control across the lower Waterford Formation margin shows long-term trend for successive parasequences to become thicker and increasingly dominated by proximal facies in the north, which can indicate a long term stepping of the system to the north. However, even in a study area with exceptional lateral outcrop control such as the lower Waterford margin (~20 km) is may still be difficult to record large scale delta lobe shifting. Despite the long term stepping of the system to the north all parasequences (aside from WfC 1) can be correlated across the study area which suggests the lateral extent of individual sandbodies and their intervening transgressive intervals exceed ~20 km. Additionally, the landward extent of the fine grained transgressive intervals suggests that shoreface sandstones were backed by landward extensive low-gradient subaqueous delta tops, which reinforces the argument that delta lobe switching was not the main driver of transgressive and regressive episodes in the lower Waterford Formation. For this reason the lower Waterford parasequences are interpreted as extensive shore-parallel shoreface sandstones that are subject to limited delta lobe switching and are likely to have been subject to significant redistribution of sediment along the margin by oscillatory and geostrophic wave and storm processes.

Eight consecutive parasequences totalling 300 m of shelf deposits with regionally correlatable low-gradient subaqueous delta tops indicates that the margin was subject to relatively high subsidence rates across the study area that likely controlled long term accommodation. The ability to correlate parasequences across the study area is consistent with regional tectonic subsidence which in the case of shelf edge delta settings is often attributed to collapse of the over steepened basin margin.

Abundance of shelf confined soft sediment deformation suggests that the margin was also subject to high rates of sediment supply, which generally outpaced subsidence in order to deliver sediment to the slope without exposure of the shelf edge rollover or the development of incised valley systems. The occurrence of upper slope deposits, associated with the transgressive systems tract WfC 5, is further evidence that supports the premise that high sediment supply rates allowed sediment to be delivered to the upper slope. Therefore the lower Waterford Formation is considered a high accommodation and high sediment supply system (Fig. 6.1).

The exclusion of delta lobe shifting as the principal control on transgressive-regressive cyclicity and the establishment of a long term tectonic subsidence across the lower Waterford Formation margin suggests that eustatic sea level change represents the key mechanism that controls the transgression and regression of the lower Waterford system

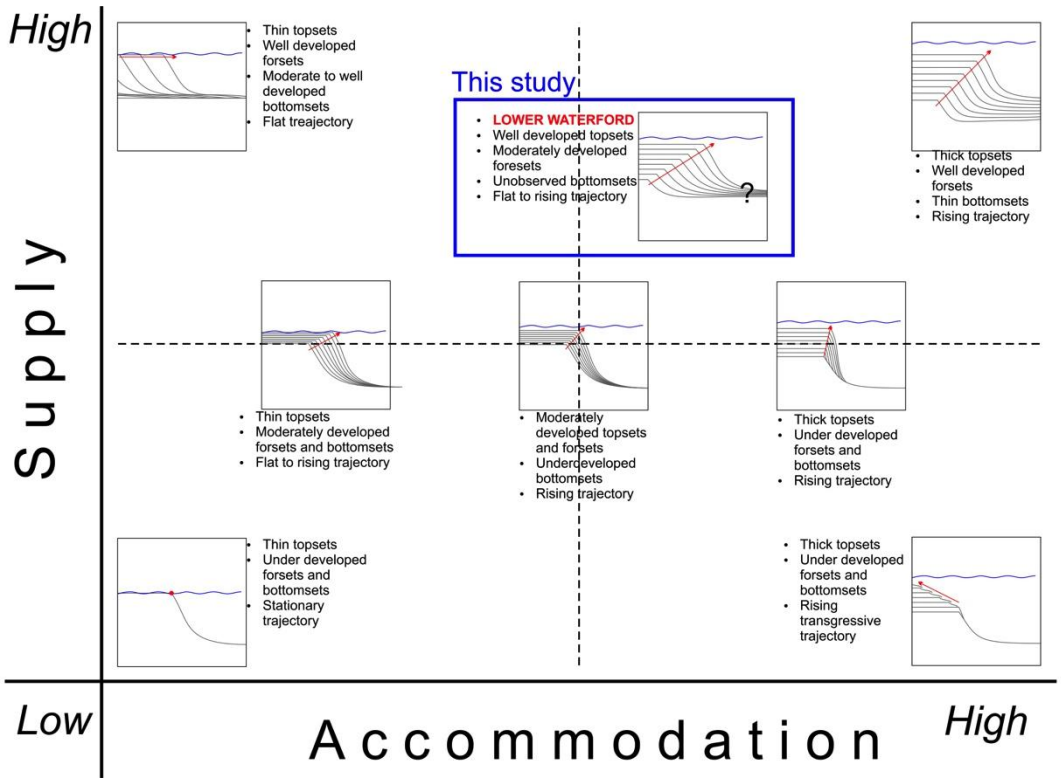

Figure 6.1: Sediment supply vs. Accommodation and the resulting margin geometries. Note the position of the lower Waterford Formation in the Laingsburg area as a high supply, high accommodation system.

CHAPTER 7.
CONCLUSIONS

This chapter combines the findings of the previous chapters and addresses the key research questions set out in chapter 1. Answers to the four key research questions integrate and reflect on the results and discussions presented in chapters 3, 4, 5 and 6, and synthesize the spatial and temporal evolution of Karoo Basin margin as represented by the lower Waterford Formation. In addition, a number of recommendations for future work are made that will build on the research presented here.

Response to initial questions posed in this thesis

A. What factors control the spatial and temporal variability of sand delivery to the slope and basin floor, and is fluvial incision of the shelf rollover necessary for the delivery of sand to deep marine settings?

Chapters 3-6 have addressed the influence each of the key mechanisms had on the spatial and temporal variability of sediment bypass across the shelf, the details of which are summarized below and shown in figure 7.1.

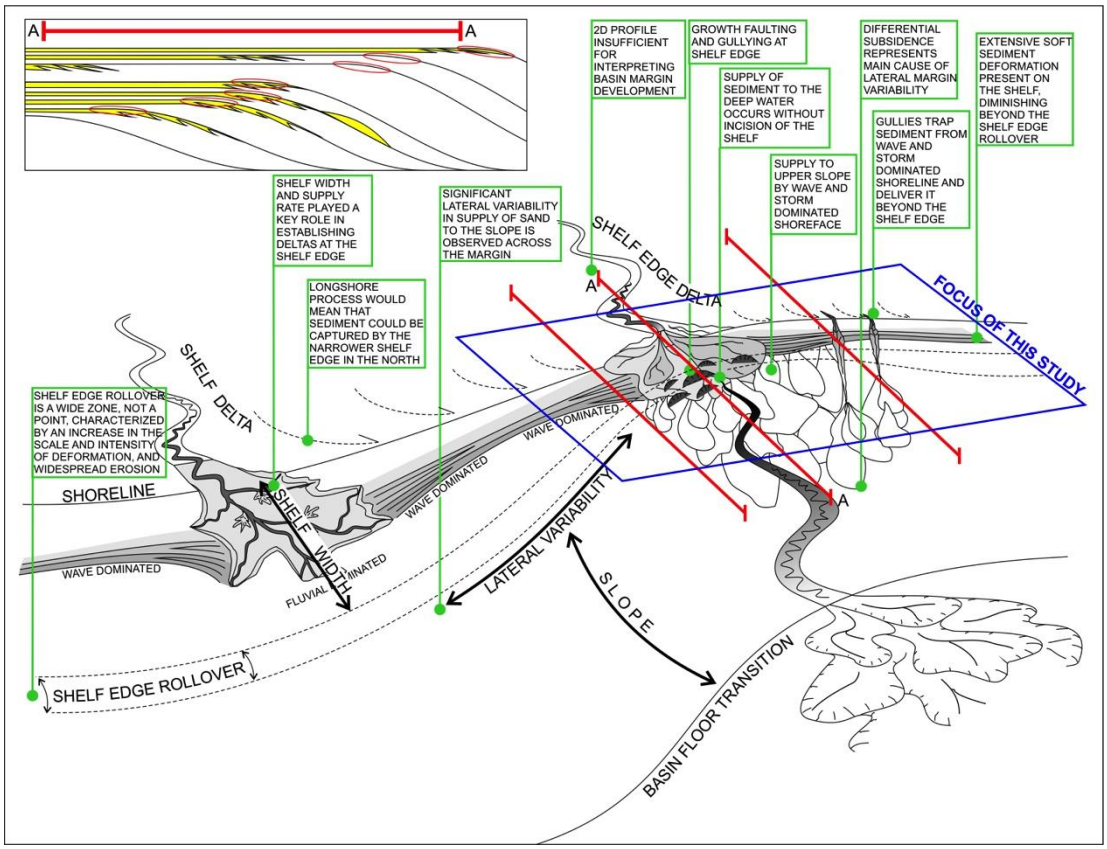

Figure 7.1: Cartoon to illustrate variability across a basin margin. Highlighted is the area on which this study focuses i.e. shelf edge delta systems. Flags correspond to the key question addresses in this thesis. The three red lines correspond to the three basin margin profiles that represent the dataset upon which this study is based; they demonstrate how variable a basin margin setting may be and the limitations of s single 2D profile.

Relative sea-level: Lowering of relative sea-level below the shelf edge break is widely postulated as a prerequisite condition for the delivery of sediment to the deep water settings due to a lack of accommodation on the shelf, which results in the initiation of fluvial incision (Posamentier & Vail, 1988b; Van Wagoner *et al.*, 1990; Milton & Dyce, 1995; Marjanac, 1996; Normark *et al.*, 1998; Steel & Olsen, 2002; Johannessen & Steel, 2005;

Porębski & Steel, 2006; Ainsworth *et al.*, 2008; Steel *et al.*, 2008). Yet local conditions such as high fluvial discharge (Kolla & Perlmutter, 1993; Weber *et al.*, 1997), headward erosion of submarine canyons and/or transport of sediment into canyons by shelf-parallel currents (Boyd *et al.*, 2008; Covault & Graham, 2010) promote sediment transport off the shelf into deep water without sea-level fall below the shelf edge and fluvial incision (Talling, 1998). Chapter 4 provides strong evidence that WfC 4 delivered significant amounts of sediment to the upper slope, producing a thick package of upper slope turbidites. However, the absence of evidence for widespread subaerial exposure associated with this increased sediment supply to the slope suggests that it is not necessary for relative sea-level to fall below the shelf edge rollover to initiate delivery of sediment to deeper parts of the basin. It also indicates that factors other than relative sea-level can force deltaic systems beyond the shelf edge.

Process regime: Dixon *et al.* (2012b) have shown a strong positive correlation between process regime at the shelf edge and delivery of sand to the deep water that is not necessarily tied to relative sea-level position or stacking pattern. Other authors have also advocated the importance of a focussed fluvial supply in order to drive the deltaic system to the shelf edge and bypass sediment to the slope and basin floor (Morton & Suter, 1996; Johannessen & Steel, 2005; Carvajal & Steel, 2009). It has also been postulated that a dominance of storm and wave processes at the margin is less efficient in the potential for delivery of sediment beyond the shelf edge (Brami *et al.*, 2000; Carvajal & Steel, 2006). The detailed sedimentological investigation of WfC 3 and 4 along the Baviaans North profile, summarized in chapter 4, shows that despite the sand-prone portion of the delta reaching the shelf edge, the fluvial dominated WfC 3 did not deliver coarse-grained sediment to the slope. In contrast, the wave and storm dominated WfC4 was more efficient at supplying coarse-grained sediment across the shelf edge rollover. This suggests that in the case of the lower Waterford Formation, the process regime at the shelf edge had relatively little influence on margin construction and delivery to the slope and basin floor.

Sediment supply: The lower Waterford is considered to have been dominated by high sediment supply rates due to the abundance of shelf-confined soft sediment deformation. High sediment supply combined with limited accommodation on the shelf is interpreted to have enabled rapid delta progradation across a pre-existing muddy shelf, which resulted in instability and failure at the delta front, similar to the over-pressured and undercompacted mud deformation driven by the high sediment supply on the Mississippi delta (Prior *et al.*,

1979; Prior & Coleman, 1980). Parasequence thickness data and stacking pattern analysis show that WfC 4 is the most heavily deformed and thinnest of the lower Waterford parasequences, which leads to the interpretation that the parasequence was subject to reduced accommodation as a result of relative sea-level fall, which when combined with high sediment supply rates caused WfC 4 to prograde rapidly across the mud-prone shelf and suffer widespread deformation as it delivered sediment to the upper slope.

Basin physiography: chapter 5 explores how across-strike variability in basin margin physiography strongly affects spatial and temporal variability of sediment delivery to the slope and basin floor. A long-term trend for greater sediment supply beyond the shelf edge in the north of the region is demonstrated through regional correlations. Plotting the shelf edge rollover in map view using criteria established in chapter 1, combined with isopach thickness maps, reveals that the lower Waterford Formation margin was not linear, and was slightly embayed to the north resulting in a narrower shelf. The narrower shelf in the north of the study area is therefore interpreted to have enabled successive shoreface and deltaic systems (WfC 3, 4 and 5) to transit more rapidly across and establish at the shelf edge earlier (and for longer periods), therefore supplying greater amounts of sediment to the deep water. The earlier establishment might also have influenced sediment routing across the shelf, although this is not testable with the current dataset.

The detailed study of depositional architecture and facies variability along the three main basin profiles has revealed how high sediment supply rates, relative sea-level variability, combined with variability in basin margin physiography played an important role in establishing shoreface and deltaic systems at the shelf edge and controlled the delivery of sediment to deep marine settings. The lack of widespread or deep shelf incision (no valley fills in the shelf stratigraphy have been identified) has shown that, given sufficient sediment supply, deltaic systems can deliver sediment to the slope and basin floor without exposure and incision of the shelf. The findings of chapter 4 also caution against using process regime at the shelf edge as a predictor of down dip sand deposits. The across-strike control afforded by the three dip profiles has provided an understanding of the spatial distribution of sediment supplied basinward of the shelf edge, and shows that considerable variability can occur across a margin as well as emphasizing the limitations of basing interpretation and prediction of down dip sand deposits on a 2D profile.

B. How is the shelf edge rollover identified at outcrop?

Although the shelf edge rollover can be readily identified in reflection seismic datasets, the published literature of exhumed examples is limited. This study is unique in identifying the physical transition from shelf to slope in multiple successive clinothems and across three sub-parallel dip-profiles that cover a 900 km^2 area. Steel *et al.* (2000) suggested that the key criterion in the recognition of the shelf edge rollover is the identification of the gradient increase associated with the transition from a relatively flat shelf to a steeper slope setting. Establishing the position of the shelf edge rollover from outcrop or well datasets is more difficult due to the limitations of exposure, especially in low gradient systems where the change in gradient from the shelf (0.01°) (Miall, 1991; Cattaneo & Steel, 2003; Sømme *et al.*, 2009) to the slope may be <1° (Wild *et al.*, 2009).

Chapter 4 establishes a number of facies and architecture based criteria to aid the identification of exhumed shelf edge rollovers based on the Baviaans North dip panel. These include: increased and widespread erosion or gullying, extensional growth faults, an increase in large scale (m's) soft-sediment deformation, and basinward thickening of parasequences coincident with increased amounts of turbidite beds. Rather than a defined point, as suggested by 2D seismic lines, the sedimentological changes observed on the Baviaans North dip profile occur over a zone of several kilometres. Although these criteria were developed based on observations made in a low gradient setting they are likely to provide a starting point for the interpretation of other more complicated margin settings or datasets with limited outcrop of borehole data.

The large scale outcrops along the Baviaans North profile enabled the physical correlation of two successive clinothems from the shelf to the upper slope, and permitted the detailed study of the process regime and architecture present at the shelf edge rollover zone. The correlations show that there can be significant variability between successive clinothems in the shelf edge rollover setting. WfC 3 is fluvially dominated, resulting in local unidirectional sediment supply to the shelf edge. High supply rates are interpreted to drive growth faulting by loading at the shelf edge, resulting in the trapping of sediment and overall thickening of the parasequence. The limited delivery of sediment over the shelf edge indicates that the sediment supply was not high enough to outpace the growth faulting. This is largely consistent with the typical shelf edge delta characteristics described by Johannessen & Steel (2005). In contrast, the overlying parasequence (WfC 4) is wave and storm dominated, but shows extensive erosion at the shelf edge, beyond which WfC 4

transitions into a thick wedge of upper slope turbidite deposits that are incised by an upper slope channel. This suggests that significant coarse-grained sediment was bypassed into the deeper parts of the basin during the later stages of WfC 4.

C. What is the relationship between soft-sediment deformation processes and proximity to the shelf edge?

The occurrence of abundant soft sediment deformation has commonly been attributed to increased gradient at the shelf edge rollover and has been used to identify the rollover position (e.g. Stow, 1994; Galloway, 1998; Lee *et al.*, 2009; Pratson *et al.*, 2009; Oliveira *et al.*, 2011). The extensive dip correlation profiles of the lower Waterford Formation, combined with the application of criteria for identifying shelf edge rollover position (outlined in chapters 4) show that soft sediment deformation is largely confined to shelf settings (landward of the shelf edge rollover) and is attributed to shelf delta-scale instability (gradient) and rapid sedimentation (overpressured and/or undercompacted fines). Commonly, soft-sediment deformation deposits with evidence of disaggregation and downslope movement (debrites) are overlain by *in-situ* deformed units, indicating a physical connection and process continuum between soft-sediment deformation features. However, an increase in the scale and a change in the process of deformation can be observed at the shelf edge rollover; WfC 3 on the Baviaans North profile exhibits large, rotational growth faulting at the rollover position. These features are analogous in scale and architecture to structures observed in other shelf edge deltas that encounter increased gradient at the shelf edge (Rider, 1978; Coleman *et al.*, 1998). The scale of the growth faulting is significantly larger than any failure features observed landward of the rollover position. The confinement of soft sediment deformation to the shelf and the marked decrease in its occurrence beyond the shelf edge rollover indicates that soft-sediment deformation should be used with caution as an indicator of rollover position, and that the scale and process of deformation are more accurate indicators of proximity to the shelf edge rollover zone.

D. What role does differential subsidence play on the stratigraphic development of the Karoo Basin margin during deposition the lower Waterford Formation?

Recognising the mechanisms that fundamentally control lateral variability is critical for understanding the distribution of deep water sand deposits and the long term development of a basin margin. High sediment supply rates and relative sea-level change have been identified as the primary mechanism by which the lower Waterford deltaic system was able to prograde to a position at the shelf edge and deliver sediment to the slope. Shelf width, rather than regional sediment supply rates across the Waterford margin, is cited as the principal reason for the observed lateral variability in the delivery of coarse grained material to the upper slope, although local sediment supply rates might be influenced by basin margin physiography. Chapter 5 documents the spatial and temporal variability of supply beyond the shelf edge rollover, and shows a trend for greater long-term delivery to the slope in the north of the region. The long-term trend for increasing parasequence thickness toward the north of the region suggests that greater accommodation was present in this area. Therefore, along-margin variability is attributed to differential subsidence. The thickness of the Waterford Formation points to long-term tectonic subsidence, although compaction of underlying strata is an alternative mechanism, which may have had contributed to the differential subsidence. Long-term differential subsidence across the Waterford margin would have had significant influence on sediment routing pathways, diverting them northward toward the area of greatest subsidence. Increased subsidence, and therefore accommodation, would also have impeded progradation and maintained a narrower shelf during multiple delta transits, and a more pronounced and steeper gradient change at the shelf edge. Chapter 5 emphasizes the importance of a balanced approach to understanding how basin margins develop and the prediction of coarse grained deep water deposits. It cautions against reliance upon eustatic sea-level change as the primary means for interpreting margin development, and demonstrates how differential subsidence can significantly affect routing and sediment flux rates along a basin margin.

7.1. Future work

The detailed work carried out during this project raised a number of questions that lay outside the remit of this project, but would provide a good basis for future work. They include the following:-

7.1.1. When and by what means do basin margins prograde?

Established models suggest that basin margins prograde largely during sea-level still stand and fall, when sedimentation in topsets is limited by low accommodation, and deltas are able to prograde to the outer shelf, and are in a position to deliver significant quantities of relatively coarse grained material to the slope (Steel & Olsen, 2002; Porębski & Steel, 2006; Ainsworth *et al.*, 2008; Steel *et al.*, 2008). This results in accretion at the shelf margin and generation of basin margin scale clinoforms.

The three regional dip correlation panels produced as part of this work reveal significant basinward stepping of the clinoform rollover position between WfC 5 and WfC 8, i.e. during a relative sea-level high stand. WfC 5 represents the last parasequence when the sand-prone portion of the shelf delta encountered the shelf edge rollover before drowning of the shelf relating to the overlying maximum flooding surface that formed prior to progradation of WfC 6, 7, and 8. The sandy components of WfC 6 and 7 appear to be entirely shelf confined whereas WfC 8 exhibits significant basinward progradation of shelf facies (lower shoreface and deformed facies) well beyond the shelf edge previously established by WfC 5. This suggests that the shelf edge must have prograded through siltstone accretion during the long-term highstand period while the sand-prone portions of WfC 6 and 7 remained shelf confined in order to create a shelf platform over which WfC 8 could prograde, as suggested in chapter 6.

An implicit assumption in shelf edge trajectory analysis and sequence stratigraphy that employs uncalibrated 2D and 3D reflection seismic lines, is that sandy components of shelf deltas must always reach the shelf edge rollover to enable progradation of the margin, although 3D reflection seismic datasets indicate that this is not the case (Sanchez *et al.*, 2012b). Margin progradation is considered to occur predominantly through accretion of coarse grained sediment when deltas are at the shelf edge (Carvajal & Steel, 2006; Carvajal & Steel, 2009; Covault *et al.*, 2009), but this outcrop dataset indicates that margin progradation can operate in a fundamentally different manner through the accretion of silt

during highstand conditions ahead of the sandy section of the parasequence. In exceptional exposures it may be possible to observe features at the muddy shelf edge that are consistent with increased gradient such as deformation, evidence of bypass or subtle facies change within very low density, silty turbidites. Detailed process sedimentological observations will be needed to identify gravity and density driven fine-grained flows, such as wave-enhanced sediment gravity flows (WESGCs) (Macquaker *et al.*, 2007). The ability to document criteria relating to a muddy shelf to slope transition is significant if equivalent seismic expressions are to be identified, and for margin progradation via fine grained material to be documented. In addition, further investigations are required to determine what processes are able to transport fine grained material across the shelf and beyond the shelf edge rollover during highstand conditions.

7.1.2. In basin-fill successions, are shallow-marine systems representative of the sediment delivery regime that supplied the underlying basin-floor and slope?

The limitations of outcrop-based datasets mean that time-equivalent shelf, slope and basin floor deposits are commonly not observed (Wild et al., 2009, Dixon et al, 2012a). Yet a starting assumption is that the juxtaposed shelf successions are similar in character to those that supplied underlying basin-floor stratigraphy, particularly on shallow progradational margins (Wild et al., 2009). The well-documented channelized slope and basin floor stratigraphy of the Laingsburg and Fort Brown Formations that underlie the lower Waterford Formation represent lowstand systems tracts to sequences and composite sequences (Flint et al 2011). The ability to document a complete basin fill succession in the Laingsburg depocentre raises the question as to whether the observed lower Waterford Formation could have supplied a time equivalent channelized slope, and delivered comparable quantities of sediment to the slope and basin floor to those recorded in Units A - F.

7.1.3. Regional variability of the Waterford Formation

Shallow water facies crop out across the Karoo region, as far north as the towns of Carnarvon and Calvinia (Fig. 7.2), several hundred kilometres from the study area. Reconnaissance fieldwork undertaken as part of this study recognized a number of key differences from the shallow marine Waterford Formation in the Laingsburg area. Extended log sections through the shallow marine strata in the Northern Cape Province reveal a significantly thinner shallow-marine succession (Fig. 7.2) The characteristic thickness of the

lower Waterford Formation in the Laingsburg area has been linked to significant rates of local subsidence, which by implication would suggest that areas to the north and to the east around the town of Prince Albert were subject to less subsidence, which may have had a significant impact on margin architecture and progradation rates. The prevalence of soft sediment deformation is a key feature of the stratigraphy in the Laingsburg area, however, it seems that widespread soft sediment deformation is not the norm based on observations from elsewhere in the basin. A number of outcrops showed consistent coarsening and thickening upward of parasequences, from heterolithic siltstones to amalgamated wave and storm dominated shoreface deposits. Other localities display a transition from a mudstone-succession dominated by sandstone filled erosive gullies (Fig. 7.3) into amalgamated shoreface and mouth bar facies. The muddy package containing the erosive gulley feature replaces the deformed interval typically recorded in parasequences found in the Laingsburg area, which leads to speculation that such facies are a precursor to extensive deformation. Understanding the regional variability of the shallow marine stratigraphy across the larger Karoo region will provide context for the detailed work carried out by Wild *et al.* (2009), Dixon *et al.* (2012a) and this study, and will provide greater understanding of how the wider basin evolution has affected the margin architecture.

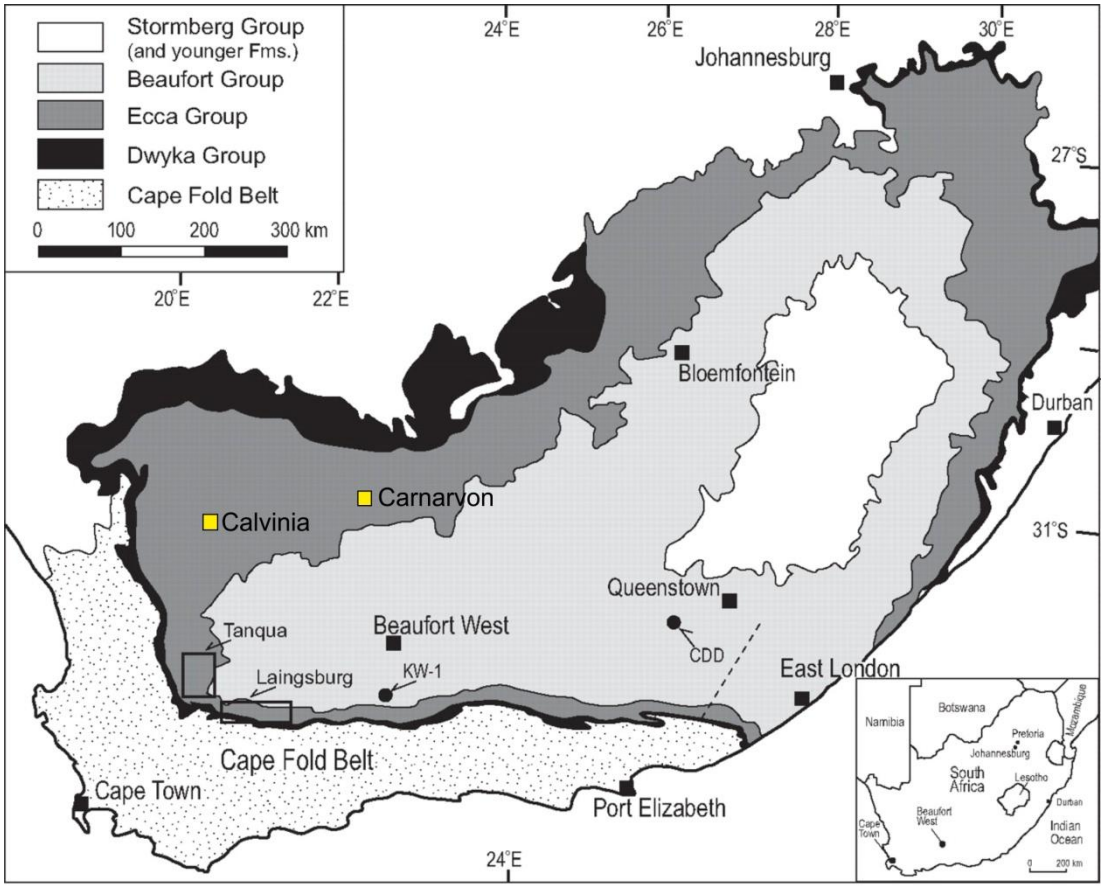

Modified from Fildani et al., 2009

Figure 7.2 Regional geological map of South Africa showing the extent of the Ecca Group and locations of Carnarvon and Calvinia

Figure 7.3: Keiskie Pass, South of Calvinia. Photo shows a silt dominated lower slope consisting of heterolithic facies with an abrupt change to thick amalgamated sandstone parasequences. The parasequences only include one thin (~1-m-thick) *in-situ* deformed package.

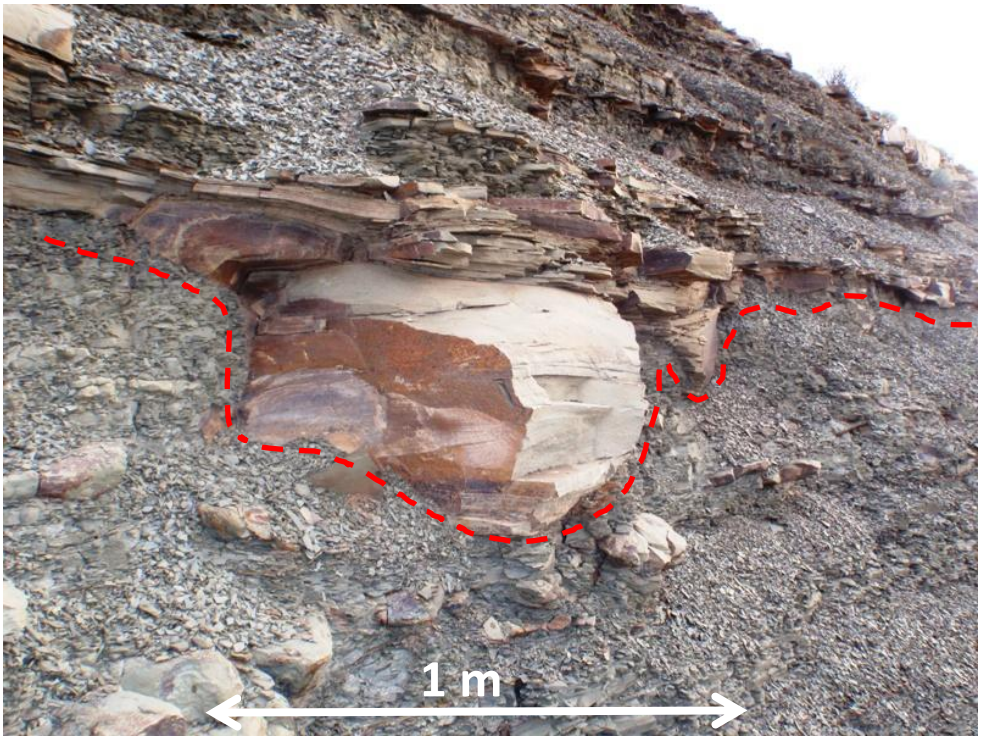

Figure 7.4: Siltstone dominated interval underlying amalgamated shoreface facies. Mudstones are cut by erosive gully features that range in size from a few centimetres up to 3 m across. Possible interpretations include a delta front setting with gutter casts. Mudstone intervals cut by gully feature replace deformed facies in a typical parasequence facies succession observed in the Laingsburg area, therefore it may be speculated that such gullied delta front settings are a forerunner to extensive deformation.

REFERENCES

Ainsworth, R. B., Flint, S. S., & Howell, J. A., 2008, Predicting coastal depositional style: Influence of basin morphology and accommodation to sediment supply ratio within a sequence stratigraphic framework: *in* Hampson, G.J., Steel, R., Burgess, P.B. & Dalrymple, R.W. eds., Recent Advances in Models of Siliciclastic Shallow-marine Stratigraphy: Society of Economic Paleontologists and Mineralogists no. Special Publication No. 90, p. 237-263.

Al-Aasm, I. S., Morad, S., Durocher, S., & Muir, I., 1996, Sedimentology, C-S-Fe relationships and stable isotopic compositions in Devonian black mudrocks, Mackenzie Mountains, Northwest Territories, Canada: Sedimentary Geology, v. 106, no. 3-4, p. 279-298.

Allen, G. P., & Posamentier, H. W., 1994, Transgressive facies and sequence architecture in mixed tide and wave-dominated incised valleys: example from the Gironde estuary, France: In: R.W. Ashley, G.M. and Sheridan, R.E., 1994. Depositional model for valley fills on a passive continental margin. In: R.W. Dalrymple, R.J. Boyd and B.A. Zaitlin (Eds), Incised valley systems : Origin and sedimentary Sequences. SEPM (Soc. Sediment. Geol.) Spec. Publ., Tulsa,, v. 51, p. 285-301.

Allen, P. A., 2008, From landscapes into geological history: Nature, v. 451, p. 274.

Anderson, J. B., Rodriguez, A., Abdulah, K. C., Fillon, R. H., Banfield, L. A., Mckeown, H. A., & Wellner, J. S., 2004, Late quaternary stratigraphic evolution of the northern Gulf of Mexico margin: a synthesis: Society for Sedimentary Geology, v. 79.

Andersson, P. O. D., Worden, R. H., Hodgson, D. M., & Flint, S., 2004, Provenance evolution and chemostratigraphy of a Palaeozoic submarine fan-complex: Tanqua Karoo Basin, South Africa: Marine and Petroleum Geology, v. 21, no. 5, p. 555-577.

Ashton E., 2002, Transgressive-Regressive (T_-R) Sequence Stratigraphy: Gulf Coast Association of Geological Societies Transactions, v. 52, p. 151-172.

Bangert, B., Stollhofen, H., Lorenz, V., & Armstrong, R., 1999, The geochronology and significance of ash-fall tuffs in the glaciogenic Carboniferous-Permian Dwyka Group of Namibia and South Africa: Journal of African Earth Sciences, v. 29, no. 1, p. 33-49.

Barnes, P. M., & Lewis, K. B., 1991, Sheet slides and rotational failures on a convergent margin: the Kidnappers Slide, New Zealand: Sedimentology, v. 38, no. 2, p. 205-221.

Bertram, G., Griffiths, C., Milton, N., Reynolds, T., M., R., & S., S., 2006, Sequence stratigraphy: Blackwell publishing, v. 297.

Bhattachary, J. P., 2006, Deltas. In: Facies Models Revisited (Eds H.W. Posamentier and R.G. Walker): SEPM Special Publication, v. 84, p. 237-292.

Bhattacharya, J. P., & Walker, R. G., 1992, Deltas. In: Facies Models: Response to Sea-Level Change (Eds R.G. Walker and N.P. James),: Geological Association of Canada, St Johns, p. 157-177.

Boyd, R., Ruming, K., Goodwin, I., Sandstrom, M., & Schröder-Adams, C., 2008, Highstand transport of coastal sand to the deep ocean: A case study from Fraser Island, southeast Australia: Geology, v. 36, no. 1, p. 15-18.

Brami, T. R., Pirmez C., Archie, C., Heeralal, S., & Holman, K. L., 2000, Late Pleistocene Deep-Water Stratigraphy and Depositional Processes, Offshore Trinidad & Tobago: In: Deep-water reservoirs of the world: Gulf Coast Section-SEPM 20th Annual Research Conference, Huston Texas, December 3-6, p. 104-115.

Broquet, C. A. M., 1992, The sedimentary record of the Cape Supergroup: a review: Inversion tectonics of the Cape Fold Belt, Karoo and Cretaceous basins of southern Africa, p. 159-183.

Brunt, R. L., Di Celma, C., Hodgson, D. M., Flint, S. S., Kavanagh, J. P., & van der Merwe, W. C., 2013, Driving a channel through a levee when the levee is high: an outcrop example of submarine down-dip entrenchment: Marine and Petroleum Geology.

Burgess, P. M., & Hovius, N., 1998, Rates of delta progradation during highstands: consequences for timing of deposition in deep-marine systems: Journal of the Geological Society [London], v. 155, no. 2, p. 217-222.

Carvajal, C., & Steel, R., 2009, Shelf-edge architecture and bypass of sand to deep water: Influence of shelf-edge processes, sea level, and sediment supply: Journal of Sedimentary Research v. 79, no. 9, p. 652-672.

Carvajal, C., Steel, R., & Petter, A., 2009, Sediment supply: The main driver of shelf-margin growth: Earth-Science Reviews, v. 96, no. 4, p. 221-248.

Carvajal, C. R., & Steel, R. J., 2006, Thick turbidite successions from supply-dominated shelves during sea-level highstand: Geology, v. 34, no. 8, p. 665-668.

Cattaneo, A., & Steel, R. J., 2003, Transgressive deposits: a review of their variability: Earth-Science Reviews, v. 62, no. 3-4, p. 187-228.

Catuneanu, O., 2002, Sequence stratigraphy of clastic systems: concepts, merits, and pitfalls: Journal of African Earth Sciences, v. 35, no. 1, p. 1-43.

-, 2004, Basement control on flexural profiles and the distribution of foreland facies: The Dwyka Group of the Karoo Basin, South Africa: Geology, v. 32, no. 6, p. 517-520.

Catuneanu, O., Abreu, V., Bhattacharya, J. P., Blum, M. D., & Dalrymple, R. W., 2009, Towards the standardization of sequence stratigraphy: Earth-Sci. Rev., v. 92, p. 1.

Catuneanu, O., Hancox, P. J., & Rubidge, B. S., 1998, Reciprocal flexural behaviour and contrasting stratigraphies: a new basin development model for the Karoo retroarc foreland system, South Africa: Basin Research, v. 10, no. 4, p. 417-439.

Charvin, K., Hampson, G. J., Gallagher, K. L., & Labourdette, R., 2010, Intra-parasequence architecture of an interpreted asymmetrical wave-dominated delta: Sedimentology, v. 57, no. 3, p. 760-785.

Chough, S. K., Hwang, I. G., & Choe, M. Y., 1990, The Miocene Doumsan fan-delta, Southeast Korea; a composite fan-delta system in back-arc margin: Journal of Sedimentary Research, v. 60, no. 3, p. 445-455.

Coe, A. L., Bosence D.W.J., Church K.D., Flint S.S., Howell J.A., & Wilson R.C.L., 2003, The Sedimentary Record of Sea-Level Change: Cambridge University Press.

Cole, D. I., 1992, Evolution and development of the Karoo Basin. In: De Wit, M.J. and Ransome, I.G.D. (eds),Inversion Tectonics of the Cape Fold Belt, Karoo and Cretaceous Basins of Southern Africa.: Balkema, Rotterdam, p. 87-99.

Cole, D. I., & Whipplinger, P. E., 2001, Sedimentology and molybdenum potential Beaufort Group in the Karoo Basin: Council for Geoscience, Geological Survay of South Africa, v. Memoir 80.

Coleman, J. M., Walker, H. J., & Grabau, W. E., 1998, Sediment instability in the Mississippi River Delta: Journal of Coastal Research, v. 14, no. 3, p. 872-881.

Collinson, J. D., Martinsen, O., Bakken, B., & Kloster, A., 1991, Early fill of the Western Irish Namurian Basin: a complex relationship between turbidites and deltas: Basin Research, v. 3, no. 4, p. 223-242.

Covault, J. A., & Graham, S. A., 2010, Submarine fans at all sea-level stands: Tectono-morphologic and climatic controls on terrigenous sediment delivery to the deep sea: Geology, v. 38, no. 10, p. 939-942.

Covault, J. A., Normark, W. R., Romans, B. W., & Graham, S. A., 2007, Highstand fans in the California borderland: The overlooked deep-water depositional systems: Geology, v. 35, no. 9, p. 783-786.

Covault, J. A., Romans, B. W., & Graham, S. A., 2009, Outcrop expression of a continental-margin-scale shelf-edge delta from the Cretaceous Magallanes Basin, Chile: Journal of Sedimentary Research v. 79, no. 7, p. 523-539.

Dail, M. B., Reide Corbett, D., & Walsh, J. P., 2007, Assessing the importance of tropical cyclones on continental margin sedimentation in the Mississippi delta region: Continental Shelf Research, v. 27, no. 14, p. 1857-1874.

Dalrymple, R. W., Zaitlin, B. A., & Boyd, R., 1992, Estuarine facies models; conceptual basis and stratigraphic implications: Journal of Sedimentary Research, v. 62, no. 6, p. 1130-1146.

Damuth, J. E., 1994, Neogene gravity tectonics and depositional processes on the deep Niger Delta continental margin: Marine and Petroleum Geology, v. 11, no. 3, p. 320-346.

De Wit, M., & Ransome., I. D. G., 1992, Regional inversion tectonics along the southern margin of Gondwana: *in* De Wit, M.J., Ransome, I.D.G., Inversion Tectonics of the Cape Fold Belt. Karoo and Cretaceous Basins of South Africa. A.A. Balkema, Rotterdam, p. 15-21.

Deibert, J. E., Benda, T., Løseth, T., Schellpeper, M., & Steel, R. J., 2003, Eocene Clinoform Growth in Front of a Storm-Wave-Dominated Shelf, Central Basin, Spitsbergen: No Significant Sand Delivery to Deepwater Areas: Joutnal of Sedimentary Research, v. 73, no. 4, p. 546-558.

Dixon, J. F., Steel, R. J., & Olariu, C., 2012a, River-dominated, shelf-edge deltas: delivery of sand across the shelf break in the absence of slope incision: Sedimentology, v. 59, p. 1133-1157, doi: 1110.1111/j.1365-3091.2011.01298.x.

Dixon, J. F., Steel, R. J., & Olariu, C., 2012b, Shelf-Edge Delta Regime As A Predictor of Deep-Water Deposition: Journal of Sedimentary Research, v. 82, no. 9, p. 681-687.

Driscoll, N. W., & Karner, G. D., 1999, Three-dimensional quantitative modeling of clinoform development: Marine Geology, v. 154, no. 1–4, p. 383-398.

Droz, L., Marsset, T., Ondréas, H., Lopez, M., Savoye, B., & Spy-Anderson, F. L., 2003, Architecture of an active mud-rich turbidite system: The Zaire Fan (Congo–Angola margin southeast Atlantic): Results from ZaïAngo 1 and 2 cruises: AAPG Bulletin, v. 87, no. 7, p. 1145-1168.

Edwards, M. B., 1981, Upper Wilcox Rosita delta system of South Texas; growth-faulted shelf-edge deltas: AAPG Bulletin, v. 65, no. 1, p. 54-73.

Emery, D., & Myers, K., 1996, Sequence stratigraphy: Oxford, Blackwell Science.

Enge, H. D., Howell, J. A., & Buckley, S. J., 2010, Quantifying clinothem geometry in a forced-regressive river-dominated delta, Panther Tongue Member, Utah, USA: Sedimentology, v. 57, no. 7, p. 1750-1770.

Faure, K., & Cole, D., 1999, Geochemical evidence for lacustrine microbial blooms in the vast Permian Main Karoo, Parana, Falkland Islands and Huab basins of southwestern Gondwana: Palaeogeography, Palaeoclimatology, Palaeoecology, v. 152, no. 3, p. 189-213.

Fernández-Salas, L. M., Lobo, F. J., Sanz, J. L., Díaz-del-Río, V., García, M. C., & Moreno, I., 2007, Morphometric analysis and genetic implications of pro-deltaic sea-floor undulations in the northern Alboran Sea margin, western Mediterranean Basin: Marine Geology, v. 243, no. 1–4, p. 31-56.

Figueiredo, J. J. P., Hodgson, D. M., Flint, S. S., & Kavanagh, J. P., 2010, Depositional environments and sequence stratigraphy of an exhumed Permian mudstone-dominated submarine slope succession, Karoo Basin, South Africa: Journal of Sedimentary Research, v. 80, no. 1, p. 97-118.

Fildani, A., Drinkwater, N. J., Weislogel, A., McHargue, T., Hodgson, D. M., & Flint, S. S., 2007, Age Controls on the Tanqua and Laingsburg Deep-Water Systems: New Insights on the Evolution and Sedimentary Fill of the Karoo Basin, South Africa: Journal of Sedimentary Research, v. 77, no. 11, p. 901-908.

Fildani, A., Weislogel, A., Drinkwater, N. J., McHargue, T., Tankard, A., Wooden, J., Hodgson, D., & Flint, S., 2009, U-Pb zircon ages from the southwestern Karoo Basin, South Africa—Implications for the Permian-Triassic boundary: Geology, v. 37, no. 8, p. 719-722.

Flint, S. S., Hodgson, D. M., Sprague, A. R., Brunt, R. L., & Van der Merwe, W. C., 2011a, Depositional architecture and sequence stratigraphy of the Karoo basin floor to shelf-edge succession, Laingsburg depocentre, South Africa: Mar. Pet. Geol., v. 28, p. 658.

Flint, S. S., Hodgson, D. M., Sprague, A. R., Brunt, R. L., Van der Merwe, W. C., Figueiredo, J., Prélat, A., Box, D., Di Celma, C., & Kavanagh, J. P., 2011b, Depositional architecture and sequence stratigraphy of the Karoo basin floor to shelf edge succession, Laingsburg depocentre, South Africa: Marine and Petroleum Geology, v. 28, no. 3, p. 658-674.

Flood, R. D., & Piper, D. J. W., 1997, Amazon fan sedimentation: the relationship to equatorial climate change, continental denudation, and sea-level fluctuations: Proceedings of the Ocean Drilling Program, Scientific Results, v. 155, no. 653-675.

Frazier, D. E., 1976, Recent Deltaic Deposits of the Mississippi River: Their Development and Chronology: Gulf Coast Association of Geological Societies Transactions, v. 17, p. 287-315.

Fulthorpe, C. S., & Austin, J. A., 2008, Assessing the significance of along-strike variations of middle to late Miocene prograding clinoformal sequence geometries beneath the New Jersey continental shelf: Basin Research, v. 20, no. 2, p. 269-283.

Galloway, W. E., 1975, Process framework for describing the morphologic andstratigraphic evolution of deltaic depositional systems. In: Broussard, M.L. (ed.). Deltas: models for exploration.: Houston Geological Society, Houston, USA, p. 87-98.

-, 1989, Genetic stratigraphic sequences in basin analysis; II, Application to Northwest Gulf of Mexico Cenozoic basin: AAPG Bulletin, v. 73/2, p. 125-142.

Galloway, W. E., 1998, Siliciclastic slope and base-of-slope depositional systems; component facies, stratigraphic architecture, and classification: AAPG Bulletin, v. 82, no. 4, p. 569-595.

Gilbert, G. K., 1990, Lake Bonneville: U.S. Geol. Surv. Monogr. 1,, v. 438.

Goff, J. A., Allison, M. A., & Gulick, S. P. S., 2010, Offshore transport of sediment during cyclonic storms: Hurricane Ike (2008), Texas Gulf Coast, USA: Geology, v. 38, no. 4, p. 351-354.

Gresse, P. G., Theron, J. N., Fitch, F. J., & Miller, J. A., 1992, Tectonicinversion and radiometric resetting of the basement in the Cape Fold Belt. In: DeWit, M. J. and Ransome, I. D.(eds) Inversion tectonics of the Cape Fold Belt, Karoo and Cretaceous basins of Southern Africa:: Balkema, Rotterdam p. 217-228.

Hälbich, I. W., 1993, Tectonogenesis of the Cape Fold Belt (CFB), In: Söhnge, A.P.G. and Hälbich, I.W. (eds) Geodynamics of the Cape Fold Belt: Special Publication of the Geological Society of South Africa, v. 12, p. 165-175.

Hampson, G. J., 2000, Discontinuity Surfaces, Clinoforms, and Facies Architecture in a Wave-Dominated, Shoreface-Shelf Parasequence: Journal of Sedimentary Research, v. 70, no. 2, p. 325-340.

Hampson, G. J., Gani, M. R., Sharman, K. E., Irfan, N., & Bracken, B., 2011, Along-strike and down-dip variations in shallow-marine sequence stratigraphic architecture: Upper Cretaceous Star Point Sandstone, Wasatch Plateau, Central Utah, U.S.A: Journal of Sedimentary Research, v. 81, no. 3, p. 159-184.

Hampson, G. J., & Howell, J. A., 2005, Sedimentologic and geomorphic characterization of ancient wave-dominated deltaic shorelines: Upper Cretaceous Blackhawk

Formation, Book Cliffs, Utah, U.S.A: SPECIAL PUBLICATION- SEPM, no. 83, p. 133-154.

Hart, B. S., & Long, B. F., 1996, Forced regressions and lowstand deltas; Holocene Canadian examples: Journal of Sedimentary Research, v. 66, no. 4, p. 820-829.

Hart, B. S., Sibley, D. M., & Flemings, P. B., 1997, Seismic stratigraphy, facies architecture, and reservoir character of a Pleistocene shelf-margin delta complex, Eugene Island Block 330 Field, offshore Louisiana: AAPG Bulletin, v. 81, no. 3, p. 380-397.

Helland-Hansen, W., 2010, Facies and stacking patterns of shelf-deltas within the Palaeogene Battfjellet Formation, Nordenskiöld Land, Svalbard: implications for subsurface reservoir prediction: Sedimentology, v. 57, no. 1, p. 190-208.

Helland-Hansen, W., & Gjelberg, J. G., 1994, Conceptual basis and variability in sequence stratigraphy: a different perspective: Sedimentary Geology, v. 92, no. 1-2, p. 31-52.

Helland-Hansen, W., & Hampson, G. J., 2009, Trajectory analysis: concepts and applications: Basin Research, v. 21, no. 5, p. 454-483.

Helland-Hansen, W., Steel, R. J., & Somme, T. O., 2012, Shelf Genisis Revisited: Journal of Sedimentary Research, v. 82, p. 133-148.

Henriksen, S., Hampson, G. J., Helland-Hansen, W., Johannessen, E. P., & Steel, R. J., 2009, Shelf edge and shoreline trajectories, a dynamic approach to stratigraphic analysis: Basin Research, v. 21, no. 5, p. 445-453.

Henriksen, S., Helland-Hansen, W., & Bullimore, S., 2011, Relationships between shelf-edge trajectories and sediment dispersal along depositional dip and strike: a different approach to sequence stratigraphy: Basin Research, v. 23, no. 1, p. 3-21.

Hesthammer, J., & Fossen, H., 1999, Evolution and geometries of gravitational collapse structures with examples from the StatfJord Field, northern North Sea: Marine and Petroleum Geology, v. 16, no. 3, p. 259-281.

Hiscott, R. N., 2001, Depositional sequences controlled by high rates of sediment supply, sea-level variations, and growth faulting: the Quaternary Baram Delta of northwestern Borneo: Marine Geology, v. 175, no. 1–4, p. 67-102.

Hodgson, D. M., Di Celma, C. N., Brunt, R. L., & Flint, S. S., 2011a, Submarine slope degradation and aggradation and the stratigraphic evolution of channel-levee systems: Journal of the Geological Society, v. 168, no. 3, p. 625-628.

Hodgson, D. M., van der Merwe, W. C., & Flint, S. S., 2011c, Distribution of submarine mass movement deposits: an exhumed basin perspective: In: Y. Yamada, K. Kawamura, K. Ikehara, Y. Ogawa, R. Ureles, D. Mosher, J. Chaytor, M. Strasser (Eds.)

Advances in Natural and Technological Hazards Research - Submarine Mass Movements and Their Consequences, 4th Edition., p. 619-628.

Holmes, A., 1965, Principals of Physical Geology: Thomas Nelson, London, p. 1288.

Houseknecht, D. W., Bird, K. J., & Schenk, C. J., 2009, Seismic analysis of clinoform depositional sequences and shelf-margin trajectories in Lower Cretaceous (Albian) strata, Alaska North Slope: Basin Research, v. 21, no. 5, p. 644-654.

Hovius, N., 1998, Controls on Sediment Supply by Large Rivers. In: Shanley, K.W., McCabe, P.J. (Eds.), Relative Role of Eustasy, Climate and Tectonism in Continental Rocks.: Society of Economic Paleontologists and Mineralogists, Special Publication, v. 59, p. 3 - 16, Tulsa.

Howell, J. A., & Flint, S. S., 1996, A model for high resolution sequence stratigraphy within extensional basins: London, Geological Society [London] Special Publication, v. 104, no. 1, p. 129-137.

Hubbard, S. M., Fildani, A., Romans, B. W., Covault, J. A., & McHargue, T., 2010, High-relief slope clinoform development: insights from outcrop, Magallanes Basin, Chile: J. Sediment. Res., v. 80, p. 357.

Jervey, M. T., 1988, Quantitative geological modelling of siliciclastic rock sequences and their seismic expressions In: Wilgus, C.K., Hastings, B.S., Ross, C.A., Posamentier, H.W., Van Wagoner, J.C. & Kendall, C.G.St.C. (eds.). Sea-level changes: An integrated approach:: Society of Economic Palaeontologists and Mineralogists Special Publication, v. 42, p. 47-69.

Johannessen, E. P., & Steel, R. J., 2005, Shelf-margin clinoforms and prediction of deepwater sands: Basin Research, v. 17, no. 4, p. 521-550.

Johnson, M. R., 1991, Sandstone petrography, provenance and plate tectonic setting in Gondwana context of the southeastern Cape-Karoo Basin: South African Journal of Geology, v. 94, no. 2-3, p. 137-154.

Johnson, M. R., van Vuuren, C. J., Visser, J. N. J., Cole, D. I., de van Wickens, H., Christie, A. D. M., & Roberts, D. L., 1997, The foreland Karoo Basin, South Africa *in* Selley, R.C. (ed.) African Basins. Sedimentary Basins of the World. Amsterdam, Elsevier Science, 3, p. 269-317.

Johnson, S. D., Flint, S., Hinds, D., & De Ville Wickens, H., 2001, Anatomy, geometry and sequence stratigraphy of basin floor to slope turbidite systems, Tanqua Karoo, South Africa: Sedimentology, v. 48, no. 5, p. 987-1023.

Jones, G. E. D., Hodgson, D. M., & Flint, S. S., 2013, Contrast in the process response of stacked clinothems to the shelf-slope rollover: Geosphere.

Kane, I. A., & Hodgson, D. M., 2011, Sedimentological criteria to differentiate submarine channel levee subenvironments: Exhumed examples from the Rosario Fm. (Upper Cretaceous) of Baja California, Mexico, and the Fort Brown Fm. (Permian), Karoo Basin, S. Africa: Marine and Petroleum Geology, v. 28, no. 3, p. 807-823.

Kindinger, J. L., 1988, Seismic stratigraphy of the Mississippi-Alabama shelf and upper continental slope: Marine Geology, v. 83, no. 1–4, p. 79-94.

Kolla, V., Biondi, P., Long, B., & Fillon, R., 2000, Sequence stratigraphy and architecture of the Late Pleistocene Lagniappe delta complex, northeast Gulf of Mexico: Geological Society, London, Special Publications, v. 172, no. 1, p. 291-327.

Kolla, V., & Perlmutter, M. A., 1993, Timing of turbidite sedimentation on the Mississippi Fan: AAPG Bulletin, v. 77, no. 7, p. 1129-1141.

Krassay, A. A., & Totterdell, J. M., 2003, Seismic stratigraphy of a large, Cretaceous shelf-margin delta complex, offshore southern Australia: AAPG Bulletin, v. 87, no. 6, p. 935-963.

Laberg, J. S., & Vorren, T. O., 2000, The Trænadjupet Slide, offshore Norway — morphology, evacuation and triggering mechanisms: Marine Geology, v. 171, no. 1–4, p. 95-114.

Lee, H. J., Locat, J., Desgagnés, P., Parsons, J. D., McAdoo, B. G., Orange, D. L., Puig, P., Wong, F. L., Dartnell, P., & Boulanger, E., 2009, Submarine Mass Movements on Continental Margins, Continental Margin Sedimentation, Blackwell Publishing Ltd., p. 213-274.

Lobo, F. J., Fernández-Salas, L. M., Moreno, I., Sanz, J. L., & Maldonado, A., 2006, The sea-floor morphology of a Mediterranean shelf fed by small rivers, northern Alboran Sea margin: Continental Shelf Research, v. 26, no. 20, p. 2607-2628.

López-Gamundí, O. R., & Rossello, E. A., 1998, Basin fill evolution and paleotectonic patterns along the Samfrau geosyncline: the Sauce Grande basin–Ventana foldbelt (Argentina) and Karoo basin–Cape foldbelt (South Africa) revisited: Geologische Rundschau, v. 86, no. 4, p. 819-834.

Løseth, T. M., Steel, R. J., Crabaugh, J. P., & Schellpeper, M., 2006, Interplay between shoreline migration paths, architecture and pinchout distance for siliciclastic shoreline tongues: evidence from the rock record: Sedimentology, v. 53, no. 4, p. 735-767.

Macquaker, J. H. S., Taylor, K. G., & Gawthorpe, R. L., 2007, High-Resolution Facies Analyses of Mudstones: Implications for Paleoenvironmental and Sequence Stratigraphic Interpretations of Offshore Ancient Mud-Dominated Successions: Journal of Sedimentary Research, v. 77, no. 4, p. 324-339.

Maloney, D., Davies, R., Imber, J., & King, S., 2012, Structure of the footwall of a listric fault system revealed by 3D seismic data from the Niger Delta: Basin Research, v. 24, no. 1, p. 107-123.

Marjanac, T., 1996, Deposition of megabeds (megaturbidites) and sea-level change in a proximal part of the Eocene-Miocene flysch of central Dalmatia (Croatia): Geology, v. 24, no. 6, p. 543-546.

Martinsen, O. J., & Helland-Hansen, W., 1995, Strike variability of clastic depositional systems: Does it matter for sequence-stratigraphic analysis?: Geology, v. 23, no. 5, p. 439-442.

Matteucci, T. D., & Hine, A. C., 1987, Evolution of the Cape Fear Terrace: A complex interaction between the Gulf Stream and a paleo-shelf edge delta: Marine Geology, v. 77, no. 3–4, p. 185-205.

Mayall, M. J., Yeilding, C. A., Oldroyd, J. D., Pulham, A. J., & Sakurai, S., 1992, Facies In A Shelf-Edge-Delta - An Example From The Subsurface Of The Gulf Of Mexico, Middle Pliocene, Mississippi Canyon, Block-109: Aapg Bulletin-American Association of Petroleum Geologists, v. 76, no. 4, p. 435-448.

McMaster, R. L., Boer, J. d., & Ashraf, A., 1970, Magnetic and seismic reflection studies on continental shelf off Portuguese Guinea, Guinea, and Sierra Leone, west Africa: AAPG Bulletin, v. 54, no. 1, p. 158-167.

Meisling, K. E., Kanschat, K. A., Armentrout, J. M., Dyer, R., Tsakma, J. J., & Bassey, F. A., 2000, Slope deformation control on trap and reservoir development in turbidite systems, southeastern Niger Delta, offshore Nigeria. : American Association of Petroleum Geologists, 2000 Annual Meeting Expanded Abstract,, p. 97.

Mellere, D., Breda, A., & Steel, R. J., 2003, Fluvial-incised shelf-edge deltas and linkage to upper-slope channels (Central Tertiary Basin, Spitsbergen). : In Robers, H.H., Rosen, N.C., Fillon, R.H., and Anderson, J.B., 2003. Shelf -Margin Deltas and Linked Downslope Petroleum Systems; Global Significance and Future Exploration Potential, Gulf Coast Section:23rd Annual Research Conference Houston, Texas, p. 231-266.

Mellere, D., Plink-Bjorklund, P., & Steel, R., 2002, Anatomy of shelf deltas at the edge of a prograding Eocene shelf margin, Spitsbergen: Sedimentology, v. 49, no. 6, p. 1181-1206.

Miall, A. D., 1991, Stratigraphic sequences and their chronostratigraphic correlation: Journal of Sedimentary Research, v. 61, no. 4, p. 497-505.

Milliman, J. D., & Syvitski, J. P. M., 1992, Geomorphic/Tectonic Control of Sediment Discharge to the Ocean: The Importance of Small Mountainous Rivers: The Journal of Geology, v. 100, no. 5, p. 525-544.

Milton, N., & Dyce, M., 1995, Systems tract geometries associated with Early Eocene lowstands, imaged on a 3D seismic dataset from the Bruce area, UK North Sea: *in* Steel, R. J.; Felt, V. L.; Johannessen, E. P.; and Mathieu, C., eds. Sequence stratigraphy on the northwest European margin. Norwegian Petroleum Society, Special Publication no. 5, p. 429-449.

Mitchum, R. M., Jr. & Vail, P.R., 1977, Seismic stratigraphy and global changes in sea level, part 7: stratigraphic interpretation of seismic reflection patterns in depositional sequences: Memoir of the American Association of Petroleum Geologists, v. 39, no. Seismic Stratigraphy - Applications to Hydrocarbon Exploration, p. 116-139.

Mitrovica, J. X., Beaumont, C., & Jarvis, G. T., 1989, Tilting of continental interiors by the dynamical effects of subduction: Tectonics, v. 8, no. 5, p. 1079-1094.

Monteverde, D. H., Mountain, G. S., & Miller, K. G., 2008, Early Miocene sequence development across the New Jersey margin: Basin Research, v. 20, no. 2, p. 249-267.

Moore, J. G., & Shannon, P. M., 1991, Slump structures in the Late Tertiary of the Porcupine Basin, offshore Ireland: Marine and Petroleum Geology, v. 8, no. 2, p. 184-197.

Morton, R. A., & Suter, J. R., 1996, Sequence Stratigraphy and Composition of Late Quaternary Shelf-Margin Deltas, Northern Gulf of Mexico: AAPG Bulletin, v. 80, no. 4 (April), p. 505-530.

Moscardelli, L., Wood, L. J., & Dunlap, D. B., 2012, Shelf-edge deltas along structurally complex margins: A case study from eastern offshore Trinidad: AAPG Bulletin, v. 96, no. 8, p. 1483-1522.

Mountain, G., & Proust, J. N., 2010, The New Jersey margin scientific drilling project (IODP expedition 313): Untangling the record of global and local sea-level changes: Scientific Drilling, no. 10, p. 26-34.

Muto, T., & Steel, R. J., 1992, Retreat of the front in a prograding delta: Geology, v. 20, no. 11, p. 967-970.

-, 2002, In Defense of Shelf Edge Delta Development during Falling and Lowstand of Relative Sea Level: The Journal of Geology, v. 110, no. 4, p. 421-436.

Mutti, E., & Davoli, G., 1992, Turbidite Sandstones, AGIP - Istituto di Geologia, Università di Parma.

Mutti, E., & Ricci Lucchi, F., 1975, Turbidite facies and facies associations: In: Examples of Turbidite Facies and Facies Associations from Selected Formations of the Northern Apennines (by E. Mutti, G.C. Parea, F. Ricci Lucchi, M. Sagri, G. Zanzucchi, G. Ghibaudo and S. Jaccarino), v. IX International Congress of Sedimentology, Field Trip A-11, p. 21–36.

Nemec, W., Steel, R. J., Gjelberg, J., Collinson, J. D., Prestholm, E., & Oxnevad, I. E., 1988, Anatomy of collapsed and re-established delta front in Lower Cretaceous of eastern Spitsbergen; gravitational sliding and sedimentation processes: AAPG Bulletin, v. 72, no. 4, p. 454-476.

Nichol, S. L., Boyd, R., & Penland, S., 1996, Sequence stratigraphy of a coastal-plain incised valley estuary, Lake Calcasieu, Louisiana: Journal of Sedimentary Research, v. 66, no. 4, p. 847-857.

Normark, Piper, & Hiscott, 1998, Sea level controls on the textural characteristics and depositional architecture of the Hueneme and associated submarine fan systems, Santa Monica Basin, California: Sedimentology, v. 45, no. 1, p. 53-70.

O'Grady, D. B., Syvitski, J. P. M., Pratson, L. F., & Sarg, J. F., 2000, Categorizing the morphologic variability of siliciclastic passive continental margins: Geology, v. 28, no. 3, p. 207-210.

Olariu, C., & Bhattacharya, J. P., 2006, Terminal distributary channels and delta front architecture of river-dominated delta systems: Journal of Sedimentary Research, v. 76, no. 2, p. 212-233.

Olariu, C., & Steel, R. J., 2009, Influence of point-source sediment-supply on modern shelf-slope morphology: implications for interpretation of ancient shelf margins: Basin Research, v. 21, no. 5, p. 484-501.

Oliveira, C. M. M., Hodgson, D. M., & Flint, S. S., 2011, Distribution of soft-sediment deformation structures in clinoform successions of the Permian Ecca Group, Karoo Basin, South Africa: Sedimentary Geology, v. 235, no. 3-4, p. 314-330.

Orton, G. J., 1988, A spectrum of middle Ordovician fan and braidplain deltaic sequences,North Wales: a consequence of varying fluvial input.: In: Fan Deltas: Sedimentology and Tectonic Settings (Ed. by W. Nemec & R. J. Steel) p. 23-49. Blackie, Glasgow.

Orton, G. J., & Reading, H. G., 1993, Variability of deltaic processes in terms of sediment supply, with particular emphasis on grain size: Sedimentology, v. 40, no. 3, p. 475-512.

Petter, A. L., & Steel, R. J., 2006, Hyperpycnal flow variability and slope organization on an Eocene shelf margin, Central Basin, Spitsbergen: AAPG Bulletin, v. 90, no. 10, p. 1451-1472.

Pinous, O. V., Levchuk, M. A., & Sahagian, D. L., 2001, Regional Synthesis of the Productive Neocomian Complex of West Siberia: Sequence Stratigraphic Framework: AAPG Bulletin, v. 85, no. 10, p. 1713-1730.

Piper, D. J. W., & Normark, W. R., 2001, Sandy Fans-From Amazon to Hueneme and Beyond: AAPG Bulletin, v. 85, no. 8, p. 1407-1438.

Plink-Bjorklund, P., Mellere, D., & Steel, R. J., 2001, Turbidite variability and architecture of sand-prone, deep-water slopes: Eocene clinoforms in the Central Basin, Spitsbergen: Journal of Sedimentary Research, v. 71, no. 6, p. 895-912.

Plink-Björklund, P., & Steel, R. J., 2004, Initiation of turbidity currents: outcrop evidence for Eocene hyperpycnal flow turbidites: Sedimentary Geology, v. 165, no. 1–2, p. 29-52.

Plint, A. G., & Nummedal, D., 2000, The falling stage systems tract: recognition and importance in sequence stratigraphic analysis: Geological Society, London, Special Publications, v. 172, no. 1, p. 1-17.

Poag, C. W., Swift, B. A., Schlee, J. S., Ball, M. M., & Sheetz, L. L., 1990, Early Cretaceous shelf-edge deltas of the Baltimore Canyon Trough: Principal sources for sediment gravity deposits of the northern Hatteras Basin: Geology, v. 18, no. 2, p. 149-152.

Ponten, A., & Plink-Bjorklund, P., 2009, Process Regime Changes Across a Regressive to Transgressive Turnaround in a Shelf-Slope Basin, Eocene Central Basin of Spitsbergen: Journal of Sedimentary Research, v. 79, no. 1, p. 2-23.

Porębski, S. J., & Steel, R. J., 2003, Shelf-margin deltas: their stratigraphic significance and relation to deepwater sands: Earth-Science Reviews, v. 62, no. 3-4, p. 283-326.

Porębski, S. J., & Steel, R. J., 2006, Deltas and sea-level change: Journal of Sedimentary Research, v. 76, no. 3, p. 390-403.

Posamentier, H. W., & Allen, G. P., 1993, Variability of the sequence stratigraphic model: effects of local basin factors: Sedimentary Geology, v. 86, no. 1-2, p. 91-109.

Posamentier, H. W., & Allen, G. P., 1999, Siliciclastic sequence stratigraphy-concepts and applications: SEPM (Society for Sedimentary Geology) v. Concepts in Sedirnentology and Paleontology No. 7.

Posamentier, H. W., Allen, G. P., James, D. P., & Tesson, M., 1992, Forced regressions in a sequence stratigraphic framework; concepts, examples, and exploration significance: AAPG Bulletin, v. 76, no. 11, p. 1687-1709.

Posamentier, H. W., Jervey, M. T., & Vail, P. R., 1988, Eustatic controls on clastic deposition I - conceptual framework. : *in* C.K. Wilgus, B.S. Hastings, C.G.S.C. Kendall, H.W. Posamentier, C.A. Ross and J.C. Van Wagoner eds., Sea Level Changes - An Integrated Approach, SEPM Special Publication, v. 42.

Posamentier, H. W., & Vail, P. R., 1988a, Eustatic controls on clastic deposition II-Sequence and systems tract models: *in* C.K Wilgus B.S. Hastings, C.G.ST.C. Kendall, H.W. Posamentier, C.A. Ross & J.C. Van Wagoner, eds., Sea-Level Changes - An Intergrated Approach, SEPM Special Publication, v. 42, p. 125-154.

Posamentier, H. W., & Vail, P. R., 1988b, Eustatic controls on clastic deposition II – sequence and systems tract models. In: Sea-Level Changes – An Integrated Approach (Ed. by C.K.Wilgus, B.S.Hastings, C.G.St.C.Kendall, H.W.Posamentier, C.A.Ross & J.C.Van Wagoner),: SEPM Spec. Publ., v. 42, p. 125-154.

Postma, G., 1995, Sea-level-related architectural trends in coarse-grained delta complexes: Sedimentary Geology, v. 98, no. 1-4, p. 3-12.

Pratson, L. F., Nittrouer, C. A., Wiberg, P. L., Steckler, M. S., Swenson, J. B., Cacchione, D. A., Karson, J. A., Murray, A. B., Wolinsky, M. A., Gerber, T. P., Mullenbach, B. L., Spinelli, G. A., Fulthorpe, C. S., O'Grady, D. B., Parker, G., Driscoll, N. W., Burger, R. L., Paola, C., Orange, D. L., Field, M. E., Friedrichs, C. T., & Fedele, J. J., 2009, Seascape Evolution on Clastic Continental Shelves and Slopes, Continental Margin Sedimentation, Blackwell Publishing Ltd., p. 339-380.

Prélat, A., & Hodgson, D. M., 2013, The full range of turbidite bed thickness patterns in submarine lobes: controls and implications: Journal of the Geological Society, v. 170, no. 1, p. 209-214.

Prior, D. B., & Coleman, J. M., 1980, Sonograph mosaics of submarine slope instabilities, Mississippi River Delta: Marine Geology, v. 36, no. 3-4, p. 227-239.

Prior, D. B., Coleman, J. M., & Garrison, L. E., 1979, Digitally acquired undistorted side-scan sonar images of submarine landslides, Mississippi River delta: Geology, v. 7, no. 9, p. 423-425.

Pulham, A. J., 1989, Controls on internal structure and architecture of sandstone bodies within Upper carboniferous fluvial-dominated deltas, County Clare, western Ireland. In: Whatley, M.K.G. & Pickering, K.T. (eds) Deltas: sites and traps for fossil fuels,: Geological Society Special Publication, v. 41, p. 179-203.

Pyles, D., & Slatt, R., 2007, Applications to understanding shelf edge to base-of-slope changes in stratigraphic architecture of prograding basin margins: Stratigraphy of the Lewis Shale, Wyoming, USA: *in* Nilsen, T.H., Shew, R.D., Steffens, G.S., and Studlick, J.R.J. eds., Atlas of Deep-Water Outcrops: American Association of Petroleum Geologists.

Reading, H., & Collinson, J. D., 1996, Clastic coasts: In: Reading H. G. (Ed.), SedimentaryEnvironments: Processes. Facies and Stratigraphy. Blackwell, Oxford p. 154-231.

Rich, J. L., 1951, Three critical environments of deposition, and criteria for recognition of rocks deposited in each of them: Geological Society of America Bulletin, v. 62, no. 1, p. 1-20.

Rider, M. H., 1978, Growth faults in Carboniferous of Western Ireland: Aapg Bulletin-American Association of Petroleum Geologists, v. 62, no. 11, p. 2191-2213.

Rogers, K. G., & Goodbred, S. L., 2010, Mass failures associated with the passage of a large tropical cyclone over the Swatch of No Ground submarine canyon (Bay of Bengal): Geology, v. 38, no. 11, p. 1051-1054.

Romans, B. W., & Graham, S. A., 2013, A Deep-Time Perspective of Land-Ocean Linkages in the Sedimentary Record: Annual Review of Marine Science, v. 5, no. 1, p. 69-94.

Romans, B. W., Hubbard, S. M., & Graham, S. A., 2009, Stratigraphic evolution of an outcropping continental slope system, Tres Pasos Formation at Cerro Divisadero, Chile: Sedimentology, v. 56, no. 3, p. 737-764.

Rubidge, B. S., Hancox, P. J., & Catuneanu, O., 2000, Sequence analysis of the Ecca-Beaufort contact in the southern Karoo of South Africa: South African Journal of Geology, v. 1, no. 103, p. 81-96.

Ryan, M. C., Helland-Hansen, W., Johannessen, E. P., & Steel, R. J., 2009, Erosional vs. accretionary shelf margins: the influence of margin type on deepwater

sedimentation: an example from the Porcupine Basin, offshore western Ireland: Basin Research, v. 21, no. 5, p. 676-703.

Saller, A. H., Noah, J. T., Ruzuar, A. P., & Schneider, R., 2004, Linked lowstand delta to basin-floor fan deposition, offshore Indonesia: An analog for deep-water reservoir systems: AAPG Bulletin, v. 88, no. 1, p. 21-46.

Sanchez, C. M., Fulthorpe, C. S., & Steel, R. J., 2012a, Middle Miocene–Pliocene siliciclastic influx across a carbonate shelf and influence of deltaic sedimentation on shelf construction, Northern Carnarvon Basin, Northwest Shelf of Australia: Basin Research, p. n/a-n/a.

-, 2012b, Miocene shelf-edge deltas and their impact on deepwater slope progradation and morphology, Northwest Shelf of Australia: Basin Research, p. n/a-n/a.

Sangree, J. B., & Widmier, J. M., 1978, Seismic Stratigraphy and Global Changes of Sea Level, Part 9: Seismic Interpretation of Clastic Depositional Facies: AAPG Bulletin, v. 62, no. 5, p. 752-771.

Scheepers, R., & Armstrong, R., 2002, New U-Pb SHRIMP zircon ages of the Cape Granite Suite: implications for the magmatic evolution of the Saldania Belt: South African Journal of Geology, v. 105, no. 3, p. 241-256.

Schomacker, E. R., Kjemperud, A. V., Nystuen, J. P., & Jahren, J. S., 2010, Recognition and significance of sharp-based mouth-bar deposits in the Eocene Green River Formation, Uinta Basin, Utah: Sedimentology, v. 57, no. 4, p. 1069-1087.

Sixsmith, P. J., Flint, S. S., Wickens, H. D. V., & Johnson, S. D., 2004, Anatomy and stratigraphic development of a basin floor turbidite system in the Laingsburg formation, main Karoo basin, South Africa: Journal of Sedimentary Research, v. 74, no. 2, p. 239-254.

Sømme, T. O., Helland-Hansen, W., & Granjeon, D., 2009, Impact of eustatic amplitude variations on shelf morphology, sediment dispersal, and sequence stratigraphic interpretation: Icehouse versus greenhouse systems: Geology, v. 37, no. 7, p. 587-590.

Sømme, T. O., Helland-Hansen, W., & Granjeon, D., 2010, Impact of eustatic amplitude variations on shelf morphology, sediment dispersal, and sequence stratigraphic interpretation: Icehouse versus greenhouse systems: REPLY: Geology, v. 38, no. 6, p. e209.

Southard, J. B., & Stanley, D. J., 1976, Shelf-break processes and sedimentation.: In: Marine Sediment Transport and Environmental Management (Eds D.J. Stanley and D.J.P. Swift), Wiley-Interscience, New York, p. 351–377.

Steel, R., & Olsen, T., 2002, Clinoforms, clinoform trajectories and deepwater sands.: *in* Sequence stratigraphic models for exploration and production: Evolving models and application histories: Proceedings of the Gulf Coast Section Society for Sedimentary geology (GCSSEPM), v. 22nd Research Conference (CD-ROM) eds J.M.Armentrout & N.C.Rosen, p. 367–381.

Steel, R. J., Carvajal, C., Petter, A., & Uroza, C., 2008, Shelf and shelf-margin growth in scenarios of rising and falling sea level: *in* Hampson, G.J., Steel, R.J., Burgess, P.M., and Dalrymple, R.W., eds., Recent Advances in Models of Siliciclastic Shallow-Marine Stratigraphy, SEPM Society for Sedimentary Geology, no. Special Publication 90, p. 47-71.

Steel, R. J., Crabaugh, J., Schelpepper, M., Mellere, D., Plink-Björklund, P., Deibert, J., & Løseth, T., 2000, Deltas vs. rivers on the shelf edge: their relative contributions to the growth of shelf-margins and basin-floor fans (Barremian and Eocene, Spitsbergen). In: Deep-Water Reservoirs of the World: 20th Annual Gulf Coast SEPM Bob F. Perkins Research Conference (Ed. by P.Weimer, R.M.Slatt, J.Coleman, N.C.Rosen, H.Nelson, A.H.Bouma, M.J.Styzen & D.T.Lawrence), p. 981–1009.

Stewart, S. A., 2011, Vertical exaggeration of reflection seismic data in geoscience publications 2006–2010: Marine and Petroleum Geology, v. 28, no. 5, p. 959-965.

Stow, D. A. V., 1994, Sedimentology and Stratigraphy, 2nd Edition: *in* Pye, K eds., Sediment Transport and Depositional Processes: Black Scientific Publication.

Suter, J. R., & Berryhill, H. L., 1985, Late Quaternary shelf-margin deltas, Northwest Gulf of Mexico: AAPG Bulletin, v. 69, no. 1, p. 77-91.

Sydow, J., & Roberts, H. H., 1994, Stratigraphic framework of a late Pleistocene shelf-edge delta, Northeast Gulf of Mexico: AAPG Bulletin, v. 78, no. 8, p. 1276-1312.

Syvitski, J. P. M., & Milliman, J. D., 2007, Geology, Geography, and Humans Battle for Dominance over the Delivery of Fluvial Sediment to the Coastal Ocean: The Journal of Geology, no. 1, p. 1.

Talling, P. J., 1998, How and where do incised valleys form if sea level remains above the shelf edge?: Geology, v. 26, no. 1, p. 87-90.

Tankard, A., Welsink, H., Aukes, P., Newton, R., & Stettler, E., 2009, Tectonic evolution of the Cape and Karoo basins of South Africa: Marine and Petroleum Geology, v. 26, no. 8, p. 1379-1412.

Tankard, A. J., Jackson, M. P. A., Eriksson, K. A., Hobday, D. K., Hunter D.R., & W.E.L., M., 1982, Crustal evolution of South Africa: 3.8 billion years of Earth History, p. 523.

Tesson, M., Allen, G. P., & Ravenne, C., 2009, Late Pleistocene Shelf-Perched Lowstand Wedges on the Rhône Continental Shelf, Sequence Stratigraphy and Facies Associations, Blackwell Publishing Ltd., p. 181-196.

Tesson, M., Gensous, B., Allen, G. P., & Ravenne, C., 1990, Late Quaternary deltaic lowstand wedges on the Rhône continental shelf, France: Marine Geology, v. 91, no. 4, p. 325-332.

Turner, B. R., 1999, Tectonostratigraphical development of the Upper Karooforeland basin: Orogenic unloading versus thermally-induced Gondwana rifting: Journal of African Earth Sciences, v. 28, no. 1, p. 215-238.

Uličný, D., Nichols, G., & Waltham, D., 2002, Role of initial depth at basin margins in sequence architecture: field examples and computer models: Basin Research, v. 14, no. 3, p. 347-360.

Uroza, C. A., & Steel, R. J., 2008, A highstand shelf-margin delta system from the Eocene of West Spitsbergen, Norway: Sedimentary Geology, v. 203, no. 3-4, p. 229-245.

Vail, P. R., Audemar, F., Bowman, S. A., Eisner, P. N., & Perez-Cruz, C., 1991, The stratigraphic signatures of tectonics, eustasy and sedimentology - and overview. : *in*: G. Einsele, W. Ricken & A. Seilacher ed. Cycles and Events in Stratigraphy, Springer-Verlag, Berlin Heidelberg, p. 617-659.

Vail, P. R., Mitchum R. M. J., & I., T. S., 1977b, Seismic stratigraphic and globalchanges in sea level, part 3. In. C.E. Playton (eds.), Seismic Stratigraphy - Application to Hydrocarbon Exploration: AAPG Memoir. Tulsa, v. 26, p. 63-82.

Vail, P. R., Todd R.G., & J.B., S., 1977d, Seismic stratigraphy - applications to hydrocarbon exploration, p. 292.

van der Merwe, W. C., Flint, S. S., & Hodgson, D. M., 2010, Sequence stratigraphy of an argillaceous, deepwater basin-plain succession: Vischkuil Formation (Permian), Karoo Basin, South Africa: Marine and Petroleum Geology, v. 27, no. 2, p. 321-333.

van der Merwe, W. C., Hodgson, D. M., & Flint, S. S., 2009, Widespread syn-sedimentary deformation on a muddy deep-water basin-floor: The vischkuil formation (Permian), Karoo Basin, South Africa: Basin Research, v. 21, no. 4, p. 389-406.

Van Lente, B., 2004, Chemostratigraphic trends and provenance of the Permian Tanqua and Laingsburg depocentres, South Western Karoo Basin, South Africa: [unpublished Ph.D. thesis]: University of Stellenbosch, p. 339.

Van Wagoner, J. C., Mitchum, R. M., Campion, K. M., & Rahmanian, V. D., 1990, Siliciclastic sequence stratigraphy in well logs, cores, and outcrops, Related Information: AAPG methods in exploration series, No. 7.

Van Wagoner, J. C., Posamentier, H. W., Mitchum, R. M., Vail, P. R., Sarg, J. F., Loutit, T. S., & Hardenbol, J., 1988, An overview of sequence stratigraphy and key definitions.: SEPM Special Publication, v. 42, p. 39 - 45.

Vanessa Kertznus, & Ben Kneller, 2009, Clinoform quantification for assessing the effects of external forcing on continental margin development: Basin Research, v. 9999, no. 9999.

Veevers, J. J., Cole, D. I., & Cowan, E. J., 1994, Southern Africa: Karoo Basin and Cape Fold Belt: *in* Veevers, J.J. and Powell, C. McA. eds., Permian-Triassic Pangean basins and foldbelts along the Panthalassan Margin of Gondwanaland. Geological Society America Memoir, , v. 184, p. 223-279.

Viljoen, J. H. A., 1994, Sedimentology of the Collingham Formation, Karoo Supergroup: South African Journal of Geology, v. 97, no. 2, p. 167-183.

Visser, J. N. J., 1987, The palaeogeography of part of southwestern Gondwana during the Permo-Carboniferous glaciation: Palaeogeography, Palaeoclimatology, Palaeoecology, v. 61, no. 0, p. 205-219.

Visser, J. N. J., 1993, Sea-level changes in a back-arc-foreland transition: the late Carboniferous-Permian Karoo Basin of South Africa: Sedimentary Geology, v. 83, no. 1-2, p. 115-131.

-, 1997, Deglaciation sequences in the Permo-Carboniferous Karoo and Kalahari basins of Southern Africa; a tool in the analysis of cyclic glaciomarine basin fills: Sedimentology, v. 44, no. 3, p. 507-521.

Visser, J. N. J., & Praekelt, H. E., 1998, Subduction, mega-shear systems and late Palaeozoic basin development in the African segment of Gondwana: Journal of African Earth Sciences, v. 26, no. 2, p. VIII-VIII.

Weber, M. E., Wiedicke, M. H., Kudrass, H. R., Hübscher, C., & Erlenkeuser, H., 1997, Active growth of the Bengal Fan during sea-level rise and highstand: Geology, v. 25, no. 4, p. 315-318.

Wickens, H. D., 1994, Basin Floor Fan Building Turbidites of the Southwestern Karoo Basin, Permian Ecca Group, South Africa [unpublished Ph.D. Thesis]: University of Port Elizabeth, Port Elizabeth, p. 233.

Wignall, P. B., & Best, J. L., 2004, Sedimentology and kinematics of a large, retrogressive growth-fault system in Upper Carboniferous deltaic sediments, western Ireland: Sedimentology, v. 51, no. 6, p. 1343-1358.

Wild, R., Flint, S. S., & Hodgson, D. M., 2009, Stratigraphic evolution of the upper slope and shelf edge in the Karoo Basin, South Africa: Basin Research, v. 21, no. 5, p. 502-527.

Winn, R. D., Roberts, H. H., Kohl, B., Fillon, R. H., Bouma, A. H., & Constans, R. E., 1995, Latest Quaternary deposition on the outer shelf, northern Gulf of Mexico: Facies and sequence stratigraphy from Main Pass Block 303 shallow core: Geological Society of America Bulletin, v. 107, no. 7, p. 851-866.

APPENDIX A: PALAEO-FLOW MEASURMENTS

This appendix present the palaeo-flow dataset acquired in this work. A total of 1,228 individual measurements were taken across the study area. Both unidirectional measurements acquired from foresets of ripple cross lamination, and bidirectional data, from ripple crest orientation, flutes and grooves are included. The data are grouped based on individual units / parasequences and separated into unidirectional and bidirectional data.

The raw data were processed using the EZ-ROSE software (Baas, 2000).

Unit G

Unidirectional

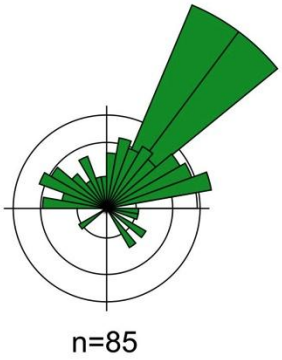

Bidirectional

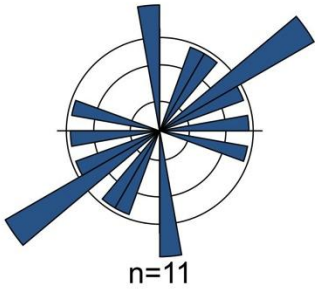

WfC 1

Unidirectional

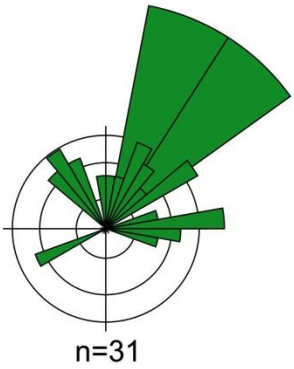

Bidirectional

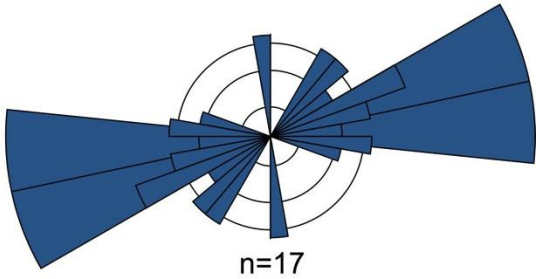

WfC 2

Unidirectional

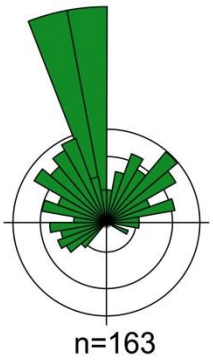

Bidirectional

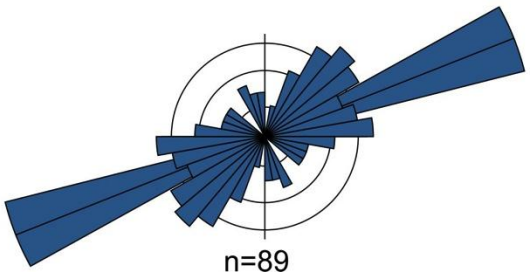

WfC 3

Unidirectional

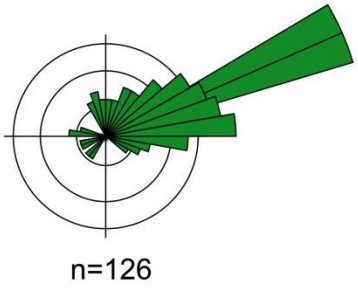

n=126

Bidirectional

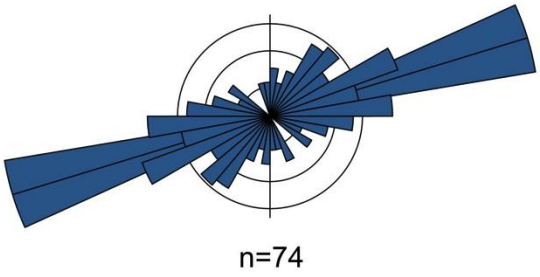

n=74

WfC 4

Unidirectional

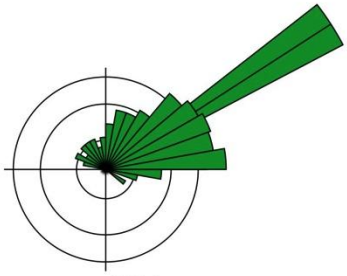

n=165

Bidirectional

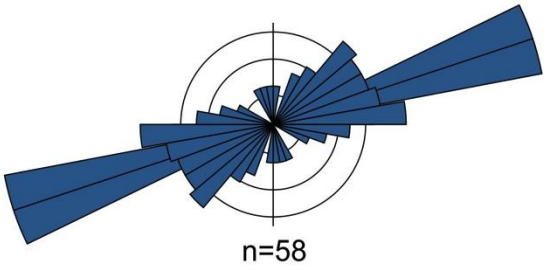

n=58

WfC 5

Unidirectional

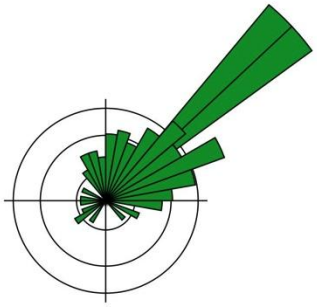

n=134

Bidirectional

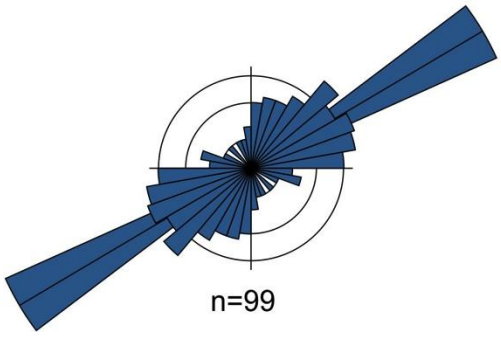

n=99

WfC 6

Unidirectional

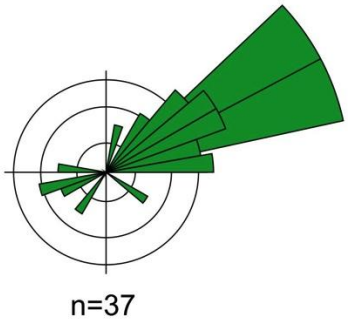

Bidirectional

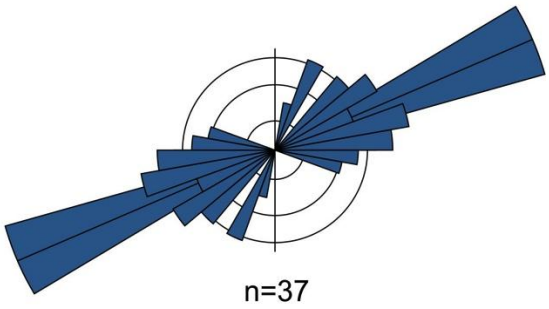

WfC 7

Unidirectional

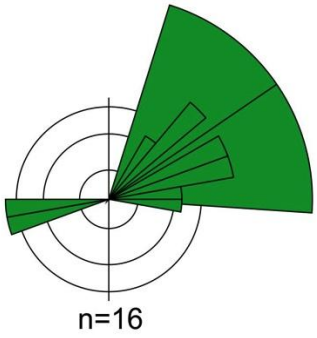

Bidirectional

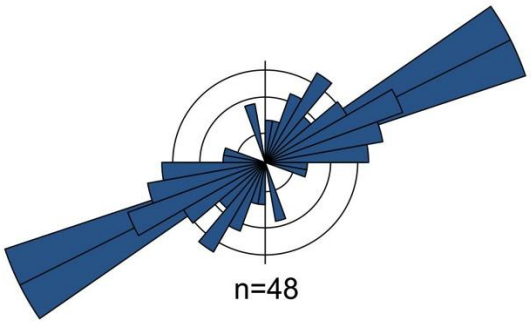

WfC 8

Unidirectional

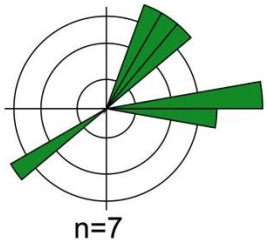

Bidirectional

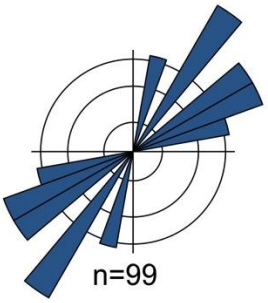

APPENDIX B: LOG LOCALITIES

Location of logs within the studied Waterford succession (Karoo 21 E)

Log Locality	LogName			Base of log	
Baviaans South profile	Kranz 2	X	477458	Y	6323994
Baviaans South profile	Kranz	X	481986	Y	6323707
Baviaans South profile	Ladikranz	X	482506	Y	6323938
Baviaans South profile	Ladikranz 2	X	485014	Y	6324075
Baviaans South profile	Ladismith road	X	436775	Y	6324220
Baviaans South profile	Ladigeel	X	488575	Y	6323921
Baviaans South profile	Geelbec 2	X	490331	Y	6324095
Baviaans South profile	Geelbec 3	X	492041	Y	6324088
Baviaans South profile	Geelbec 1	X	496200	Y	6324599
Baviaans South profile	Geelbec river	X	498267	Y	6324618
Baviaans South profile	Hart B	X	505889	Y	6324808
Baviaans South profile	Hart B 2	X	511678	Y	6325329
Baviaans South profile	6.6	X	513809	Y	6325703
Baviaans South profile	Spitskop south	X	517582	Y	6326297
Baviaans North profile	Ouplaas	X	478218	Y	6326375
Baviaans North profile	Ouplaas 2	X	479355	Y	6326435
Baviaans North profile	Vischkuil Station	X	483691	Y	6326516
Baviaans North profile	Vischkuil Station 2	X	489904	Y	6326136
Baviaans North profile	Viaduct cut	X	485990	Y	6326422
Baviaans North profile	Rail cut	X	486894	Y	6326624
Baviaans North profile	N1 log	X	489659	Y	6327165
Baviaans North profile	Fillin log	X	490908	Y	6327412
Baviaans North profile	Geelbec north	X	492492	Y	6327809
Baviaans North profile	Geelblock	X	494423	Y	6328592
Baviaans North profile	Geelblock 2	X	496274	Y	6328208
Baviaans North profile	Blockhouse	X	498518	Y	6329105
Baviaans North profile	Blockhouse east	X	49959	Y	6329520
Baviaans North profile	Vleifountein station	X	504827	Y	6330773
Baviaans North profile	Turb log	X	508009	Y	6331662
Baviaans North profile	Spitskop	X	598518	Y	6329105
Zoutkloof profile	Zout river	X	497013	Y	6333112
Zoutkloof profile	Zout-brff	X	485185	Y	333451
Zoutkloof profile	Buf rep (H)	X	488624	Y	6332052
Zoutkloof profile	Buffles north rep	X	488771	Y	6332418
Zoutkloof profile	Buffles north rep 2	X	488771	Y	6332418
Zoutkloof profile	Zout TT	X	498085	Y	6332841
Zoutkloof profile	Zout TT 2	X	492085	Y	6332841
Zoutkloof profile	Faberskraal	X	497743	Y	6334122
Zoutkloof profile	Fab farm	X	500505	Y	6334951
Zoutkloof profile	Fab 3	X	502476	Y	6335325

Zoutkloof profile	Log 6.5	X	505998	Y	6335764
Zoutkloof profile	Log 6.4	X	508414	Y	6336133
Zoutkloof profile	Log 6.2	X	511459	Y	6336295
Zoutkloof profile	Oskop	X	513885	Y	6336328
Zoutkloof profile	Becksflakte	X	516957	Y	6336522
Zoutkloof profile	Koup station	X	524402	Y	6334394

APPENDIX C: CORRELATION PANELS

Baviaans South, Baviaans North and Zoutkloof correlation panels.

Baviaans Southern Profile

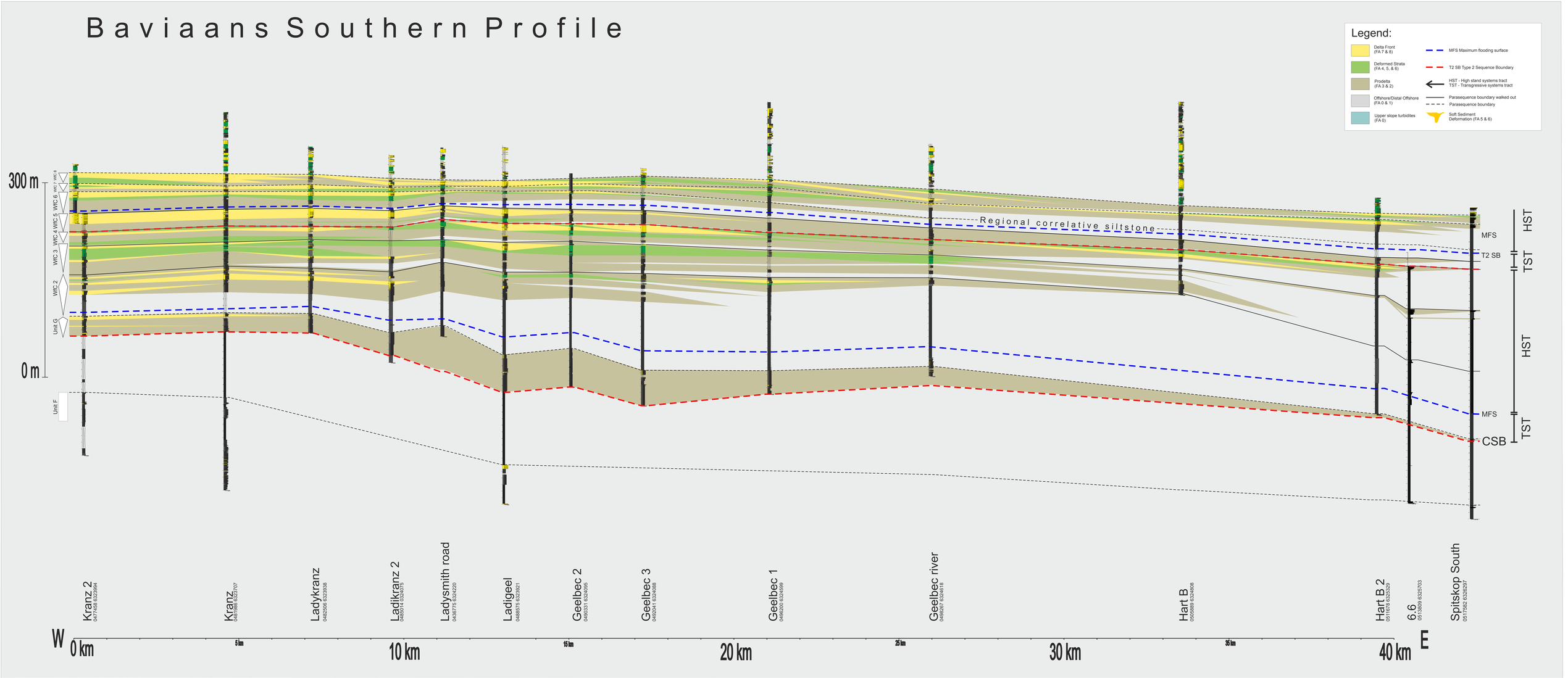

Baviaans North Profile

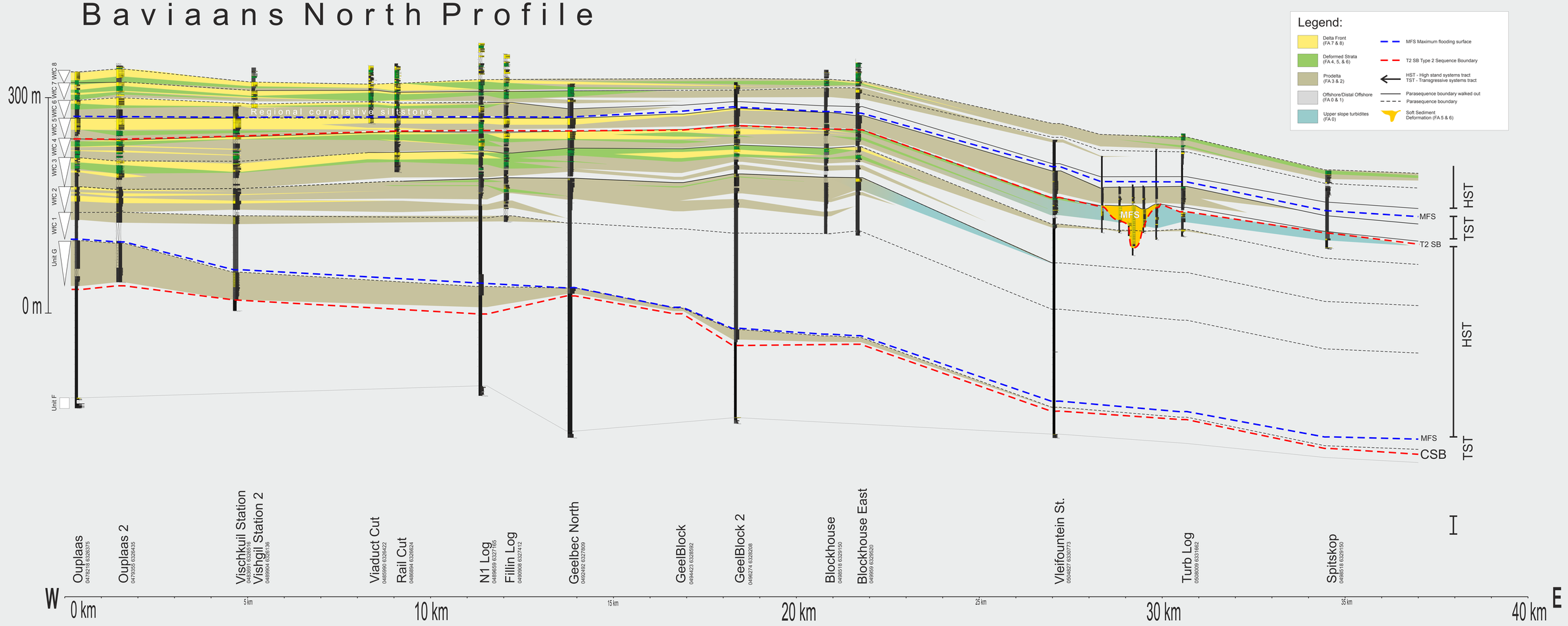

Zoutkloof Profile